Universidad de Huelva

Departamento de Ciencias de la Tierra

Valorización de residuos no peligrosos para la elaboración de tecnosuelos aplicados a la recuperación de espacios mineros abandonados

Memoria para optar al grado de doctora
presentada por:

Sandra Fernández Landero

Fecha de lectura: 2 de diciembre de 2025

Bajo la dirección de los doctores:

Juan Carlos Fernández Caliani

Pablo José Hidalgo Fernández

Huelva, 2025

Universidad de Huelva

Valorización de residuos no peligrosos para la elaboración de tecnosuelos aplicados a la recuperación de espacios mineros abandonados

Tesis Doctoral

Sandra Fernández Landero

Huelva, 2025

Universidad de Huelva

Programa oficial de doctorado en Ciencia y Tecnología Industrial y Ambiental

Valorización de residuos no peligrosos para la elaboración de tecnosuelos aplicados a la recuperación de espacios mineros abandonados

Memoria para optar al Grado de Doctora presentada por:

Sandra Fernández Landero

Huelva, 2025

Bajo la dirección de los doctores:

Juan Carlos Fernández Caliani

Pablo José Hidalgo Fernández

FINANCIACIÓN

La investigación de esta tesis ha sido financiada por la Junta de Andalucía y el Fondo Europeo de Desarrollo Regional Andalucía 2014-2020, a través del Proyecto P-18-TP-3503, realizado en colaboración con la empresa DSM Soluciones Medioambientales.

AGRADECIMIENTOS

Me gustaría comenzar estas palabras de agradecimiento dando las gracias de todo corazón a todos los que, de una forma u otra, han ayudado a la realización de esta tesis doctoral. Ha sido un camino largo y con pequeños contratiempos, pero también gratificante.

En primer lugar, quiero agradecer a Inmaculada Giráldez Díaz, cuya contribución fue determinante para el desarrollo y la culminación de esta tesis. Aunque no fue posible reconocer formalmente su función como codirectora, su dedicación y cariño al enseñarme todo lo relacionado con el trabajo de laboratorio, desde preparación de muestras y técnicas analíticas hasta el tratamiento de datos, han sido imprescindible. Inma, gracias por ser tan amable y entregada, por tu paciencia y por siempre estar dispuesta a ayudar con una sonrisa.

También me gustaría agradecer profundamente a mi tutor y director, Juan Carlos Fernández Caliani, por su enorme paciencia. Ha sido mi guía constante y ha hecho que este difícil camino se sintiera más fácil gracias a su apoyo y motivación incansable.

A Pablo J. Hidalgo Fernández, también mi director, quiero expresar mi gratitud por ser mi guía en la parte botánica de esta tesis. Su orientación fue esencial para el éxito de los ensayos con plantas y para entender mejor la interacción de los tecnosuelos con las plantas.

También doy las gracias a los demás miembros del equipo de investigación: Emilio Morales Carrillo de Albornoz, Cinta Barba Brioso, Mercedes Ruiz Montoya, Manuel Jesús Díaz Blanco e Isabel González. Gracias por vuestro esfuerzo, dedicación y por el tiempo tan generoso que habéis invertido en este proyecto.

A Manuela Abreu y Paula Gonçalves, del Instituto Superior de Agronomía, muchas gracias por hacer que mi estancia en Lisboa fuera tan agradable y por enseñarme todo lo necesario para el análisis de la actividad enzimática del suelo.

Quiero hacer un agradecimiento especial a Manuela por su cálido trato y su constante disposición a ayudarme.

A Rosa León, gracias por enseñarme técnicas de extracción de ADN genómico del suelo. Aunque los resultados no fueron los esperados, su sonrisa y actitud positiva hicieron que el trabajo en el laboratorio fuera mucho más agradable.

También quiero expresar mi agradecimiento a Nereida Pascual, Lourdes Vales y Alicia Rodríguez, de DSM Soluciones Medioambientales (Centro Ambiental de Nerva), por su valiosa colaboración durante este trabajo. Su ayuda en la recogida de muestras de residuos y la información técnica facilitada fueron fundamentales para el desarrollo de una parte clave de esta tesis. Gracias por vuestra disposición, profesionalidad y amabilidad en todo momento.

A mis padres, Julia y Matías, no tengo palabras para expresar todo lo que les debo. Gracias por bridarme el apoyo emocional y material necesario para llegar hasta aquí. Vuestra confianza en mí ha sido el pilar sobre el que se sostiene esta tesis.

A mis amigas incondicionales, Victoria, Rocío, María H., Zaida, Yulia, Cristina y Joaquín, María P., gracias por estar siempre ahí, por vuestras palabras de ánimo y por hacer que los momentos menos buenos fueran más llevaderos.

Y no puedo olvidar a mi querido gato Makki, por acompañarme en las largas tardes al ordenador, ofreciéndome su compañía, algún que otro bocado y muchos pelos en el teclado.

Por último, quiero agradecer la financiación recibida por el proyecto P-18-TP-3503 y por el grupo de investigación Geología y Geoquímica Ambiental (RNM 347), sin la cual esta tesis no hubiera sido posible.

Muchas gracias a todos, no podría haber completado este trabajo sin vosotros.

RESUMEN

Los tecnosuelos constituyen una alternativa de remediación ambiental basada en la formulación de mezclas sólidas de residuos no peligrosos (RNP) para la recuperación ambiental de ecosistemas degradados. La tesis se enmarca en este contexto de economía circular y desarrollo sostenible, con el propósito de valorizar RNP y regenerar suelos contaminados por la minería metálica. Los objetivos abarcan la caracterización de suelos afectados, el diseño de tecnosuelos innovadores y la evaluación de su eficacia para neutralizar la acidez, estabilizar contaminantes y mejorar la fertilidad y el crecimiento vegetal.

Se estudiaron cinco emplazamientos contaminados por metales pesados o afectados por drenaje ácido de minas (DAM) en Riotinto y Tharsis, así como en el estero de Domingo Rubio (estuario de Huelva). La caracterización de los suelos incluyó análisis granulométricos, electroquímicos (pH_{H_2O}, pH_{KCl} y pH_{ox}, Eh, conductividad eléctrica), mineralógicos (DRX, FESEM-EDS) y químicos (ICP-OES, EPMA). El potencial de generación de acidez se cuantificó mediante dos pruebas estáticas: el balance ácido-base (ABA) y el ensayo de generación de acidez neta (NAG).

Los resultados confirmaron que los suelos afectados son sistemas hiperácidos (acidez neta hasta 663 mmol H^+ kg^{-1}), con una marcada deficiencia de nutrientes, materia orgánica y bases de cambio, lo que impide el desarrollo natural de la vegetación. Excepcionalmente, en el suelo contaminado con residuos piríticos del estero de Domingo Rubio crecen plantas tolerantes como *Nicotiana glauca, que* acumulan As, Pb y Cu en sus raíces, favoreciendo su fitoestabilización.

En general, se detectaron altos contenidos de S pirítico y en forma de sulfato y niveles preocupantes de As, Pb, Cd, Cu, Zn y Tl. En algunos casos, As y Pb superaron 5000 mg kg^{-1}, lo cual supone un riesgo potencial significativo. Los análisis químicos puntuales por microsonda de electrones (EPMA) revelaron que estos contaminantes

están asociados principalmente a sulfuros, sulfatos y óxidos de hierro derivados de los residuos mineros. El sistema edáfico ha agotado su capacidad amortiguadora, actuando como una fuente activa de efluentes ácidos y elementos traza potencialmente tóxicos (EPT).

A partir de este diagnóstico, se seleccionaron diversos RNP, orgánicos e inorgánicos, para formular tecnosuelos destinados a la restauración ambiental. La selección se basó en criterios de idoneidad técnico-ambiental, disponibilidad y buen comportamiento en los ensayos de lixiviación. Se evaluaron propiedades como granulometría, pH, conductividad eléctrica, contenidos de C orgánico e inorgánico, N y S totales, P y K asimilables. Las concentraciones de los EPT se analizaron por ICP-OES y los hidrocarburos totales del petróleo mediante TD-GC-MS. Los residuos seleccionados se combinaron para lograr capacidad neutralizante, adsorción de metales y poder fertilizante, con el fin de anular la acidez neta, inmovilizar metales pesados y corregir las carencias de nutrientes esenciales de los suelos a tratar.

Se formularon ocho tecnosuelos con una proporción de 60% de residuo orgánico y 40% inorgánico, y se mezclaron con diferentes proporciones de suelo minero (95, 85, 80, 75, 70, 60 y 50%). Las mezclas, junto con los suelos sin tratar (control), se sometieron a ensayos de lixiviación normalizados y los eluatos se analizaron por ICP-OES, ICP-MS y cromatografía iónica para determinar las concentraciones de EPT y aniones. Los equilibrios geoquímicos se modelaron con el programa PHREEQC para identificar las especies iónicas dominantes y calcular los índices de saturación. Además, se realizaron extracciones químicas con $CaCl_2$, EDTA y HNO_3 para evaluar la movilidad y bioaccesibilidad de los contaminantes.

Los suelos sin tratar generaron lixiviados extremadamente ácidos (pH 2,5–3,5), con elevados niveles de Cu (hasta 556 mg kg^{-1}), Pb (hasta 90 mg kg^{-1}) y Zn (hasta 28 mg kg^{-1}). Con la aplicación de los tecnosuelos, el pH se elevó hasta un promedio de 7,6 y la fracción móvil de los metales disminuyó a menos del 0,10%, debido a la formación de fases menos solubles (hidróxidos y carbonatos). El tratamiento también incrementó los niveles de cationes básicos y nutrientes.

A partir de estos resultados, se seleccionaron 15 mezclas con mayor capacidad neutralizante y eficacia en la inmovilización de los contaminantes. Estas formulaciones fueron llevadas a una segunda fase de experimentación en macetas. Tras una incubaron de 14 días para alcanzar el equilibrio físico-químico, se sembraron cinco plántulas de *Brassica juncea* por maceta. En total, se emplearon 36 macetas con tecnosuelos (en triplicado), cinco controles con suelos sin tratar y dos macetas con mantillo comercial (control positivo).

Durante cinco meses (enero-junio de 2023), las macetas se mantuvieron en condiciones de invernadero, con exposición a luz natural y riego periódico. Se monitorizó el pH, la conductividad eléctrica y la composición química del agua de poro extraída con sondas Rhizon. El pH osciló entre 5,8 y 8,2 durante todo el periodo, evidenciando la estabilidad del efecto neutralizante. Las concentraciones de Fe, Al, sulfato y EPT disueltos disminuyeron en varios órdenes de magnitud en comparación con los controles, reduciendo significativamente su movilidad y disponibilidad para las plantas. Al mismo tiempo, aumentaron los niveles de Ca, Mg, K, bicarbonato, nitrato y P asimilable, mejorando la condición del suelo para el desarrollo vegetal.

Brassica juncea mostró una alta tasa de germinación en los suelos tratados, aunque su desarrollo varió según el tecnosuelo aplicado. Los indicadores de crecimiento vegetal, como la altura de la planta, el número de hojas y la biomasa producida, confirmaron la mejora en las condiciones edáficas, evidenciando el potencial de los tecnosuelos diseñados para la revegetación de áreas mineras degradadas.

En conclusión, la aplicación de tecnosuelos mejoró significativamente la calidad ambiental y la capacidad de regeneración del sistema edáfico, por lo que constituye una alternativa viable para la valorización de residuos industriales y la mitigación de los efectos de la minería metálica histórica. No obstante, su eficacia debe validarse mediante pruebas piloto antes de su aplicación a escala real.

ABSTRACT

Technosols offer an environmental remediation approach based on the formulation of solid mixtures of non-hazardous wastes (NHW) for the ecological recovery of degraded ecosystems. This research, aligned with principles of the circular economy and sustainable development, was aimed to both valorize NHW and restore soils contaminated by historic mining activities. The objectives included characterizing affected soils, designing innovative technosols, and evaluating their effectiveness to neutralize acidity, stabilize contaminants and improve fertility and plant growth.

Five sites affected by acid mine drainage (AMD) and potentially contaminated with heavy metals were studied in Riotinto and Tharsis mining districts, as well as in the Domingo Rubio tidal creek (Huelva estuary). Soil characterization involved granulometric, electrochemical (pH_{H_2O}, pH_{KCl}, pH_{ox}, Eh, electrical conductivity), mineralogical (XRD, FESEM-EDS), and chemical (ICP-OES, EPMA) analyses. To quantify the acid generation potential, two static tests were used: acid-base accounting (ABA) and net acid generation (NAG) assay.

Results confirmed that the affected soils are hyperacidic systems, with net acidity reaching up to 663 mmol H^+ kg^{-1}. They showed significant deficiencies in nutrients, organic matter, and exchangeable bases, thus hindering natural vegetation development. Remarkably, tolerant plants such as *Nicotiana glauca* were found growing on sulfide waste-contaminated soil at the Domingo Rubio site. This species accumulates As, Pb and Cu in its roots, supporting a potential role in phytostabilization.

In general, high contents of pyritic and sulfate sulfur and concerning levels of As, Pb, Cd, Cu, Zn and Tl were detected. In some cases, As and Pb exceeded 5000 mg kg^{-1}, posing a potential environmental risk. Microchemical analyses by EPMA revealed that these contaminants are mainly associated with sulfides, sulfates, and iron oxides

derived from mining wastes. The environmental assessment indicated that these soils have lost their buffering capacity and now act as active sources of acid effluents and potentially toxic elements (PTE).

In response, various organic and inorganic NHW were selected to formulate technosols for environmental restoration. Selection criteria prioritized technical-environmental suitability, availability and good performance in leaching tests. Granulometry, pH, electrical conductivity, organic and inorganic carbon content, total N and S, assimilable P and K were thoroughly evaluated. PTE concentrations were analyzed by ICP-OES and total petroleum hydrocarbons by TD-GC-MS. The selected NHW were combined to achieve optimal neutralizing capacity, metal adsorption, and fertilizing power, aiming to eliminate net acidity, immobilize heavy metals and correct nutrient deficiencies in the mine soils.

Eight technosols were formulated with a 60% organic and 40% inorganic waste ratio and mixed with varying proportions of mine soil (95, 85, 80, 75, 70, 60 and 50%). These mixtures, along with untreated soils (controls), underwent standardized leaching tests. The leachates were then analyzed by ICP-OES, ICP-MS and ion chromatography to determine PTE and anion concentrations. Geochemical equilibria were modeled using the PHREEQC software to identify the dominant ionic species and calculate saturation indices. Furthermore, chemical extractions with $CaCl_2$, EDTA and HNO were performed to assess contaminant mobility and bioaccessibility.

Untreated soils generated extremely acidic leachates (pH 2.5–3.5), with elevated levels of Cu (up to 556 mg kg^{-1}), Pb (up to 90 mg kg^{-1}) and Zn (up to 28 mg kg^{-1}). Technosol application raised pH to an average of 7.6 and reduced the mobile fraction of metals to less than 0.10% due to the formation of less soluble phases (hydroxides and carbonates). Technosol treatment also increased the levels of basic cations and nutrients.

From these promising results, 15 mixtures with the highest neutralizing capacity and contaminant immobilization efficacy were selected for a second

experimental phase in potted trials. Following a 14-day incubation to achieve physicochemical equilibrium, five *Brassica juncea* seedlings were planted per pot. In total, 36 technosol pots (in triplicate), five untreated soil controls, and two pots with commercial mulch (positive control) were used.

For five months (January–June 2023), the pots were kept under greenhouse conditions with natural light exposure and periodic irrigation. pH, electrical conductivity, and the chemical composition of pore water extracted with Rhizon probes were monitored. pH ranged from 5.8 to 8.2 throughout the period, confirming the stability of the neutralizing effect. Concentrations of dissolved Fe, Al, sulfate and PTE decreased by several orders of magnitude compared to controls, significantly reducing their mobility and phytoavailability. Concurrently, levels of Ca, Mg, K, bicarbonate, nitrate and assimilable P increased, improving soil conditions for plant growth.

Brassica juncea showed high germination rates in treated soils, with plant growth varying depending on the technosol applied. Plant growth indicators such as height, leaf count and biomass indicated significant improvements in soil quality, demonstrating the effectiveness of the designed technosols for restoring vegetation in degraded mining areas.

In conclusion, the application of technosols significantly enhanced environmental quality and the regenerative capacity of the soil system, offering a viable strategy for the valorization of industrial wastes and the rehabilitation of mining-impacted areas. However, the technosol effectiveness should be further validated through pilot-scale tests prior to large-scale implementation.

CONTENIDO

1. INTRODUCCIÓN

1.1. El suelo: un recurso crítico para la sostenibilidad ambiental

El suelo es un recurso natural limitado, no renovable e irremplazable, de vital importancia para la sostenibilidad del planeta. Esta capa superior de la corteza terrestre, situada entre el lecho rocoso y la superficie, es un ecosistema complejo, dinámico y polifásico. Está compuesto por partículas minerales, materia orgánica, agua, aire y organismos vivos, y cumple numerosas funciones, tanto naturales como de uso (Blum, 2005).

El sistema edáfico desempeña un papel fundamental en la regulación de los ciclos biogeoquímicos, actuando como reservorio y procesador de nutrientes esenciales para el desarrollo vegetal, como nitrógeno, fósforo y potasio. También interviene en el ciclo del agua, al regular su flujo, infiltración y almacenamiento, lo que ayuda a prevenir eventos extremos como inundaciones y sequías. Además, el suelo es un sumidero de carbono orgánico que contribuye significativamente a la mitigación y adaptación frente al cambio climático (Lal, 2004). Asimismo, proporciona el hábitat natural para una gran biodiversidad de organismos, mejorando la funcionalidad del ecosistema.

El suelo ofrece una amplia gama de servicios ecosistémicos o funciones para el beneficio de los seres humanos, como la provisión de agua, biomasa, alimentos y materias primas. Como servicio ecosistémico esencial, constituye la base de la agricultura, ya que suministra el soporte físico y los nutrientes indispensables para el crecimiento de los cultivos, siendo un factor determinante en la seguridad alimentaria mundial. Se estima que el 95% de nuestros alimentos depende directa o indirectamente del suelo (FAO, 2015).

Por otra parte, el suelo actúa como una barrera protectora contra la propagación de contaminantes hacia otros sistemas más vulnerables, mediante procesos físicos, químicos y biológicos que filtran, descomponen, neutralizan o inmovilizan dichos contaminantes. Sin embargo, su capacidad amortiguadora es limitada y puede verse superada ante cargas contaminantes excesivas, dando lugar a

procesos de degradación y pérdida de funcionalidad (Jiménez-Ballesta, 2017; Weil y Brady, 2016).

A pesar de ser recurso natural esencial para la vida, el suelo a menudo es subestimado. Los impactos de las actividades humanas son más rápidos y de mayor alcance que los procesos naturales de formación del suelo, que son lentos y complejos. Actividades como la intensificación de la agricultura, la urbanización, la industrialización, la minería, los conflictos armados y el cambio climático alteran directa e indirecta las propiedades y procesos del suelo, generando efectos negativos en su estabilidad y funcionalidad. Se estima que entre el 60% y el 70% de los suelos de la Unión Europea (UE) no se encuentran en buen estado (European Commission, 2021). Por tanto, es fundamental diseñar e implementar estrategias destinadas a mitigar los efectos adversos y restaurar la calidad del suelo, asegurando así la sostenibilidad ambiental a largo plazo (Sandor et al., 2023).

1.2. Contaminación de suelos: una realidad oculta

La contaminación del suelo constituye un problema ambiental de escala global, con efectos directos en la salud de las personas y en los ecosistemas. En la UE se han identificado unos 2,8 millones de emplazamientos potencialmente contaminados (Jones et al., 2012), mientras que en Estados Unidos más de 1300 sitios contaminados se encuentran registrados en la Lista de Prioridades Nacionales del Superfondo (USEPA, 2024). Estas cifras ilustran la magnitud del problema y ponen de relieve la urgente necesidad de abordar la contaminación del suelo con un enfoque global y coordinado.

En España, la Ley 7/2022, de 8 de abril, de residuos y suelos contaminados para una economía circular, define el suelo contaminado como aquel cuyas características han sido alteradas negativamente por la presencia de componentes químicos de carácter peligroso procedentes de la actividad humana, en concentración tal que comporte un riesgo inaceptable para la salud humana o el medio ambiente, de

acuerdo con los criterios y estándares establecidos en el Real Decreto 9/2005, de 14 de enero.

Las principales fuentes de contaminación del suelo son las actividades industriales, mineras y agrícolas. Los suelos afectados por actividades industriales contienen, en general, una amplia variedad de contaminantes en altas concentraciones, como metales pesados, hidrocarburos y contaminantes orgánicos persistentes. Las actividades mineras y metalúrgicas, en particular, ocasionan un impacto significativo en los ecosistemas locales, ya que los metales y metaloides, como As, Cd, Cu, Ni, Pb, Zn y Tl, se acumulan en los suelos y pueden transferirse a través de la cadena trófica, poniendo en riesgo la salud de los organismos vivos (Alloway, 1996; Kabata-Pendias y Mukherjee, 2007). Además, la minería provoca una profunda alteración del paisaje al dejar grandes huecos excavados y generar enormes volúmenes de residuos, destruyendo la topografía, el suelo, la vegetación, el hábitat natural y afectando la calidad del agua y la hidrología de la zona (Arenas-Lago et al., 2014).

En el ámbito agrícola, el uso excesivo de fertilizantes y pesticidas de base metálica añade un componente tóxico al suelo, acumulando elementos potencialmente tóxicos, como As, Cd, Mn, U, y Zn, además de compuestos orgánicos con propiedades pesticidas (Mirsal, 2008). El uso continuado de fertilizantes químicos reduce la materia orgánica y la fertilidad del suelo, y puede contaminar masas de aguas cercanas y alterar la calidad del aire (Pahalvi et al., 2021).

En las últimas décadas, los países desarrollados han implementado legislaciones cada vez más estrictas para limitar el impacto de las actividades potencialmente contaminantes y promover prácticas sostenibles de manejo del suelo. No obstante, los efectos contaminantes de actividades históricas realizadas sin regulación ambiental, hoy en día continúan representando una amenaza persistente para la salud del suelo. Aunque los problemas derivados de la contaminación del suelo están ganando mayor visibilidad y concienciación social, esta forma de degradación sigue siendo una realidad oculta (Rodríguez-Eugenio et al., 2019).

1.3. Los suelos mineros

Los suelos afectados por las actividades mineras están potencialmente contaminados y han sufrido profundas alteraciones en su estructura y en sus propiedades físicas, químicas y biológicas debido a las operaciones de extracción, procesamiento de minerales y generación de residuos.

La degradación física es uno de los efectos más inmediatos de la minería. Se caracteriza por la destrucción de la estructura edáfica, afectando a su estabilidad y a la formación de agregados que facilitan la retención de agua y nutrientes (Rabot et al., 2018). La pérdida de estructura y de cobertura vegetal hace que estos suelos sean más vulnerables a la erosión. Además, el uso de maquinaria pesada provoca una compactación severa que reduce la porosidad del suelo y su capacidad para filtrar agua y permitir el paso de aire.

La degradación química del suelo conlleva una serie de problemas que complican su restauración. La oxidación de sulfuros metálicos como la pirita en contacto con agua y oxígeno produce ácido sulfúrico, dando lugar al drenaje ácido de minas (DAM) (Nordstrom y Alpers, 1997; Blowes et al., 2003). Este proceso ocasiona una acidificación extrema del suelo, limitando la disponibilidad de nutrientes y aumentando la solubilidad de los metales pesados (Grantcharova y Fernández-Caliani, 2022). Los residuos mineros suelen contener EPT (As, Cd, Co, Cu, Pb, Tl y Zn, entre otros) que persisten en el suelo durante largos períodos y representan un riesgo para la salud humana y los ecosistemas. En suelos ácidos, la movilidad de estos contaminantes es alta, lo que facilita su dispersión hacia aguas subterráneas y superficiales, amplificando el impacto ambiental.

La degradación biológica en los suelos mineros disminuye drásticamente su capacidad para sustentar vida. La pérdida del horizonte orgánico superficial y la exposición a condiciones de alta acidez y toxicidad reducen la disponibilidad de nutrientes esenciales. Asimismo, el bajo contenido de arcillas y materia orgánica disminuye la capacidad de intercambio catiónico, afectando la retención de nutrientes (Weil y Brady, 2016). Estas condiciones adversas impactan gravemente la

actividad microbiana, reduciendo la biodiversidad y afectando a toda la cadena trófica, lo que dificulta aún más la restauración de los ecosistemas en las zonas mineras.

En España, la conciencia sobre la conservación del medio natural en entornos mineros se afianzó a finales del siglo XX, dando lugar a normativas como el Real Decreto 2994/1982, de 15 de octubre, que estableció las normas para la restauración de espacios naturales alterados por actividades extractivas. Esta regulación fue pionera en su momento y promovió una minería más responsable, reconociendo la necesidad de restablecer las condiciones ambientales en las áreas afectadas para mitigar sus impactos negativos. Sin embargo, muchas minas fueron abandonadas antes de la entrada en vigor de esta normativa, cuando la restauración ambiental aún no era obligatoria. Esta situación provocó que numerosos emplazamientos mineros quedaran sin intervención, generando focos de contaminación persistente y pasivos ambientales de difícil remediación.

1.4. Tecnosuelos como estratégica de recuperación natural asistida

Actualmente existe un amplio abanico de técnicas fisicoquímicas y biológicas para recuperar suelos contaminados (Meuser, 2013). Los tratamientos físico-químicos incluyen: a) técnicas de aislamiento, como la disposición en vertederos y la estabilización/solidificación; b) técnicas de extracción, como el lavado de suelos y extracción con solventes; y c) técnicas de transformación de contaminantes, como la oxidación y la desorción térmica. Aunque estas técnicas suelen ser rápidas y efectivas, resultan muy costosas y pueden afectar la funcionalidad del suelo. Por otra parte, las técnicas biológicas aprovechan la capacidad de algunos organismos vivos para remediar suelos contaminados a través de procesos como biorremediación y fitorremediación. Estas técnicas son más sostenibles y menos invasivas, aunque requieren más tiempo para lograr resultados óptimos (Aparicio et al., 2022).

Los suelos mineros presentan propiedades singulares que dificultan su recuperación ambiental, como hiperacidez, altas concentraciones de metales pesados, sulfatos y especies alumínicas tóxicas, además de una limitada actividad biológica. Las estrategias de remediación deben abordar tanto a la estabilización química de los contaminantes como la restauración ecológica del suelo. Entre los tratamientos más comunes destaca el uso de enmiendas alcalinas y/o férricas para neutralizar la acidez y reducir la movilidad de los metales pesados, junto con aditivos orgánicos para mejorar la fertilidad del suelo (Adriano et al., 2004; Kumpiene et al., 2008; Bolan et al., 2014; Palansooriya et al., 2020; Fernández-Caliani et al., 2021).

En este contexto, los tecnosuelos han surgido como una alternativa prometedora frente a los métodos tradicionales de restauración minera. Son suelos artificiales, con al menos un 20% de artefactos o materiales generados, modificados o extraídos por el ser humano (WRB, 2006). Esta técnica, impulsada en España por el Prof. Dr. Felipe Macías desde el Laboratorio de Tecnología Ambiental de la Universidad de Santiago de Compostela (LTA-USC), pretende corregir las alteraciones ambientales, aumentar la carga crítica de contaminantes y potenciar la capacidad de autorrecuperación del suelo (Macías, 2001, 2004).

La creciente preocupación social por la contaminación ha incentivado el desarrollo de soluciones sostenibles, como la valorización de residuos para producir tecnosuelos. Estos suelos artificiales, formulados con residuos no peligrosos (RNP), funcionan como sustratos vegetales que imitan a los suelos naturales, contribuyendo a la restauración de ambientes degradados (Macías, 2015). Su desarrollo se alinea con la economía circular, al reincorporar residuos al ciclo productivo para crear nuevos productos o materias primas. Además, cumplen con las políticas europeas de gestión de residuos, como la Directiva 2008/98/CE y la Decisión 96/350/CE, mediante la operación de valorización R10 para mejorar los suelos de forma ecológica o agronómica.

El diseño de tecnosuelos exige un conocimiento exhaustivo de las condiciones del suelo a tratar, los contaminantes presentes, los residuos disponibles y los

procesos biogeoquímicos implicados (Macías, 2004). Para garantizar su eficacia, los tecnosuelos deben tener una textura y estructura óptimas, junto con propiedades físico-químicas y biogeoquímicas que neutralicen procesos contaminantes y estabilicen metales pesados o aniones tóxicos mediante mecanismos como adsorción, complejación o precipitación. Asimismo, deben ser capaces de estabilizar carbono orgánico, aumentar la actividad biológica y promover un desarrollo edafogenético similar al de los suelos naturales (Macías-García et al., 2009a; Macías, 2015; Santos et al., 2014, 2016).

Algunos residuos que actualmente se depositan en vertedero podrían aprovecharse para producir tecnosuelos, reduciendo costes de gestión y tratamiento, e integrándolos en los ciclos biogeoquímicos (Macías et al., 2007). Los tecnosuelos se elaboran con dos tipos de residuos: a) fermentables (orgánicos), que aportan materia orgánica y nutrientes; y b) acondicionadores (inorgánicos), que estabilizan compuestos orgánicos y regulan propiedades como la solubilidad, el pH y el estado redox. Estos materiales deben estar libres de agentes tóxicos, patógenos y olores, y cumplir estrictos estándares que minimicen riesgos ambientales y sanitarios, conforme a la Estrategia de Protección del Suelo en Europa para 2030 (European Commission, 2021).

La aplicación de esta técnica de recuperación natural asistida en emplazamientos mineros degradados ha demostrado ser efectiva para contrarrestar los efectos del DAM, fomentando la regeneración del suelo y mejorando la calidad ambiental del entorno. Un caso emblemático es la mina de Touro, en Galicia. Esta mina de cobre fue explotada entre 1974 y 1988, dejando unas 600 ha de terrenos contaminados. La oxidación de los residuos mineros abandonados generó aguas hiperácidas e hiperoxidantes, con altas concentraciones de sulfatos, Al, Fe, Mn, Cu y Zn. El uso combinado de tecnosuelos especializados y humedales reactivos permitió neutralizar la acidez, aportar nutrientes esenciales y recuperar la actividad biológica del suelo (Macías-García et al., 2009a,b; Macías y Nieto, 2012; Bolaños-Guerrón, 2014; Forján et al., 2015).

Otro ejemplo significativo es la mina de sulfuros metálicos de São Domingo, en Portugal, donde se emplearon tecnosuelos elaborados con residuos mineros mezclados con materiales orgánicos y residuos de cantera de caliza (Santos et al., 2016, 2017). Esto mejoró las características químicas de los lixiviados, aumentó la actividad enzimática y estimuló la germinación y el crecimiento de las plantas. En el distrito minero de Cartagena-La Unión (Murcia), se ensayaron tecnosuelos con biocarbones y residuos de la industrial del mármol, logrando estabilizar metales pesados y mejorar el contenido de carbono orgánico y nitrógeno (Moreno-Barriga et al., 2017). Asimismo, la mina Fe (Salamanca), antigua explotación de uranio, se ha beneficiado del uso de tecnosuelos con propiedades ándicas y eutróficas, que mejoraron significativamente las características físicoquímicas y biológicas de los residuos mineros y sus lixiviados, reduciendo su impacto ecotoxicológico (Arán et al., 2022).

Estos resultados positivos avalan la viabilidad técnica y ambiental de los tecnosuelos, aunque su implementación sigue en fase de investigación y desarrollo, y carece de una regulación estatal específica. Galicia ha sido pionera con la publicación de una instrucción técnica sobre formulación y uso de tecnosuelos, tomando como base la experiencia de la mina de Touro. Se trata de la Instrucción Técnica de Residuos ITR/01/08 (Xunta de Galicia, 2008). Este documento establece los criterios de admisión de los residuos y las características que deben cumplir los tecnosuelos para garantizar su eficacia y seguridad ambiental. Aunque no tiene carácter normativo, esta instrucción técnica se ha convertido en una referencia para ensayos y proyectos de investigación en otras comunidades autónomas.

En definitiva, los tecnosuelos ofrecen múltiples ventajas ambientales y económicas (Macías y Nieto, 2012): permiten valorizar residuos, reciclar nutrientes, secuestrar carbono y sustituir recursos naturales como tierra vegetal. También mejoran las propiedades físicas, químicas y biológicas del suelo, a la vez que inmovilizan contaminantes reduciendo su biodisponibilidad. Esta estrategia proporciona una solución sostenible y rentable para restaurar ecosistemas degradados, al descontaminar suelos y aguas, reciclar nutrientes, estimular la

biomasa y capturar carbono partir de RNP (Santos et al., 2016; Rodríguez-Vila et al., 2016, 2017; Forján et al., 2017; Moreno-Barriga et al., 2017). La eficacia de los tecnosuelos ha sido demostrada no sólo en la recuperación de suelos contaminados, sino también en la cubrición de escombreras y el sellado de vertederos (Fernández-Caliani et al., 2024).

1.5. Justificación, hipótesis de partida y objetivos

En la provincia de Huelva se estima que existen entre 4200 y 4800 hectáreas de suelos afectados directamente por la minería histórica de la FPI (Fernández-Caliani et al., 2009; Grande et al., 2014). Los suelos mineros han superado la carga crítica de acidez y la capacidad amortiguadora de la contaminación, por lo que constituyen un riesgo potencial para la salud de las personas y los ecosistemas.

La remediación de estos suelos presenta costes elevados, debido tanto al grado y tipo de contaminación como a la gran extensión de los terrenos afectados. Hasta el momento, se han llevado a cabo actuaciones puntuales en algunas minas abandonadas para corregir la acidez, aunque se espera que la Junta de Andalucía impulse nuevos proyectos de recuperación en numerosos emplazamientos que soportaron actividades mineras contaminantes en el pasado, de acuerdo con lo previsto en el Reglamento Andaluz de Suelos Contaminados (Junta de Andalucía, 2015). Además, la reactivación que ha experimentado la minería en la FPI durante los últimos años incrementará la necesidad de desarrollar nuevos proyectos de restauración ambiental, conforme a la legislación vigente, lo que justifica la importancia de buscar soluciones tecnológicas innovadoras para la recuperación de estos suelos.

Por otra parte, el centro de gestión de residuos industriales de Nerva (Huelva) gestiona residuos de distinta naturaleza, como escorias, residuos cálcicos, yesos, tierras, escombros, etc. Estos materiales, con códigos LER (Lista Europea de Residuos) autorizados para su depósito directo en vaso de RNP, podrían

aprovecharse como componentes en la elaboración de tecnosuelos a costes económicos y ambientales asumibles. Asimismo, Huelva cuenta con un número considerable de empresas y factorías industriales que generan una amplia variedad de residuos valorizables, algunos de los cuales tienen un alto potencial para la producción de tecnosuelos.

En este contexto, la **hipótesis de partida** de esta tesis plantea que la elaboración de tecnosuelos a partir de RNP locales podría ser una alternativa económicamente viable y ambientalmente sostenible para la recuperación de suelos mineros, siempre que sean de calidad adecuada y se apliquen conforme a las instrucciones técnicas y procedimientos establecidos. Por ello, el estudio se centra en el desarrollo de formulaciones y aplicaciones específicas basadas en la valorización biogeoquímica de RNP, con el objetivo de abordar necesidades concretas, como la regeneración de suelos ácidos de mina en un marco de economía circular y desarrollo sostenible.

Los **objetivos específicos** que se pretenden conseguir con la tesis son los siguientes:

- Caracterizar la persistencia y la dinámica de la contaminación en suelos mineros altamente impactados.
- Revalorizar y reutilizar RNP, actualmente sin salida al mercado y cuya única vía de gestión es el depósito en vertedero, cerrando así su ciclo de vida.
- Desarrollar formulaciones innovadoras de tecnosuelos a partir de estos residuos, como técnica de recuperación natural asistida de suelos ácidos contaminados por actividades mineras.
- Evaluar la eficacia de los tecnosuelos formulados para neutralizar la acidez, estabilizar los elementos traza potencialmente tóxicos y mejorar la fertilidad de los suelos mineros.
- Comprobar que los tecnosuelos ofrecen las condiciones adecuadas para promocionar el crecimiento vegetal, garantizando que su aplicación no genera efectos adversos en el medio ambiente y la salud de las personas.

1.6. Estructura de la tesis

Esta tesis se presenta como un compendio de cinco artículos publicados en revistas internacionales revisadas por pares, e indexadas en el primer o segundo cuartil de alguna de las categorías del Journal Citation Reports (Web of Science):

- **Artículo 1.** *Soil contaminated with hazardous waste materials at Rio Tinto mine (Spain) is a persistent secondary source of acid and heavy metals to the environment.*

  S. Fernández-Landero, J.C. Fernández-Caliani, M.I. Giráldez, E. Morales, C. Barba Brioso, I. González
  Minerals (2023) 456
  DOI: https://doi.org/10.3390/min13040456
  Factor de impacto: JCR 2,5 (Q2) – CiteScore 4,1 (Q2)
  Número de citas: 7 (WoS) – 9 (Scopus) – 13 (Google Académico)

- **Artículo 2.** *Phytoaccumulation of trace elements (As, Cd, Co, Cu, Pb, Zn) by Nicotiana glauca and Euphorbia segetalis growing in a Technosol developed on legacy mine wastes (Domingo Rubio wetland, SW Spain).*

  C. Barba-Brioso, P.J. Hidalgo, **S. Fernández-Landero**, M.I. Giráldez, J.C. Fernández-Caliani
  Environmental Geochemistry & Health 45 (2023) 9541-9557
  DOI: https://doi.org/10.1007/s10653-023-01523-w
  Factor de impacto: JCR 3,2 (Q2) – CiteScore 8,0 (Q1)
  Número de citas: 5 (WoS) – 6 (Scopus) – 8 (Google Académico)

- **Artículo 3.** *Long-term sustainability of marble waste sludge in reducing soil acidity and heavy metal release in a contaminated mine Technosol.*

  J.C. Fernández-Caliani, M.I. Giráldez, **S. Fernández-Landero**, C. Barba-Brioso, E. Morales
  Applied Sciences 12 (2022) 6998
  DOI: https://doi.org/10.3390/app12146998
  Factor de impacto: JCR 2,7 (Q2) – CiteScore 5,3 (Q1)
  Número de citas: 9 (WoS) – 11 (Scopus) – 16 (Google Académico)

- **Artículo 4.** *Unveiling a Technosol-based remediation approach for enhancing plant growth in an iron-rich acidic mine soil from the Rio Tinto Mars analog site.*

  J.C. Fernández-Caliani, **S. Fernández-Landero**, M.I. Giráldez, P.J. Hidalgo, E. Morales
  Science of the Total Environment 922 (2024) 171217
  DOI: https://doi.org/10.1016/j.scitotenv.2024.171217
  Factor de impacto: JCR 9.8 (Q1) – CiteScore 16.8 (Q1)
  Número de citas: 3 (WoS) – 3 (Scopus) – 3 (Google Académico)

- **Artículo 5.** *Successful plant growth in acid mine drainage-impacted soil using pot-based experiments with waste amendments.*

  S. Fernández-Landero, J.C. Fernández-Caliani, M.I. Giráldez, P.J. Hidalgo, E. Morales
  Land Degradation & Development 922 (2024) 171217
  DOI: https://doi.org/10.1002/ldr.5211
  Factor de impacto: JCR 4.7 (Q2) – CiteScore 7.2 (Q1)
  Número de citas: 1 (WoS) – 1 (Scopus) – 1 (Google Académico)

Los artículos tienen una clara **coherencia temática y metodológica.** Todos ellos comparten un marco conceptual centrado en la contaminación de suelos generada por la minería metálica, con énfasis en el DAM y la liberación de EPT, y abordan la remediación de suelos en un contexto geo-ambiental unificado. A través de diversas metodologías, los estudios convergen en la problemática común de la contaminación de suelos por metales pesados, explorando el uso de tecnosuelos derivados de RNP como solución sostenible.

Los estudios emplean una amplia gama de metodologías (análisis químicos y mineralógicos, ensayos de lixiviación, modelado de especiación acuosa, experimentación en campo y en macetas, evaluación de la respuesta vegetal) que, en conjunto, se complementan entre sí para ofrecer una visión integral del problema y de las soluciones.

Una vez presentado en esta introducción general (**Capítulo 1**) el marco conceptual y los objetivos de la tesis, en el **Capítulo 2** se describe el área de estudio,

contextualizando históricamente la actividad minera y sus impactos ambientales. En el **Capítulo 3** se detallan los métodos y técnicas empleados en los diferentes trabajos, mientras que los resultados más relevantes de los artículos se sintetizan y discuten en el **Capítulo 4**. Por último, en el **Capítulo 5** se exponen las conclusiones generales de la tesis y se plantean nuevas líneas de investigación actualmente en desarrollo.

En conjunto, estos artículos conforman un cuerpo de trabajo coherente, complementario y científicamente relevante, no solo en términos de promoción general del conocimiento sino también ofrecen un potencial de transferencia de resultados, aportando soluciones prácticas para la valorización de RNP, la gestión sostenible de pasivos mineros y la restauración ecológica de entornos degradados.

2. ÁREA DE ESTUDIO

2.1. Localización geográfica

El área de estudio comprende tres emplazamientos diferentes de la provincia de Huelva (Fig. 1): el estero de Domingo Rubio, un humedal costero asociado al estuario de Huelva, y las cuencas mineras de Riotinto y Tharsis, en la comarca de El Andévalo.

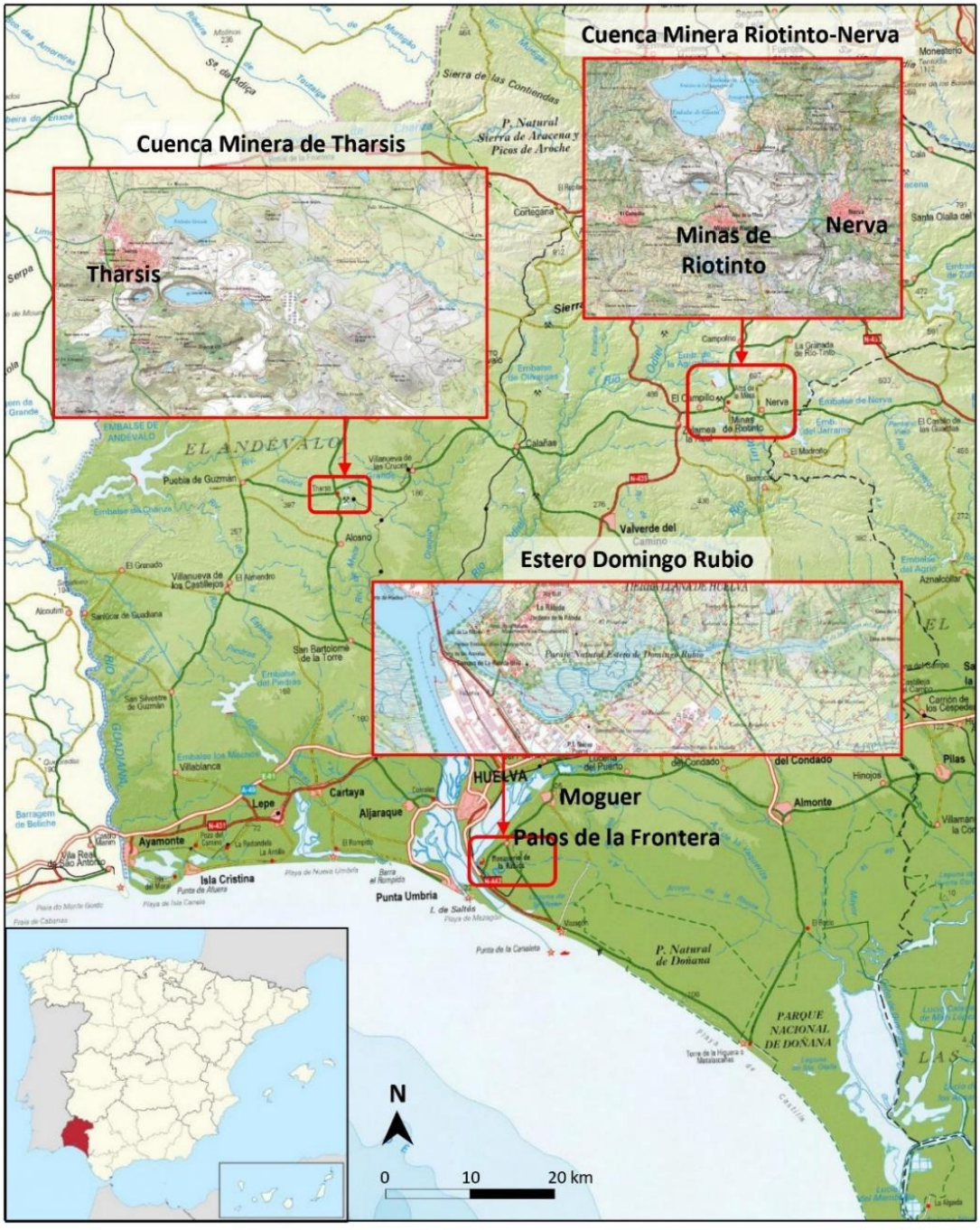

Fig. 1. Mapa de localización de los emplazamientos estudiados en la provincia de Huelva. Elaboración propia a partir del visor Iberpix del Instituto Geográfico Nacional.

2.2. Rasgos fisiográficos y edafológicos

La provincia de Huelva, como el resto de Andalucía, presenta un clima mediterráneo templado, pero existen diversos factores como la disposición del relieve y la altimetría que establecen ciertas zonaciones bioclimáticas. Según la Red de Información Ambiental de Andalucía (REDIAM), la unidad territorial Litoral Atlántico, donde se encuadra el estero de Domingo Rubio, tiene un clima mediterráneo oceánico, caracterizado por unas temperaturas medias anuales entre 17 y 19 °C, y precipitaciones medias anuales de 500 a 700 mm. Por otro lado, la comarca minera de El Andévalo se integra dentro de la unidad Sierra Morena Occidental, donde prevalece un clima mediterráneo de influencia continental, con temperaturas medias más bajas (12-17 °C) y precipitaciones medias más elevadas (400-1000 mm).

Desde el punto de vista hidrográfico, las áreas mencionadas se encuadran dentro de la Demarcación Hidrográfica del Tinto, Odiel y Piedras, con una extensión total de 4955 km^2. En la zona más septentrional de la demarcación (Sierra de Aracena), se alcanzan cotas de 900 m.s.n.m., que desciende hasta el litoral. La altitud varía entre 200 y 600 m.s.n.m. en Minas de Riotinto, 200-400 en Tharsis y 0-10 en el estero de Domingo Rubio (Junta de Andalucía, 2023).

En el estero de Domingo Rubio, la dinámica de los procesos de los aportes fluviales junto con las corrientes de marea, han formado un paisaje de marisma con caños y esteros. Sus suelos se clasifican edafológicamente como Fluvisol sálico, Fluvisol gleyco, Regosol esquelético, Regosol arénico, Arenosol calcárico y Tecnosol espólico. Presentan valores de pH medio ligeramente ácidos, aunque se pueden encontrar puntos con acidez extrema en los Tecnosoles (Barba-Brioso, 2011). Los suelos dominantes en los distritos mineros de Rio Tinto y Tharsis se clasifican como Cambisol eútrico, Regosol eútrico, Leptosol úmbrico, Luvisol crómico y Luvisol órtico, según el Portal Ambiental de Andalucía (Junta de Andalucía, 2023).

El Andévalo se caracteriza por un relieve ondulado, dominado por suaves colinas cubiertas de matorral mediterráneo (jaras, lentiscos y brezos), y algunas

dehesas de encinas y alcornoques dedicadas a usos agropecuarios tradicionales como la cría de ganado y la producción de corcho. En algunas zonas también se encuentran repoblaciones de pinos y eucaliptos. La actividad minera ha modificado considerablemente el paisaje, transformándolo con la presencia de grandes escombreras, cortas a cielo abierto, infraestructuras industriales abandonadas y suelos degradados, con una vegetación escasa y adaptada a condiciones extremas, como *Erica andevalensis*. Los suelos predominantes son Leptosoles líticos, es decir suelos delgados, ácidos y pobres en nutrientes, derivados de las rocas metamórficas y volcano-sedimentarias que conforman el sustrato geológico de la región.

El estero de Domingo Rubio forma parte de un conjunto de zonas húmedas en la desembocadura de los ríos Tinto y Odiel, y está integrado en la Red de Espacios Naturales Protegidos de Andalucía por su alto valor ecológico. Además, está incluido en la Red Natura 2000 como Lugar de Importancia Comunitaria (LIC) y Zona de Especial Protección para las Aves (ZEPA). El humedal comprende dos tramos con características ambientales claramente diferenciadas: a) una zona de marisma, atravesada por un canal mareal meandriforme y formada por Fluvisoles salinos con vegetación halófila como *Salicornia* y *Spartina*; y b) una zona lacustre de agua dulce, creada artificialmente por el represamiento del arroyo, con vegetación acuática y ribereña. Este ecosistema alberga una avifauna rica y diversa, sirviendo de refugio para numerosas aves migratorias (Junta de Andalucía, 2005).

Sin embargo, el estero de Domingo Rubio está sometido a múltiples amenazas ambientales, como la contaminación hidroquímica difusa del estuario de Huelva y los aportes contaminantes del polígono industrial del puerto exterior de Huelva y de las explotaciones agrícolas cercanas (Madejón et al., 2009; Barba-brioso et al., 2010). Además, existen focos de contaminación puntual, como una escombrera de pirita abandonada en las proximidades de la marisma. La oxidación de la pirita ha desencadenado un proceso de acidificación del suelo y lixiviación de metales pesados, que pone en riesgo el ecosistema del humedal (Barba-Brioso et al., 2021).

2.3. Marco geológico

Desde el punto de vista geológico, el área de estudio abarca dos contextos bien diferenciados. Por un lado, el estero de Domingo Rubio se localiza en el sector noroccidental de la Cuenca del Guadalquivir y, por otro lado, los distritos mineros de Rio Tinto y Tharsis se ubican en la Zona Surportuguesa del Macizo Ibérico, concretamente en el dominio de la Faja Pirítica Ibérica (FPI) (Fig. 2).

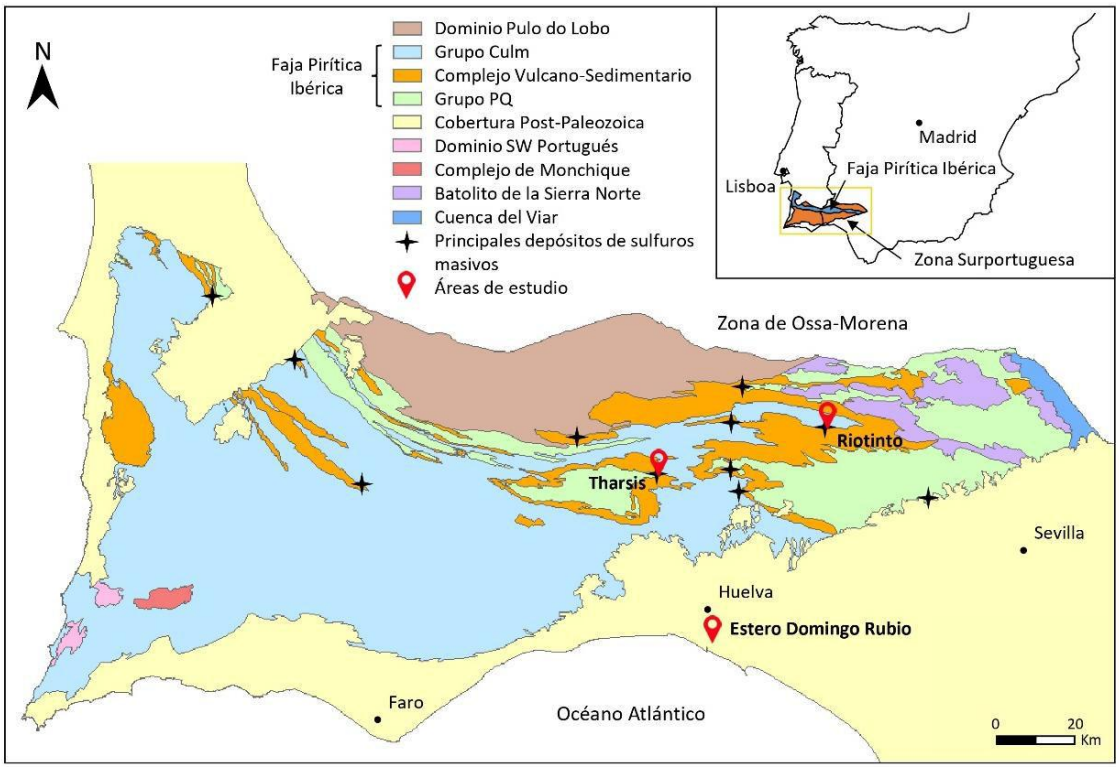

Fig. 2. Mapa geológico de la Zona Surportuguesa (modificado de Mapa Geológico de España, 1:1.000.000) y localización de los emplazamientos estudiados.

El estero de Domingo Rubio es un pequeño valle inundable, conectado al estuario de Huelva a través de un canal mareal meandriforme que discurre entre colinas rojizas constituidas por limos, arenas y gravas plio-pleistocénicas en su margen derecha, y por formaciones de dunas estables en su margen izquierdo. Estas dunas separan al estero del canal principal del estuario de Huelva, protegiéndolo de la acción directa del oleaje.

La FPI es una de las provincias metalogénicas más importantes a nivel mundial, con más de 1700 Mt de sulfuros masivos que presentan leyes medias de 1,2% Cu, 1% Pb y 3% Zn (Ruiz de Almodóvar y Sáez, 1992; Tornos, 2006; Sáez et al., 2024). Está compuesta por tres grandes unidades litoestratigráficas (Schermerhorn, 1971): el Grupo de Pizarras y Cuarcitas (PQ), de edad Devónico medio a superior; el Complejo Vulcano-Sedimentario (CVS), del Devónico superior al Carbonífero inferior; y el Grupo Culm, formado por una secuencia turbidítica de pizarras y areniscas del Carbonífero inferior a medio. Los depósitos de sulfuros masivos, compuestos principalmente por pirita y cantidades menores de calcopirita, esfalerita y galena, se encuentran en el CVS, donde forman masas estratiformes concordantes con las rocas encajantes (rocas volcánicas félsicas o pizarras negras).

Los distritos mineros de Rio Tinto y Tharsis son los más importantes de la FPI, tanto por el volumen de sus yacimientos como por su historial minero. El distrito de Rio Tinto, con más de 500 Mt de pirita (masas San Dionisio, Filón Sur, Filón Norte y Planes-San Antonio) y más de 2000 Mt de stockwork mineralizado (Cerro Colorado), constituye una de las mayores concentraciones de sulfuros del mundo (Ribeiro de Mello et al., 2022). Por su parte, el distrito de Tharsis también cuenta con depósitos de sulfuros masivos que superan 100 Mt, entre los que destacan los cuerpos mineralizados de Filón Norte, Filón Sur, Filón Centro y Sierra Bullones.

2.4.Breve historial minero

El Andévalo es una de las comarcas mineras más importantes del mundo, con una tradición que se extiende desde tiempos prehistóricos hasta la actualidad. Las primeras evidencias de actividad minera y metalúrgica datan de la Edad del Cobre (Pérez Macías, 1998), aunque los períodos de mayor auge tuvieron lugar durante la época romana (siglos I-II d.C.) y, especialmente, con la segunda Revolución Industrial de finales del siglo XIX.

En particular, Riotinto fue uno de los distritos mineros y metalúrgicos más destacados del mundo antiguo (Salkield, 1987). Los tartesios extraían cobre y plata para la fabricación de herramientas y objetos ornamentales, y comerciaban con fenicios y otros pueblos mediterráneos. Los romanos desarrollaron métodos avanzados de extracción y fundición, convirtiendo las minas de Huelva en importantes centros productores de cobre, plata y oro. Tras la caída del imperio romano en el siglo IV, la minería entró en declive y permaneció casi inactiva hasta el siglo XIX. Con la Revolución Industrial, las minas de Huelva despertaron el interés internacional debido a la creciente demanda de cobre y pirita. A finales del siglo XIX, las compañías británicas The Tharsis Sulphur and Copper y The Rio Tinto Company Limited revitalizaron la actividad minera, situando nuevamente a la provincia como un referente mundial en la producción de minerales (Pinedo, 1963).

La minería en Rio Tinto no solo se centró en la extracción de minerales, sino también en procesos metalúrgicos que evolucionaron con el tiempo, reflejando los avances tecnológicos de cada época. Durante la etapa británica, se emplearon dos métodos de obtención de cobre: hidrometalurgia (vía húmeda) y pirometalurgia (vía seca).

Los minerales de baja ley en cobre (<2-3%) eran beneficiados por cementación natural y/o artificial (Delgado, 2023). Estos procesos hidrometalúrgicos transformaban el cobre de los sulfuros insolubles en sulfato de cobre soluble en agua, y se precipitaba por intercambio iónico con hierro para su posterior afino. En la cementación natural, se formaban montones de minerales cobrizos regados con aguas ácidas durante varios años, lo que provocaba la oxidación de la pirita generando soluciones enriquecidas en cobre que hacían precipitar en canales de cementación con chatarra de hierro. Para acelerar el proceso, se recurrió a la cementación artificial, consistente en la oxidación forzada de la pirita mediante calcinación al aire libre en montones llamados *teleras*. El mineral calcinado se lixiviaba con aguas ácidas en pilones o diques, y las soluciones resultantes se conducían a los canales de cementación para obtener la cáscara de cobre.

Los minerales ricos en cobre se trataban mediante procesos pirometalúrgicos, que consistían en oxidar los sulfuros con aire caliente, liberando el cobre y formando una escoria fayalítica (silicato de hierro) que se amontonaba en escombreras junto a las fundiciones. En Rio Tinto, las operaciones pirometalúrgicas continuaron hasta 1970, cuando la fundición de cobre se trasladó al Polo Químico de Huelva.

A finales del siglo XX, todas las minas cerraron debido a la crisis de la pirita como fuente de azufre para la fabricación de ácido sulfúrico y la caída de los precios del cobre. Sin embargo, en los últimos años, la minería de Huelva ha resurgido gracias a la creciente demanda de minerales en industrias tecnológicas, energías renovables y para la electrificación del transporte. Actualmente, las explotaciones en yacimientos como Aguas Teñidas, Sotiel y Magdalena se centran en los depósitos de sulfuros masivos polimetálicos (Cu-Pb-Zn), mientras que Rio Tinto se enfoca en el stockwork de cobre.

2.5. Impacto de la minería en el suelo

La intensa actividad minera y metalúrgica desarrollada en la FPI a lo largo de su historia ha dejado una profunda huella de degradación ambiental en la región (Fernández-Caliani, 2008, 2022), originando problemas como la contaminación persistente de suelos y aguas, la acidificación de ríos y la pérdida de biodiversidad.

La excavación de grandes cortas a cielo abierto ha causado una pérdida irreversible de suelo natural y generado enormes cantidades de residuos mineros, acumulados en terreros, diques, balsas y escombreras (Grande et al., 2014). Estos residuos liberan aguas ácidas cargadas de metales pesados hacia los suelos del entorno (Romero-Baena et al., 2021) y emiten partículas contaminantes a la atmósfera (Castillo et al., 2013; Fernández-Caliani et al., 2013). Entre los materiales residuales con mayor potencial contaminante destacan la pirita cruda y lixiviada, las cenizas de tostación, las escorias, los lodos de los procesos de concentración y los estériles de mina (Romero et al., 2011; Cánovas et al., 2021).

Aunque los datos disponibles sobre los residuos mineros y el DAM en la FPI son abundantes (e.g. Galán et al., 2003; Sánchez-España et al., 2006; Sarmiento et al., 2009; Olías et al., 2010), los estudios centrados en los suelos mineros son relativamente escasos, a pesar de su relevancia. Según Fernández-Caliani et al., (2009), estos suelos son sistemas extremadamente ácidos, con una escasa capacidad de intercambio iónico efectiva, bajos niveles de materia orgánica y nutrientes esenciales, y una clase textural desequilibrada. Además, contienen fases portadoras de metales pesados, principalmente pirita y sus productos derivados de oxidación como jarosita y oxi-hidróxidos de hierro, y carecen de carbonatos lo que contribuye a su elevado potencial de acidificación neto.

En consecuencia, los suelos mineros presentan una elevada carga de elementos traza contaminantes, especialmente As, Cu, Pb y Zn (Chopin y Alloway, 2007; Fernández-Caliani et al., 2009), cuyas concentraciones superan ampliamente los valores de fondo regional (Galán et al, 2008; Martín-Méndez et al., 2023), y los niveles genéricos de referencia (NGR) para suelos de Andalucía (Junta de Andalucía, 2015). Su limitada capacidad para neutralizar la acidez y fijar contaminantes agrava su peligrosidad ambiental. Esta problemática es particularmente preocupante en los suelos agrícolas y urbanos cercanos a las zonas mineras, donde una fracción significativa de los metales más móviles podría estar biodisponible y transferirse a la cadena trófica.

En los suelos agrícolas del entorno minero, aunque los niveles de contaminación son similares a los de los suelos mineros (López et al., 2008), los metales se encuentran estabilizados por procesos de precipitación, adsorción y fijación en el complejo de cambio. Los metales analizados en las hortalizas no suelen alcanzar los niveles fitotóxicos (Madejón et al., 2011). Sin embargo, en algunos huertos próximos a las minas, el riesgo para la salud humana supera el umbral legalmente establecido (Gabari y Fernández-Caliani, 2017; Fernández-Caliani et al., 2019).

En los suelos urbanos de Minas de Riotinto, las concentraciones de As y Pb se mantienen dentro de los valores de fondo regional, aunque en algunos puntos superan los NGR, generando un riesgo potencial para la salud de los residentes (Parviainen et al., 2022).

En definitiva, los espacios mineros abandonados de la FPI y los suelos de su entorno están contaminados por EPT, y requieren la adopción de medidas de recuperación ambiental que reduzcan los niveles de riesgo a valores tolerables para la proteger la salud humana y los ecosistemas. Aunque no existe una legislación que obligue a restaurar las minas históricas abandonadas, en la FPI se han realizado intervenciones puntuales para corregir la acidez del suelo y revegetar algunas minas, como Poderosa, Castillo de las Guardas y Tharsis (Sáiz y Ceacero, 2008; Madejón et al., 2021), con el apoyo de fondos europeos (FEDER). La aplicación de enmiendas alcalinas y orgánicas ha demostrado mejorar la calidad del suelo en estos enclaves mineros (Fernández-Caliani y Barba-Brioso, 2010; Fernández-Caliani et al., 2021). Sin embargo, la mayoría de las minas abandonadas permanecen en un estado de deterioro ambiental alarmante.

3. METODOLOGÍA

El plan de trabajo diseñado para alcanzar los objetivos planteados comprende diversas actividades de campo, laboratorio y gabinete (Fig. 3).

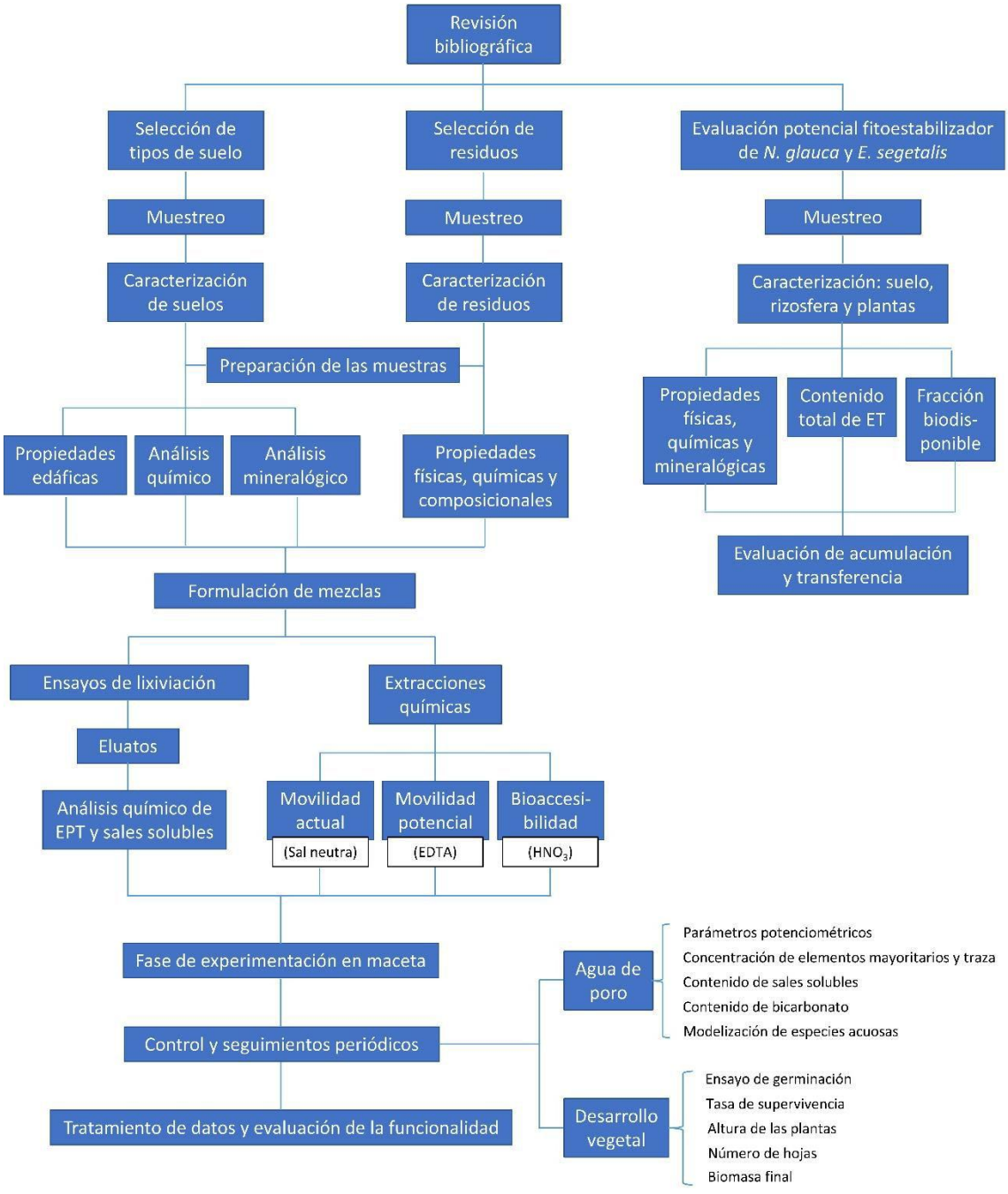

Fig. 3. Diagrama de flujo metodológico.

3.1. Revisión del estado de la técnica

En primer lugar, se realizó una revisión bibliográfica para conocer la situación actual de la técnica y sus últimos avances. Esta revisión permitió adquirir un conocimiento exhaustivo de los antecedentes relacionados con la naturaleza y el comportamiento de los materiales empleados en la elaboración de tecnosuelos, así como de los resultados obtenidos en sus diversas aplicaciones.

3.2. Materiales

3.2.1. Selección y muestreo de los suelos a tratar

Los suelos mineros se caracterizan por una gran heterogeneidad química, mineralógica y textural. Para prevenir errores derivados de tanta variabilidad, se realizó un reconocimiento de campo con el objetivo de identificar los diversos procesos y residuos minero-metalúrgicos que podrían ser fuentes de contaminación para los suelos (Fig. 4).

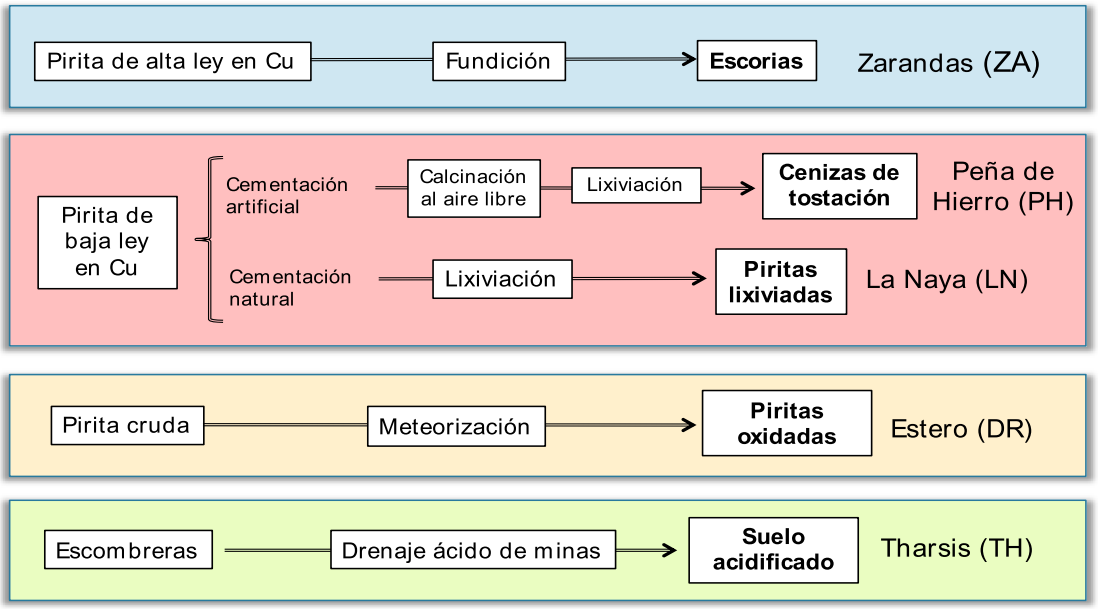

Fig. 4. Tipología de contaminantes de los suelos seleccionados para este estudio, con indicación de las fuentes de contaminación y de los procesos involucrados en su generación.

Este estudio preliminar permitió seleccionar cinco tipos de suelos potencialmente contaminados por EPT procedentes de las actividades mineras y metalúrgicas desarrolladas en su entorno (Tabla 1).

Tabla 1

Tipología de los suelos seleccionados

Suelo	Contaminante	Ubicación	Referencia
S1	Residuos de pirita abandonados	Estero de Domingo Rubio (estuario de Huelva)	DR
S2	Cenizas de tostación de pirita	Peña de Hierro (Nerva)	PH
S3	Escorias de cobre	Fundición Piritas, Zarandas (Minas de Riotinto)	ZA
S4	Sulfuros lixiviados	Zona de cementación de La Naya (Minas de Riotinto)	LN
S5	Drenaje ácido de minas	Filón Norte (Minas de Tharsis)	TH

En cada uno de estos emplazamientos se seleccionaron 3 puntos de muestreo representativos de los suelos (Fig. 5).

En cada punto se tomaron cinco muestras, compuestas a su vez por cinco submuestras cada una (una central y cuatro perimetrales) para asegurar una mayor representatividad. El muestreo se realizó con una barrena Edelman, extrayendo los primeros 20 cm de suelo (Fig. 6).

Las muestras fueron secadas al aire, desagregadas suavemente, homogeneizadas y tamizadas a 2 mm, y una alícuota fue molida en un mortero de ágata y tamizada por 63 µm para su análisis químico.

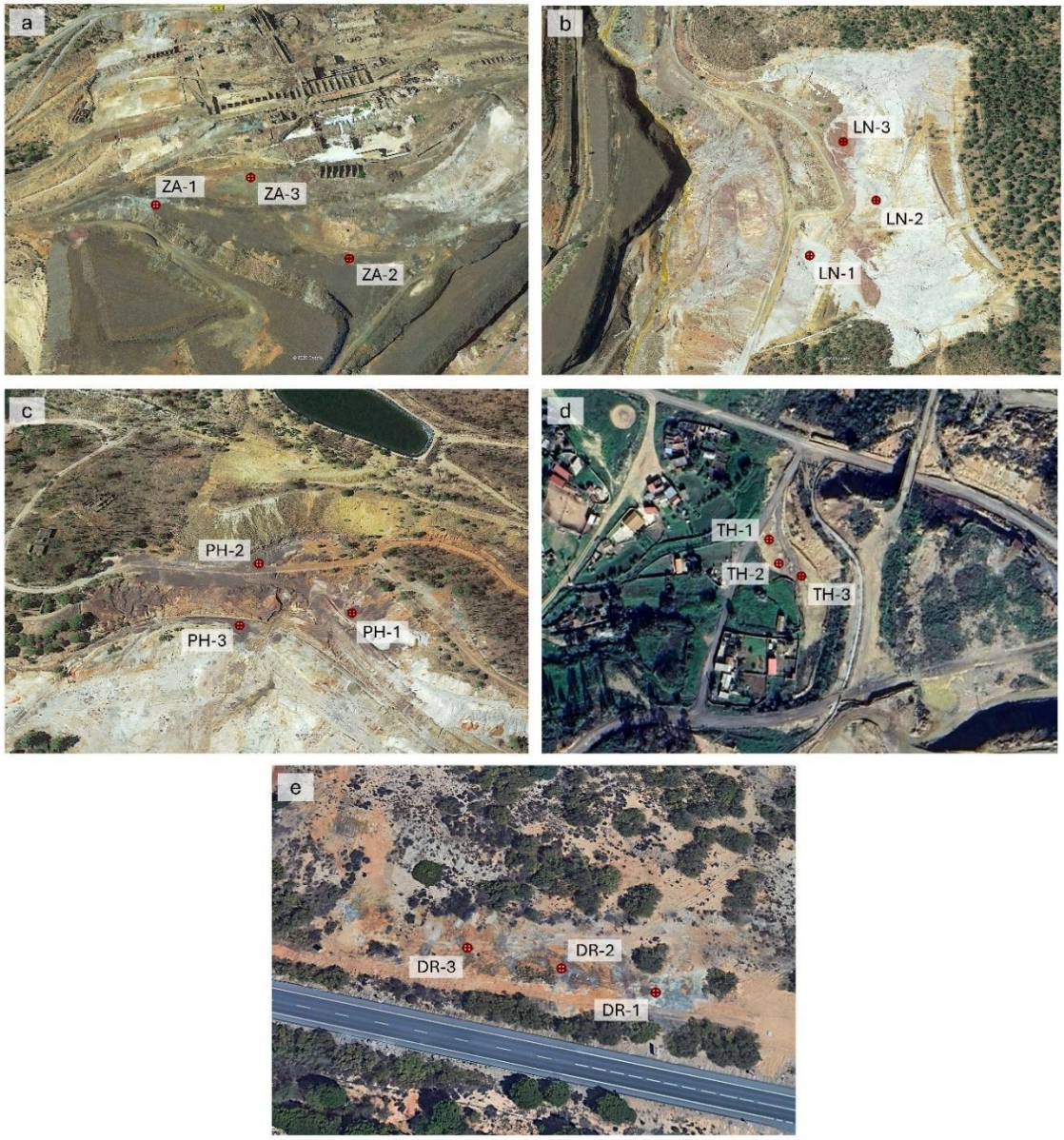

Fig. 5. Localización de los puntos de muestreo en las zonas de estudio: a) antigua Fundición de Piritas en Zarandas (Minas de Riotinto); b) antiguos terreros de cementación natural en La Naya (Minas de Riotinto); c) antigua plaza de calcinación de pirita en Peña de Hierro (Nerva); d) escombrera de Filón Norte (Tharsis); y e) residuos de pirita cruda en el estero de Domingo Rubio (Palos de la Frontera). Imágenes tomadas de Google Earth.

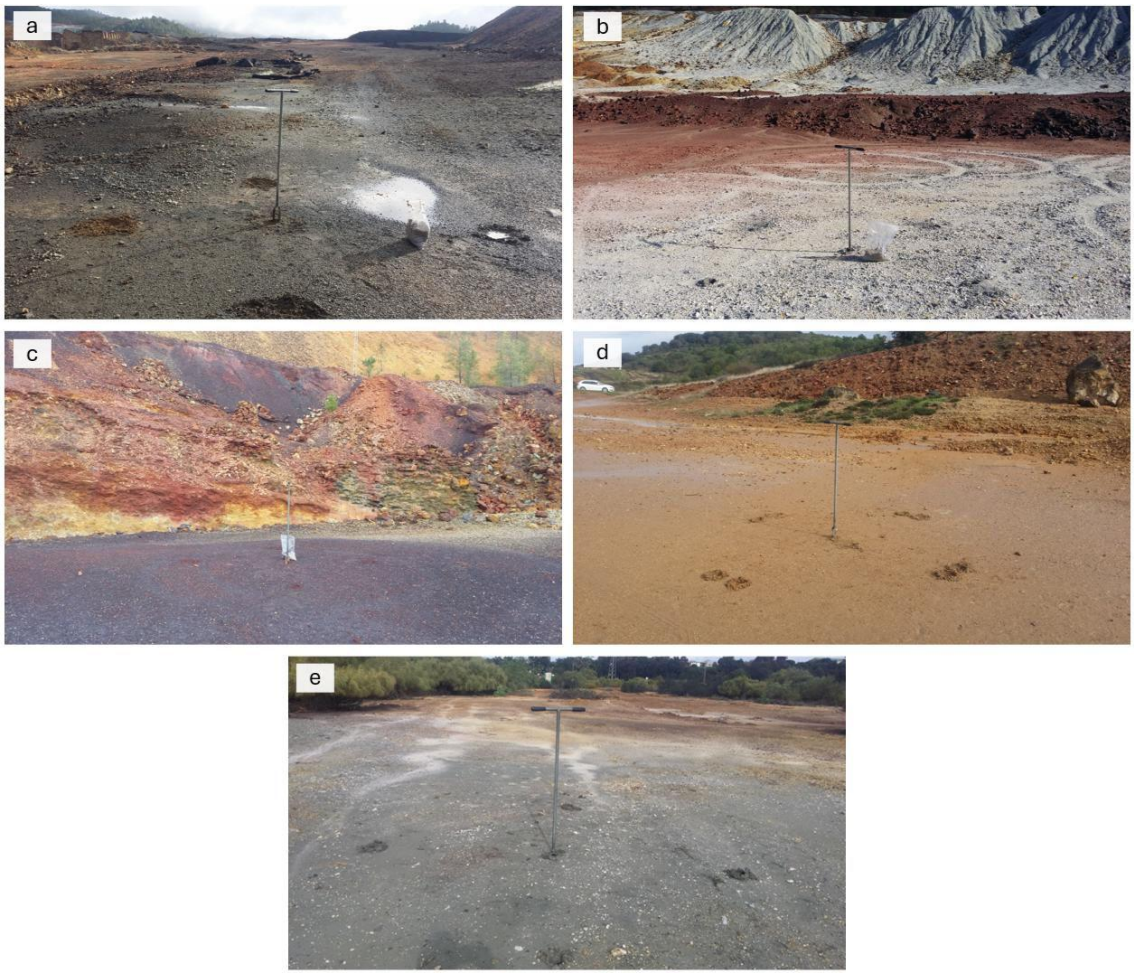

Fig. 6. Toma de muestras de los suelos contaminados por: a) escorias de cobre; b) sulfuros lixiviados; c) cenizas de tostación de pirita; d) drenaje ácido de minas; y e) pirita cruda.

Además, se recolectaron muestras de plantas (*Nicotiana glauca* y *Euphorbia segetalis*) en el suelo del estero de Domingo Rubio contaminado con residuos piríticos (Fig. 7), con el fin de analizar las concentraciones de metales pesados en raíces, tallos y hojas. Las muestras se lavaron y sonicaron con agua destilada, se secaron a 40 °C durante 5 días y se molieron hasta un tamaño de 0,5 mm.

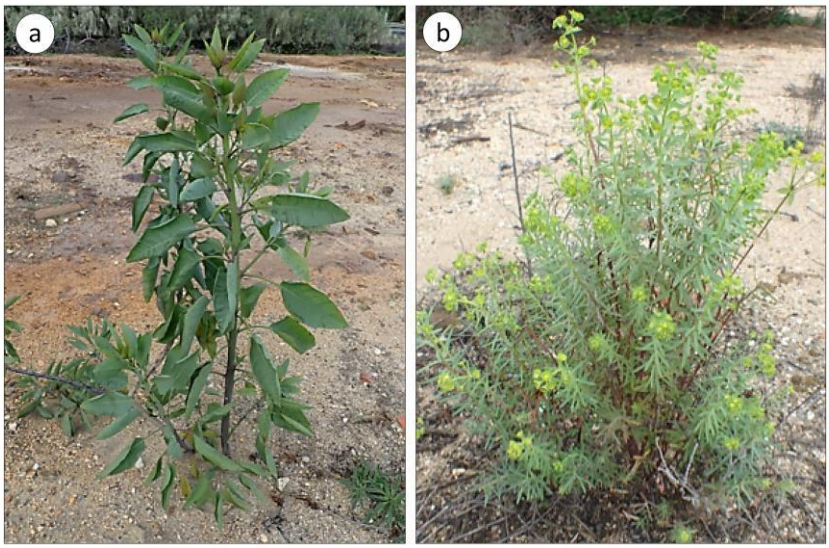

Fig. 7. Aspecto de campo de la vegetación desarrollada en el suelo contaminado del estero de Domingo Rubio (a) *Nicotiana glauca* y (b) *Euphorbia segetalis*.

3.2.2. Selección y muestreo de los residuos empleados

En el proceso de preselección de los RNP adecuados para su aplicación funcional en tecnosuelos, se tomaron en consideración los siguientes criterios: 1) cumplen las especificaciones técnicas y ambientales requeridas (sus códigos LER están incluidos en el anexo 1 de la Xunta de Galicia (2008); 2) se gestionan regularmente en el centro de gestión de residuos industriales de Nerva (Huelva); y 3) presentan un comportamiento aceptable en los ensayos de lixiviación realizados por la empresa gestora (Ditecsa Soluciones Medioambientales, DSM).

Finalmente, se seleccionaron ocho tipos de RNP (Tabla 2), cuya composición y resultados en los ensayos de lixiviación proporcionados por la empresa demostraron su potencial como ingredientes de tecnosuelos.

El muestreo de los residuos se ajustó a la norma UNE-EN 14899:2007, y la preparación de las muestras fue similar a la de los suelos, a excepción de los lodos, que se secaron en estufa a 40 °C.

Tabla 2

Relación de residuos no peligrosos seleccionados

Residuo	Código LER	Descripción	Origen o procedencia
R1	010413	Lodos del corte y aserrado del mármol	Planta de elaboración de mármol
R2	030311	Lodos de depuradora	Planta de biomasa
R3	190902	Lodos de la clarificación del agua	Estación de tratamiento de agua potable (ETAP)
R4	050110	Lodos biológicos	Tratamiento biológico de efluentes industriales
R5	100202	Escorias blancas	Industria del acero
R6	100903	Escorias de horno	Fundición de hierro
R7	061101	Yesos rojos	Producción de pigmentos de dióxido de titanio
R8	190112	Escorias de incineradora	Incineración de residuos sólidos urbanos

3.3. Métodos analíticos

3.3.1. Caracterización de los suelos mineros

A continuación, se describen brevemente los métodos y técnicas analíticas utilizadas para determinar las propiedades edáficas y la composición del suelo.

- Análisis granulométrico

Las muestras se pasaron por un tamiz de 2 mm para separar y cuantificar la fracción más gruesa (pedregosidad). La clasificación textural del suelo se determinó en función de las proporciones de arcilla, limo y arena. La distribución del tamaño de las partículas se midió por difracción láser con un analizador Mastersizer 2000 (Malvern Instruments).

- Análisis mineralógico

La composición mineralógica de las fases mayoritarias se determinó por difracción de rayos-X (DRX) con un difractómetro BRUKER modelo D8I 90 Advance A25, usando radiación Kα de Cu (30 mA, 40 kV). La abundancia semicuantitativa de los minerales se estimó aplicando factores de intensidad que ponderan el área de los picos de las reflexiones diagnósticas (Kahle et al., 2002).

Para la identificación de minerales accesorios portadores de elementos pesados y de fases amorfas, se utilizó un microscopio electrónico de barrido de emisión de campo (JEOL JSM-IT500HR) equipado con un espectrómetro de energías dispersivas de rayos-X (Oxford Instruments X-Max EDS), operando a alto vacío (2,5 nA, 20 kV).

Además, se cuantificó la composición elemental de fases seleccionadas en mediante microanálisis de sonda electrónica (JEOL JXA-8200 SuperProbe). Las condiciones instrumentales fueron: voltaje de aceleración a 20 kV, corriente de haz a 20 nA y diámetro de haz hasta 5 mm.

- pH, Eh y conductividad eléctrica

El pH en agua, el potencial redox (Eh) y la conductividad eléctrica (CE) se midieron por el método potenciométrico en una suspensión suelo:agua (1:2,5 m/v). Las suspensiones se agitaron durante 5 min y se dejaron reposar media hora antes de realizar las mediciones, obteniendo así valores representativos de la acidez activa o actual, de las condiciones redox y de la salinidad del suelo.

Para evaluar la acidez potencial o intercambiable, se determinó el pH en una disolución 1M de KCl (pH_{KCl}) con la misma relación suelo/solución. Este parámetro cuantifica los protones adsorbidos en las partículas del suelo que pueden ser desplazados mediante intercambio iónico con una solución salina neutra.

Asimismo, para evaluar el efecto de la oxidación de los sulfuros, se determinó el pH de oxidación (pH_{OX}). Para ello, las muestras se trataron con H_2O_2 al 30% (pH ajustado a 5,5) en una relación suelo/solución de 1:20 (m/v) y se agitaron hasta completar la reacción de oxidación (Urrutia et al., 1992).

- Fósforo (P) asimilable

El P disponible para las plantas se determinó por el método Olsen (Olsen y Sommers, 1982), usando una solución 0,5 M de $NaHCO_3$ a pH 8,5 en una relación suelo-solución de 1:20 (m/v). La concentración de P en el extracto se midió por colorimetría en un espectrofotómetro UV-Vis GENESYS 10UV.

- Carbono (C), nitrógeno (N) y azufre (S) totales

Las concentraciones totales de C, N y S se cuantificaron con un analizador elemental ELTRA CHS-580A. Este método se basa en la oxidación completa de la muestra por combustión a alta temperatura en atmósfera de oxígeno purificado. Los gases liberados (CO_2, SO_2 y NO_X) se determinaron por espectroscopía infrarroja.

- Carbono inorgánico (C_{INORG}), orgánico (C_{ORG}) y materia orgánica (MO)

La cuantificación de la MO se abordó calcinando las muestras a 400 °C durante 16 h (Nelson y Sommers, 1996). El C_{ORG} se obtuvo restando el C_{INORG} del carbono total. Finalmente, la concentración de MO se estimó indirectamente multiplicando el C_{ORG} por un factor de conversión (1,72).

- Azufre jarosítico (S_{JAR}) y azufre pirítico (S_{PYR})

La extracción de S_{JAR} se realizó con una solución de oxalato de amonio 0,2 M a pH 3 (Dold, 2003). Las muestras fueron molidas y tamizadas a un tamaño de partícula inferior a 250 µm. Posteriormente, se preparó una suspensión sólido-líquido de 1:50 (m/v), que fue agitada a 80 °C durante 2 h. El sobrenadante se separó por centrifugación (5000 rpm, 10 min) y se filtró (0,45 µm) para su análisis.

El residuo sólido se utilizó para extraer el S_{PYR} mediante la adición de HNO_3 6M en una relación sólido-líquido de 1:15 (m/v), siguiendo el método ASTM D2492-02. La suspensión se incubó a 120 °C durante 30 min, con agitación manual periódica. Finalmente, el sobrenadante se separó por centrifugación y se filtró para su análisis.

Las concentraciones de S_{JAR} y S_{PYR} se cuantificaron mediante espectroscopía de emisión óptica de plasma acoplado inductivamente (ICP-OES), utilizando un instrumento Agilent 5110.

- Potencial de acidez total y acidez neta

Para predecir el riesgo de drenaje ácido de los suelos se aplicaron dos ensayos estáticos: *Acid-Base Accounting* (ABA) y *Net Acid Generation* (NAG).

El ensayo ABA permite evaluar el balance entre la capacidad del suelo para generar acidez total y su capacidad de neutralización de la acidez (CNA). En suelos sulfatados ácidos, la acidez puede provenir de diversas fuentes (Ahern et al., 2004):

- Potencial de acidez sulfídica (PA_{PYR}): generado por la oxidación de los sulfuros, principalmente pirita. El PA_{PYR} se calculó multiplicando el contenido de S_{PYR} por 0,625, un factor estequiométrico basado en que la oxidación de un mol de azufre en la pirita libera dos moles de protones (H^+):

$$PA_{PYR}\ (mol\ H^+\ kg^{-1}) = S_{PYR}\ (\%) * 0{,}625$$

- Acidez real titulable (ART): incluye tanto la acidez soluble como la intercambiable. Se midió mediante titulación con NaOH 0,1 M de una suspensión de suelo en KCl 1 M (1:2,5, m/v) hasta alcanzar un pH neutro.

- Acidez retenida (PA_{JAR}): asociada a jarosita ($KFe_3(SO_4)_2(OH)_6$), el sulfato que liberaría la mayor cantidad de acidez antes cambios en las condiciones del medio como, por ejemplo, alcalinización durante la remediación. Se calculó

a partir del contenido de S_{JAR}, multiplicando por 0,468, considerando que un mol de azufre en la jarosita libera 1,5 moles de H^+:

$$PA_{JAR}\,(mol\ H^+\ kg^{-1}) = S_{JAR}\,(\%) * 0{,}468$$

La acidez neta (AN) se calculó mediante la siguiente ecuación:

$$AN = PA_{PYR} + ART + PA_{JAR} - CNA$$

Cuando la acidez intercambiable no alcanza la neutralidad ($pH_{KCl} < 5{,}5$), se asume que su capacidad de neutralización ha sido superada; en tal caso, la CNA se considera nula, ya que cualquier capacidad remanente de neutralización sería inefectiva (Ahern et al., 2004).

Por otro lado, el ensayo NAG proporciona una medida directa del potencial de generación de acidez neta mediante la oxidación forzada con H_2O_2 al 30%. Este método considera la acidez generada por los sulfuros, así como cualquier neutralización simultánea, pero no evalúa la acidez retenida en jarosita, ya que este mineral permanece estable en las condiciones del ensayo. Tras la oxidación, el extracto se tituló con NaOH 0,1 M hasta alcanzar un pH de 7 (Ahern et al., 2004).

- Capacidad de intercambio iónico (CIC)

La CIC se determinó al pH natural del suelo (Saiz, 2004), usando una disolución no tamponada de NH_4Cl 1M en una relación suelo-solución de 1:12 (m/v). Se realizó una segunda extracción para asegurar la completa recuperación de los cationes intercambiables. Las concentraciones de K^+ y Na^+ se midieron por espectrometría de emisión atómica con llama (FEAS) y las de Ca^{2+} y Mg^{2+} por absorción atómica con llama (FAAS), utilizando un equipo Varian SpectrAA 50B. Los cationes ácidos (H^+ y Al^{3+}) se estimaron por valoración con NaOH 0,01 N.

- Composición química total

Las concentraciones totales de elementos mayoritarios y traza se analizaron por ICP-OES, tras un proceso de digestión multi-ácida ($HClO_4$ + HNO_3 + HCl + HF). Los análisis se llevaron a cabo en Actlabs (Ancaster, Ontario, Canadá), un laboratorio reconocido y acreditado internacionalmente, que opera bajo estrictos estándares de calidad, incluyendo las certificaciones ISO 9001 e ISO/IEC 17025.

- Elementos traza fitodisponibles en la rizosfera

Las concentraciones de EPT disponibles por las plantas en la rizosfera se estimaron mediante una extracción con $CaCl_2$ 0,01 M (1:10 m/v). Las muestras se agitaron durante 2 horas a 30 rpm (Houba et al., 1990; Rivera et al., 2016), se centrifugaron y filtraron (0,45 µm), y los elementos extraídos se analizaron por ICP-MS.

- Análisis químicos de las plantas

Las concentraciones de metales pesados en los órganos vegetales (raíces, tallos y hojas) de *Nicotiana glauca* y *Euphorbia segetalis*, especies que crecen en el suelo contaminado del estero de Domingo Rubio, se analizaron por espectrometría de masas con plasma acoplado inductivamente (ICP-MS), usando un equipo Agilent 7700. Previamente, las muestras fueron sometidas a una digestión ácida con HNO_3 concentrado (Madejón et al., 2011).

3.3.2. Caracterización de los residuos

Para caracterizar los residuos, se usaron los mismos métodos empleados en el análisis de suelos para determinar la composición mineralógica, la granulometría, los parámetros potenciométricos, los contenidos totales de C, N, S y de P asimilable. Además, se realizaron las siguientes determinaciones:

- Potasio (K) asimilable

Se extrajo con una solución de $CaCl_2$ 0,01 M, con una relación residuo-solución 1:10 (m/v), agitadas durante 2 h a 30 rpm (Houba et al., 1996). Seguidamente, las muestras fueron una centrifugadas (5000 rpm, 10 min) y el K asimilable se cuantificó por FAAS en un equipo Varian SpectrAA 50B.

- Nitratos lixiviables

Se determinaron siguiendo la Norma Europea EN-12457-4 mediante un ensayo de lixiviación con agua milli-Q en una relación líquido-sólido de 10:1, con agitación durante 24 h a 10 rpm. Los eluatos obtenidos fueron centrifugados, filtrados y analizados por cromatografía iónica (Metrohm 883 Basic IC plus).

- Hidrocarburos totales del petróleo (TPH)

Se determinaron mediante un sistema acoplado de desorción térmica, cromatografía de gases y espectrometría de masas (TD-GC-MS). Las muestras de residuo se colocaron en viales con un *twister* recubierto de polidimetilsiloxano para la extracción de los analitos en el espacio de cabeza, bajo atmósfera de nitrógeno. La extracción se realizó por calentamiento a 200 °C durante 5 min (TPH) y 30 min (PAH), y posteriormente se analizaron los *twisters*.

- Elementos traza potencialmente tóxicos

Las concentraciones pseudototales de As, Cd, Cr, Cu, Hg, Ni, Pb y Zn se determinaron tras una digestión parcial del residuo con agua regia. Los extractos fueron analizados por ICP-MS en el laboratorio acreditado de Actlabs (Canadá).

3.4.Formulación y composición de los tecnosuelos

De entre los residuos caracterizados, se comprobó que los lodos de depuradora (R2) excedían los valores límite establecidos en la Xunta de Galicia (2008)

para Cd, Cu, Ni y Zn, así como las escorias de incineradora de residuos sólidos urbanos (R8) para Zn. Por tanto, estos residuos se descartaron para su uso en la elaboración de los tecnosuelos. En cambio, los resultados obtenidos permitieron seleccionar dos tipos de residuos orgánicos (R3 y R4), que aportan materia orgánica y nutrientes esenciales, y cuatro tipos de residuos inorgánicos o acondicionadores (R1, R5, R6 y R7), que estabilizan los compuestos orgánicos y proporcionan las propiedades físico-químicas deseadas para regenerar suelos degradados.

Los residuos seleccionados para regenerar los suelos mineros se combinaron de manera sistemática y estratégica hasta lograr las propiedades clave deseadas, tales como: capacidad neutralizante para reducir o anular la acidez neta del suelo; capacidad de adsorción de EPT, para evitar su solubilización en la solución del suelo; y poder fertilizante, para aportar materia orgánica y nutrientes vitales para las plantas y los microorganismos del suelo.

Se realizaron múltiples pruebas y ajustes en las cantidades formuladas hasta alcanzar una composición óptima capaz de hacer frente a los desafíos ambientales específicos de los suelos a tratar, como la hiperacidez, la movilidad y toxicidad de los metales pesados, y superar los factores limitantes del crecimiento vegetal, como el bajo grado de saturación en bases y la carencia o deficiencias en nutrientes esenciales.

Inicialmente se crearon 15 tecnosuelos diferentes con una proporción de 60% residuo orgánico y 40% residuo inorgánico en peso (Tabla 3). Se formularon 72 mezclas con distintas proporciones de suelo minero/tecnosuelo en las dosis de 50:50 y 75:25. Posteriormente, en una fase de reajuste, se realizaron 36 nuevas mezclas con diferentes proporciones de tecnosuelo (40, 35, 30, 20, 15 y 5%). En total, se probaron 108 combinaciones suelo/tecnosuelo diferentes.

Tabla 3

Composición de los tecnosuelos ensayados para la recuperación de los suelos mineros. La descripción de los suelos (S) y de los residuos empelados (R) se presenta en las Tablas 1 y 2, respectivamente.

Tecnosuelo	Composición		Formulación	
S1T2-25	75% suelo 1	25% residuos R3,R5,R7	60% R3	20% R5+20% R7
S1T5-25	75% suelo 1	25% residuos R3,R6,R7	60% R3	20% R6+20% R7
S1T11-30	70% suelo 1	30% residuos R3,R6	60% R3	40% R6
S2T8-25	75% suelo 2	25% residuos R3,R5	60% R3	40% R5
S2T11-10	90% suelo 2	10% residuos R3,R6	60% R3	40% R6
S2T11-25	75% suelo 2	25% residuos R3,R6	60% R3	40% R6
S3T3-5	95% suelo 3	5% residuos R4,R5,R7	60% R3	20% R5+20% R7
S3T5-25	75% suelo 3	25% residuos R3,R6,R7	60% R3	20%R6+20% R7
S3T11-25	75% suelo 3	25% residuos R3,R6	60% R3	40% R6
S4T5-20	80% suelo 4	20% residuos R3,R6,R7	60% R3	20% R6+20% R7
S4T6-15	85% suelo 4	15% residuos R3,R5,R6	60% R3	20% R5+20% R6
S4T11-25	75% suelo 4	25% residuos R3,R6	60% R3	40% R6
S5T2-25	75% suelo 5	25% residuos R3,R5,R7	60% R3	20% R5+20% R7
S5T8-5	95% suelo 5	5% residuos R3,R5	60% R3	40% R5
S5T11-35	65% suelo 5	35% residuos R3,R6	60% R3	40% R6

3.5. Funcionalidad de los tecnosuelos

Además de analizar la composición química total y los contenidos de TPH y PAH según los métodos expuestos, se llevaron a cabo ensayos específicos para evaluar la funcionalidad de los tecnosuelos.

- Ensayo de lixiviación

Con el objetivo de estimar la movilidad potencial de los contaminantes en las distintas formulaciones de tecnosuelos y evaluar su efectividad, se llevaron a cabo ensayos de lixiviación de acuerdo con la Norma Europea EN 12457-4. Las muestras se mezclaron con agua Milli-Q en una proporción líquido-sólido de 10:1 (L/kg), se

agitaron durante 24 h y posteriormente se centrifugaron (5000 rpm 10 min) y filtraron a través de una membrana de 0,45 µm (Fig. 8).

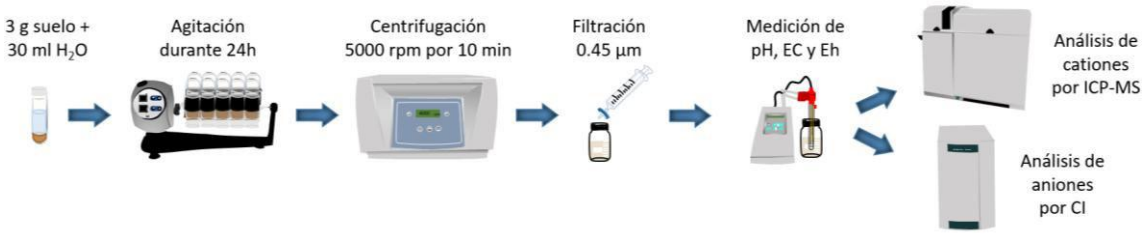

Fig. 8. Esquema metodológico del ensayo de lixiviación.

Los elementos mayoritarios se cuantificaron mediante ICP-OES utilizando un equipo Agilent 5110, mientras que EPT se analizaron por ICP-MS con un equipo Agilent 7700.

Las soluciones lixiviadas también fueron analizadas para determinar las concentraciones de aniones (nitrato, fluoruro y cloruro) mediante cromatografía iónica (Metrohm 883 Basic IC plus). El contenido de bicarbonato se cuantificó por el método de Warder, mediante titulación con HCl 0,02 M, empleando naranja de metileno como indicador del punto final.

La calidad del agua de los suelos mineros, tanto originales como tratados con tecnosuelos, se clasificó usando un diagrama de Ficklin modificado (Ficklin et al., 1992), considerando la carga metálica disuelta (suma de las concentraciones de Cd, Cu, Ni, Pb y Zn) y el pH de los lixiviados.

Para estimar el riesgo potencial, se calculó el coeficiente promedio de peligrosidad (CPP_{LAB}), comparando el contenido de EPT de los eluatos con un estándar de calidad de agua predefinido (Alberruche et al., 2014):

$$CPP_{LAB} = \frac{1}{n} * \sum^{n} \frac{[X]_{LIX-LAB}}{NCA_X}$$

donde $[X]_{LIX\text{-}LAB}$ es la concentración medida en el lixiviado para el elemento *X*; NCA_X es el contenido máximo admisible en el agua correspondiente al elemento *X*; y *n* es el número de elementos cuya concentración supera al nivel adoptado como estándar.

A partir del CPP_{LAB} se estimó el factor de toxicidad (F_{TOX}), que clasifica la toxicidad relativa en una escala de 0 a 5. Si CPP_{LAB} es superior a 400, se le asigna la toxicidad máxima (5); si CPP_{LAB} es inferior o igual a 400, entonces el F_{TOX} se calcula mediante la siguiente ecuación:

$$F_{TOX} = CPP_{LAB} * 0{,}0125$$

- Ensayos de movilidad y bioaccesibilidad

Para determinar la fracción de EPT más fácilmente disponible se realizó una extracción con una disolución no tamponada de $CaCl_2$ 0,01 M (Houba et al., 1996), que simula la fuerza iónica de la solución del suelo. La movilidad potencial se estimó con una solución de EDTA 0,05 M a pH neutro (Ure et al., 1993). Por último, la bioaccesibilidad de los EPT estimó mediante una extracción con HNO_3 0,43 M, sobre la fracción granulométrica inferior a 250 µm, que simula las condiciones ácidas que se encuentran en el tracto digestivo de algunos organismos (Rodrigues et al., 2010).

Todos los protocolos de extracción se llevaron a cabo usando una relación sólido-líquido de 1:10 (m/v), agitación (30 rpm, 2 h), centrifugación (5000 rpm, 10 min) y filtración (0,45 µm). Los EPT extraídos se analizaron por ICP-MS (Agilent 7700).

- Contenido de bicarbonato en el agua de poro

El contenido de bicarbonato en el agua intersticial de los tecnosuelos se cuantificó mediante titulación con HCl 0,002 M, empleando naranja de metileno como indicador.

- Modelización de especies acuosas con PHREEQC

Los índices de saturación de minerales y la distribución de especies acuosas en la solución del suelo se calcularon utilizando el software de modelización geoquímica PHREEQC (Parkhurst y Appelo, 2013) y la base de datos Minteq.v4 (Allison et al., 1999), ampliada con datos de Bigham et al. (1996) para incluir la schwertmannita. El índice de saturación (IS) para cada mineral previsto se calculó mediante la ecuación:

$$IS = log \frac{IAP}{Ks}$$

donde *IAP* es el producto de la actividad iónica y *Ks* es la constante del producto de solubilidad. El IS permitió inferir procesos de disolución o precipitación de minerales, esenciales para entender la disponibilidad de los elementos tóxicos en el suelo. Un valor de IS próximo a cero indica que la solución está en equilibrio con respecto al mineral considerado. Un IS positivo implica sobresaturación y posible precipitación, mientras que un IS negativo indica subsaturación, lo que sugiere una tendencia hacia la disolución.

3.6. Capacidad de arraigo y crecimiento vegetal

3.6.1. Ensayo de germinación

Para evaluar la aptitud de los tecnosuelos como sustrato para el desarrollo vegetal, se realizaron ensayos de germinación utilizando semillas de *Brassica juncea* (mostaza india). Se comparó la tasa de germinación en los tecnosuelos con dos controles: suelo minero sin tratar (negativo) y mantillo comercial (positivo).

Se colocaron 30 semillas de *B. juncea* (variedad scala) por placa de Petri con una fina capa de cada sustrato. Las semillas se humedecieron regularmente con agua de grifo (pH= 6,85; CE= 0,65 mS/cm) y se mantuvieron a temperatura ambiente (14–24 °C) bajo luz natural con fotoperiodo de 10-14 h. Transcurridos 6 días, se procedió al recuento de semillas germinadas, considerándose como tales aquellas cuyas radículas habían alcanzado una longitud superior a 3 mm (ISTA, 2005).

3.6.2. Experimentación en macetas

El objetivo de este ensayo fue evaluar el efecto de los tecnosuelos sobre el establecimiento y desarrollo de *B. juncea*. Esta planta herbácea fue elegida por su adaptabilidad a diversas condiciones climáticas y edáficas, por su rápido crecimiento, sistema radicular denso, tolerancia a metales pesados y uso en procesos de fitoestabilización de suelos contaminados (Novo y González, 2014; Pérez-Esteban et al., 2014; Forján et al., 2018). Además, *B. juncea* es un buen indicador de fitodisponibilidad, empleado para evaluar la eficacia de los tratamientos de remediación (Clemente et al., 2005).

Los tecnosuelos se humidificación y estabilizaron durante 14 días a temperatura ambiente, en macetas de 15 cm de diámetro y profundidad, con orificios de drenaje y una capa de grava en la base para evitar encharcamientos. En aquellos tecnosuelos que consiguieron neutralizar la acidez, se plantaron 5 plántulas con cotiledones completamente desplegados. Cada tratamiento se replicó por triplicado. Se establecieron además dos controles: uno negativo (suelo minero sin tratar) y otro positivo (mantillo).

Las macetas se mantuvieron en condiciones de invernadero durante 4 meses (febrero-mayo 2023) con temperaturas entre 10 y 42 °C, humedad relativa 25–80%, y luz natural diaria de 10,5–14,5 h. La humedad del suelo se mantuvo mediante riego periódico con agua de grifo.

Mensualmente, se muestreó el agua de poro, tanto en los suelos tratados como en los controles. Las muestras se obtuvieron a capacidad máxima de retención de agua, utilizando muestreadores de succión Rhizon (Fig. 9) insertados con una inclinación de 45° (Clemente et al., 2008). Se determinaron el pH, Eh, conductividad eléctrica y las concentraciones totales de elementos mayoritarios y traza. Además, se evaluaron indicadores del desarrollo vegetal, como la tasa de supervivencia, altura de las plantas, número de hojas, tiempo hasta la floración y producción final de biomasa. El estado aparente de salud de las plantas se valoró mediante observación visual, considerando síntomas como marchitez, clorosis, necrosis u otros signos de estrés.

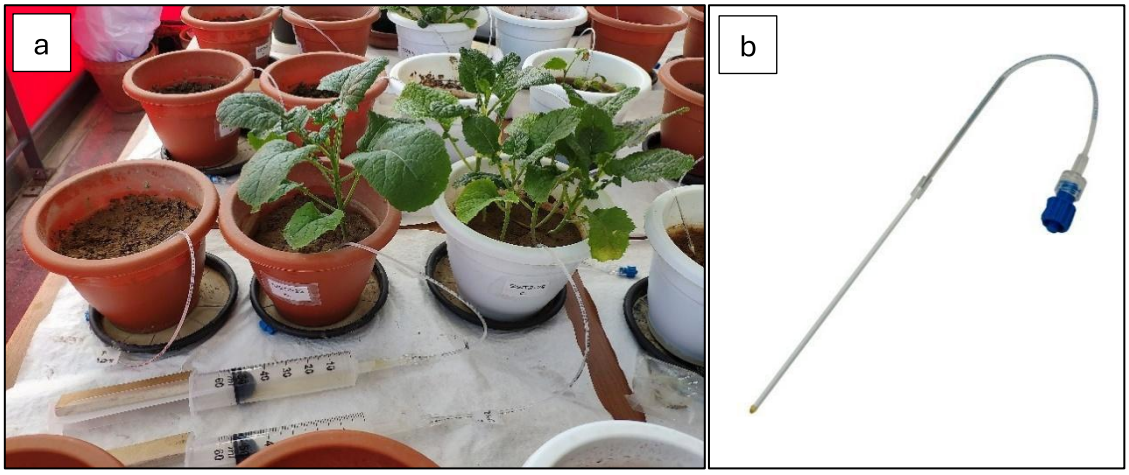

Fig. 9. Muestreo del agua de poro con muestreadores Rhizon: a) extracción por vacío con jeringa; b) detalle de la sonda de succión.

3.7. Control de calidad

Para asegurar la fiabilidad de los resultados, se implementaron rigurosas medidas de control de calidad en todas las etapas del análisis.

Se utilizaron reactivos de alta pureza, específicamente de calidad analítica "para análisis" (Merck, Sigma-Aldrich) o de grado "Suprapur" (Merck). El agua empleada en los procedimientos analíticos fue ultrapura tipo I (18,2 MΩ·cm a 25 °C, <5 ppb TOC), obtenida mediante un sistema Milli-Q (Merck Millipore).

El material de laboratorio se descontaminó meticulosamente mediante inmersión en una disolución de DERQUIN al 10% (Panreac), seguido de una limpieza con HNO_3 al 10% durante 24 h. Posteriormente, se enjuagó con agua ultrapura y se secó a temperatura ambiente o en estufa a 120 °C según el tipo de material.

La cuantificación de los analitos se realizó mediante calibración externa con patrones certificados. Para los EPT medidos por ICP-MS, se utilizó una disolución de Ge, Rh, Sc y Tb a 10 µg L^{-1} como patrón interno.

El control de calidad analítica incluyó blancos de laboratorio, patrones de comprobación de la calibración y análisis por duplicado para evaluar la exactitud y precisión de los resultados. La precisión, expresada como desviación estándar relativa (RSD) fue inferior al 8% para todos los parámetros. La exactitud del método se validó con materiales de referencia certificados, adecuados a la naturaleza de cada tipo de muestra:

- Suelos mineros y residuos analizados: Se usaron los materiales de referencia OREAS 13b, OREAS 98 y OREAS 101b. Los resultados mostraron una exactitud con errores relativos inferiores al 10% y una excelente precisión (RSD < 2%).

- Lixiviados y agua de poro: Se utilizó el material de referencias SRM 1640a. Las recuperaciones de los elementos certificados oscilaron entre 95% y 106%, con una precisión inferior al 10%.

- Tejidos vegetales: Se empleó material INCT-OBTL-5 (hojas de plantas de tabaco Oriental Basma). La recuperación media fue del 92% y la precisión del 8%.

3.8. Tratamiento estadístico

El análisis estadístico de los datos experimentales se realizó con los paquetes de software STATISTICA versión 10.0 (StatSoft Inc., 2011) y SPSS versión 27.0 (SPSS Inc., 2021) para Windows. Cuando los resultados se encontraron por debajo del límite de detección (LD), se les asignó un valor equivalente a la mitad del LD, una práctica común en estudios ambientales para minimizar el sesgo.

Para la comparación de medias entre grupos, se aplicaron pruebas estadísticas univariantes. Se utilizó la prueba *t de Student* para comparaciones entre dos grupos y el análisis de varianza (ANOVA) para comparaciones entre más de dos grupos. Previamente al ANOVA, se comprobó la homogeneidad de la varianza de los datos con la prueba de Levene, y sólo se procedió con el análisis paramétrico cuando se

cumplió este supuesto. En todos los casos, el nivel significancia estadística se fijó en $\alpha = 0,05$ (intervalo de confianza del 95%).

Además, se emplearon análisis bivariantes y multivariantes para explorar patrones y relaciones entre las variables estudiadas. En particular, el análisis de componentes principales (PCA) se utilizó como técnica multivariante para reducir la dimensionalidad del conjunto de datos y visualizar la influencia integrada de múltiples variables químicas en la respuesta de las plantas en los suelos remediados. Antes de aplicar el PCA, se verificó la existencia de correlaciones significativas entre las variables, un requisito fundamental para este tipo de análisis.

4. RESULTADOS Y DISCUSIÓN

4.1. Los suelos mineros de Rio Tinto actúan como una fuente secundaria y persistente de ácido y metales pesados

Basado en el artículo:

Soil contaminated with hazardous waste materials at Rio Tinto mine (Spain) is a persistent secondary source of acid and heavy metals to the environment. Minerals 13 (2023) 456

Este artículo investiga la contaminación del suelo por residuos mineros, y su impacto en el medio ambiente como fuente secundaria persistente de ácido y metales pesados. El trabajo se centró en el distrito minero de Rio Tinto, un área con una larga historia de actividad minera y metalúrgica que ha dejado tras de sí un legado de extensas áreas de suelos contaminados. Los objetivos del estudio fueron: 1) cuantificar la acidez actual y predecir el potencial de formación de ácido por la oxidación de sulfuros; y 2) determinar las concentraciones de EPT lixiviados de los suelos y evaluar su movilidad y contribución a la contaminación hídrica. Para ello, se seleccionaron tres tipos de suelos contaminados con diferentes residuos minero-metalúrgicos (cenizas de calcinación de pirita, escorias de cobre y minerales sulfurados lixiviados) y se realizaron análisis mineralógicos, ensayos de reactividad estáticos, experimentos de lixiviación y modelización de la especiación de los metales en los lixiviados.

4.1.1. Resultados más relevantes

a) Composición del suelo y partículas portadoras de metales pesados

El suelo contaminado con cenizas de pirita (PH) está compuesto principalmente hematites, jarosita y cuarzo, con cantidades menores de filosilicatos, feldespatos y barita. Además, se encontró anglesita, generalmente formando sobrecrecimientos epitaxiales sobre cristales de barita. El análisis FESEM-EDS mostró trazas (< 0,5%) de Cu, As, Sb y S en los óxidos de hierro. La presencia de jarosita es particularmente relevante, ya que es un mineral que almacena acidez y puede liberarla en determinadas condiciones.

El suelo contaminado con escorias de cobre (ZA) presenta una composición más variada: cuarzo, filosilicatos y feldespatos, con cantidades variables de jarosita (hasta un 25%), y hematites, barita y yeso como accesorios, además de fragmentos de escoria fayalítica con magnetita diseminada e inclusiones de mata de cobre. También se encontraron partículas de minerales de hierro portadoras de As y fases complejas con S-Fe-Pb-As, que se atribuyen a minerales del grupo de la jarosita. Excepcionalmente, la muestra ZA-3 presentó un contenido relativamente alto de pirita (20-25%).

El suelo contaminado con minerales sulfurados lixiviados (LN) muestra una composición mineralógica formada por cuarzo, pirita, mica, y minerales del grupo de la jarosita como componentes principales, con una menor presencia de hematites, feldespatos, barita y anglesita. En este caso, la jarosita también contiene cantidades significativas de Pb y As. En este suelo conviene destacar la presencia de abundante pirita, principal fase responsable de la generación de ácido.

b) Acidez y potencial de generación de ácido

Las muestras de los suelos estudiados mostraron, en su mayoría, una reacción extremadamente ácida, con valores de pH_{H_2O} inferiores a 3,5, aunque los suelos contaminados por las escorias (ZA) presentaron valores entre 3,0 y 5,4. Aunque el pH_{H_2O} es un indicador de la acidez actual del suelo, no proporciona información sobre la capacidad de generación total. Los tres tipos de suelos mineros de Riotinto exhibieron una elevada capacidad total de generación de ácido (LN: 1365 $mmolH^+/kg$, ZA: 1503 $mmolH^+/kg$ y PH: 708 $mmolH^+/kg$), siendo la acidez sulfídica la principal fuente de acidez en las muestras de LN y ZA-3, debido a la presencia de sulfuros residuales. Sin embargo, la acidez actual (acidez soluble e intercambiable) fue relativamente baja (LN: 29 $mmolH^+/kg$, ZA: 12 $mmolH^+/kg$ y PH: 51 $mmolH^+/kg$), en comparación con la acidez potencial sulfídica. La acidez retenida en la jarosita también contribuyó significativamente a la acidez neta, particularmente en el suelo PH y ZA, donde representa el 79–86% de la capacidad total de generación de ácido. La jarosita se forma en ambientes ácidos y, bajo ciertas condiciones, puede disolverse liberando la acidez retenida. Como era de esperar por la ausencia de carbonatos y

otras fases neutralizantes, la capacidad de neutralización de la acidez de los suelos fue muy baja, obteniéndose valores de generación neta de acidez positivos (LN: 578 $mmolH^+/kg$, ZA: 438 $mmolH^+/kg$ y PH: 114 $mmolH^+/kg$), lo que implica un riesgo ambiental persistente por drenaje ácido.

c) Movilización de elementos traza

En términos de concentraciones totales, los suelos reflejaron niveles extremadamente altos de As, Cu, Pb y Zn, superando ampliamente los límites de referencia para suelos no contaminados.

Los lixiviados mostraron un pH fuertemente ácido, sobre todo en los suelos PH y LN, con valores de pH entre 2,5 y 3,5. Se midieron concentraciones elevadas de EPT, principalmente en los lixiviados de PH y ZA, con valores máximos de 55,6 mg L^{-1} para Cu, 2,25 mg L^{-1} para Zn, 2,62 mg L^{-1} para Pb, 97,5 g L^{-1} para As y 37,8 g L^{-1} para Cd. El Pb se lixivió con mayor facilidad en el suelo LN, donde la pirita es una fase más abundante, con una extracción de hasta 9,02 mg L^{-1}.

A pesar de las altas concentraciones totales de metales en los suelos, la fracción móvil liberada en los ensayos de lixiviación fue limitada, generalmente inferior al 1% del total, excepto en algunas muestras donde Cd y Cu alcanzaron valores máximos de liberación de 12,6% y 10,3%, respectivamente. Esto sugiere que gran parte de los metales se encuentran en formas relativamente estables o inmovilizadas en la matriz del suelo. Sin embargo, incluso una fracción pequeña de concentraciones tan elevadas puede representar un riesgo significativo, especialmente en un ambiente de lixiviación continua a largo plazo.

4.1.2. Discusión

Los resultados confirmaron que los suelos mineros de Rio Tinto actúan como una fuente secundaria de acidez y metales pesados, incluso décadas o siglos después del cese de la actividad minera. La pirita fue la principal fuente de acidez, especialmente en los suelos LN y ZA-3, mientras que, en el resto de las muestras (PH y ZA-1/ZA-2), la acidez retenida en la jarosita fue la dominante. El hecho de no

presentar una capacidad de neutralización efectiva agrava el impacto ambiental. La acidez extrema y las altas concentraciones de metales en los lixiviados evidencian la continua reactividad de los sulfuros residuales y la disolución de minerales que almacenan acidez, contribuyendo así a la generación persistente de ácido.

El pH es el factor más crítico que controla la movilidad de los metales. A valores de pH extremadamente ácidos, como los observados en Rio Tinto, la solubilidad de la mayoría de los metales aumenta drásticamente, lo que facilita su transporte en el agua. No obstante, también existen otros factores que controlan la movilidad y especiación de los metales, como la composición mineralógica. La presencia de sulfuros (principalmente pirita), jarosita y óxidos de hierro influye en la especiación y la liberación de metales. Los sulfuros son una fuente directa de metales al oxidarse, mientras que los óxidos de hierro pueden adsorber metales a pH más altos. La modelización geoquímica reveló que los metales se presentan principalmente como iones libres o complejos de sulfato en las soluciones ácidas. Estas formas son altamente móviles y biodisponibles, lo que aumenta su potencial tóxico, mientras que el As se liberó en forma oxianiones de arseniato ($H_2AsO_4^-$).

Los elevados índices de contaminación calculados para los suelos ZA (C_d = 420) y LN (C_d = 204) permite clasificarlos como ultra-altamente contaminados, indicando un elevado riesgo ambiental. La liberación continua de EPT en los lixiviados contribuye directamente a la contaminación de las aguas superficiales.

4.1.3. Conclusiones

Este trabajo ha proporcionado una evidencia sólida de que los suelos contaminados por la actividad minera en Rio Tinto no son solo un pasivo ambiental de la minería histórica, sino también un problema ambiental activo que exige una atención y acción inmediata para mitigar sus impactos.

Los suelos contaminados con residuos minero-metalúrgicos actúan como reservorio y como fuente secundaria y constante de acidez y metales pesados. Este impacto no es puntual sino un proceso continuo que se mantendrá a largo plazo si no

se toman medidas correctoras. La alta acidez de los suelos, combinada con la presencia de sulfuros oxidables y la escasa capacidad de neutralización, genera un drenaje ácido persistente. La liberación de metales tóxicos en estas condiciones ácidas representa un riesgo ambiental potencial para la calidad del agua y los ecosistemas afectados.

En definitiva, a la luz de estos resultados, se necesitan estrategias de recuperación del suelo para neutralizar la acidez y reducir la movilidad de los metales a niveles ambientalmente sostenibles, y establecer una cubierta vegetal para estabilizar el suelo, reducir la erosión y, en algunos casos, bioacumular o fitoestabilizar los metales.

minerals

MDPI

Article

Soil Contaminated with Hazardous Waste Materials at Rio Tinto Mine (Spain) Is a Persistent Secondary Source of Acid and Heavy Metals to the Environment

Sandra Fernández-Landero [1], Juan Carlos Fernández-Caliani [1,*], María Inmaculada Giráldez [2], Emilio Morales [2], Cinta Barba-Brioso [3] and Isabel González [3]

[1] Department Earth Sciences, University of Huelva, 21071 Huelva, Spain; sandra.fernandez@dct.uhu.es
[2] Department Chemistry, University of Huelva, 21071 Huelva, Spain; giraldez@uhu.es (M.I.G.); albornoz@uhu.es (E.M.)
[3] Department Crystallography, Mineralogy and Agricultural Chemistry, University of Seville, 41071 Seville, Spain; cbarba@us.es (C.B.-B.); igonza@us.es (I.G.)
* Correspondence: caliani@uhu.es

Abstract: Mineralogical analysis and laboratory-based leaching tests coupled with speciation modeling were undertaken to quantify the potential for short-term acid generation and the release of trace elements from soils heavily contaminated with mine waste at Rio Tinto. Three different waste materials were considered as case studies: roasted pyrite, copper slags, and leached sulfide ores. The results showed elevated values of net acid generation (up to 663 mmol H^+/kg), the major pools being potential sulfidic acidity and acidity retained in jarosite. Remarkable contents of As and toxic heavy metals were found especially in the slag-contaminated soil. Copper, Zn, and Pb were the most abundant metals in the acid leach solutions resulting from mine soil-water interaction, with peak values of 55.6 mg L^{-1}, 2.77 mg L^{-1}, and 2.62 mg L^{-1}, respectively. Despite the high total contents of trace elements occurring in soil, the mobile fraction was limited to maximum release values of 12.60% for Cd and 10.27% for Cu, according to the test leaching. Speciation calculations indicated that free metal ions (M^{2+}) and sulfate species (MSO_4^0) accounted for most of the dissolved load. Acid soil drainage is a secondary source of acid and heavy metals in the mine site and, therefore, an effective land reclamation program should ensure that acidity and metal mobility are reduced to environmentally sustainable levels.

Keywords: Technosol; mine wastes; soil contamination; acidity; leaching test; metal release; speciation; ICP-OES/MS; acid soil drainage; Iberian Pyrite Belt

Citation: Fernández-Landero, S.; Fernández-Caliani, J.C.; Giráldez, M.I.; Morales, E.; Barba-Brioso, C.; González, I. Soil Contaminated with Hazardous Waste Materials at Rio Tinto Mine (Spain) Is a Persistent Secondary Source of Acid and Heavy Metals to the Environment. *Minerals* **2023**, *13*, 456. https://doi.org/10.3390/min13040456

Academic Editors: Saglara S. Mandzhieva and Maria Economou-Eliopoulos

Received: 7 February 2023
Revised: 20 March 2023
Accepted: 21 March 2023
Published: 23 March 2023

1. Introduction

Soil is a vital and non-renewable resource that is increasingly under pressure from a range of human activities, with mining being one of the leading anthropogenic forces driving environmental degradation. Acid generation and metal release from the oxidative dissolution of sulfide minerals in mine wastes is a well-documented issue in many historic mining districts [1–3]. Acid mine drainage (AMD) and heavy metal-bearing mineral particles arising from abandoned mine lands may pose a serious threat to human health and ecosystems [4–8]. Hence, a great deal of work has been undertaken to characterize the mineralogy, geochemistry, and environmental impacts of mine wastes [9–13]. However, there are still gaps in the research on mining-affected soil systems that need to be addressed.

The pollutants enter surrounding soils by seepage and run-off from mine wastes, AMD discharges, and atmospheric fallout, resulting in a legacy of mine-related anthropogenic soils that can be classified as Technosols according to IUSS Working Group WRB [14]. Mine Technosols contaminated with waste materials may have lost their natural resilience and adaptive capacity to retain harmful contaminants and, therefore, can generate acidic

effluents and release sulfate and potentially toxic elements (PTEs) into surface and pore waters [15]. This can be referred to as acid soil drainage (ASD) in analogy to AMD. Soil erosion and leaching are intensive during rain events leading to the dispersion of PTEs, either bound to suspended particles or as dissolved species. Knowledge of ASD is important for understanding the mobility and environmental availability of PTEs at historically contaminated sites, and also for developing sustainable remediation options to reduce the dispersion of contaminants and their associated risks [16]. Accurate prediction of ASD is challenging but essential to minimize the environmental impact of these soils.

The goal of this work was to assess the potential mobilization of acid and PTEs from mine Technosols contaminated with various types of mining and metallurgical wastes in the mining district of Rio Tinto (Spain). These drastically disturbed mine soils have been subjected to chemical loading for over two centuries in the absence of legal and regulatory frameworks. The sources and relative contributions of acid and PTEs from the mine Technosols are currently not well understood. Thus, the specific objectives of the study were: (1) to quantify the existing acidity and to predict the acid-forming potential from sulfide oxidation, and (2) to determine the element concentrations leached from the mine soils and then to evaluate the mobility of PTEs and their contribution for water pollution.

2. Site Description and Historical Background

Rio Tinto mine, located in Huelva province, Spain (Figure 1), is an internationally renowned mine not only for the giant size of its ore body but also because of its long history of mining and extractive metallurgy, dating back to pre-Roman times. It is the largest of the volcanogenic massive sulfide (VMS) deposits of the Iberian Pyrite Belt (IPB), with over 500 million tons of VMS ores averaging 45 wt.% S, 40 wt.% Fe, 0.8 wt.% Cu, 2.1 wt.% Zn, 0.8 wt.% Pb, 0.5 g/t Au, and 26 g/t Ag [17], and about 2 billion tons of low-grade stockwork mineralization including zones of economic copper ore (186 million tons at 0.38 wt.% Cu according to Noble [18]) that are currently being mined at Cerro Colorado open pit. Previous research on the geology and metallogeny of the Rio Tinto VMS deposit has been described in detail recently ([19] and references therein).

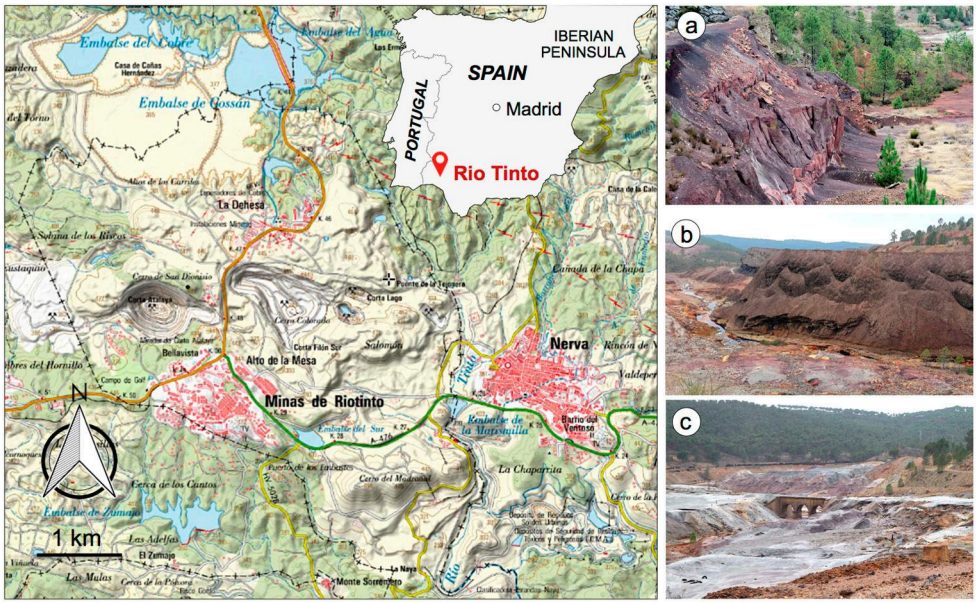

Figure 1. Location map of the Rio Tinto mining area (viewfinder SIGPAC), and representative photographs of the extensive mine wastes: (**a**) roasted pyrite piles; (**b**) slag dumps; and (**c**) heap leaching grounds (photo A. Delgado).

The Rio Tinto mining area is also an example of large-scale environmental degradation caused by long-lasting mining, ore processing, and smelting activities. It is generally accepted that Rio Tinto was extensively mined since at least the Late Bronze Age [20], being a major source of copper, gold, and silver in the Roman era, as evidenced by a large number of ancient slags widespread in the area (about 6 million tons according to Rothenberg and García-Palomero [21]).

Modern mining started in the middle of the 19th century with the extraction of cupreous pyrites, and major technological changes took place involving the smelting of high-grade ores in blast furnaces and converters. Slags produced during smelting were accumulated in significant amounts over time. Further details of the smelting works are given in Salkield [22]. The low-grade copper ores that were deemed unsuitable for smelting were converted into water-soluble sulfates by open-air roasting in heaps locally known as teleras. The roasted mineral (i.e., pyrite ash) was washed with acidic water to leach out the soluble metal-sulfate salts, leaving a solid residue enriched in ferric iron (red waste), while the leach liquors were conducted into cementation tanks where dissolved copper was precipitated by iron scrap chips. The red wastes resulting from that ancient process can be found today at the Planes and Peña de Hierro sites (Figure 1a).

In 1873 the British Rio Tinto Company (RTC) was formed to operate the mines and the scale of the operations was dramatically increased. The ore body was extensively worked from several open-pit and underground mines, focusing on copper-rich ores and massive pyrite for the manufacture of sulfuric acid. During the period of RTC operations (1873–1954), the total output of pyrite ores was almost 110 million tons [22]. The pyrite concentrates were transported by railway to Huelva port causing adverse impacts on the local soil environment due to hazardous cargo spills [23]. Pyrite smelting operated until 1970 to melt massive sulfide concentrates to produce blister copper, and at the same time to recover the excess sulfur in the elemental form. The smelting operations produced a vast volume of slag (at least 10 million tons with an average grade of 0.44 wt.% Cu according to Lottermoser [24]) placed along the banks of the Tinto River, in the industrial complex of Zarandas (Figure 1b).

Heap leaching was another widely used extraction method for low-grade ores since the early 20th century. An average of about 2000 tons of ore per day was delivered from the mines to the heaps by railway wagons, with La Naya becoming the main center of operations (Figure 1c). In more recent times, high-grade copper stockwork mineralization and gold-bearing gossan, which overlies the VMS deposit, were exploited by opencast mining. The Rio Tinto mine was last operated in 2001 and restarted operations in 2015 owing to the rise in the copper price. The current open pit mining operation is focused on the Cerro Colorado deposit, including Filón Sur and Filón Norte orebodies.

Extensive opencast workings and smelting activities as well as the lack of environmental protection have resulted in land contamination arising from past waste disposal practices. The natural soil was irreversibly damaged or transformed into degraded land unable to support plant life over a bare area of about 1000 ha (Figure 2). Huge quantities of mine and metallurgical wastes, including sulfide-rich waste dumps, ore stockpiles, slag deposits, roasted pyrite residues, heap leaching grounds, and tailings impoundments were left without any environmental control. These hazardous materials have the potential for releasing a variety of dissolved metals and metalloids that are usually present in the ores as minor or trace elements, such as Cu, Pb, Zn, As, Cd, Sb, and Tl, thus causing serious environmental pollution to the surrounding soils and vegetation [25–30].

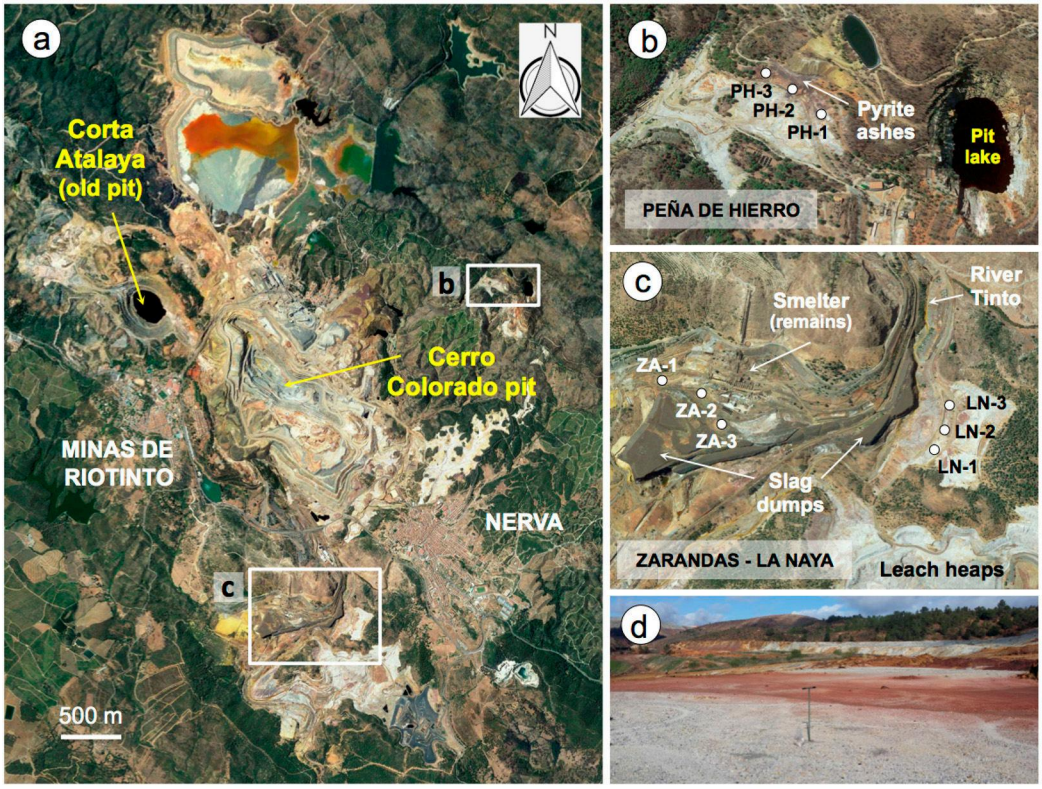

Figure 2. Satellite view (Google Earth) of the Rio Tinto copper mine showing: the mining-affected area (**a**); the location of the sampling sites at Peña de Hierro (**b**) and Zarandas-La Naya (**c**); and the method for taking soil samples with hand auger (**d**).

3. Materials and Methods

3.1. Sample Selection and Preparation

Three different Technosols containing abundant artifacts in the form of mine waste particles were selected for this study: (1) Technosol contaminated with roasted pyrite wastes from the Peña de Hierro mine site (hereafter referred to as PH; Figure 2b); (2) Technosol contaminated with copper slags from the old smelter *Fundición Piritas* at Zarandas (hereafter referred to as ZA; Figure 2c); and (3) Technosol contaminated with leached sulfide ores from the leach heap grounds of La Naya (hereafter referred to as LN; Figure 2c). These areas have experienced considerable environmental damage and were selected on the basis of being representative of mine-related anthropogenic soils in the mining district of Rio Tinto.

Within each selected area, soil samples were collected with an Edelman hand auger from the surface layer (0–20 cm) at three randomly selected sites and stored in airtight polyethylene bags. At each sampling site, a composite sample of about 10 kg was obtained by bulking five topsoil samples taken in crossing directions and spaced approximately 1.5 m around the central point (Figure 2d). The composite samples were thoroughly mixed to ensure optimal homogenization, dried at room temperature (20 ± 1 °C), gently disaggregated, and sieved to 2 mm. A portion of the sieved sample was ground in an agate mortar and passed through a 63 µm sieve for analysis.

3.2. Soil Characterization Methods

Soil reaction (pH), redox potential (Eh), and electrical conductivity (EC) were determined by stirring 10 g of soil in 25 mL of deionized water, after shaking for 5 min, and left to stand for 30 min. Soil pH was also determined in 1 M KCl suspension at the soil-to-solution ratio of 1:2.5 (*m*/*v*), and in a suspension of soil after digestion by 30% hydrogen peroxide (H_2O_2) in a 1:20 (*m*/*v*) soil-to-solution ratio [31]. The reaction was allowed to continue until the bubbling stopped (about 6 h after the addition of H_2O_2). The pH values in water

(pH_{H2O}), KCl (pH_{KCl}), and H_2O_2 (pH_{ox}) suspensions were measured with a digital pH meter properly calibrated with two buffer solutions at pH 4 and 7. All measurements were performed in triplicate and averaged.

Mineralogical analysis of the bulk sample was performed by X-ray diffraction (XRD) with a BRUKER AXS D8-Advance powder diffractometer (CITIUS, University of Seville) using monochromatic Cu-Kα radiation. The instrument was operated under standard conditions: 40 kV voltage and 30 mA current in the angular range of 3–70° 2θ with a step size of 0.015° and a scan speed of 0.1 s per step. Intensity factors weighting integrated peak area values of diagnostic reflections in combination with the 100% approach [32] were applied to obtain semiquantitative mineral abundances.

To assist in the identification of metal-bearing accessory minerals and poorly crystallized phases, the samples were coated with a thin layer of sputtered carbon and examined by field-emission scanning electron microscopy (FESEM) with a JEOL JSM-IT500HR instrument (University of Huelva) fitted with an energy dispersive X-ray spectroscopy (EDS) detector (Oxford Instruments). The samples were observed in both secondary electron (SE) and backscattered electron (BSE) modes. The working distance was set at 10 mm, accelerating voltage at 20 kV, and probe current at 2.5 nA.

Quantitative analysis of the elemental composition of selected phases was conducted on polished sections by electron probe microanalysis (EPMA) using a JEOL JXA-8200 SuperProbe (University of Huelva) equipped with four wavelength dispersive X-ray spectrometers. The instrumental operating conditions were accelerating voltage at 20 kV, beam current at 20 nA, and beam diameter up to 5 μm allowing point-by-point element determination. A set of synthetic materials and well-characterized minerals was used as standards for calibration.

The composite bulk soil samples were analyzed for the determination of the total contents of PTEs of environmental significance (As, Cd, Co, Cr, Cu, Ni, Pb, Sb, Tl, and Zn). First, a 0.25 g sample was digested with four acids beginning with HF, followed by a mixture of HNO_3 and $HClO_4$, and then heated in several ramping and holding cycles. After incipient dryness was attained, samples were brought back into the solution using aqua regia. The analysis was conducted by inductively coupled plasma optical emission spectrometry (ICP-OES) with an Agilent 735 instrument at Activation Laboratories (Ancaster, ON, Canada), which is accredited to ISO 9001 and ISO/IEC 17,025 standards. ICP-OES has a proven history as an appropriate tool to assess metal contamination [33].

Quality control of the analytical method included the use of reagent blanks, replicate analysis of two samples, and a range of certified reference materials (OREAS 13b, OREAS 98, OREAS 101b). Analysis of the reference materials yields values that deviated from the certified contents by less than 10% (relative standard deviation, RSD). Reproducibility of the analytical data was better than 2% RSD for most of the elements reported and always better than 5% RSD.

3.3. Static Test Methods

Acid-forming potential (net acidity) was quantified for acid soil drainage prediction using an acid-base accounting (ABA) approach that involves determining the total acid-generating capacity and the acid-neutralizing capacity of the soils. In the context of acid sulfate soils, the total acid-generating capacity comprises the potential sulfidic acidity in addition to the existing acidity, which in turn includes actual (soluble plus exchangeable) and retained acidity [34]. Thus, the global ABA equation can be expressed in the following form: Net acidity = Potential sulfidic acidity + actual acidity + retained acidity − acid neutralizing capacity.

Potential sulfidic acidity (PSA) was determined by measuring the pyrite sulfur (S_{pyr}) extracted with 6 M HNO_3 solution heated at 120 °C for 30 min, performed on the residue remaining after sulfate extraction with hot dilute HCl acid, according to the standard test method ASTM D2492-02 optimized for Fe-rich soils. The S_{pyr} concentration of the extract was analyzed by ICP-OES using an Agilent 5110 instrument (University of Huelva,

Supplementary Table S1), and then used to calculate the potential pool of sulfidic acidity. The weight percent of S_{pyr} was multiplied by the stoichiometric factor of 625 to give the PSA value in mmol H^+/kg, based on the theoretical assumption that each mole of pyrite releases two moles of sulfuric acid [35,36].

Acidity existing in the soil as a consequence of previous sulfide oxidation, resulting either from the dissolution of readily soluble sulfates (actual acidity) or from acid adsorbed onto negative exchange sites of the soil particles (exchangeable acidity), was measured directly by titrating a 1 M KCl soil suspension with 0.1 M NaOH to a pH endpoint of 7.0 [37]. Additional existing acidity stored in sparingly soluble hydroxy-sulfate minerals, particularly jarosite (a conspicuous product of pyrite oxidation), was calculated from the concentration of sulfate sulfur (S_{jar}) extracted with a 0.2 M NH_4-oxalate solution adjusted to pH 3.0 and heated at 80 °C for 2 h [38]. The extract solutions were analyzed for S_{jar} using the Agilent 5110 ICP-OES. The weight percent of NH_4-oxalate extracted sulfur was multiplied by the stoichiometric factor of 468 to convert the S_{jar} values to equivalent acidity units (mmol H^+/kg) on the basis that one mole of sulfur in jarosite releases 1.5 moles of acidity.

Alternatively, a direct approach to give an indication of acid-forming potential was made for measuring net acid generation (NAG) using an H_2O_2-based static test. For the NAG test, 2 g of dry soil was treated with 40 mL of 30% H_2O_2 to accelerate the oxidation of pyrite, followed by measurement of the pH of the extract solution and titration with 0.1 M NaOH until pH 7 was reached, thus allowing the product to react with the acid-neutralizing minerals, if any.

3.4. Leaching Test

The leaching test was performed according to European Standard EN-12457-4 [39] in order to determine the element concentrations leached from the mine Technosols, and then to assess the mobility of PTEs and their potential impact on water resources.

Following this test procedure (Figure 3), a dry mass of soil was placed in contact with distilled water under a liquid-to-solid (L/S) ratio of 10 L kg^{-1}, and kept under agitation for 24 h. The solid residue was separated by filtration using a 0.45 µm membrane filter, and the PTE concentrations (As, Cd, Cr, Cu, Ni, Pb, and Zn) in the leachates were analyzed by inductively coupled plasma mass spectrometry (ICP-MS) using an Agilent 7700 instrument (University of Huelva, Supplementary Table S1). Multi-element standard-2A Agilent solutions were used for external calibration, and 10 µg L^{-1} of Ge, Rh, Sc, and Tb were used as internal standards. The accuracy and reproducibility of the analytical data were better than 10% RSD for most analyzed elements.

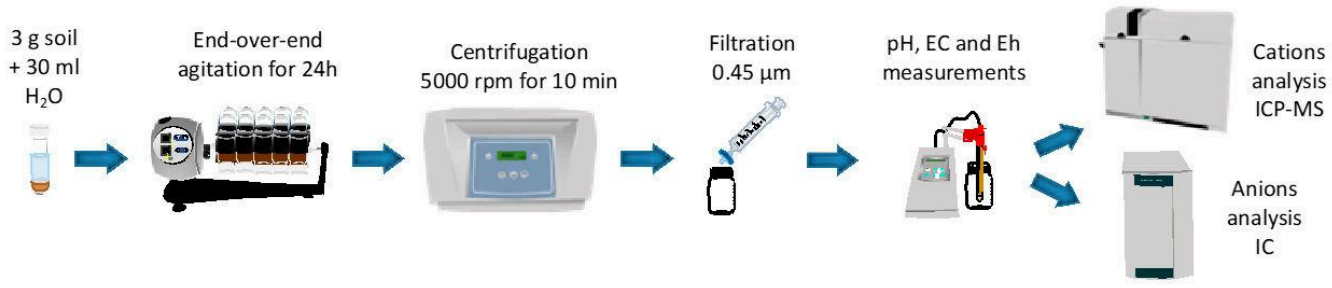

Figure 3. Simplified flow diagram of the static leaching test.

The eluate solution recovered from the leaching test was also analyzed for sulfate, nitrate, and chloride anions by ion chromatography with a Metrohm 883 Basic IC plus instrument (University of Huelva), and the leaching conditions were recorded in terms of pH, electrical conductivity and redox potential (Eh) values.

4. Results and Discussion

4.1. Soil Components with Emphasis on Heavy Metal-Bearing Particles

Combined results from XRD and FESEM-EDS analysis of the bulk fraction (<2 mm) revealed that the mine soils impacted by waste materials have a contrasting mineral composition (Table 1). The chemical composition of randomly selected heavy metal-bearing particles obtained from EPMA is also listed in Table 1.

The soil contaminated with roasted pyrite wastes (PH) is mineralogically composed of well-crystalized iron oxides (hematite), jarosite, and quartz, with subordinate amounts of phyllosilicates (mica and kaolinite), feldspars, and barite. Hematite is responsible for the distinctive weak red color (Munsell 10R 4/2) of this Technosol. The essential mineralogy is in line with that described in the literature for historic pyrite ash wastes of the Rio Tinto mining area [40,41]. The XRD patterns displayed a high background signal indicating the occurrence of amorphous or poorly ordered material in the PH samples. Moreover, the FESEM-EDS examination (Figure 4) allowed the identification of anglesite, often forming overgrowths on barite crystals, and confirmed the presence of abundant iron oxide aggregates with a porous texture (Figure 4a). EPMA analysis of representative hematite particles (Table 1) showed that they are almost chemically pure with only trace amounts (less than 0.5 wt.%) of Cu, As, Sb and S. The EPMA study also revealed Pb-rich barite veins filling pre-existing cracks within barite (Figure 4b).

Table 1. Mineral composition of the Technosols and EPMA analysis of selected mineral particles.

Technosol	**Peña de Hierro (PH)**					**Zarandas (ZA)**					**La Naya (LN)**			
Major minerals Accessories	Hem + Jrs + Qz Mca + Fsp + Brt + Ang					Mca + Chl/Kln + Qz ± Jrs ± Py Fsp + Brt ± Hem ± Jrs ± Gp					Qz + Py + Mca ± Jrs Fsp + Brt + Ang ± Jrs ± Hem ± Gp			
Oxides (wt.%)	Hem_1	Hem_2	Hem_3	Ang_1	Ang_2	Jarosite-like minerals				Ang	Jarosite-like minerals		Pb-rich phosphate	
Fe_2O_3	99.74	99.17	97.96			45.78	27.94	42.38	53.73		38.02	37.45	7.21	4.34
SO_3	0.05	0.03	0.03	25.60	27.05	17.93	14.01	23.44	21.97	26.17	23.66	22.88	5.29	4.48
As_2O_5		0.04				4.00	9.88	2.66	4.97		0.70	3.14	1.67	2.34
Sb_2O_5	0.04	0.05	0.02	0.05	0.05	0.15	3.55	0.20	0.11		0.34	0.44	0.07	0.13
P_2O_5													12.13	11.67
PbO				73.97	72.19	1.40	12.55	8.30	1.98	73.11	14.88	12.31	32.60	31.69
CuO	0.05	0.05	0.03			0.24	0.24	0.68	0.21		0.45	0.20	0.13	0.13
ZnO							0.06	0.06						
K_2O						1.24	0.53	1.19	1.40		1.54	3.68	0.39	0.41

Mineral abbreviations: Ang (anglesite); Brt (barite); Chl (chlorite); Fsp (feldspar); Gp (gypsum); Hem (hematite); Jrs (jarosite-like minerals); Kln (kaolinite); Mca (mica); Py (pyrite); Qz (quartz).

The slag-contaminated soil samples from Zarandas (ZA) are made up of quartz, phyllosilicates (mica, chlorite, and/or kaolinite), and feldspars along with variable quantities of jarosite (up to 25 wt.%) and accessory hematite, barite, and gypsum. This Technosol contains numerous copper slag fragments consisting of feathery crystals of fayalite with the interstices filled with glassy material (Figure 4c), in which tiny crystals of magnetite and more rarely matte particles and spherical copper nanoparticles are disseminated, as detected by FESEM-BSE-EDS (Figure 4d). The fayalitic slag often had a vesicular texture with jarosite-lined voids. In addition, the EDS spectra indicated the occurrence of As-bearing iron mineral particles attributable to amorphous ferric arsenate or scorodite, and complex phase mixtures containing S-Fe-Pb-As-(Cu)-(Sb). The results of EPMA analyses (Table 1) of selected micro-areas suggest that the chemical composition of such phases may be compatible with jarosite-like minerals (Pb-jarosite and Pb-As-jarosite) that appear mixed with iron oxides. Interestingly, the sample ZA-3 showed a strikingly high content of pyrite (20–25 wt.%), most likely sourced from sulfide ores used for manufacturing sulfuric acid in a plant adjacent to the smelter site. The presence of readily water-soluble sulfate salts in the slag-contaminated soil (Figure 5a) and the widespread occurrence of efflorescent sulfate minerals at seepage points of the slag dumps [24], support the idea that these metallurgical wastes are chemically active long after the mining period.

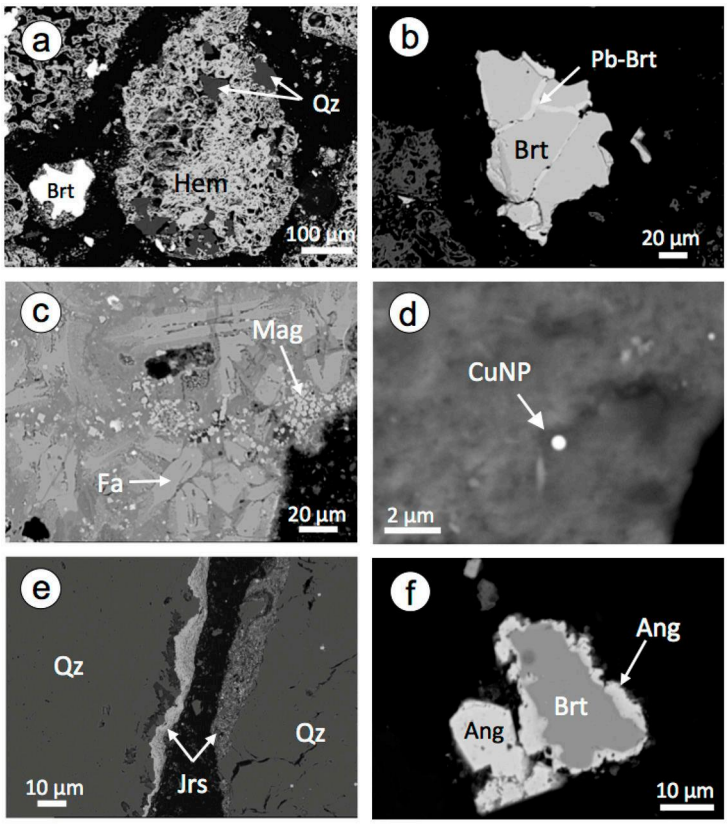

Figure 4. BSE images of polished sections showing in detail some textural and compositional features of the Technosols. (**a**) Aggregates of hematite (Hem) with inclusions of quartz (Qz) (sample PH-2); (**b**) Pb-rich barite (Pb-Brt) occurring as crack fillings in barite (sample PH-2); (**c**) slag artifact (sample ZA-1) composed of lath-shaped fayalite (Fa) and disseminated magnetite (Mag); (**d**) Copper nanoparticle (CuNP) embedded in the fine-grained matrix of the slag; (**e**) quartz (Qz) grains coated by Pb-As-bearing jarosite (Jrs) rims (sample LN-3); (**f**) Barite (Brt) crystals enclosed by anglesite (Ang) overgrowths (sample LN-3).

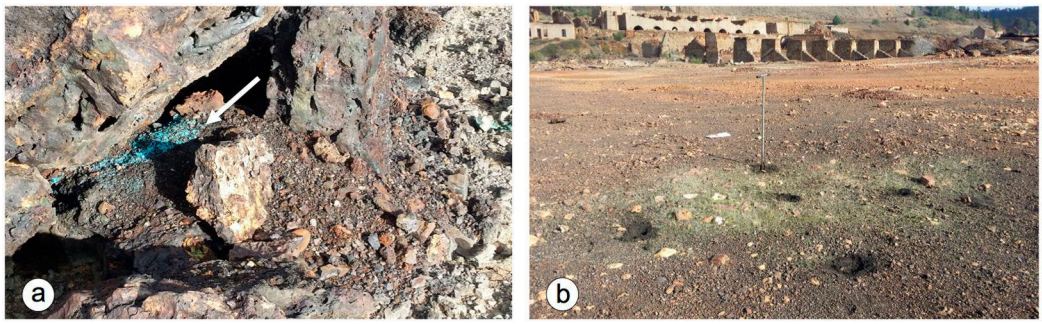

Figure 5. Field pictures of the Technosol ZA showing: (**a**) sulfate precipitate occurring as greenish blue efflorescence (white arrow) on the slag-contaminated soil; and (**b**) grass plants growing in the vicinity of the old smelter site on patches of soil with a moderately acid reaction.

The Technosol contaminated with leached ores from the heap leaching grounds of La Naya (LN) is comprised of mixtures of quartz, pyrite, mica, and jarosite-group minerals, with minor hematite, feldspars, barite, and anglesite. The FESEM-EDS study showed actively oxidizing crystals of pyrite with pitted surfaces. Jarosite was commonly found forming aggregates of euhedral pseudo-cubic crystals, but also appeared as coatings and rims covering grains of quartz or feldspars (Figure 4e). BSE images on polished sections revealed the occurrence of barite crystals enclosed by anglesite (Figure 4f). The jarosite-like

minerals contain significant amounts of Pb and As, and minor levels of Sb and Cu, as determined by EPMA analysis (Table 1), which also allowed us to infer the presence of Pb-rich phosphate particles with additional amounts of Fe, S, and As.

Therefore, the mining-affected soils are variable in mineral composition. Besides quartz, feldspars, and phyllosilicates, which are remnants of the original soil, a variety of heavy metal-bearing particles have been inferred as both primary contaminants of mine wastes (pyrite, hematite, copper slags) and secondary products of oxidation, dissolution, and precipitation reactions (jarosite-group minerals, amorphous iron oxyhydroxides, scorodite, anglesite, and gypsum). Overall, this mineral assemblage is consistent with the mineralogy of the alluvium contaminated by metal mining in the Rio Tinto area [16].

4.2. Total Acid Generating Capacity and Net Acidity

The soils of the areas under study were mostly extremely acidic in reaction when suspended in water, with pH_{H2O} values below 3.5, although the slag-contaminated soil samples (Technosol ZA) spanned a range of values between 3.0 and 5.4 (Table 2). A few patches of grass were seen at the site growing on the least acid soil (Figure 5b). They are all well aerated with Eh values consistently over +500 mV reflecting strongly oxidizing conditions. The soil electrical conductivity was always lower than 2 mS cm^{-1}, which is indicative of a relatively low soluble salt concentration in the soil solution. Similar results were obtained when the soil pH was measured in a 1M KCl solution (pH_{KCl} = 2.4–5.3), with the exception of the sample ZA-2 whose average pH_{KCl} value was 1.2 units lower than that measured in water. Nonetheless, the pH measured after complete oxidation of the sample with H_2O_2 varied noticeably among the different mine soils, depending on the relative abundance of pyrite. The lowest pH_{ox} levels (1.7–1.9) were found in the Technosol LN, where pyrite is a ubiquitous mineral, revealing a latent acid-generating capacity after sulfide oxidation. The Technosol PH showed pH_{ox} values close to those measured in water and KCl solution due to the lack or scarcity of sulfide minerals, while the pH_{ox} of the Technosol ZA varied between around 2.0 (samples ZA-1 and ZA-2) and 5.1 (sample ZA-3). However, it must be pointed out that the sample ZA-3 had a pH_{ox} of 3.0 after 2 min of contact with H_2O_2, indicating a likelihood of potential sulfidic acidity. Thus, all samples are potentially acid generating as the pH values after H_2O_2-reaction were less than 4.0 in the short term.

Table 2. Soil pH values, sulfur speciation, and major pools of acidity.

Sample	pH		Sulfur Speciation (wt.%)				Acidity (mmol H^+/kg)				
	H_2O	KCl	H_2O_2	S_{total}	S_{pyr}	S_{jar}	PSA	TAA	RA	TAG	NAG
PH-1	2.96	3.00	2.83	2.60	0.18	1.71	111	90	800	1001	144
PH-2	2.51	2.57	2.45	2.75	0.15	0.78	93	27	367	487	104
PH-3	2.14	2.58	2.41	2.63	0.16	1.07	97	36	503	636	93
ZA-1	2.96	2.75	1.86	2.53	0.16	2.44	102	19	1146	1267	442
ZA-2	4.56	3.36	2.20	0.55	0.11	0.24	66	10	110	186	632
ZA-3	5.35	5.34	5.08	6.80	3.54	1.78	2214	7	835	3056	240
LN-1	2.68	2.49	1.85	2.97	2.00	0.32	1248	26	151	1425	663
LN-2	2.51	2.44	1.65	3.15	1.42	1.66	890	30	780	1700	609
LN-3	3.02	3.01	1.78	1.67	1.26	0.33	786	31	153	971	463

PSA (Potential Sulfidic Acidity); TAA (Titratable Actual Acidity); RA (Retained Acidity); TAG (Total Acid Generation); NAG (Net Acid Generation).

Even though pH is a primary index for soil acidity, it gives no indication of the total acid-generating capacity of the Technosols. The measurement of total sulfur (S_{total}) is an option widely used for estimating the maximum potential acidity from sulfide sources [34]. According to the S_{total} content measured in soil (Table 2), the potential acid release should be in the range of 340–4250 mmol H^+/kg. But this conservative approach overestimates the potential acid risk of the studied soils, in which a fraction of sulfur is in the form of jarosite and non-acid-producing sulfate minerals, such as gypsum and barite, and additionally,

no account is made for acid-neutralizing potential. This fact highlights the importance of quantifying the various pools of acidity in the mine soils (Table 2).

Among the acid-generating components of the soil, pyrite is by far the major contributor to acid production at the mine Technosols. As noted previously, no other sulfide minerals were detected in any sample. Based on the stoichiometry of pyrite oxidation, one mole of sulfur in pyrite produces two moles of protons through the reaction:

$$FeS_2 + {}^{15}/_4O_2 + {}^{7}/_2H_2O \rightarrow Fe(OH)_3 + 4H^+ + 2SO_4{}^{2-}$$

The content of S_{pyr} in the Technosol LN ranged from 1.26 to 2.00 wt.%, which is compatible with a latent acidity of 780–1250 mmol H^+/kg in soil, equivalent to a potential sulfidic acidity (PSA) of 38.6–61.2 kg H_2SO_4/t. Conversely, the S_{pyr} percent was quite low (0.15–0.18 wt.%) in the Technosol PH, confirming that very few remnants of unroasted sulfide ores were present in the soil contaminated with pyrite ashes. So, the latent acidity released from sulfide oxidation is expected to be consistently low (around 100 mmol H^+/kg equivalent to the production of 3.06 kg H_2SO_4/t). The acid-production capacity due to sulfide oxidation of the Technosol ZA varied from sample to sample, reaching a maximum of 2210 mmol H^+/kg (about 108 kg H_2SO_4/t) in the sample ZA-3 due to its high content of pyrite (S_{pyr} = 3.54 wt.%). The samples ZA-1 and ZA-2 showed a latent acidity (3.4–4.9 kg H_2SO_4/t) considerably lower than the median acid producing potential (47.5 kg H_2SO_4/t) of the Zarandas slag deposit [24].

Soluble and exchangeable acidity existing in the soil as a consequence of previous oxidation of pyrite was relatively low, with mean values of titratable actual acidity (TAA) ranging from 12 mmol H^+/kg (Technosol ZA) to 51 mmol H^+/kg (Technosol PH). These findings are indicative that acidic conditions resulting from either dissolution of readily soluble sulfates (actual acidity), or acid adsorbed at the exchange sites of the soil particles (replaceable acidity), are limited. The eventual occurrence of soluble sulfate salts is likely to be an instantaneous source of acidity upon dissolution [42], and the presence of exchangeable and soluble Al species may be also an additional component of the existing acidity [37].

It is noteworthy that the oxidation of pyrite did not reach completion. The mine soils contain actively oxidizing crystals of pyrite in variable amounts, and their oxidation products other than iron oxy-hydroxides and sulfuric acid were and are being formed, such as poorly soluble iron hydroxy sulfate minerals. In fact, a portion of the sulfate ions and acid generated by pyrite oxidation appears to be stored in jarosite-like minerals, which are a major source of retained acidity under the oxidizing and acidic (pH < 3.5) conditions prevailing in the mine soils, where they are present in substantial amounts. The retained acidity values were within the ranges of 360–800 mmol H^+/kg (Technosol PH), 110–1150 mmol H^+/kg (Technosol ZA), and 150–780 mmol H^+/kg (Technosol LN) on the basis of the content of S_{jar} in soil samples. This retained acidity (RA) represents the less available form of the existing acidity that may be slowly released over time by hydrolysis of jarosite-like minerals [34], assuming that one mole of sulfur in jarosite would produce 1.5 moles of protons through the reaction:

$$KFe_3(SO_4)_2(OH)_6 + 3H_2O \rightarrow K^+ + 3Fe(OH)_3 + 2SO^{2-} + 3H^+$$

Thus, the total acid generating (TAG) capacity of the Technosols, comprising potential sulfidic acidity and existing acidity (i.e., soluble plus exchangeable and retained acidity) showed the following order of increasing acidity expressed in mmol H^+/kg: Technosol PH (710) < Technosol $ZA_{SAMPLES\ 1-2}$ (730) < Technosol LN (1360) < Technosol $ZA_{SAMPLE\ 3}$ (3060). The potential sulfidic acidity of the Technosol LN and Technosol ZA (sampling site ZA-3) accounted for 71% and 73% of TAG, respectively. The acidity retained in jarosite was the dominant acidity pool in the Technosol PH and Technosol ZA (sampling sites ZA-1 and ZA-2), comprising 79%–86% of TAG, respectively, while actual acidity accounted for less than 7% (Figure 6).

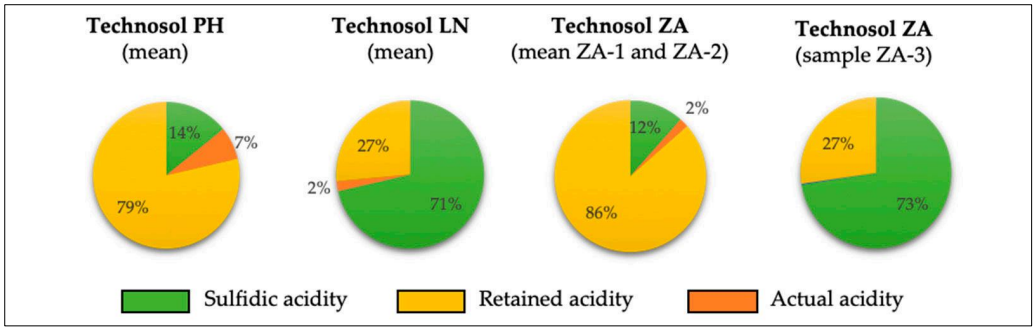

Figure 6. Pie charts comparing the percentage distribution of sulfidic, retained, and actual acidity in the Technosols.

The Technosols have a low buffering capacity to neutralize the amount of acid that is being produced, or has been produced, given the lack of carbonates and other reactive acid-neutralizing minerals. Certainly, the results from an H_2O_2-based static test (Table 2) suggest that the sulfidic acidity is unable to be neutralized by potential acid-consuming phases, as shown by the following mean values of net acid generation (NAG): 114 mmol H^+/kg (Technosol PH), 438 mmol H^+/kg (Technosol ZA) and 578 mmol H^+/kg (Technosol LN). It should be noted that these figures are an estimate of the acidity in the surface 20 cm only, and the NAG values provide a direct measure of the net amount of acid produced by the soil assuming that acid generation and acid neutralization reactions occur simultaneously [43,44]. The occurrence of labile or existing acidity is another indication that the acid-neutralizing capacity of the mine soils seems to be not effective [37].

4.3. Heavy Metal Contamination

The total contents of PTEs in the mine soil samples are listed in Table 3, including those below the detection limit and over-range values. For comparative purposes, Table 3 also provides PTE contents compiled from the literature for mine wastes of the Rio Tinto mining area, pedogeochemical baseline levels, and reference values for PTEs in soils around the abandoned mines of the IPB.

Trace element geochemistry of the Technosols is clearly dominated by chalcophile elements, with Cu, Pb, As and Zn being the major contributors to the heavy metal budget. Unusually high contents of Cu (>10,000 mg kg^{-1}), Pb (>5000 mg kg^{-1}), As (>5000 mg kg^{-1}), and Zn (up to 3810 mg kg^{-1}) were measured in some slag-contaminated soil samples. It was found that the Pb content also exceeded 5000 mg kg^{-1} in all Technosol LN samples. These levels are more than two orders of magnitude above the regional baseline values, and they are comparable, or even higher, than those reported for mine wastes in the reference sites [24,40,41,45], as well as in other severely polluted mine soils of the IPB [27] and elsewhere in the world [46,47].

Furthermore, the contents of Bi (up to 260 mg kg^{-1}), Tl (up to 81 mg kg^{-1}), Sb (up to 42 mg kg^{-1}), and Cd (up to 28 mg kg^{-1}) were higher than those reported in the literature for natural soils and sediments [48]. In contrast to the chalcophile elements, the contents of Cr, Ni, and Co in most samples were found to be within, or slightly above, the typical range of the regional soils, indicating that they are naturally occurring. However, some contamination was found at the sampling site ZA-3, where the Co content was over 7-fold higher than the baseline level.

As evidenced from the results of mineral characterization, a considerable amount of PTEs seems to be bonded to secondary phases, such as jarosite-group minerals, iron oxyhydroxides, anglesite, and Pb-rich phosphate, which would have scavenged contaminants from the soil solution, notably Pb and As, through structural incorporation, surface adsorption or co-precipitation mechanisms. Jarosite minerals also likely served as a secondary host of Tl, as described in mine soils and AMD systems elsewhere [40,49]. Altogether, the above findings support the claim that soil acted not only as a storage for heavy metal-bearing

particles (pyrite, hematite, fayalitic slag, etc.) eroded from the wasteland, but also as a geochemical sink for PTEs released into solution by sulfide oxidation. The content of Cu in the Technosol ZA was between 50 and 300 times higher compared to the background. This abnormally high Cu content could be reasonably explained by the occurrence of slag fragments with entrapped matte particles that represent the copper loss in the slag during the smelting process.

Table 3. Chemical composition of trace elements measured in the bulk soil samples (<2 mm) by ICP-OES and reference values reported for comparison.

Element (mg kg^{-1})	As	Bi	Cd	Co	Cr	Cu	Ni	Pb	Sb	Tl	Zn
Detection Limit	3	2	0.3	1	1	1	1	3	5	5	1
Technosol PH											
PH-1	319	86	3.0	46	18	504	8	2340	<5	12	415
PH-2	150	108	3.3	46	7	400	8	3420	19	17	314
PH-3	152	100	3.1	47	9	384	9	2980	19	15	311
Roasted pyrite wastes (mean)											
Peña de Hierro [1] (N = 3)	665		2.3	36	21	474	11	2707			561
Planes [2] (N = 3)	1026					338		4515		70	267
Technosol ZA											
ZA-1	>5000	121	4.9	15	67	1660	24	>5000	42	81	576
ZA-2	532	20	1.0	43	89	4370	70	1850	11	<5	1790
ZA-3	3630	174	27.8	142	149	>10,000	101	>5000	24	16	3810
Copper slag wastes (mean)											
Zarandas [3] (N = 6)	110	5.6	4.5	283		4410	17	2088	380	5.5	
Technosol LN											
LN-1	868	133	1.7	12	21	939	5	>5000	6	15	655
LN-2	2030	260	1.7	7	31	178	5	>5000	7	56	400
LN-3	1040	116	1.1	8	14	199	6	>5000	<5	9	266
Heap leaching wastes											
Rio Tinto [4]	4310		0.7	25	77	537	11	7056	765	9	478
Reference values											
Regional geochemical baseline [5]	25			19	95	32	35	38			76
Mine soils of Iberian Pyrite Belt [6]	361		0.7	15	78	412	19	1080			298

Data source: [1] [40]; [2] [41]; [3] [24]; [4] [45]; [5] [50]; [6] [51].

Based on calculation methods that relate the total contents of PTEs in soil and their regional baseline levels, an estimation of the extent of multi-element contamination was made by taking the four highest enriched elements (As, Cu, Pb, and Zn) and using the following formula [52]:

$$C_d = \sum_{i=1}^{n} C_f^i$$

where C_d is the contamination degree, n is the number of considered elements (n = 4 in this study), and C_f is the contamination factor for a given element (i), which is defined as the quotient between the PTE content measured in the soil (C_s) and the regional baseline (C_b), as follows:

$$C_f = \frac{C_s}{C_b}$$

The mean C_f values of the four elements of concern were in the following descending order: Pb ≫ Cu > As > Zn for Technosol PH; Cu > Pb > As ≫ Zn for Technosol ZA; and Pb ≫ As ≫ Cu > Zn for Technosol LN.

The pollution load index (PLI) of Tomlinson [53] was also used to calculate the degree of soil contamination as a geometric mean of C_f values based on the following formula:

$$PLI = \left(C_{f\,As} \times C_{f\,Cu} \times C_{f\,Pb} \times C_{f\,Zn}\right)^{1/4}$$

The results showed that all samples of the Technosols ZA and LN were found to be ultra-high contaminated, with ZA-3 (C_d = 639) and ZA-1 (C_d = 391) being the most contaminated sampling sites (Figure 7), whereas the samples of the Technosol PH (C_d = 96–113) showed extremely high contamination, according to the descriptive classes of soil contamination [54]. Consistently, the PLI values ranged widely from 12 (samples PH-2 and PH-3) to a maximum of 132 (sample ZA-3).

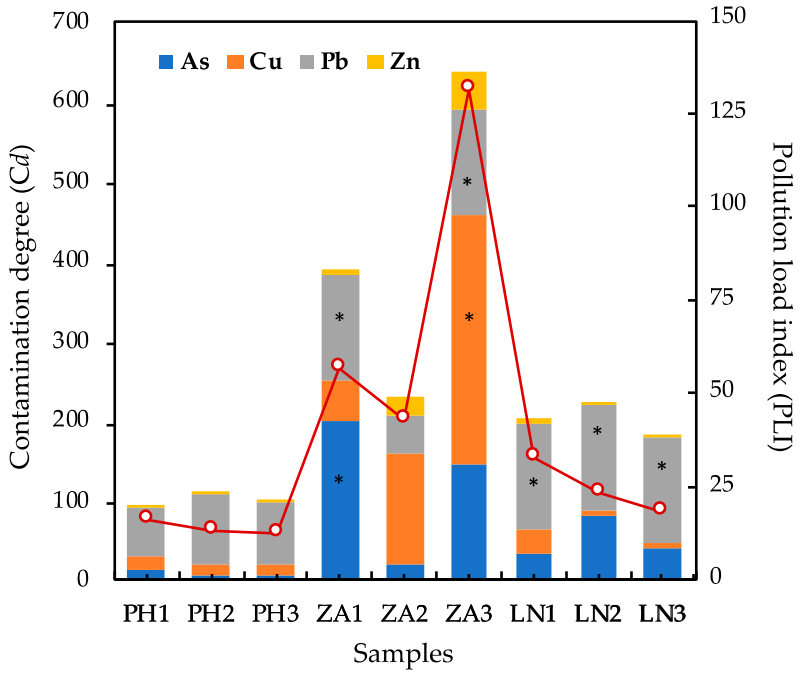

Figure 7. Combined bar and line chart showing the contamination degree (C_d) and the pollution load index (PLI) values, respectively. The stacked bar graph is divided into sub-bars that represent the proportional contribution or contamination factor (C_f) of each element. C_f values determined by using the maximum values of the detection range are marked with asterisks.

4.4. Potential for Metal Release

The results from the short-term leach test conducted to estimate the potential metal release are given in Table 4, along with pH, Eh, and electrical conductivity values, as well as the anion composition (sulfate, nitrate, and chloride) of the leach solutions. The PTE concentrations leached from the soil samples are compared graphically to the total soil contents in Figure 8.

The eluates recovered from the leaching test had pH values equal to or slightly higher than soil pH values (in water). The Technosols PH and LN as well as the sample ZA-1 produced extremely acidic solutions (pH = 2.5–3.5), while the extract solutions from the samples ZA-2 and ZA-3 were moderately acidic (pH = 5.2–5.7). The leachates were characterized by a high redox potential (Eh > 570 mV) with the exception of the sample ZA-3 (Eh = 381 mV). Sulfate was the prevailing anion in all soil extracts, reaching concentrations of up to 652 mg L^{-1} in the sample PH-1. The highest values of electrical conductivity (up to 1.13 mS cm^{-1}) were also observed in the Technosol PH, which is consistent with the water-soluble salt (sulfate) concentration.

Table 4. Physicochemical parameters and trace element concentrations extracted from the Technosols by applying the standard EN-12457-4 leaching test.

Technosol Sample	pH	Eh mV	CE mS/cm	Sulfate mg/L	Nitrate µg/L	Chloride mg/L	Cr µg/L	Ni µg/L	Cu mg/L	Zn mg/L	As µg/L	Cd µg/L	Pb mg/L
PH-1	3.34	665	0.71	652	440	13	1.6	14.8	5.18	2.25	1.9	37.8	0.05
PH-2	2.50	747	1.13	384	330	1.7	1.1	<0.2	0.23	0.49	3.4	1.8	2.62
PH-3	2.74	731	1.12	618	320	2.4	5.5	7.3	1.43	0.79	7.7	10.4	0.31
ZA-1	3.24	668	0.63	343	540	1.7	1.7	9.2	2.57	2.77	97.5	21.3	0.04
ZA-2	5.18	688	0.03	25	630	1.5	<0.4	2.7	0.14	0.03	0.8	0.2	0.02
ZA-3	5.66	381	0.28	170	560	4.7	<0.4	135.9	55.6	0.79	18.3	36.1	0.02
LN-1	3.07	574	0.49	191	230	6.6	3.2	2.6	0.72	0.04	35.0	0.7	5.55
LN-2	3.22	612	0.59	215	240	1.2	6.9	3.6	0.13	0.24	4.8	3.3	4.36
LN-3	3.54	571	0.18	80	270	2.6	<0.4	<0.2	0.08	0.07	5.1	0.3	9.02

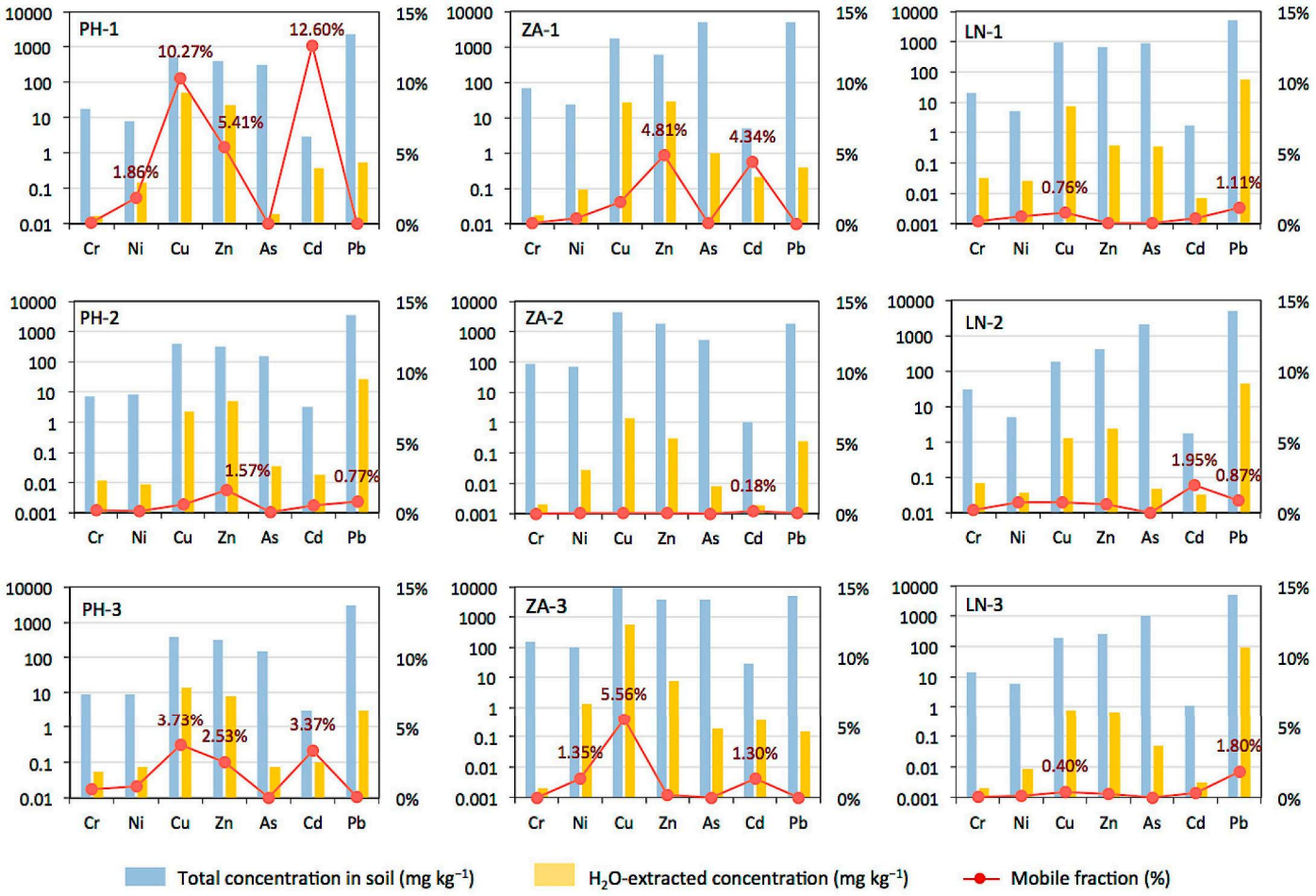

Figure 8. Bar charts comparing the contents of trace elements measured in soil and those measured in leachate (extracted with deionized water), and line charts showing the fraction (%) of metals and metalloids released from the soil (mobile fraction).

The acid leach solutions resulting from the minesoil-water interaction enhanced the solubilization of PTEs to a variable extent, depending on the element involved and the matrix. Copper, Zn, Pb, Cd, and As, in this order of decreasing median concentration, were the most abundant PTEs in the leachates of the Technosols PH and ZA, with peak values of 55.6 mg L^{-1} for Cu (sample ZA-3), 2.25 mg L^{-1} for Zn (sample ZA-1), 2.62 mg L^{-1} for Pb (sample PH-2), 97.5 µg L^{-1} for As (sample ZA-1), and 37.8 µg L^{-1} for Cd (sample PH-1). Interestingly, Pb was released substantially more easily from the Technosol LN,

where pyrite is a ubiquitous phase, with a maximum extraction yield of 9.02 mg L^{-1}. The other PTEs measured in the leachates (Cr and Ni) were found at levels usually below 0.1 mg L^{-1}. The soluble concentrations of Cu and Pb, but also As and Cd, greatly exceeded the safe drinking water standards established in international water quality guidelines (e.g., European Council Directive 98/83/EC and World Health Organization).

In general, the potential metal release from the Technosols when contacted with water is markedly lower in magnitude than that reported for abandoned mine wastes of the Rio Tinto area [45], although Cu and Pb were leached from some soil samples at comparable levels. There are likely to be important contributions of PTEs to surface and shallow groundwater chemistry, which may have an adverse impact on the quality of receiving water bodies. Therefore, in addition to the mine wastes, the mine soils generate drainage that flows into the headwaters of the nearby Tinto River and contributes to its acidification and dissolved metal load.

The samples were classified using a modified Ficklin plot [55] on the basis of the dissolved metal load (sum of Cd, Cu, Ni, Pb, and Zn concentrations) and the pH values of the leach solutions (Figure 9). Most of the samples lie in the acid to high-acid and high-metal to extreme-metal fields, thus showing a hydro-chemical signature similar to that of acid mine waters of the IPB [56–58]. Exceptionally, the sample ZA-3 was classified in the near-neutral extreme-metal class due to the elevated concentration of Cu released into the solution. This can be attributed to the occurrence of soluble hydrated salts that can be easily dissolved under the leach conditions, and serve as a transient pool of available Cu.

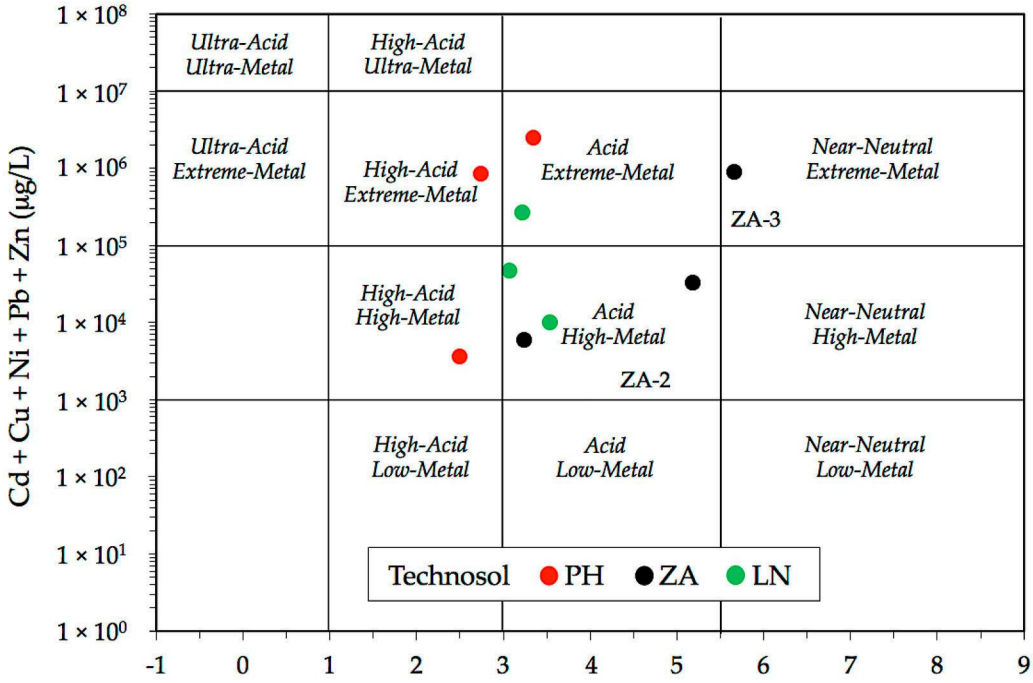

Figure 9. Ficklin diagram plotting the sum of metal concentrations leached from the soil samples against the pH of the leachates.

To further compare the leach test results, the line chart of Figure 8 shows the proportion of the total metal pool that was released from the soil and may be available for plant uptake and leached by percolation. Notwithstanding the high total contents of PTEs occurring in soil, the average values of the water-extractable proportion (Figure 10) were relatively low (less than 5.5%), suggesting that metal mobility was limited for all elements, with maximum release values of 12.60% for Cd and 10.27% for Cu. It is important to note that some of these percentages correspond, nevertheless, to elevated contents of PTEs, which is an issue of concern. The extremely high degree of contamination of the Technosols did

not have a significant correlative effect on the amount of extractable PTEs. This is in good agreement with the results obtained from mine soil samples elsewhere in the IPB [25,59].

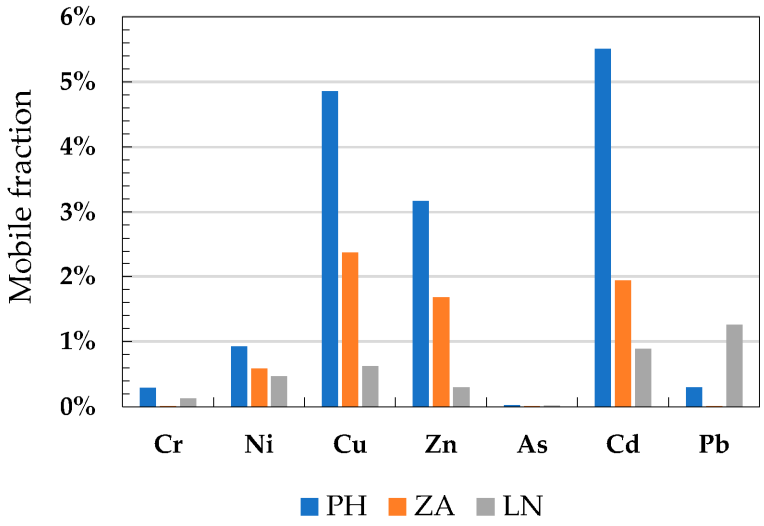

Figure 10. Average values of the trace element fraction extracted from the Technosols by applying the standard EN-12457-4 leaching test.

In most samples PTEs showed the following order of decreasing mobility: Cu > Zn > Cd > Ni > Pb > Cr > As, although Pb was more efficiently leached from the Technosol LN. Accordingly, Cd, Cu, and Zn are the most labile PTEs in mine soils, as they are likely stored in soluble sulfate salts. The fraction of As extracted in the course of the leach test was found to be practically negligible (less than 0.1%), despite the high level of contamination occurring in the Technosols. The low leachability of As with water is consistent with the fact that most of this contaminant could be accommodated by arsenate-for-sulfate substitution in the crystal structure of jarosite [60,61], which is sparingly soluble in water under the acidic and oxidizing conditions prevailing in the mine sites. Besides, the solubility of As could have been limited by adsorption on, or coprecipitation with, iron oxyhydroxide minerals [62] and precipitation of arsenic minerals like scorodite [63], as inferred from the mineralogical analysis. Similarly, the low concentration of Pb in the leach solutions indicated that this heavy metal resides to a large extent in the fixed pool, tightly bonded to soil constituents such as jarosite-like minerals, anglesite, and Pb-bearing phosphate phases. From these findings, it can be arguably claimed that the environmental availability of As and Pb in the short term is very low because, in general, they were not leached abundantly from the mine soils.

According to the aqueous speciation calculations performed using the PHREEQC code [64] with the wateq4f thermodynamic database, the most labile PTEs in soil occurred in the leach solutions in the form of a variety of ionic species (Table 5).

Free metal ion (M^{2+}) was the largely dominant form over the pH range of 2.5 to 5.7, with median values accounting for 100% of dissolved Cd, around 85% of dissolved Cu, Ni, and Zn, and about 70% of dissolved Pb. Sulfate species (MSO_4^0) accounted for most of the remaining species, comprising between 8% and 29% of the median dissolved load of Ni, Cu, Zn, and Pb. Other inorganic complexes such as chloride, nitrate, and hydroxyl ions were not predicted to be significant complexing ligands, because their concentrations in the acid solutions leached from the Technosols were not high enough to be competitive with sulfate ions for PTE speciation. Arsenic release from the soil was present as oxyanion species in the form of arsenate, mainly $H_2AsO_4^-$ and, to a lesser extent, H_3AsO_4. Similar speciation patterns have been reported in previous studies on the modeling of PTE behavior in acidic drainage waters [56,65].

Table 5. Distribution of aqueous species of trace elements of environmental significance in the acid leach solutions indicated as a percent of the total dissolved species.

Element	Species (%)	PH-1	PH-2	PH-3	ZA-1	ZA-2	ZA-3	LN-1	LN-2	LN-3	Median
As	$H_2AsO_4^-$	93.52	65.01	77.15	91.04	100	95.23	86.82	90.53	95.09	91.04
	$HAsO_4^{2-}$						4.77				
	H_3AsO_4	6.48	34.99	22.85	8.96			13.18	9.47	4.91	8.96
Cd	Cd^{2+}	100	100	100	100	100	100	100	100	100	100
Cu	Cu^{2+}	90.29	75.31	82.04	73.28	96.26	93.59	82.76	86.57	89.49	86.57
	$CuSO_4$	9.68	24.69	17.95	26.71	3.61	5.58	17.21	13.43	10.51	13.43
	$CuOH^+$					0.13	0.28				
	$Cu(OH)_2$						0.22				
	$CuCl^+$	0.03		0.01	0.01		0.02	0.03			0.01
	$Cu_2(OH)_2^{2+}$						0.32				
Ni	Ni^{2+}	91.32		83.42	74.71	96.58	94.86	83.68	87.4		83.68
	$NiSO_4$	8.68		16.58	25.29	3.42	5.14	16.32	12.6		8.68
Pb	Pb^{2+}	77.33	51.49	62.29	48.79	90.44	86.15	62.89	69.81	74.66	69.81
	$PbSO_4$	21.87	47.53	36.87	50.18	9.56	13.85	36.4	29.84	25.06	29.84
	$PbCl^+$	0.44	0.06	0.09				0.34	0.06	0.17	0.06
	$Pb(SO_4)_2^{2-}$	0.36	0.91	0.75	1.03			0.37	0.28	0.12	0.36
Zn	Zn^{2+}	88.78	72.13	79.45	69.91	95.86	93.52	80.5	84.72	88.09	84.72
	$ZnSO_4$	10.9	27.02	19.9	29.12	4.11	6.38	19.17	15.05	11.82	15.05
	$ZnOH^+$					0.01	0.02				
	$Zn(SO_4)_2^{2-}$	0.29	0.84	0.64	0.97	0.01	0.05	0.31	0.22	0.09	0.29
	$ZnCl^+$	0.03		0.01	0.01	0.01	0.02	0.03			0.01

The leach solutions from the Technosol ZA displayed a more complex speciation pattern. The activity of sulfate species decreased noticeably with increasing pH from 3.2 (sample ZA-1) to 5.7 (sample ZA-3), while the contribution of hydroxyl complexes of Cu and Zn in the aqueous solution was shown to increase, although to a still relatively very low level. Therefore, the distribution of major species seems to be related to the solution pH.

The saturation index (SI) values for solid phases were computed with PHREEQC by comparing measured solution activity, expressed as an ion activity product (IAP) with the theoretical solubility product constant (Ksp), as follows:

$$SI = log\left(\frac{IAP}{K_{sp}}\right)$$

The geochemical modeling approach of the mine soil-water interaction indicated a slight supersaturation with respect to anglesite (SI = 0.16–0.21) in the Technosol LN, which is consistent with the observed mineralogy, and also with copper-rich secondary minerals, like brochantite (SI = 2.15) and antlerite (SI = 1.19), that may form from evaporation at the site ZA-3. The extracts were undersaturated (SI < 0) with all the Cd- and Zn-bearing minerals in the database, so it is unlikely that such phases are present as precipitates under the prevailing conditions.

5. Conclusions

This paper has highlighted the importance of determining the various forms of acidity and the potential for the release and mobilization of PTEs at historically contaminated mine sites in order to assess the risk of water contamination by leaching through the soil. Specifically, it has been shown that soils contaminated with hazardous mine waste at Rio Tinto have become secondary source areas of acidic effluents and harmful contaminants to the surrounding environment. These soils have a remarkable acid-production capacity due to sulfide oxidation and an existing acidity, albeit often neglected, that may be slowly released by hydrolysis of jarosite-like minerals. It was also found that they contain anomalous

contents of As, Pb, Cu, and Zn, mostly linked to heavy metal-bearing particles inherited from the wasteland, but also structurally bound in soil-forming minerals thus limiting their environmental significance. Notwithstanding, there still is a persistent reservoir of readily leachable Cu, Cd, Zn, and Pb, in the form of free metal ions and sulfate species that are being flushed into the Tinto River system. The extreme acidity and metal release will likely be maintained over time due to the occurrence of actively oxidizing pyrite. Ultimately, in light of these findings, an effective mine land reclamation program should not be limited to abandoned mine wastes but should also ensure that acidity and metal mobility in the mining-affected soils are reduced to environmentally sustainable levels.

Supplementary Materials: The following supporting information can be downloaded at: https://www.mdpi.com/article/10.3390/min13040456/s1, Table S1: ICP-OES and ICP-MS operating conditions.

Author Contributions: S.F.-L.: investigation; formal analysis; data curation; software; visualization; writing-original draft preparation. J.C.F.-C.: investigation; conceptualization; methodology; visualization; validation; original draft preparation; supervision; project administration; M.I.G.: investigation; formal analysis; methodology; validation; writing-review and editing; resources. E.M.: investigation; formal analysis; validation; writing-review and editing. C.B.-B.: investigation; formal analysis; validation; writing-review and editing. I.G.: investigation; formal analysis; validation; writing-review and editing. All authors have read and agreed to the published version of the manuscript.

Funding: This research was supported by the Regional Government of Andalusia (Spain) and the European Regional Development Fund Andalusia 2014–2020 through Project P-18-TP-3503, in collaboration with DSM Soluciones Medioambientales.

Data Availability Statement: The authors confirm that the data supporting the findings of this study are available within the manuscript.

Conflicts of Interest: The authors declare no conflict of interest.

Abbreviations

ABA: Acid-Base Accounting. AMD: Acid Mine Drainage. ASD: Acid Soil Drainage. ASTM: American Standard Test Method. BSE: Back Scattered Electron. EC: Electrical Conductivity. EDS: Energy Dispersive X-ray Spectroscopy. EPMA: Electron Probe Micro Analysis. FESEM: Field-Emission Scanning Electron Microscopy. ICP-MS: Inductively Coupled Plasma Mass Spectrometry. ICP-OES: Inductively Coupled Plasma Optical Emission Spectrometry. IPB: Iberian Pyrite Belt. ISO: International Organization for Standardization. IUSS: International Union of Soil Sciences. NAG: Net Acid Generation. PLI: Pollution Load Index. PSA: Potential Sulfidic Acidity. PTE: Potentially Toxic Trace Elements. RA: Retained Acidity. RSD: Relative Standard Deviation. RTC: Rio Tinto Company. SE: Secondary Electron. SI: Saturation Index. TAA: Titratable Actual Acidity. TAG: Total Acid Generation. VMS: Volcanogenic Massive Sulfide. WRB: World Reference Base. XRD: X-ray Diffraction.

References

1. Salomons, W. Environmental impact of metals derived from mining activities. *J. Geochem. Explor.* **1995**, *53*, 53–56.
2. Nordstrom, D.K. Hydrogeochemical processes governing the origin, transport and fate of major and trace elements from mine wastes and mineralized rock to surface waters. *Appl. Geochem.* **2011**, *26*, 1777–1791. [CrossRef]
3. Hudson-Edwards, K. Tackling mine wastes. *Science* **2016**, *352*, 288–290. [CrossRef]
4. Plumlee, G.S.; Morman, S.A. Mine wastes and human health. *Elements* **2011**, *7*, 399–404. [CrossRef]
5. Sánchez de la Campa, A.; De la Rosa, J.D.; Fernández-Caliani, J.C.; González-Castanedo, Y. Impact of abandoned mine waste on atmospheric respirable particulate matter in the historic mining district of Rio Tinto (Iberian Pyrite Belt). *Environ. Res.* **2011**, *111*, 1018–1023. [CrossRef] [PubMed]
6. Castillo, S.; De la Rosa, J.; Sánchez de la Campa, A.; González-Castanedo, Y.; Fernández-Caliani, J.C.; González, I.; Romero, A. Contribution of mine wastes to atmospheric metal deposition in the surrounding area of an abandoned heavily polluted mining district (Rio Tinto mines, Spain). *Sci. Total Environ.* **2013**, *449*, 363–372. [CrossRef] [PubMed]
7. Romero, A.; González, I.; Martín, J.M.; Vázquez, M.A.; Ortiz, P. Risk assessment of particle dispersion and trace element contamination from mine-waste dumps. *Environ. Geochem. Health* **2015**, *37*, 273–286. [CrossRef]

8. Helser, J.; Vassilieva, E.; Cappuyns, V. Environmental and human health risk assessment of sulfidic mine waste: Bioaccessibility, leaching and mineralogy. *J. Hazard. Mat.* **2022**, *424*, 127313. [CrossRef]
9. Jambor, J.L. Mine-waste mineralogy and mineralogical perspectives of acid-base accounting. In *Environmental Aspects of Mine Wastes*; Jambor, J.L., Blowes, D.W., Ritchie, A.I.M., Eds.; Mineralogical Association of Canada Short Course: Ottawa, ON, Canada, 2003; Volume 31, pp. 117–146.
10. Lottermoser, B.G. Mine Wastes. In *Characterization, Treatment and Environmental Impacts*, 3rd ed.; Springer: Berlin/Heidelberg, Germany, 2010.
11. Jamieson, H.E.; Stephen, S.R.; Parsons, M.B. Mineralogical characterization of mine waste. *Appl. Geochem.* **2015**, *57*, 85–105. [CrossRef]
12. Cánovas, C.R.; De La Aleja, C.G.; Macías, F.; Pérez-López, R.; Basallote, M.D.; Olías, M.; Nieto, J.M. Mineral reactivity in sulphide mine wastes: Influence of mineralogy and grain size on metal release. *Eur. J. Mineral.* **2019**, *31*, 263–273. [CrossRef]
13. Arranz, J.C.; Rodríguez-Gómez, V.; Fernández-Naranjo, F.J.; Vadillo, L. Assessment of the pollution potential of a special case of abandoned sulfide tailings impoundment in Riotinto mining district (SW Spain). *Environ. Sci. Pollut. Res.* **2021**, *28*, 14054–14067. [CrossRef]
14. IUSS Working Group WRB. World Reference Base for Soil Resources 2014. In *International Soil Classification System for Naming Soils and Creating Legends for Soil Maps, Update 2015*; World Soil Resources Reports; FAO: Rome, Italy, 2015; Volume 106, pp. 1–192.
15. Gómez-González, M.A.; Voegelin, A.; García-Guinea, J.; Bolea, E.; Laborda, F.; Garrido, F. Colloidal mobilization of arsenic from mining-affected soils by surface runoff. *Chemosphere* **2016**, *144*, 1123–1131. [CrossRef] [PubMed]
16. Hudson-Edwards, K.A.; Schell, C.; Macklin, M.G. Mineralogy and geochemistry of alluvium contaminated by metal mining in the Rio Tinto area, southwest Spain. *Appl. Geochem.* **1999**, *14*, 1015–1030. [CrossRef]
17. García-Palomero, F. Mineralizaciones de Riotinto (Huelva): Geología, génesis y modelos geológicos para su explotación y evaluación de reservas minerales. In *Recursos Minerales de España*; Martínez-Frías, J., García-Guinea, J., Eds.; Consejo Superior de Investigaciones Científicas, Textos Universitarios: Madrid, Spain, 1992; Volume 15, pp. 1325–1352.
18. Noble, A.C. Technical Report on the Riotinto Copper Project. 2022. Available online: https://atalayamining.com/wp-content/uploads/2022/09/Technical-Report-on-the-Riotinto-Project_Sept2022_FINAL.pdf (accessed on 2 February 2023).
19. De Mello, C.R.; Tornos, F.; Conde, C.; Tassinari, C.C.G.; Farci, A.; Vega, R. Geology, geochemistry, and geochronology of the giant Rio Tinto VMS deposit, Iberian Pyrite Belt, Spain. *Econ. Geol.* **2022**, *117*, 1149–1177. [CrossRef]
20. Dutrizac, J.E.; Jambor, J.L.; O'Reilly, J.B. Man's first use of jarosite: The pre-Roman mining-metallurgical operations at Rio Tinto, Spain. *Can. Min. Metall. Bull.* **1983**, *76*, 78–82.
21. Rothenberg, B.; García-Palomero, F. The Rio Tinto enigma-no more. *Inst. Archaeo-Metall. Stud. Newsl.* **1986**, *8*, 3–5.
22. Salkield, L.U. *A Technical History of the Rio Tinto Mines: Some Notes on Exploitation from Pre-Phoenician Times to the 1950s*; The Institution of Mining and Metallurgy: London, UK, 1987; p. 116.
23. Gallego, L.; Fernández-Caliani, J.C. Pyrite ore cargo spills as a source of soil pollution and ecological risk along the abandoned railway corridors of the Tharsis and Rio Tinto mines (Spain). *Environ. Monit. Assess.* **2023**, *195*, 97. [CrossRef] [PubMed]
24. Lottermoser, B.G. Evaporative mineral precipitates from a historical smelting slag dump, Rio Tinto, Spain. *Neues Jb. Miner. Abh.* **2005**, *181*, 183–190. [CrossRef]
25. Chopin, E.I.B.; Alloway, B.J. Trace element partitioning and soil particle characterisation around mining and smelting areas at Tharsis, Riotinto and Huelva, SW Spain. *Sci. Total Environ.* **2007**, *373*, 488–500. [CrossRef] [PubMed]
26. López, M.; González, I.; Romero, A. Trace element contamination of agricultural soils affected by sulphide exploitation (Iberian Pyrite Belt, SW Spain). *Environ. Geol.* **2008**, *54*, 805–818. [CrossRef]
27. Fernández-Caliani, J.C.; Barba-Brioso, C.; González, I.; Galán, E. Heavy metal pollution in soils around the abandoned mine sites of the Iberian Pyrite Belt (Southwest Spain). *Water Air Soil Pollut.* **2009**, *200*, 211–226. [CrossRef]
28. González, I.; Galán, E.; Romero, A. Assessing soil quality in areas affected by sulfide mining. Application to soils in the Iberian Pyrite Belt (SW Spain). *Minerals* **2011**, *1*, 73–108. [CrossRef]
29. Arranz, J.C.; Cala, V.; Iribarren, I. Geochemistry and mineralogy of surface pyritic tailings impoundments at two mining sites of the Iberian Pyrite Belt (SW Spain). *Environ. Earth Sci.* **2012**, *65*, 669–680. [CrossRef]
30. Romero-Baena, A.J.; Barba-Brioso, C.; Ross, A.; González, I.; Aparicio, P. Mobility of potentially toxic elements in family garden soils of the Riotinto mining area. *Appl. Clay Sci.* **2021**, *203*, 105999. [CrossRef]
31. Urrutia, M.M.; García-Rodeja, E.; Macias, F. Sulfide oxidation in coal-mine dumps: Laboratory measurement of acidifying potential with H_2O_2 and its application to characterize spoil materials. *Environ. Manag.* **1992**, *16*, 81–89. [CrossRef]
32. Kahle, M.; Kleber, M.; Jahn, R. Review of XRD-based quantitative analyses of clay minerals in soils: The suitability of mineral intensity factors. *Geoderma* **2002**, *109*, 191–205. [CrossRef]
33. Bussan, D.; Harris, A.; Douvris, C. Monitoring of selected trace elements in sediments of heavily industrialized areas in Calcasieu Parish, Louisiana, United States by inductively coupled plasma-optical emission spectroscopy (ICP-OES). *Microchem. J.* **2019**, *144*, 51–55. [CrossRef]
34. Ahern, C.R.; McElnea, A.E.; Sullivan, L.A. *Acid Sulfate Soils Laboratory Methods Guidelines*; Queensland Department of Natural Resources, Mines and Energy: Indooroopilly, Australia, 2004.
35. Nordstrom, D.K. Aqueous pyrite oxidation and the consequent formation of secondary iron minerals. In *Acid Sulfate Weathering*; Kittrick, J.A., Fanning, D.S., Hossner, L.R., Eds.; SSSA Special Publications; Soil Science Society of America: Madison, WI, USA, 1982; Volume 10, pp. 37–56.

36. Dold, B. Acid rock drainage prediction: A critical review. *J. Geochem. Explor.* **2017**, *172*, 120–132. [CrossRef]
37. McElnea, A.E.; Ahern, C.R.; Menzies, N.W. The measurement of actual acidity in acid sulfate soils and the determination of sulfidic acidity in suspension after peroxide oxidation. *Austr. J. Soil Res.* **2002**, *40*, 1133–1157. [CrossRef]
38. Dold, B. Speciation of the most soluble phases in a sequential extraction procedure adapted for geochemical studies of copper sulfide mine waste. *J. Geochem. Explor.* **2003**, *80*, 55–68. [CrossRef]
39. *EN 12457-2:2002*; European Standard EN 12457-2 Characterization of Waste–Leaching–Compliance Test for Leaching of Granular Waste Materials and Sludges, Part 2: One Stage Batch Test at a Liquid to Solid Ratio of 10 l/kg for Materials with Particle Size below 4 mm (without or with Size Reduction). European Committee for Standardization: Brussels, Belgium, 2002.
40. López-Arce, P.; Garrido, F.; García-Guinea, J.; Voegelin, A.; Göttlicher, J.; Nieto, J.M. Historical roasting of thallium- and arsenic-bearing pyrite: Current Tl pollution in the Riotinto mine area. *Sci. Total Environ.* **2019**, *648*, 1263–1274. [CrossRef]
41. Romero, A.; González, I.; Galán, E. Estimation of potential pollution of waste mining dumps at Peña del Hierro (Pyrite Belt, SW Spain) as a base for future mitigation actions. *Appl. Geochem.* **2006**, *21*, 1093–1108. [CrossRef]
42. Jerz, J.K.; Rimstidt, J.D. Efflorescent iron sulfate minerals: Paragenesis, relative stability, and environmental impact. *Am. Miner.* **2003**, *88*, 1919–1932. [CrossRef]
43. Miller, S.; Robertson, A.; Donahue, T. Advances in acid drainage prediction using the net acid generating (NAG) test. In Proceedings of the fourth International Conference on Acid Rock Drainage, Vancouver, BC, Canada, 31 May–6 June 1997; Volume 2, pp. 533–547.
44. Karlsson, T.; Räisänen, M.L.; Lehtonen, M.; Alakangas, L. Comparison of static and mineralogical ARD prediction methods in the Nordic environment. *Environ. Monit. Assess.* **2018**, *190*, 719. [CrossRef] [PubMed]
45. Cánovas, C.R.; Quispe, D.; Macías, F.; Callejón-Leblic, B.; Arias-Borrego, A.; García-Barrera, T.; Nieto, J.M. Potential release and bioaccessibility of metal/loids from mine wastes deposited in historical abandoned sulfide mines. *Environ. Pollut.* **2023**, *316*, 120629. [CrossRef]
46. Li, Z.; Ma, Z.; Van der Kuijp, T.J.; Yuan, Z.; Huang, L. A review of soil heavy metal pollution from mines in China: Pollution and health risk assessment. *Sci. Total Environ.* **2014**, *468–469*, 843–853. [CrossRef] [PubMed]
47. Barsova, N.; Yakimenko, O.; Tolpeshta, I.; Motuzova, G. Current state and dynamics of heavy metal soil pollution in Russian Federation—A review. *Environ. Pollut.* **2019**, *249*, 200–207. [CrossRef] [PubMed]
48. Reimann, C.; Caritat, P. *Chemical Elements in the Environment*; Springer: Berlin/Heidelberg, Germany, 1998; p. 398.
49. Grantcharova, M.M.; Fernández-Caliani, J.C. Soil acidification, mineral neoformation and heavy metal contamination driven by weathering of sulphide wastes in a Ramsar wetland. *Appl. Sci.* **2022**, *12*, 249. [CrossRef]
50. Galán, E.; Fernández Caliani, J.C.; González, I.; Aparicio, P.; Romero, A. Influence of geological setting on geochemical baselines of trace elements in soils. Application to soils of South-West Spain. *J. Geochem. Explor.* **2008**, *98*, 89–106. [CrossRef]
51. Fernández-Caliani, J.C. La contaminación del suelo por la minería metálica de la Faja Pirítica Ibérica. *Macla* **2022**, *26*, 1–2.
52. Hakanson, L. An ecological risk index for aquatic pollution control: A sedimentological approach. *Water Res.* **1980**, *14*, 975–1001. [CrossRef]
53. Tomlinson, D.L.; Wilson, J.G.; Harris, C.R.; Jeffrey, D.W. Problems in the assessment of heavy-metal levels in estuaries and the formation of a pollution index. *Helgol. Meeresunters.* **1980**, *33*, 566–575. [CrossRef]
54. Abrahim, G.M.S.; Parker, R.J. Assessment of heavy metal enrichment factors and the degree of contamination in marine sediments from Tamaki Estuary, Auckland, New Zealand. *Environ. Monit. Assess.* **2007**, *136*, 227–238. [CrossRef] [PubMed]
55. Ficklin, W.H.; Plumlee, G.S.; Smith, K.S.; McHugh, J.B. Geochemical classification of mine drainages and natural drainages in mineralized areas. In Proceedings of the 7th International Symposium on Water-Rock Interaction, Park City, UT, USA, 13–18 July 1992; pp. 381–384.
56. Sánchez-España, J.; López-Pamo, E.; Santofimia, E.; Aduvire, O.; Reyes-Andrés, J.; Barettino, D. Acid mine drainage in the Iberian Pyrite Belt (Odiel river watershed, Huelva, SW Spain): Geochemistry, mineralogy and environmental implications. *Appl. Geochem.* **2005**, *20*, 1320–1356. [CrossRef]
57. Romero, A.; González, I.; Galán, E. Stream water geochemistry from mine wastes in Peña de Hierro, Riotinto Area, SW Spain. A case of extreme acid mine drainage. *Environ. Earth Sci.* **2011**, *62*, 645–656. [CrossRef]
58. Durães, N.; Bobos, I.; Ferreira da Silva, E. Speciation and precipitation of heavy metals in high-metal and high-acid mine waters from the Iberian Pyrite Belt (Portugal). *Environ. Sci. Pollut. Res.* **2017**, *24*, 4562–4576. [CrossRef] [PubMed]
59. Madejón, P.; Barba-Brioso, C.; Lepp, N.W.; Fernández-Caliani, J.C. Traditional agricultural practices enable sustainable remediation of highly polluted soils in Southern Spain for cultivation of food crops. *J. Environ. Manag.* **2011**, *92*, 1828–1836. [CrossRef]
60. Paktunc, D.; Dutrizac, J.E. Characterization of arsenate-for-sulfate substitution in synthetic jarosite using X-ray diffraction and X-ray absorption spectroscopy. *Canad. Mineral.* **2003**, *41*, 905–919. [CrossRef]
61. Asta, M.P.; Cama, J.; Martínez, M.; Giménez, J. Arsenic removal by goethite and jarosite in acidic conditions and its environmental implications. *J. Hazard. Mater.* **2009**, *171*, 965–972. [CrossRef]
62. Morin, G.; Calas, G. Arsenic in soils, mine tailings, and former industrial sites. *Elements* **2006**, *2*, 97–101. [CrossRef]
63. Haffert, L.; Craw, D. Mineralogical controls on environmental mobility of arsenic from historic mine processing residues, New Zealand. *Appl. Geochem.* **2008**, *23*, 1467–1483. [CrossRef]

64. Parkhurst, D.L.; Appelo, C.A.J. Description of input and examples for PHREEQC version 3—A computer program for speciation, batch-reaction, one-dimensional transport, and inverse geochemical calculations. *US Geol. Surv. Tech. Methods* **2013**, *6*, 497.
65. Plumlee, G.S.; Smith, K.S.; Montour, M.R.; Ficklin, W.H.; Mosier, E.L. Geologic controls on the composition of natural waters and mine waters draining diverse mineral–deposit types. In *The Environmental Geochemistry of Mineral Deposits. Part B: Case Studies and Research Topics*; Filipek, L.H., Plumlee, G.S., Eds.; Reviews in Economic Geology; Society of Economic Geologists: Littleton, CO, USA, 1999; Volume 6B, pp. 373–432.

4.2. Fitoacumulación de elementos traza en un Tecnosol desarrollado sobre residuos mineros abandonados en el Estero de Domingo Rubio

Basado en el artículo:

Phytoaccumulation of trace elements (As, Cd, Co, Cu, Pb, Zn) by Nicotiana glauca and Euphorbia segetalis growing in a Technosol developed on legacy mine wastes (Domingo Rubio wetland, SW Spain). Environmental Geochemistry & Health 45 (2023) 9541-9557

La fitorremediación es una estrategia sostenible y respetuosa con las funcionalidades del suelo que permite descontaminar o estabilizar contaminantes. Sin embargo, su aplicación efectiva requiere identificar y caracterizar especies vegetales que sean tolerantes a los metales pesados y capaces de acumular o inmovilizar estos elementos. En este contexto, se investiga el comportamiento de dos especies vegetales, *Nicotiana glauca* (tabaco moruno) y *Euphorbia segetalis* (euforbia), que crecen de forma espontánea en un Arenosol calcárico contaminado con residuos piríticos abandonados en el estero de Domingo Rubio, un humedal costero asociado al estuario de Huelva. El objetivo principal de la investigación fue evaluar la capacidad de fitorremediación de estas dos especies vegetales.

Se tomaron muestras representativas de un suelo fuertemente impactado por los residuos piríticos, así como de los principales órganos (raíces, tallos y hojas) de ambas plantas. Las muestras de suelo fueron analizadas para caracterizar sus propiedades fisicoquímicas, el contenido de materia orgánica y las concentraciones totales de As, Cd, Co, Cu, Pb y Zn. Las muestras vegetales fueron digeridas con HNO_3 concentrado para determinar las concentraciones de los mismos elementos. Para evaluar la capacidad de acumulación y translocación de las plantas, se calcularon los factores de bioconcentración (BCF) y de translocación (TF), respectivamente.

4.2.1. Resultados más relevantes

Los análisis del suelo confirmaron las características esperadas de un ambiente impactado por DAM: pH extremadamente ácido (1,9-2,7), alta conductividad eléctrica (3,3-11,9 mS cm^{-1}), condiciones fuertemente oxidantes (659-756 mV) y concentraciones elevadas de sulfato y EPT, superando en muchos casos los valores de referencia. Las concentraciones de As, Cu, Zn y Pb fueron particularmente anómalas, con valores hasta 1360, 1710, 1610 y más de 5000 mg kg^{-1} respectivamente.

El pH de la rizosfera mostró una reacción ligeramente alcalina (pH = 7,0-8,1). La alta capacidad de neutralización de la acidez del suelo rizosférico fue eficaz para limitar la transferencia de los EPT hacia las plantas. No obstante, los resultados del análisis del tejido vegetal mostraron diferencias significativas en la capacidad de acumulación de elementos entre las dos especies estudiadas:

- ***N. glauca*** demostró una notable capacidad para acumular As (13,4 mg kg^{-1}), Cu (314 mg kg^{-1}) y Pb (41,8 mg kg^{-1}), principalmente en sus raíces, donde se registraron las concentraciones más altas de estos elementos. Específicamente, *N. glauca* exhibió una translocación significativa de Cd hacia las partes aéreas, con un TF a las hojas relativamente alto (5,4), lo que la clasifica como una especie hiperacumuladora de Cd. También acumuló cantidades considerables de Co y Zn, aunque con una menor eficiencia de translocación (3,1 en tallos y 1,5 en hojas, respectivamente).

- ***E. segetalis*** mostró una menor capacidad de acumulación de EPT en comparación con *N. glauca*. Aunque también acumuló ciertos elementos, como As, Cd y Pb, en sus raíces, su capacidad de translocación hacia las partes aéreas fue más limitada para la mayoría de los metales, con TF generalmente inferiores a 1, a excepción del Co (2,2 en hojas).

Los valores de BCF y TF corroboraron que *N. glauca* tiene un mayor potencial tanto para la fitoextracción (especialmente para Cd y Co) como para la

fitoestabilización (para As, Cu y Pb que acumula preferentemente en las raíces), mientras que *E. segetalis* podría contribuir más a la fitoestabilización.

4.2.2. Discusión

Los resultados de este estudio revelaron la notable resiliencia de *N. glauca* y *E. segetalis* para prosperar en un entorno edáfico altamente contaminado por residuos mineros, un hábitat donde la mayoría de las especies vegetales son incapaces de sobrevivir. La elevada acumulación de As, Pb y Cu por parte de *N. glauca* es relevante, confirmando su papel como planta hiperacumuladora de estos contaminantes, como se ha documentado en otras regiones. Esta capacidad convierte a *N. glauca* en una especie con potencial para la fitoestabilización. Al retener estos metales en el sistema radicular, la planta contribuye a inmovilizarlos en el suelo, lo que reduce su movilidad y biodisponibilidad. Por lo tanto, se aminora el riesgo de lixiviación y de entrada en la cadena trófica. Además, la traslocación de Co, Cd y Zn en las partes aéreas de *N. glauca* resalta su potencial para la fitoextracción de estos metales.

Por otro lado, *E. segetalis* mostró una menor capacidad de fitoextracción, evidenciada por sus factores de translocación generalmente bajos. A pesar de ello, la planta sobrevive en estos suelos contaminados, lo que podría indicar un mecanismo de exclusión de metales, dándose una mayor acumulación en la rizosfera o en el sistema radicular. Esto contribuye a la reducción de la dispersión y toxicidad de los contaminantes mediante fitoestabilización.

La variabilidad observada en la acumulación de contaminantes entre ambas especies, así como entre los diferentes órganos de la misma especie, puede atribuirse a una combinación de factores, como: la biodisponibilidad de los metales en el suelo, las características genéticas inherentes a cada especie, las complejas interacciones microbianas en la rizosfera, y las estrategias fisiológicas adaptativas de cada planta para tolerar el estrés por metales.

4.2.3. Conclusiones

Las especies *N. glauca* y *E. segetalis* demuestran ser tolerantes a las elevadas concentraciones de EPT presentes en un Tecnosol desarrollado sobre residuos mineros históricos en el humedal del estero de Domingo Rubio. *N. glauca* posee un considerable potencial para la biorremediación de suelos impactados por DAM. Destacada su capacidad para acumular Co, Cd y Zn en sus partes aéreas la convierte una especie adecuada para la fitoextracción de estos contaminantes. Además, su capacidad para acumular As, Pb y Cu, predominantemente en sus raíces, la hace apta para la fitoestabilización, contribuyendo a la inmovilización de estos metales en el suelo y reduciendo su dispersión ambiental. Aunque *E. segetalis* mostró una menor capacidad de fitoacumulación comparada con *N. glauca*, su presencia y tolerancia en estos ambientes extremos sugiere un valor potencial en programas de revegetación orientados a la estabilización de suelos degradados.

Environ Geochem Health (2023) 45:9541–9557
https://doi.org/10.1007/s10653-023-01523-w

ORIGINAL PAPER

Phytoaccumulation of trace elements (As, Cd, Co, Cu, Pb, Zn) by *Nicotiana glauca* and *Euphorbia segetalis* growing in a Technosol developed on legacy mine wastes (Domingo Rubio wetland, SW Spain)

C. Barba-Brioso · P. J. Hidalgo · S. Fernández-Landero · I. Giráldez · J. C. Fernández-Caliani

Received: 17 June 2022 / Accepted: 27 February 2023 / Published online: 16 March 2023

Abstract Sulfidic mine wastes have the potential to generate acid mine drainage (AMD) and release acid leachates containing high levels of iron, sulfate and potentially toxic elements (PTEs). Soils receiving AMD discharges are generally devoid of vegetation. Only a few metal-tolerant plant species can survive under such adverse soil conditions. This work investigates two plant species, *Nicotiana glauca* and *Euphorbia segetalis,* that have successfully colonized an AMD-impacted wetland area in south-western Spain. The uptake of PTEs from the soil by roots and their transfer and accumulation in the above-ground biomass were quantified. Results showed that these pioneer plants grew in patches of neutral soil within the wasteland despite the high concentrations of PTEs in the rhizosphere soil (up to: 613 mg kg^{-1} As, 18.7 mg kg^{-1} Cd, 6370 mg kg^{-1} Cu, 2210 mg kg^{-1} Pb and 5250 mg kg^{-1} Zn). The target organs of As, Cu and Pb accumulation were: root > leaf > stem in *N. glauca*, and root > stem > leaf in *E. segetalis*. Zinc and Cd showed a significant decrease in roots relative to aerial parts of *N. glauca*, and Co was preferentially partitioned in stems of *N. glauca* and leaves of *E. segetalis*. The soil–plant transfer coefficient values of PTEs in all parts of both plants were well below unity with the only exception of Cd in leaves of *N. glauca* (1.254), suggesting that roots acted as a barrier limiting the uptake of PTEs by plants. Interestingly, under the same soil conditions, *N. glauca* absorbed Cd in considerable proportions from soil and accumulated it in its leaves, while *E. segetalis* was not effective in transferring PTEs from roots shoots except for Co. In conclusion, soil pH and plant-related factors greatly influence the stabilization of PTE in the rhizospheric soil and produce inconsistencies in PTE phytoavailability. The findings of this study provide criteria to assist in natural remediation in other legacy contaminated sites worldwide.

Supplementary Information The online version contains supplementary material available at https://doi.org/10.1007/s10653-023-01523-w.

C. Barba-Brioso (✉)
Department of Crystallography, Mineralogy and Agricultural Chemistry, University of Seville, Campus Reina Mercedes, s/n., 41071 Seville, Spain
e-mail: cbarba@us.es

P. J. Hidalgo
Department of Integrated Sciences, University of Huelva, Campus El Carmen, s/n., 21071 Huelva, Spain
e-mail: hidalgo@uhu.es

S. Fernández-Landero · J. C. Fernández-Caliani
Department of Earth Sciences, University of Huelva, Campus El Carmen, s/n., 21071 Huelva, Spain
e-mail: sandra.fernandez@dct.uhu.es

J. C. Fernández-Caliani
e-mail: caliani@uhu.es

I. Giráldez
Department of Chemistry, University of Huelva, Campus El Carmen, s/n., 21071 Huelva, Spain
e-mail: giraldez@uhu.es

Keywords Soil pollution · Heavy metals · Rhizosphere · Phytoextraction · Nicotiana · Euphorbia

Introduction

Multiple pollution sources are often found around the mouth of rivers and estuaries because population and industry tend to be clustered in distinct geographic areas with favorable natural conditions and resources, such as fertile soils, water availability, and low lands for urban development (Santucci et al., 2017). Many of these conditions converge in coastal wetland areas (Li et al., 2014), where the environmental functions and ecosystem services of the soil may be dramatically disrupted by man-induced reactions involving the formation of acid sulfate soils, oxidation of organic matter and subsequent emission of carbon dioxide to the atmosphere, and potentially toxic trace elements (PTEs) release into the nearby water courses (Fernández et al., 2010). In such degraded wetlands, soils lose their filtering and storing capacity for pollutants that are eventually discharged in high amounts from liquid industrial and agricultural effluents, solid waste deposited on illegal dumping sites, or dust deposition (Conesa et al., 2011; Grantcharova & Fernández-Caliani, 2022).

Fortunately, the economic development of countries is commonly accompanied by increased environmental awareness and protection, and so research, legislative and policy efforts are being undertaken to achieve a sustainable land use and management. Thus, for example, the European Commission (2021) has launched a new soil strategy for 2030 to ensure a high level of environmental and health protection. However, for legacy contaminated sites a common approach is lacking in the European Union, which is a relevant legal gap concern.

The Domingo Rubio tidal system (Spain) is a prime example of highly polluted wetland where the polluter-pays principle cannot be applied. In addition to diffuse contamination from agriculture and water pollution caused by multiple anthropogenic sources (Barba-Brioso et al., 2010a), local soil contamination occurs by improper disposal of sulfide-rich wastes coming from past mining activities. As a result, the wetland soil adversely affected by acid and heavy metal contamination has become sterile and unproductive. Under these conditions, only some races, ecotypes or edaphoendemisms are able to colonize such altered soils. It is the case of *Erica andevalensis*, an endemic heather adapted to highly acidic soil conditions along the acidic soils of the Iberian Pyrite Belt (Márquez-García et al., 2006; Rossini-Oliva et al., 2018).

Notwithstanding the above, an incipient vegetation usually arises spontaneously over time owing to the tendency for natural processes in soils to attenuate contaminants. Initially, the vegetative cover is composed of annual grasses that are able to colonize technogenic soils developed on mine wastes. These pioneer plants play an interesting role in preventing erosion, promoting soil dynamics, and maintaining other living beings of the trophic change since they are primary producers. Alien plant species may also colonize highly altered soil ecosystems, as they are more resilient and competitive than native species in degraded areas (Dana et al., 2005). Thus, a controversial issue arises when the exotic plants play a significant role in the remediation of contaminated soils, but also pose a threat to biodiversity of native ecosystems (Mendez and Maier, 2008). Interestingly, the species *Nicotiana glauca* and *Euphorbia segetalis* are found growing on the sulfidic waste material improperly disposed of in the Domingo Rubio wetland, displaying a patchy distribution, and hence, they have been selected as the focus of this study. It can be hypothesized, therefore, that both species could tolerate high levels of PTEs in surrounding soils.

The genus *Nicotiana* comprises around 67 species distributed in America, South Pacific, Australia and Southwest of Africa. Some of them contain alkaloids derived from nicotinic acid (nicotine). *Nicotiana glauca* R.C. Graham is a glabrous scrub or small tree (up to 6 m tall), natural from South America (Argentina, Paraguay, and Bolivia) and extensively naturalized in the Mediterranean region. It is a nitrophilous plant commonly found on slopes, embankments, roadsides, river terraces, and well adapted to growing in sandy or stony and disturbed soils (Dana et al., 2005). *N. glauca* was included in the Spanish Catalogue of Invasive Alien Species (Royal Decree 630/2013) until 2015 when a ruling by the Supreme Court of Spain forced its removal from the list and, since then, its use in natural landscapes is allowed. The reason for the exclusion was that it has a great potential as an energy crop, thus helping to tackle climate change. This species has the ability to survive

in heavily polluted soils (Barazani et al., 2004), and genes associated with metal tolerance have been encoded (Shingu et al., 2005).

Euphorbia segetalis L. is an annual, biennial, or perennial herb (up to 80 cm tall), native to Mediterranean Europe, North of Africa, and Macaronesia. It is indifferent to the substrate type and occurs in a wide range of habitats, including ruderal sites, crop fields, stony pastures and rocky areas of coastal places. This species has been phytochemically characterized by its diterpene content (Jakupovic et al., 1998) and antiviral and antimicrobial activities of triterpenes isolated from *E. segetalis* have been assessed (Madureira et al., 2003). Some species of the genus *Euphorbia* (Euphorbiaceae) produce a large amount of latex that can cause severe irritation of the skin and eyes. The latex has been extensively investigated from pharmacognostic and phytochemical points of view, and many interesting antitumor molecules have been characterized (Sahai et al., 1981). To our knowledge, this is the first time that *E. segetalis* is being considered for its potential as phytoaccumulator of PTEs in a contaminated soil.

This paper was aimed at determining the environmental conditions, mineral components and degree of contamination of the technogenic soil where *N. glauca* and *E. segetalis* are growing, and the concentrations of PTEs in different organ tissues (roots, stems and leaves) in order to quantify the uptake of contaminants from soil by plant roots and their transfer and accumulation in the above-ground biomass of these spontaneous pioneer plants. The final goal is to understand the potential impact of this contamination and how it can affect the environment.

Materials and methods

Geoenvironmental setting

The Domingo Rubio wetland is a small tidal channel 6 km in length connected to the confluence of the Tinto and Odiel rivers (Pendón et al., 1998), where they form the estuary of Huelva on the southwest coast of Spain (Fig. 1a, b). The tidal wetland is located in a flooded valley, which is incised into Plio-Pleistocene detritic deposits, occupying an area of about 480 ha. It has a mild Mediterranean climate moderated by the influence of the Atlantic Ocean (Csa in the Köppen–Geiger climate classification system), with average temperature of 9° C in winter and 27° C in summer, and with most of the rain (mean annual of 525 mm) falling in winter months.

The lower wetland area consists of a tidal marshland with a pronounced marine influence. The marsh soils (Salic Fluvisols according to World Reference Base for Soil Resources) are developed on fluviomarine silty-clayey sediments, and the wetland vegetation is dominated by salt-tolerant plant species, such as *Spartina densiflora, Arthrocnemum macrostachyum* and *Halimione portulacoides* (Madejón et al., 2009). The upper wetland is a lacustrine area consisting of a freshwater reservoir artificially created by stream impoundment, which is inhabited by *Typha domingensis* and *Phragmites australis*, among others wetland species. This portion of the wetland is fed by Dehesa del Estero stream and many ephemeral creeks from a watershed impacted by intensive irrigated cropping operations (Barba-Brioso et al., 2010b).

The tideland area has been catalogued as Natural Area since 1989 and more recently as Special Protection Area of the Natura 2000 Network in October 2002 (Site code: ES6150003, Estero Domingo Rubio, Directive 92/43/EEC) hosting a total of 7 natural Habitats of Community Interest and 156 species (mainly birds) referred to in Article 4 of Directive, 2009/147/EC and listed in Annex II of Directive 92/43/EEC. Despite the legislative framework in place, the wetland receives high loads of pollutants (Online Resource 1) from diffuse agricultural and industrial sources (Barba-Brioso et al., 2009, 2010a) and acidic discharges from a Spolic Technosol developed on legacy sulfidic-rich materials due to improper past waste disposal practices.

Plant and soil sampling

A stratified random soil sampling was undertaken in three representative sites of the Spolic Technosol developed on the abandoned sulfide-rich mine wastes (sites DR1, DR-2 and DR-3 in Fig. 1c). At each site, five topsoil samples (0–20 cm depth) were collected with an Edelman auger in crossing directions around the central sampling position (Fig. 1d) and bulked in the field to form one composite sample representing the site. The plants of *N. glauca* (Fig. 1e) and *E. segetalis* (Fig. 1f) and their associated soil samples were collected at ten sites in the wasteland area (five

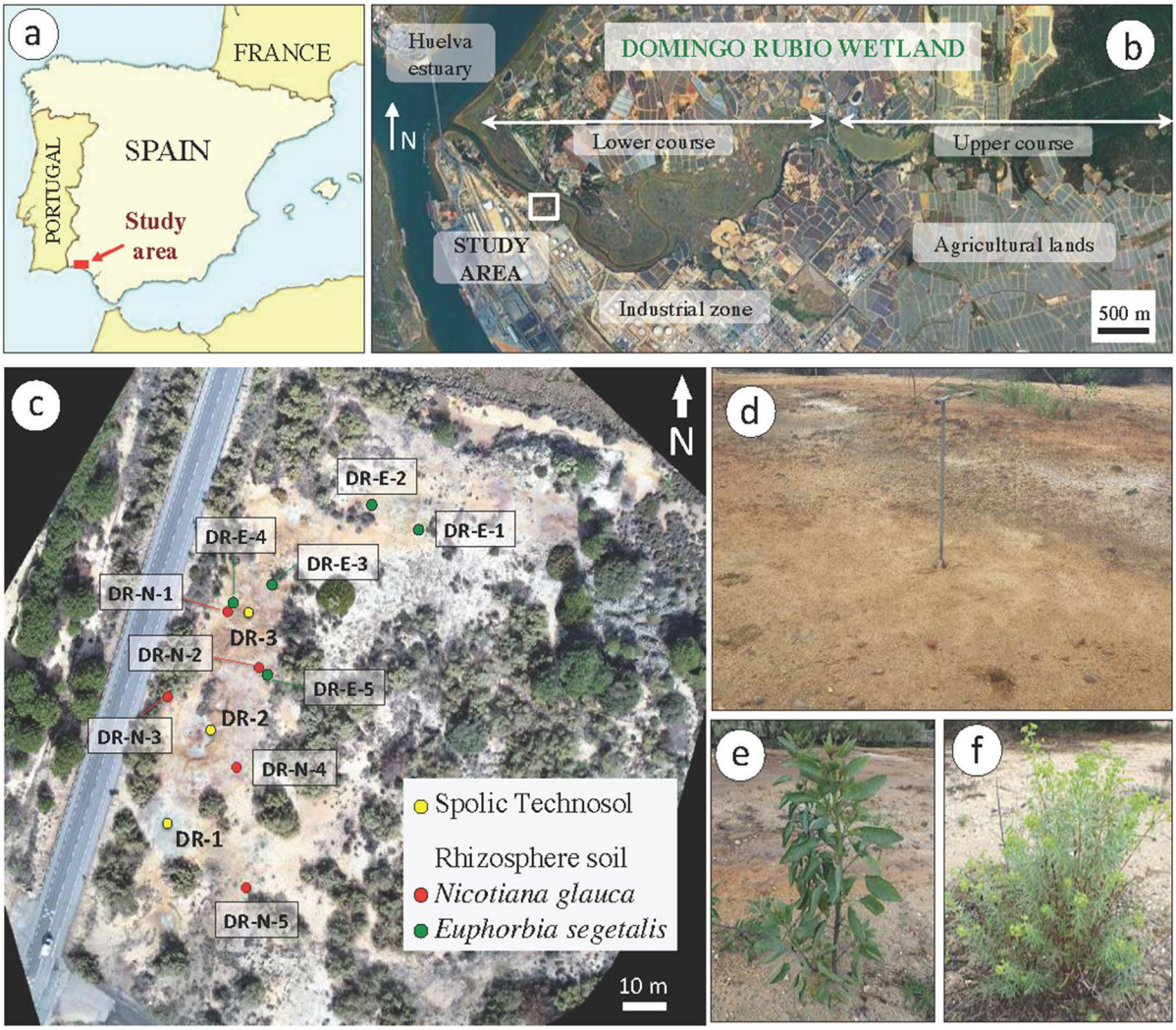

Fig. 1 **a** Location map of the Domingo Rubio wetland area in the Huelva estuary (SW Spain). **b** Google Earth® image showing the upper and lower course of the tidal channel, and the main activities developed around the study area. **c** Aerial view (drone image) of the sampling locations for soils and plants. **d** Soil sampling method using a hand auger. **e** *Nicotiana glauca* on site. **f** *Euphorbia segetalis* on site

sites per plant species) where they spontaneously grew. Plants were harvested and separated into leaves, stems and roots. This sampling scheme allowed us to compare tissue metal concentrations in different groups of organs of the two only shrubs growing on the mine wastes. As a control, plant samples of the same species and soil samples from adjacent roots were collected from seemingly uncontaminated areas elsewhere. The soil from the rhizospheric zone was collected by vigorous hand-shaking and subsequent brushing of the root mass (Luster et al., 2009). Plant and soil samples were placed in zip-lock plastic bags and immediately transported to the laboratory for processing.

Analytical methods

The soil samples were air dried, gently crushed to break the aggregates, passed through a 2-mm mesh sieve, and thoroughly mixed to ensure optimal homogenization. Soil reaction (pH), redox potential (Eh) and electrical conductivity (EC) were

potentiometrically measured in a soil/deionized water suspension of 1:2.5 (w/v), after shaking for 15 min followed by a 30 min equilibration period. Aliquots of sieved material were ground in an agate mortar and pestle until getting a nearly uniform fine powder (< 63 µm) for mineralogical and chemical analyses.

Mineralogical identification of the major crystalline phases was carried out by powder X-ray diffraction (XRD) on a BRUKER AXS D8 Advance diffractometer, using CuKα radiation at 40 kV and 30 mA. Scans of randomly oriented bulk powders were run from 3 to 65° 2θ with a step size of 0.02° and a counting time of 0.6 s per step. Relative mineral abundance was estimated by empirical intensity factors weighting the integrated peak area values of diagnostic reflections (Kahle et al., 2002). Selected samples were examined by environmental scanning electron microscopy (ESEM) on a JEOL JSM-IT500 instrument coupled with energy-dispersive X-ray spectroscopy (EDS). Back-scattered electron (BSE) images and EDS spectra were acquired at 20 kV accelerating voltage to assist in the mineral identification of accessory heavy metal-bearing particles.

Soil samples were subjected to multi-acid (HF-$HClO_4$-HNO_3-HCl) digestion followed by inductively coupled plasma-optical emission spectroscopy (ICP-OES) analysis using an Agilent 735 ICP-OES instrument to determine the total concentrations of As, Cd, Co, Cr, Cu, Pb, and Zn. The analyses were performed at Activation Laboratories Ltd. (Ancaster, Ontario, Canada), which is accredited to the ISO/IEC 17025:2005 standard. Analytical quality control was monitored by using internationally certified reference materials (OREAS 13b, OREAS 98, OREAS 101b), blank samples and laboratory replicates to check the accuracy and precision of the data. The accuracy expressed as percent recovery ranged from 78.3 to 108.3%, and the precision expressed as percent relative standard deviation (RSD) was between 2.4% and 14.7%.

A one-step extraction test with a mild neutral salt solution was used to determine the phytoavailable concentrations of PTEs in the rhizosphere (Menzies et al., 2007). For this purpose, an aliquot (1 g) of each rhizosphere soil sample (< 2 mm) was subjected to extraction with 0.01 M $CaCl_2$, in a soil/solution ratio of 1:10 (w/v), by end-over-end shaking at 30 rpm for 2 h (Houba et al., 1990; Rivera et al., 2016). The soil extract solution was then centrifuged at 3000 rpm for 10 min, and PTEs of concern were measured in the supernatant after filtration through 0.45 µm nylon filters. The analysis of PTEs in the digests was performed by ICP-MS on an Agilent 7700 instrument (Central Research Services, University of Huelva, Spain). The extraction procedure was repeated twice with similar results, and the mean value was taken. Extraction blanks were used to identify possible contamination.

In order to extract the PTEs of concern from plant tissues, all plant material (roots, stems and leaves) was washed thoroughly with tap water and rinsed with distilled water repeatedly to remove the surface dust particles and then, sonicated in a bath-type sonicator (Power Sonic 505) for 30 min. Afterward, the plant samples were dried in an oven at 40° C for 5 days, and ground to 0.5 mm in an IKA WERKE MF 10 grinder at 3250 rpm. The thicker stems were previously ground in a cutting mill RETSCH(R) model SM 2000 to pass through a 5 mm mesh sieve. An aliquot (0.05 g) of the ground sample was digested with 1 ml of concentrated HNO_3 (Madejón et al., 2011) using a microwave oven at 350 W for 1.5 min. After cooling, 1.5 ml of H_2O_2 (30%) was added to the digest solution and the heating was repeated using the same microwave program. Finally, the resulting solution was diluted to a volume of 5 ml with Milli-Q water. The analysis of PTEs in the digests was performed with the Agilent 7700 ICP-MS. The same procedure was applied for control plant samples. The validity of the analytical procedure was assessed by analyzing a certified reference material of plant leaves of Oriental Basma Tobacco Leaves (INCT-OBTL-5) (Samczyński et al., 2012). The average precision was 7.8% RSD, and the average recovery was found to be 92.1%, which is indicative of good accuracy.

Statistical treatment

All results are expressed as mean ± standard deviation. For statistical purposes, the results below the detection limit were assumed as half of the detection limit. Statistical differences between means were evaluated using Student's t-test and analysis of variance (one-way ANOVA). Prior to ANOVA analysis, the homogeneity of variance was assessed by Levene's test. The critical level of significance for all statistical tests was set at an α-value of 0.05 (95% confidence interval). Data statistical treatment

was performed with the Statistica 10.0 and MS Excel 2016 software packages.

Results and discussion

Mineral composition and environmental soil conditions

The Spolic Technosol developed on sulfide-rich mine wastes left on the marshland differed drastically in mineral composition and physico-chemical properties from the natural soils in the wetland. It was essentially composed of pyrite, jarosite, gypsum, and quartz in highly variable proportions, with minor feldspars, hematite, and accessory barite and anglesite (Table 1). In dry periods, as surface soil dries out it appears covered with yellow efflorescences of readily soluble sulfate minerals, notably ferricopiapite, as reported by Barba-Brioso et al. (2010c). The secondary mineral assemblage was clearly a result of sulfurization processes driven by weathering of the pyrite-rich wastes, with sulfate minerals being the most abundant oxidation products. Consistently, the Technosol was extremely acid (pH values below 3.0) and strongly oxidant (Eh values ranging between + 659 and + 756 mV). These surface conditions are conducive to increased release of acidity, sulfate ions and PTEs, thus limiting the soil capability to support vegetation.

Interestingly, the mineral constituents of the soil in which the plants have directly grown differed distinctly from those of the Technosol derived from the sulfidic wastes. The rhizosphere soil samples were composed mainly of quartz and clay minerals, together with minor amounts of feldspars and calcite, which coexisted with accessory gypsum and jarosite in some samples. It was noteworthy the occurrence of carbonates in most samples, indicating a good buffering capacity to neutralize the acid that has been produced, during the oxidative dissolution of pyrite in the abandoned wastes. In fact, soil active reaction was slightly alkaline, with pH_{H2O} values ranging from 7.0 to 8.1 (Table 1), which allowed specifically the growth of some species such as *N. glauca* and *E. segetalis*. The soil surrounding the plant roots showed Eh values (from + 377 to + 458 mV) and electrical conductivity values (up to a maximum of 2.65 mS cm^{-1}) lower than those of the Technosol, and within the typical range reported for natural soils of the wetland (Barba-Brioso et al., 2021). The results suggested, therefore, that these species were able to grow in soil patches subjected to contrasting environmental conditions, having less adverse effects in terms of plant tolerance. An alternative hypothesis is the potential transformation of the rhizosphere by these plants using any kind of exudates to detoxify undesirable metal pollutants in soils (Chen et al., 2017). Further research is needed to understand the origin of this extreme modification of the rhizosphere and the reason why only these species are able to survive in this extremely hostile environment.

Total and phytoavailable concentrations of trace elements

Total PTE concentrations in the technogenic soil greatly varied depending on the element considered (Table 2). The pyrite-rich material (sample DR-1) showed the highest concentrations of Pb (> 5000 mg kg^{-1}), Cu (1710 mg kg^{-1}), Zn (1610 mg kg^{-1}), Co (51 mg kg^{-1}), and Cd (8 mg kg^{-1}), whereas the maximum concentration of As (1360 mg kg^{-1}) and Cr (89 mg kg^{-1}) were measured in the samples DR-2 and DR-3, respectively. In comparison with geochemical baseline concentrations of the local wetland soils (Barba-Brioso, 2011), the Technosol was found contaminated with all PTEs, except Cr. Specifically, the concentrations measured in the Technosol exceeded the local baseline concentrations up to 9.7 times for Pb, 8.9 for As, 8.0 for Cd, 3.4 for Co, 3.2 for Zn, and 2.3 for Cu. The Cr concentration fell within the normal range of the local soils since it is not regarded as a mine-source metal in the Iberian Pyrite Belt (Fernández-Caliani et al., 2009). It was also noticeable that the total concentrations of Pb, As and Cu exceeded the generic reference levels (GRL) or threshold limits established by current regulation (Junta de Andalucía, 2015) for agricultural and other land uses, including natural areas, indicating that exposure to these contaminants may result in an unacceptable risk level for human health or ecosystems. If the GRL are exceeded, the Spanish regulation on contaminated soils establishes that a site-specific risk assessment must be performed (Tarazona et al., 2005).

The rhizosphere soil of both plant species (Table 3) contained elevated concentrations of PTEs

Table 1 Electrochemical parameters and mineral composition of the technogenic soil derived from abandoned mine wastes, of the soil surrounding the plant roots and their control soils

Sample		pH	Eh	EC	Mineral composition (wt %)						
		(in H_2O)	(mV)	(mS cm^{-1})	Pyrite	Jarosite	Gypsum	Quartz	Clay minerals	Calcite	Minor phases (< 10%)
Technosol	DR-1	1.9	659	11.9	30 – 35	25 – 30		15 – 20			Ang, Brt, Fsp, Gp, Hem
	DR-2	2.2	756	5.6		15 – 20	70 – 80				Hem, Qz
	DR-3	2.7	697	3.3		35 – 40	45 – 50	30 – 35			Hem, Brt
Rhizosphere *N. glauca*	DR-N-1	7.4	415	2.65				15 – 20	45 – 50	10 – 15	Fsp, Gp, Jrs
	DR-N-2	7.8	393	0.47				40 – 45	40 – 45		Cal, Gp, Fsp
	DR-N-3	7.0	458	0.59				35 – 40	50 – 55		Gp, Fsp, Cal
	DR-N-4	7.7	398	0.13				60 – 65	25 – 30		Cal, Gp, Fsp
	DR-N-5	7.7	413	0.07				65 – 70	20 – 25		Gp, Fsp, Cal
Control	DR-N–C	7.5	415	0.68				40 – 45	35 – 40		Cal, Dol, Gp, Fsp
Rhizosphere *E. segetalis*	DR-E-1	7.1	403	1.77			10 – 15	45 – 50	25 – 30		Cal, Fsp
	DR-E-2	7.6	377	0.16				55 – 60	30 – 35		Gp, Fsp, Cal
	DR-E-3	7.9	384	0.64				35 – 40	45 – 50		Cal, Gp, Fsp
	DR-E-4	7.0	398	2.42				15 – 20	50 – 55	10 – 15	Fsp, Gp, Jrs
	DR-E-5	8.1	399	0.13				55 – 60	25 – 30		Fsp, Gp, Cal
Control	DR-E-C	7.0	453	0.12				60 – 65	25 – 30		Fsp, Gp, Cal

Mineral symbols: Ang (anglesite); Brt (barite); Cal (calcite); Dol (dolomite); Fsp (feldspars); Gp (gypsum); Hem (hematite); Jrs (jarosite); Qz (quartz)

EC electrical conductivity

Table 2 Total trace element concentration in the technogenic soil derived from abandoned mine wastes

Trace element (mg kg^{-1})	As	Cd	Co	Cr	Cu	Pb	Zn
Detection Limit (DL)	3	0.3	1	1	1	3	1
Sample DR-1	1250	8.0	51	15	1710	> 5000	1610
Sample DR-2	1360	4.5	24	14	1570	4390	637
Sample DR-3	761	2.2	14	31	1160	2190	525
Baseline concentration*	153	< DL	15	89	732	515	508
Regulatory threshold**	36	25	24	10,000	595	275	10,000

Geochemical baseline concentrations of the local wetland soils and the generic reference levels established for soils of the Andalusia region (South Spain) are given for comparison

*Mean value in local wetland soils (Barba-Brioso, 2011)

**Junta de Andalucía (2015)

of concern, particularly Cu (up to 6370 mg kg^{-1}) and Zn (up to 5250 mg kg^{-1}) but also Pb (up to 2210 mg kg^{-1}), As (up to 613 mg kg^{-1}), and Cd (up to 18.7 mg kg^{-1}), compared to local baseline concentrations, yielding contamination factors as high as 8.7 for Cu (sample DR-E-3), 10.3 for Zn (sample DR-E-4), 4.3 for Pb (sample DR-E-4), 4.0 for As (sample DR-N-1), and 18.7 for Cd (sample DR-N-1). Consistently, the PTE concentrations in rhizosphere were significantly above the control soil levels ($p < 0.007$) in all sampling sites, except for Cu in sample DR-N-5. This may be due to the fact that the control soil had an abnormally high concentration (1990 mg kg^{-1}) arising from unexpected contamination in spite of their apparently natural trait. It could be possible due to diffuse contamination originated by re-suspension of waste material. It was also found that the sample DR-N-4 had an anomalously high content of Cr

Table 3 Trace element concentrations in the rhizospheric soil of *Nicotiana glauca* and *Euphorbia segetalis*

Trace element (mg kg^{-1})	As	Cd	Co	Cr	Cu	Pb	Zn
Detection Limit (DL)	3	0.3	1	1	1	3	1
Rhizosphere N. glauca							
DR-N-1	613	10.5	42	32	2640	1070	2150
DR-N-2	163	7.6	59	54	3210	814	4550
DR-N-3	86	1.1	7	30	1340	285	412
DR-N-4	54	3.2	20	223	3360	2210	1420
DR-N-5	69	1.7	6	17	1390	350	585
Mean	197	4.8	26.8	71.2	2388	946	1823
Std. deviation	236	4.1	23	86	972	778	1675
DR-N-control	11	< DL	4	41	65	34	98
Rhizosphere E. segetalis							
DR-E-1	208	2.5	20	28	2690	303	1220
DR-E-2	160	3.7	15	34	5730	408	1270
DR-E-3	135	6.0	19	37	6370	516	1540
DR-E-4	344	18.7	79	37	3460	1050	5250
DR-E-5	63	2.2	12	45	1110	339	1000
Mean	182	6.6	29	36	3872	523	2056
Std. deviation	105	6.9	28	6	2173	305	1796
DR-E-control	28	0.8	4	24	1990	107	273

(223 mg kg^{-1}) whose source was unclear. The pool of wastes from different sources/time slices made difficult the traceability of the materials. No significant differences were observed among the total PTE concentrations in the rhizosphere soil of the two studied plant species except for Cu, which was significantly higher in soil samples around the roots of *E. segetalis* than in those of *N. glauca* ($p = 0.018$).

Surprisingly, the levels of Cu, Zn and Cd in most rhizosphere samples were even higher than those observed in the sulfidic-rich wasteland. The contrasting soil pH values between the two soils could be a plausible explanation for the observed difference in PTE accumulation. Soil reaction is a factor of paramount importance concerning metal speciation and mobility in soil systems (McBride, 1994). Thus, a substantial fraction of Cu, Zn and Cd released by sulfide oxidation, which are relatively soluble under the acidic conditions prevailing in the Technosol, was immobilized to a large extent in some patches of neutral soil where *N. glauca* and *E. segetalis* grew spontaneously. Chemical fixation might have occurred either by precipitation, adsorption, or any other mechanism involving soil constituents with pH-dependent charge that tend to deprotonate with increasing pH, thus leading to increased metal retention. However, the highest concentrations of As and Pb were found in the Spolic Technosol, in association with relatively insoluble sulfate minerals like jarosite and anglesite. The precipitation of these secondary minerals at low pH was an efficient mechanism for decreasing the mobility of As and Pb at the source of contamination and could be the reason why some races of the studied species were able to survive.

It is generally agreed that total concentration of PTEs in soil does not provide predictive insights on mobility and availability of contaminants in relation to plant uptake (i.e., phytoavailability). The PTE pool that may be available in the rhizosphere for plant uptake (Madejón et al., 2011; Menzies et al., 2007) was assessed by single extraction with $CaCl_2$.

The results of the analysis (Table 4) showed that the extracted element concentrations varied from undetectable levels to values below 8 mg kg^{-1}. The maximum concentrations of Zn (7.40 mg kg^{-1}), As (0.07 mg kg^{-1}), Cd (0.06 mg kg^{-1}), and Co (0.06 mg kg^{-1}) were extracted from the soil surrounding the roots of *N. glauca*, whereas the highest content of extractable Cu (2.53 mg kg^{-1}) was noted in the rhizosphere of *E. segetalis* (sample DR-E-2). The Pb concentration was below the detection limit by ICP methods in all soil extracts. The t-test showed

Table 4 Trace element concentrations extracted with $CaCl_2$ from the rhizospheric soil of *Nicotiana glauca* and *Euphorbia segetalis* (< DL, below detection limit)

Element (μg kg^{-1})	As	Cd	Co	Cu	Pb	Zn
Detection Limit (DL)	3	1	5	47	7	29
Rhizosphere N. glauca						
DR-N-1	33 ± 2	6 ± 0.4	< DL	75 ± 6	< DL	< DL
DR-N-2	15 ± 0.3	< DL	< DL	< DL	< DL	< DL
DR-N-3	7.9 ± 0.2	46 ± 1	63 ± 1	925 ± 6	< DL	4382 ± 14
DR-N-4	66 ± 0.1	3.9 ± 0.03	< DL	805 ± 6	< DL	828 ± 6
DR-N-5	69 ± 0.5	59 ± 0.1	11 ± 0.1	1844 ± 30	< DL	7402 ± 143
Mean	38 ± 28	23 ± 27	15 ± 25	733 ± 690	< DL	2522 ± 3031
DR-N-Control	< DL	< DL	< DL	< DL	< DL	< DL
Rhizosphere E. segetalis						
DR-E-1	33 ± 2	3.0 ± 0.2	< DL	876 ± 38	< DL	51 ± 12
DR-E-2	46 ± 0.003	18 ± 0.1	13 ± 0.01	2570 ± 24	< DL	2340 ± 19
DR-E-3	8.6 ± 0.1	5.1 ± 0.1	< DL	388 ± 3	< DL	< DL
DR-E-4	22 ± 1	16 ± 1	< DL	65 ± 6	< DL	277 ± 21
DR-E-5	27 ± 1	4.4 ± 0.2	< DL	203 ± 1	< DL	< DL
Mean	27 ± 13	9 ± 7	4 ± 5	820 ± 949	< DL	534 ± 941
DR-E-Control	36 ± 0.01	104 ± 0.4	72 ± 0.03	14,085 ± 143	12 ± 0.4	98,872 ± 1301

no significant differences between both rhizospheric soils for the extractable concentrations of As, Cd, Co and Cu ($p > 0.057$), while the extractable Zn concentration was significantly higher in the rhizosphere soil of *N. glauca* ($p = 0.027$).

Overall, the extractability, expressed as the amount of PTE extracted with $CaCl_2$ relative to its total concentration in the soil rhizosphere, was practically negligible. The extractable fraction of contaminants accounted for less than 1% with a few exceptions concerning Cd (up to 4.18%) and Zn (up to 1.27%). The low extractability of PTEs with $CaCl_2$ suggests that only a trivial fraction of PTEs may be available for plant uptake. In this approach, the phytoavailable pool includes water-soluble and non-specifically adsorbed PTEs that are retained on soil particles, notably clay minerals, by relatively weak electrostatic interaction. Unexpectedly, the PTEs were extracted from the rhizosphere control soil of *E. segetalis* to a greater extent than from the contaminated soil. As noted previously, this could be due to unforeseen contamination with potentially mobile PTEs.

Trace element concentrations in plant tissues

A detailed comparative analysis of PTEs concentrations in plant tissues (Table 5) reflected significant differences between plant organs and species (ANOVA, $p < 10^{-5}$), with extreme values ranging from 0.034 mg kg^{-1} to 13.39 mg kg^{-1} for As, 0.123–13.16 mg kg^{-1} for Cd, 0.105–6.757 mg kg^{-1} for Co, 19.90–395.9 mg kg^{-1} for Cu, 0.621–41.83 mg kg^{-1} for Pb, and 60.51–336.9 mg kg^{-1} for Zn. Among the PTEs under investigation, only the concentrations of Cu in leaf tissue were higher than those compiled by Kabata-Pendias (2011) as excessive or toxic values, and so may pose a potential risk to the food chain. It has detected the presence of numerous rabbits in the study area. There are many rabbit latrines and clear evidence of root predation of the studied species with unpredictable consequences on the biota.

By studying distribution of PTEs among roots, stems and leaves, a similar pattern can be drawn from both species for all PTEs except Co (Fig. 2), although the fractionation pattern was somewhat more homogeneous in *E. segetalis*. Results from chemical partitioning in plant tissues showed that the roots of the two investigated species accumulate significantly more As, Cu and Pb than the above-ground biomass ($p = 0.0001$). The target organs of such PTEs accumulation appeared to be: root > leaf > stem in *N. glauca*, and root > stem > leaf in *E. segetalis*. By contrast, the mean fractions of Zn and Cd showed a significant decrease in roots relative to aerial parts of *N. glauc*a, but they did not exhibit any clear distribution pattern among the organs of *E. segetalis*. Unlike all aforementioned PTEs, Co appears to be preferentially partitioned both in stems of *N. glauca* and leaves of *E. segetalis*.

The total concentrations of PTEs measured in the narrow zone of soil subject to the influence of roots may be used as a primary indicator to assess the uptake and transmission of contaminants through the soil–plant system of *N. glauca* and *E. segetalis*. Biogeochemical processes in the rhizosphere zone are known to produce various organic compounds, which are effective in releasing PTEs from firmly fixed species in soil (Kabata-Pendias, 2011). Figure 3 depicts the relationship between mean concentrations of PTEs in rhizospheric soil and those in plant organs of the two species. In general, the distribution of PTEs appeared to follow a pattern that involves an increase in the mean concentration in both soil and plant tissues, with Cu and Zn being particularly implicated. It should be also noted the high level of Cd measured in the leaves of *N. glauca* compared to its content in soil immediately adjacent to roots. When the mean concentrations of PTEs in plant tissues are plotted versus the mean concentration of PTEs extracted with a standardized solution of $CaCl_2$ (Fig. 4), which is considered that may be available in the rhizosphere for plant uptake, a similar picture emerged for *N. glauca* and *E. segetalis*. The highest $CaCl_2$-extractable PTEs (i.e., Cu and Zn) were accumulated in plant organs to a greater extent than the others, although Pb showed a relatively high concentration in all organs of both plant species despite its low extraction yields. This could be explained by the fact that, under certain circumstances, the root exudates were capable of

Table 5 Trace element concentrations (mg kg^{-1}) in plant organs of *Nicotiana glauca* and *Euphorbia segetalis*

Plant species	Plant organ	Sample	As	Cd	Co	Cu	Pb	Zn
N. glauca	Root	DR-N-1	13.39 ± 0.14	1.907 ± 0.026	1.426 ± 0.018	149.2 ± 0.8	41.83 ± 0.28	149.3 ± 0.1
		DR-N-2	9.617 ± 0.162	1.279 ± 0.029	2.673 ± 0.048	234.8 ± 1.7	34.50 ± 0.47	281.8 ± 1.4
		DR-N-3	6.717 ± 0.091	1.397 ± 0.023	0.766 ± 0.014	313.8 ± 2.4	26.94 ± 0.27	142.1 ± 0.6
		DR-N-4	1.792 ± 0.030	0.452 ± 0.011	0.228 ± 0.007	67.54 ± 0.47	7.243 ± 0.115	135.8 ± 0.6
		DR-N-5	5.772 ± 0.072	0.577 ± 0.011	0.327 ± 0.007	132.9 ± 0.4	32.37 ± 0.29	117.8 ± 0.2
		Control	1.377 ± 0.034	0.270 ± 0.006	0.601 ± 0.018	30.95 ± 0.63	3.436 ± 0.093	53.85 ± 0.96
	Stem	DR-N-1	1.578 ± 0.023	3.940 ± 0.065	6.757 ± 0.088	39.15 ± 0.38	4.154 ± 0.063	250.5 ± 0.6
		DR-N-3	0.288 ± 0.008	0.977 ± 0.015	3.776 ± 0.050	21.76 ± 0.26	0.621 ± 0.035	107.4 ± 0.5
		DR-N-4	0.034 ± 0.005	0.577 ± 0.008	2.850 ± 0.038	19.90 ± 0.25	0.706 ± 0.037	60.51 ± 0.44
		DR-N-5	0.496 ± 0.013	1.973 ± 0.041	2.562 ± 0.048	52.45 ± 0.73	4.776 ± 0.094	134.6 ± 1.1
		Control	0.024 ± 0.004	0.170 ± 0.002	1.045 ± 0.019	7.976 ± 0.188	0.118 ± 0.032	43.30 ± 0.51
	Leaf	DR-N-1	2.139 ± 0.020	13.16 ± 0.18	0.184 ± 0.004	128.6 ± 0.1	11.46 ± 0.08	336.9 ± 1.1
		DR-N-2	0.855 ± 0.022	6.488 ± 0.182	0.406 ± 0.013	97.95 ± 1.43	6.228 ± 0.154	307.5 ± 3.6
		DR-N-3	1.147 ± 0.028	3.589 ± 0.087	0.338 ± 0.012	148.0 ± 2.3	9.333 ± 0.184	184.1 ± 2.0
		DR-N-4	1.567 ± 0.034	3.906 ± 0.098	0.220 ± 0.008	215.4 ± 2.3	9.428 ± 0.184	224.9 ± 2.0
		DR-N-5	0.946 ± 0.021	2.962 ± 0.073	0.105 ± 0.006	124.7 ± 1.3	6.335 ± 0.133	163.1 ± 1.4
		Control	0.258 ± 0.010	0.225 ± 0.009	0.020 ± 0.005	31.78 ± 0.64	0.411 ± 0.049	58.99 ± 1.15
E. segetalis	Root	DR-E-1	6.377 ± 0.117	2.004 ± 0.047	0.777 ± 0.017	395.9 ± 3.5	9.561 ± 0.166	167.5 ± 1.2
		DR-E-2	7.423 ± 0.090	0.825 ± 0.012	0.800 ± 0.013	394.4 ± 2.5	14.05 ± 0.14	120.1 ± 0.4
		DR-E-3	3.176 ± 0.012	1.019 ± 0.006	0.811 ± 0.005	254.8 ± 0.6	8.304 ± 0.017	94.73 ± 0.48
		DR-E-4	9.358 ± 0.051	2.761 ± 0.025	0.981 ± 0.008	284.1 ± 0.0	23.48 ± 0.05	163.8 ± 0.7
		DR-E-5	7.485 ± 0.043	1.636 ± 0.015	1.145 ± 0.010	322.0 ± 0.0	39.12 ± 0.07	219.8 ± 1.1
		Control	1.519 ± 0.005	0.286 ± 0.000	0.313 ± 0.003	68.27 ± 0.21	3.920 ± 0.013	95.79 ± 0.68
	Stem	DR-E-1	1.509 ± 0.029	0.963 ± 0.019	0.761 ± 0.017	172.6 ± 1.9	6.040 ± 0.105	99.23 ± 0.86
		DR-E-2	2.614 ± 0.015	0.726 ± 0.005	0.981 ± 0.008	234.0 ± 0.1	9.239 ± 0.032	116.2 ± 0.5
		DR-E-3	1.786 ± 0.010	0.315 ± 0.001	0.451 ± 0.005	134.7 ± 0.2	4.968 ± 0.024	70.97 ± 0.21
		DR-E-4	4.425 ± 0.046	1.035 ± 0.013	0.270 ± 0.007	140.9 ± 0.7	14.42 ± 0.11	85.77 ± 0.23
		DR-E-5	0.831 ± 0.007	0.432 ± 0.002	0.390 ± 0.005	87.12 ± 0.01	4.563 ± 0.028	87.71 ± 0.28
		Control	0.558 ± 0.016	0.200 ± 0.004	1.349 ± 0.031	54.52 ± 0.89	2.652 ± 0.076	158.4 ± 1.6
	Leaf	DR-E-1	1.481 ± 0.027	0.618 ± 0.015	2.771 ± 0.050	154.1 ± 1.2	8.771 ± 0.145	118.7 ± 0.8
		DR-E-2	1.964 ± 0.022	0.656 ± 0.011	3.581 ± 0.040	121.2 ± 0.2	16.16 ± 0.13	162.4 ± 0.1
		DR-E-3	0.994 ± 0.009	0.123 ± 0.003	1.254 ± 0.012	51.73 ± 0.04	4.531 ± 0.043	88.94 ± 0.24
		DR-E-4	3.476 ± 0.051	0.766 ± 0.016	0.876 ± 0.015	87.22 ± 0.48	18.92 ± 0.22	116.2 ± 0.4
		DR-E-5	0.810 ± 0.001	0.195 ± 0.001	1.410 ± 0.002	54.16 ± 0.46	4.818 ± 0.004	103.5 ± 1.1
		Control	0.704 ± 0.004	0.138 ± 0.002	11.65 ± 0.05	60.49 ± 0.28	3.689 ± 0.026	380.5 ± 3.0

forming complexes with trace element ions in solution (Mench & Martin, 1991), thus enhancing Pb mobilization and uptake by plants.

The potential mobility of PTEs from soil to plants was evaluated by the soil-to-plant transfer coefficient (TC), which is a mobility index that records the average concentration of the whole plant (C_{plant}), or certain plant parts, over that in rhizospheric soil (C_{soil}) of each element of concern (Adriano, 2001; Antoniadis et al., 2017; Kumar et al., 2013; Shaheen & Rinklebe, 2015), as follows:

$$TC = C_{plant} / C_{soil}$$

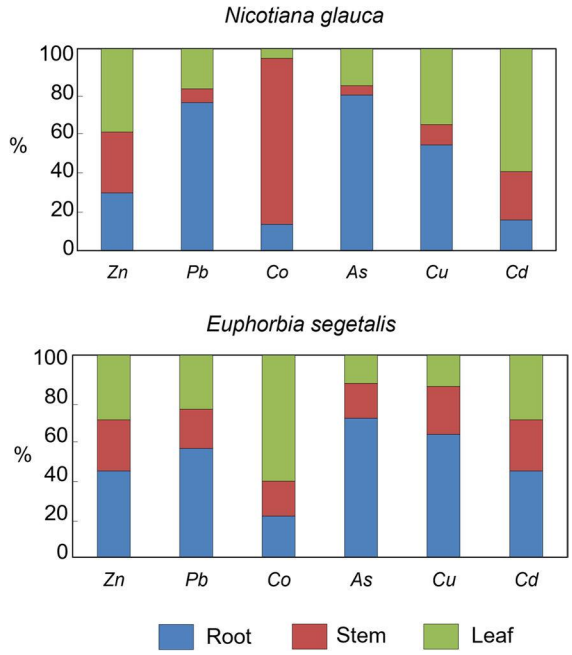

Fig. 2 Partitioning of trace elements among the plant organs of *Nicotiana glauca* and *Euphorbia segetalis*

thus allowing feasible comparisons among PTEs, as well as among different plant tissues. TC has been used as indicator of bioavailability (Adriano, 2001) and to estimate the phytoremediation potential of plants (Yoon et al., 2006).

The soil–plant transfer coefficient values of PTEs in all parts of both plants were well below unity with the only exception of Cd in leaves of *N. glauca* (Table 6), indicating that a limited fraction of PTEs was actually solubilized by root exudates and transferred to plants despite the high degree of soil contamination. This finding suggests that roots acted as a barrier limiting the uptake of PTEs by plants. Interestingly, *N. glauca* can absorb Cd in considerable proportions from rhizosphere and accumulate it in its leaves under the same soil conditions. This is in line with other studies, showing that Cd has great potential to escape the soil–plant barrier (Chaney et al., 1999).

A better way to quantify the uptake of contaminants from soil by plant roots and their transfer and accumulation in above-ground biomass is to use the translocation factor (Baker, 1981), which can be estimated through the shoot–root quotient, as follows:

$$\mathrm{TF} = C_{\text{stem or leaves}} / C_{\text{root}}$$

where TF is the translocation factor, $C_{\text{stem or leaves}}$ is the concentration of PTE in aboveground part of the plant (stem or leaves) and C_{root} is the concentration of PTE in root. A TF > 1 indicates that plants not only tolerate but utilize the PTEs in a beneficial way (Antoniadis et al., 2017).

As shown in Fig. 5, *N. glauca* translocated Cd effectively from the root to the stem (TF = 1.4) and, to a large extent, to the leaves (TF = 5.4), as well as Co from the root to the stem (TF = 3.1), and Zn from the root to the leaves (TF = 1.5), indicating that this wild plant species had high efficiency for phytoextraction of such elements from the contaminated soil. *N. Glauca* tolerance to PTEs has been previously reported (Barazani et al., 2004; Martínez-Fernández et al., 2014) related to the encode of a phytochelatin synthase and the production of nicotianamine synthetase that would promote some PTEs tolerance (Gajaje et al., 2021; Shingu et al., 2005). Instead, the capacity of *E. segetalis* was not effective in transferring PTEs from roots to shoots because the translocation factor values of PTEs were below unity except for Co, which appeared to be accumulated mainly in leaf tissues (TF = 2.2). This is a feature of metal excluder plant (Baker, 1981; Kumar et al., 2013). Therefore, marked differences in the PTE accumulating ability were found between both plant species.

Conclusions

The soil developed on legacy mine wastes (Spolic Technosol) of the Natural Area *Estero Domingo Rubio* is highly acidic and strongly contaminated with sulfate and PTEs arising from oxidative dissolution of sulfidic material, which impose severe limitations for establishing vegetation. The results from

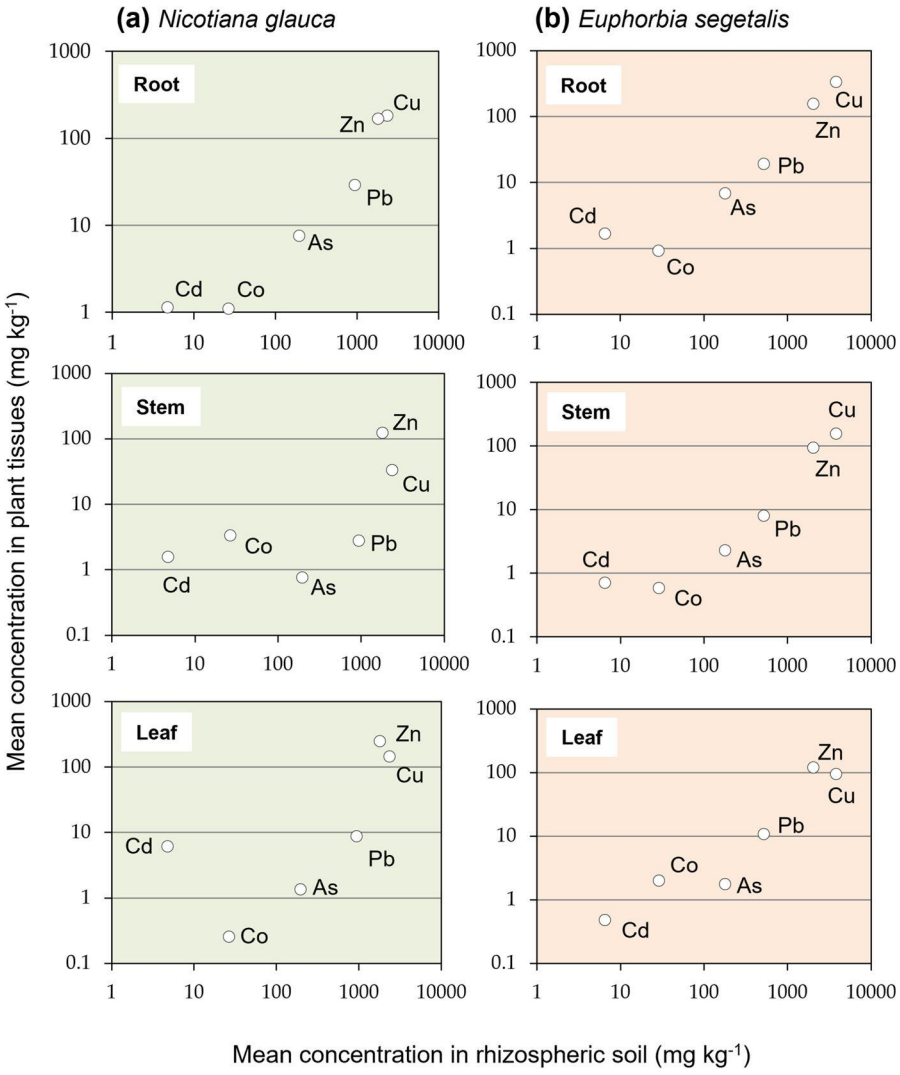

Fig. 3 **Trace** elements mean concentration in organs vs mean concentration in rhizosphere soil of **a** *Nicotiana glauca* and **b** *Euphorbia segetalis*

this study led to the conclusion that, despite these unfavorable soil conditions for plant development and growth, *N. glauca* and *E. segetalis* are able to colonize heavily contaminated soil with a slightly alkaline reaction, occurring in isolated randomly distributed patches on bare land. The high acid-neutralizing capacity of the rhizospheric soil was effective in reducing PTEs mobilization, and consistently a limited fraction of phytoavailable PTEs (i.e., extractable with $CaCl_2$) was transferred to plants. Soil acidity is regarded, therefore, as the key factor limiting plant development. Notwithstanding, the results of the plant tissue analysis showed that *N. glauca* and *E. segetalis* accumulated relatively high concentrations of As, Cu and Pb into their roots, reflecting the high degree of soil contamination, while the aerial parts of the plants were the target organs of Zn, Cd and Co. The establishment of these spontaneous metal-tolerant plants helps to mitigate the adverse impact of the mine wastes on the wetland, although the risk of PTEs entering the food chain needs to be evaluated. The new insights gained from this study provide criteria to assist in natural remediation in other legacy contaminated sites worldwide.

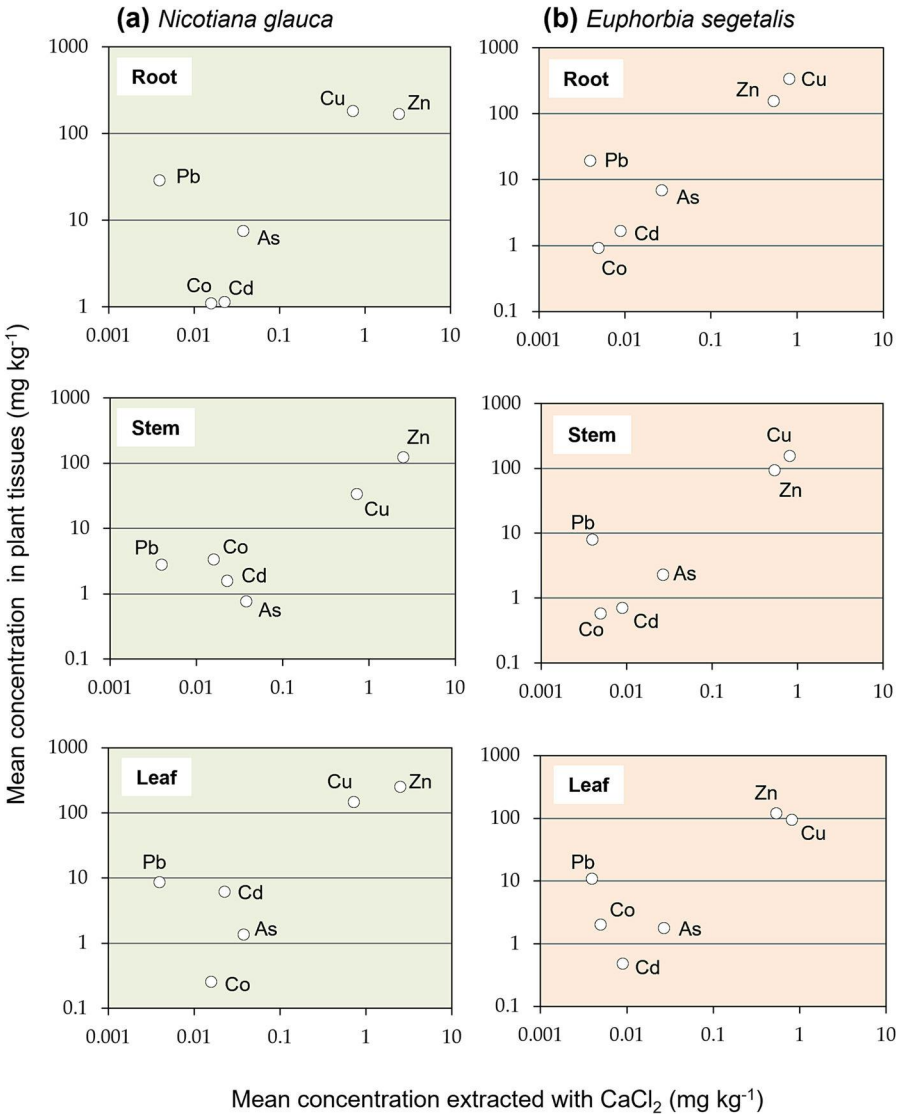

Fig. 4 Trace elements mean concentration in organs vs $CaCl_2$-extracted mean concentration in rhizosphere soil of **a** *Nicotiana glauca* and **b** *Euphorbia segetalis*

Table 6 Soil–plant transfer factors of trace elements for each plant organ of *Nicotiana glauca* and *Euphorbia segetalis*

Trace element	As	Cd	Co	Cu	Pb	Zn
Nicotiana glauca						
Root	0.038	0.234	0.040	0.075	0.030	0.091
Stem	0.004	0.322	0.123	0.014	0.003	0.067
Leaf	0.007	1.254	0.009	0.060	0.009	0.133
Euphorbia segetalis						
Root	0.037	0.250	0.031	0.085	0.036	0.075
Stem	0.012	0.105	0.020	0.040	0.015	0.045
Leaf	0.010	0.071	0.068	0.024	0.020	0.057

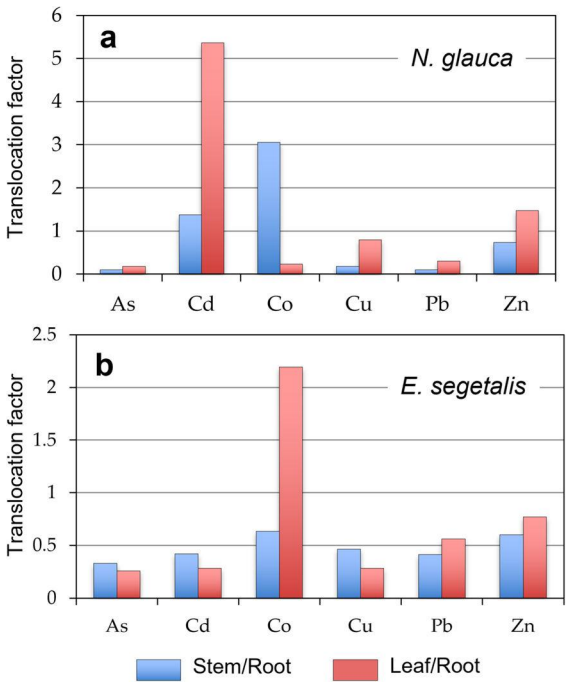

Fig. 5 Translocation factors calculated as the ratio between trace element mean concentration in aerial parts (stems and leaves) and trace element mean concentrations in the roots of **a** *Nicotiana glauca* and **b** *Euphorbia segetalis*

Acknowledgements This research was partially supported by the Regional Government of Andalusia (Spain) and the European Regional Development Fund Andalusia 2014-2020 through the Project P-18-TP-3503.

Author Contributions All authors contributed to the study conception and design. All authors collaborated in writing and commenting on previous versions of the manuscript. All authors read and approved the final manuscript.

Funding Funding for open access publishing: Universidad de Sevilla/CBUA. This research was partially supported by the Regional Government of Andalusia (Spain) and the European Regional Development Fund Andalusia 2014–2020 through the Project P-18-TP-3503.

Declarations

Competing Interests The authors have no relevant financial or non-financial interests to disclose.

References

Adriano, D. C. (2001). *Trace elements in terrestrial environments. Biogeochemistry, bioavailability, and risks of metals* (2nd ed.). Springer.

Antoniadis, V., Levizou, E., Shaheen, S. M., Ok, Y. S., Sebastian, A., Baum, C., Prasad, M. N. V., Wenzel, W. W., & Rinklebe, J. (2017). Trace elements in the soil-plant interface: Phytoavailability, translocation, and phytoremediation–A review. *Earth-Science Reviews, 171*, 621–645. https://doi.org/10.1016/j.earscirev.2017.06.005

Baker, A. J. M. (1981). Accumulators and excluders strategies in response of plants to heavy metals. *Journal of Plant Nutrition, 3*, 643–654.

Barazani, O., Sathiyamoorthy, P., Manandhar, U., Vulkan, R., & Golan-Goldhirsh, A. (2004). Heavy metal accumulation by *Nicotiana glauca* Graham in a solid waste disposal site. *Chemosphere, 54*, 867–872. https://doi.org/10.1016/j.chemosphere.2003.10.005

Barba-Brioso, C., Fernández-Caliani, J.C., Miras, A., Galán, E. (2009). Evaluation of labile metal pools in soils from a highly industrialised wetland area of southwestern Spain by single and sequential extraction methods. Geochimica Et Cosmochimica Acta, 73 (13S) *Goldschmidt 2009 Conference Abstracts* A85. ISSN 0016–7037 / 1872–9533

Barba-Brioso, C. (2011). Mineralogía, Geoquímica e implicaciones ambientales de los Suelos y Sedimentos del Paraje Natural Estero Domingo Rubio y su Entorno (Huelva). In *Tesis Doctoral*. Universidad de Sevilla.

Barba-Brioso, C., Delgado, J., Fernández-Caliani, J.C. (2021). Sulfide oxidation, chemical partitioning and environmental availability of iron and trace elements in abandoned mine wastes affecting a coastal wetland ecosystem. In *EGU General Assembly, 19-30 Apr 2021*. https://doi.org/10.5194/egusphere-egu21-5195

Barba-Brioso, C., Fernández-Caliani, J. C., Miras, A., Cornejo, J., & Galán, E. (2010a). Multi-source water pollution in a highly anthropized wetland system associated with the estuary of Huelva (SW Spain). *Marine Pollution Bulletin, 60*(8), 1259–1269. https://doi.org/10.1016/j.marpolbul.2010.03.018

Barba-Brioso, C., Otero, X. L., Fernández-Caliani, J. C., Delgado, J., Macías, F., & Galán, E. (2010c). Fraccionamiento de Fe y metales pesados en un depósito incontrolado de residuos mineros del paraje natural Estero Domingo Rubio (Huelva). *Geogaceta, 48*, 103–106.

Barba-Brioso, C., Quaranta, G., Galán, E., Fernández-Caliani, J. C., & Miras, A. (2010b). The life cycle impact assessment applied to the Domingo Rubio tidal system by the

study of seasonal variations of the aquatic eutrophication potential. *Science of the Total Environment, 408*(23), 5897–5902. https://doi.org/10.1016/j.scitotenv.2010.08.002

Chaney, R. L., Ryan, J. A., Li, Y. M., & Brown, S. L. (1999). Soil cadmium as a threat to human health. In M. J. McLaughlin & B. R. Singh (Eds.), *Cadmium in Soils and plants* (pp. 219–256). Kluwer Academic Publ.

Chen, Y. T., Wang, Y., & Yeh, K. C. (2017). Role of root exudates in metal acquisition and tolerance. *Current Opinion in Plant Biology, 39*, 66–72. https://doi.org/10.1016/j.pbi.2017.06.004

Conesa, H. M., María-Cervantes, A., Álvarez-Rogel, J., & González-Alcaraz, M. N. (2011). Influence of soil properties on trace element availability and plant accumulation in a Mediterranean salt marsh polluted by mining wastes: Implications for phytomanagement. *Science of the Total Environment, 409*(20), 4470–4479. https://doi.org/10.1016/j.scitotenv.2011.07.049

Dana, E., Sanz, M., Vivas, S., Sobrino, E. (2005). Especies Vegetales Invasoras en Andalucía. *D.G. de la Red de Espacios Naturales Protegidos y Servicios Ambientales. Consejería de Medio Ambiente. Junta de Andalucía*

Junta de Andalucía (2015). Decreto 18/2015, de 27 de enero, por el que se aprueba el reglamento que regula el régimen aplicable a los suelos contaminados. *Boletín Oficial de la Junta de Andalucía, 38*, 28–64

Directive (2009). *2009/147/EC of the European Parliament and of the Council of 30 November 2009 on the conservation of wild birds*.

European Commission (2021). EU Soil Strategy for 2030. Reaping the Benefits of Healthy Soils for People, Food, Nature and Climate. *Communication from the Commission to the European Parliament, the Council, the European Economic and Social Committee, and the Committee of the Regions. COM(2021) 699 final*.

Fernández, S., Santín, C., Marquínez, J., & Álvarez, M. A. (2010). Saltmarsh soil evolution after land reclamation in Atlantic estuaries (Bay of Biscay, North coast of Spain). *Geomorphology, 114*(4), 497–507. https://doi.org/10.1016/j.geomorph.2009.08.014

Fernández-Caliani, J. C., Barba-Brioso, C., González, I., & Galán, E. (2009). Heavy metal pollution in soils around the abandoned mine sites of the Iberian Pyrite Belt (Southwest Spain). *Water Air Soil Pollution, 200*, 211–226. https://doi.org/10.1007/s11270-008-9905-7

Gajaje, K., Venecio, U. U., Jr., Pearl, W. D., & Gaolathe, R. (2021). Rhizosphere properties and heavy metal accumulation of plants growing in the fly ash dumpsite, Morupule power plant, Botswana. *Environmental Science and Pollution Research, 28*, 20637–20649. https://doi.org/10.1007/s11356-020-11905-7

Grantcharova, M., & Fernández-Caliani, J. C. (2022). Soil acidification, mineral neoformation and heavy metal contamination driven by weathering of sulphide wastes in a Ramsar Wetland. *Applied Sciences*. https://doi.org/10.3390/app12010249

Houba, V. J. G., Novozamsky, I., Lexmond, T. M., & Der Jvnn, L. (1990). Applicability of 0.01 M $CaCl_2$ as a single extraction solution for the assessment of the nutrient status of soils and other diagnostic purposes. *Communications in Soil Science and Plant Analysis, 21*, 2281–2290. https://doi.org/10.1080/00103629009368380

Jakupovic, J., Jeske, F., Morgenstern, T., Tsichritzis, F., Marco, J. A., & Berendsohn, W. (1998). Diterpenes from *Euphorbia segetalis*. *Phytochemistry, 47*(8), 1583–1600. https://doi.org/10.1016/S0031-9422(97)00830-3

Kabata-Pendias, A. (2011). *Trace elements in soils and plants* (4th ed.). CRC Press.

Kahle, M., Kleber, M., & Reinhold, J. (2002). Review of XRD-based quantitative analyses of clay minerals in soils: The suitability of mineral intensity factors. *Geoderma, 109*, 191–205. https://doi.org/10.1016/S0016-7061(02)00175-1

Kumar, N., Bauddh, K., Kumar, S., Dwivedi, N., Singh, D. P., & Barman, S. C. (2013). Accumulation of metals in weed species grown on the soil contaminated with industrial waste and their phytoremediation potential. *Ecological Engineering, 61*, 491–495. https://doi.org/10.1016/j.ecoleng.2013.10.004

Li, Y., Shi, Y., Zhu, X., Cao, H., & Yu, T. (2014). Coastal wetland loss and environmental change due to rapid urban expansion in Lianyungang, Jiangsu, China. *Regional Environmental Change, 14*, 1175–1188. https://doi.org/10.1007/s10113-013-0552-1

Luster, J., Göttlein, A., Nowack, B., & Sarret, G. (2009). Sampling, defining, characterizing and modeling the rhizosphere – the soil science tool box. *Plant and Soil, 321*, 457–482. https://doi.org/10.1007/s11104-008-9781-3

Madejón, P., Barba-Brioso, C., Lepp, N. W., & Fernández-Caliani, J. C. (2011). Traditional agricultural practices enable sustainable remediation of highly polluted soils in Southern Spain for cultivation of food crops. *Journal of Environmental Management, 92*(7), 1828–1836. https://doi.org/10.1016/j.jenvman.2011.03.007

Madejón, P., Burgos, P., Murillo, J. M., Cabrera, F., & Madejón, E. (2009). Bioavailability and accumulation of trace elements in soils and plants of a highly contaminated estuary (Domingo Rubio tidal channel, SW Spain). *Environmental Geochemistry and Health, 31*(6), 629–642. https://doi.org/10.1007/s10653-008-9221-6

Madureira, A. M., Ascenso, J. R., Valdeira, L., Duarte, A., Frade, J. P., Freitas, G., & Ferreira, M. J. U. (2003). Evaluation of the antiviral and antimicrobial activities of triterpenes isolated from *Euphorbia segetalis*. *Natural Product Research, 17*(5), 375–380. https://doi.org/10.1080/1478641031000160584 1

Márquez-García, B., Hidalgo-Fernández, P. J., & Córdoba-García, F. (2006). How does the plant *Erica* andevalensis survive despite highly elevated soil metal contamination? *SETAC Globe, 7*, 37–38.

Martínez-Fernández, D., Arco-Lázaro, E., Bernal, M. P., & Clemente, R. (2014). Comparison of compost and humic fertiliser effects on growth and trace elements accumulation of native plant species in a mine soil phytorestoration experiment. *Ecological Engineering, 73*, 588–597.

McBride, M. B. (1994). *Environmental chemistry of soils*. Oxford University Press.

Mench, M., & Martin, E. (1991). Mobilization of cadmium and other metals from two soils by root exudates of Zea mays L., Nicotiana tabacum L. and Nicotiana rustica L. *Plant and Soil, 132*, 187–196.

Mendez, M. O., & Maier, R. M. (2008). Phytostabilization of mine tailings in arid and semiarid environments—an emerging remediation technology. *Environmental Health Perspectives, 116*, 278–283. https://doi.org/10.1289/ehp.10608

Menzies, N. W., Donn, M. J., & Kopittke, P. M. (2007). Evaluation of extractants for estimation of the phytoavailable trace metals in soils. *Environmental Pollution, 145*(1), 121–130. https://doi.org/10.1016/j.envpol.2006.03.021

Pendón, J. G., Morales, J. A., Borrego, J., Jiménez, I., & López, M. (1998). Evolution of estuarine facies in a tidal channel environment, SW Spain: Evidence for a change from tide- to wave-domination. *Marine Geology, 147*, 43–62.

Rivera, M. B., Giráldez, M. I., & Fernández-Caliani, J. C. (2016). Assessing the environmental availability of heavy metals in geogenically contaminated soils of the Sierra de Aracena Natural Park (SW Spain). Is there a health risk? *Science of the Total Environment, 560–561*, 254–265. https://doi.org/10.1016/j.scitotenv.2016.04.029

Rossini-Oliva, S., Abreu, M. M., & Leidi, E. O. (2018). A review of hazardous elements tolerance in a metallophyte model species: *Erica* andevalensis. *Geoderma, 319*, 43–51. https://doi.org/10.1016/j.geoderma.2017.12.035

Sahai, R., Dube, M. P., & Rastogi, R. P. (1981). Chemical and pharmacological study of *Euphorbia maddeni*. *Indian Journal of Pharmaceutical Sciences, 43*(6), 216–219.

Samczyński, Z., Dybczyński, R. S., Polkowska-Motrenko, H., Chajduk, E., Pyszynska, M., Danko, B., Czerska, E., Kulisa, K., Doner, K., & Kalbarczyk, P. (2012). Two new reference materials based on tobacco leaves: Certification for over a dozen of toxic and essential elements. *The Scientific World Journal*. https://doi.org/10.1100/2012/216380

Santucci, L., Carol, E., Borzi, G., & García, M. G. (2017). Hydrogeochemical and isotopic signature of surface and groundwater in a highly industrialized sector of the Rio de la Plata coastal plain (Argentina). *Marine Pollution Bulletin, 120*, 387–395. https://doi.org/10.1016/j.marpolbul.2017.05.007

Shaheen, S. M., & Rinklebe, J. (2015). Phytoextraction of potentially toxic elements by Indian mustard, rapeseed, and sunflower from a contaminated riparian soil. *Environmental Geochemistry and Health, 37*, 953–967. https://doi.org/10.1007/s10653-015-9718-8

Shingu, Y., Kudo, T., Ohsato, S., Kimura, M., Ono, Y., Yamaguchi, I., & Hamamoto, H. (2005). Characterization of genes encoding metal tolerance proteins isolated from *Nicotiana glauca* and *Nicotiana tabacum*. *Biochemical and Biophysical Research Communications, 331*, 675–680. https://doi.org/10.1016/j.bbrc.2005.04.010

Tarazona, J. V., Fernandez, M. D., & Vega, M. M. (2005). Regulation of contaminated soils in Spain - A new legal instrument (4 pp). J*ournal of Soils and Sediments, 5*(2), 121–124. https://doi.org/10.1065/jss2005.05.135

Yoon, J., Cao, X., Zhou, Q., & Ma, L. Q. (2006). Accumulation of Pb, Cu, and Zn in native plants growing on a contaminated Florida site. *Science of the Total Environment, 368*, 456–464.

4.3. Evaluación a largo plazo del uso de lodos de mármol para reducir la acidez y la movilización de metales en un suelo minero de Tharsis

Basado en el artículo:

Long-term sustainability of marble waste sludge in reducing soil acidity and heavy metal release in a contaminated mine Technosol. Applied Sciences 12 (2022) 6998

Este estudio abordó la problemática de la remediación de suelos altamente contaminados en contextos mineros, caracterizados por una acidez extrema y elevadas concentraciones de EPT, como As, Pb y Zn. En este trabajo se trató de evaluar la eficacia a largo plazo de una enmienda alcalina a base de lodos procedentes de la industria del mármol (residuo R1) para inmovilizar EPT en un suelo minero de Tharsis. Concretamente, los objetivos específicos fueron determinar el efecto de la neutralización de la acidez en la composición química del lixiviado del suelo, así como determinar la influencia del lodo carbonatado en el fraccionamiento de EPT y su disponibilidad ambiental a largo plazo.

El trabajo se centró en un tecnosuelo del entorno de Filón Norte (Minas de Tharsis), afectado por DAM. Se empleó una metodología experimental en condiciones de campo sobre una parcela de 1 x 1 m de suelo contaminado, previamente enmendada con lodos de aserrado del mármol, aplicados 12 años antes. Se extrajeron 70 cm de suelo con una barrena de tipo Edelman, tanto en el suelo enmendado como en el suelo contaminado sin tratar (control), para un análisis comparativo de los siguientes parámetros: pH, conductividad eléctrica, concentraciones de EPT en el lixiviado y en el suelo (fracción total y extractable con EDTA). Además, se estudió la especiación operacional de los EPT en la capa superficial del suelo mediante técnicas analíticas de extracción secuencial (esquema BCR).

4.3.1. Resultados y discusión

Los resultados mostraron la alta efectividad de la enmienda alcalina a base de los lodos de aserrado del mármol en el proceso de neutralización de la acidez. Se

observó un incremento significativo del pH del suelo, desde valores extremadamente ácidos (3,1-3,5) a ligeramente alcalinos (5,8-6,4) en todo el perfil del suelo enmendado. Estos valores se mantuvieron prácticamente estables durante todo el experimento, lo que indica una capacidad amortiguadora duradera de la enmienda frente a la acidez residual del suelo minero.

En el suelo tratado, se observó que la mayoría de los cristales de calcita del lodo carbonatado permanecieron relativamente inalterados a pesar del tiempo transcurrido, si bien algunos granos presentaron signos de disolución parcial y otros aparecen recubiertos por oxihidróxidos de hierro. Además, aumentó la precipitación de yeso, inducida por la disolución parcial de los carbonatos añadidos.

En comparación con el control, las concentraciones de As, Pb y Cr en el suelo enmendado fueron significativamente inferiores en los primeros 20 cm del perfil, aumentando con la profundidad hasta alcanzar valores similares a los del suelo sin tratar (1860 mg kg^{-1} de As, 72 mg kg^{-1} de Cr y 2660 mg kg^{-1} de Pb). Este patrón de distribución vertical se atribuye efecto de dilución causado por la enmienda alcalina. En cambio, los niveles de Cu (1210 mg kg^{-1}), Cd (1,4 mg kg^{-1}), Ni (38 mg kg^{-1}) y Zn (851 mg kg^{-1}) en la capa superficial del suelo enmendado fueron significativamente más altos que en las capas profundas. A pesar del efecto de dilución, esta distribución indica una retención efectiva de metales en la zona tratada del suelo.

El fraccionamiento geoquímico determinado mediante extracción secuencial reveló cambios importantes en el reparto o distribución de EPT entre las distintas fracciones geoquímicas del suelo. Con el tratamiento, se registró una marcada disminución de la fracción más lábil (intercambiable y unida a carbonatos), acompañada de un aumento en las fracciones más estables, como la unida a óxidos de Fe/Mn y la residual. Esta redistribución sugiere una transformación de los contaminantes hacia fracciones menos móviles y biodisponibles, a través de mecanismos tales como:

- **Precipitación de fases secundarias.** El incremento del pH favoreció la sobresaturación y consecuente precipitación de oxihidróxidos de Fe y Al y

carbonatos metálicos. Estas fases neoformadas pueden actuar, a su vez, como sustratos o superficies para la adsorción de EPT.

- **Coprecipitación.** Los EPT también pudieron alojarse directamente en la estructura cristalina de los carbonatos o los hidróxidos de Fe generados tras la enmienda.

- **Adsorción/intercambio iónico.** Las nuevas fases precipitadas (oxihidróxidos de Fe y Al) proporcionaron sitios de sorción para la fijación de aniones, arseniato en el caso del As.

La fracción de EPT extraíble con agua, considerada la más fácilmente lixiviable y potencialmente disponible para la absorción vegetal, fue insignificante. El EDTA mostró una mayor eficacia de extracción de EPT, aunque las cantidades variaron notablemente según el elemento y la profundidad del suelo. Dado que el EDTA es capaz de extraer EPT de todas las fases no unidas a silicatos, su acción refleja de forma más realista la disponibilidad potencial de los metales a largo plazo.

Un aspecto importante para la aplicabilidad práctica de esta estrategia de remediación es la estabilidad a largo plazo de los efectos observados. A diferencia de otras enmiendas cuya eficacia puede disminuir con el tiempo, el lodo micronizado de mármol mantuvo su capacidad neutralizante e inmovilizadora durante los 12 años posteriores a su aplicación, lo que indica una solución duradera.

4.3.2. Conclusiones

Con una sola aplicación de lodos residuales de la industria del mármol, se logró reducir eficazmente la acidez y la liberación de EPT en el suelo minero, manteniendo su efecto neutralizante 12 años después. Su capacidad para elevar y mantener el pH del suelo, junto con la promoción de mecanismos de precipitación y adsorción, se tradujo en una reducción significativa de la movilidad y disponibilidad de los contaminantes.

Estos efectos de remediación son sostenibles a largo plazo, lo que permite validar la estabilidad geoquímica de los contaminantes y la viabilidad ambiental de la enmienda como estrategia para la recuperación de extensos suelos mineros acidificados.

applied sciences

MDPI

Article

Long-Term Sustainability of Marble Waste Sludge in Reducing Soil Acidity and Heavy Metal Release in a Contaminated Mine Technosol

Juan Carlos Fernández-Caliani [1,*], Inmaculada Giráldez [2], Sandra Fernández-Landero [1], Cinta Barba-Brioso [3] and Emilio Morales [2]

[1] Department of Earth Sciences, University of Huelva, Campus de El Carmen, 21071 Huelva, Spain; sandra.fernandez@dct.uhu.es
[2] Department of Chemistry, University of Huelva, Campus de El Carmen, 21071 Huelva, Spain; giraldez@uhu.es (I.G.); albornoz@uhu.es (E.M.)
[3] Department of Crystallography, Mineralogy and Agricultural Chemistry, University of Seville, Campus de Reina Mercedes, 41071 Seville, Spain; cbarba@us.es
* Correspondence: caliani@uhu.es

Abstract: A field-based experiment was set up to evaluate the effectiveness of a single application of marble waste sludge (MWS) on chemical immobilization of potentially hazardous trace elements (PHE) within the soil profile of a mine Technosol under natural assisted remediation for 12 years. Results showed that MWS amendment significantly reduced soil acidity and PHE mobility compared to unamended soil, thus improving soil health and plant growth. The amendment application had a sustained acid-neutralizing action, as soil pH remains relatively constant at between 5.8 and 6.4 throughout the entire profile (70 cm depth). In addition to diluting pollutants, the treatment triggered a redistribution of trace elements among the various operationally defined geochemical pools, shifting the PHE speciation from water-soluble forms to fractions associated with carbonates (29% Cd), metal oxides (40–48% Zn, Cd, Cu, and Ni), organic matter (22% Cu and Ni), and insoluble secondary oxidation minerals and residual phases (80–99% As, Cr, Sb, Tl, and Pb), thereby effectively limiting its potential environmental significance. MWS treatment to immobilize PHE in the contaminated mine Technosol was effective and persistent while in the untreated soil metal release is continuing over time.

Keywords: waste recycling; soil amendment; acid neutralization; chemical partitioning; metal immobilization; mine soil

Citation: Fernández-Caliani, J.C.; Giráldez, I.; Fernández-Landero, S.; Barba-Brioso, C.; Morales, E. Long-Term Sustainability of Marble Waste Sludge in Reducing Soil Acidity and Heavy Metal Release in a Contaminated Mine Technosol. *Appl. Sci.* **2022**, *12*, 6998. https://doi.org/10.3390/app12146998

Academic Editors: Svetlana Bortnikova and Nataliya V. Yurkevich

Received: 24 May 2022
Accepted: 8 July 2022
Published: 11 July 2022

1. Introduction

Soils contaminated with potentially hazardous trace elements (PHE) arising from mining wastes and industrial discharges pose serious threat to human health and ecosystems [1,2]. Management of these environmentally significant soils [3] may require the use of sustainable remediation strategies to mitigate the dispersion of contaminants and their associated risks. Conventional soil clean-up technologies [4,5], especially those involving surface capping and landfilling, are often financially inefficient in extensive mine lands where treatments should be affordable and self-sustaining.

In situ stabilization or chemical fixation of PHE induced by the addition of immobilizing agents, such as soil amendments made of waste materials and by-products [6–8], is a cost-effective and eco-friendly option to reclaim abandoned mine lands following circular economy principles and modern waste management trends. These amendments can be referred as Technosols according to the World Reference Base for Soil Resources [9], because they form a new soil layer [10].

The immobilization technique involves PHE removal from soil solution either through precipitation, adsorption, ion exchange, or complexation mechanisms [11], thus reducing

to some extent contaminant uptake by plants and leaching into groundwater or nearby watercourses [12]. Since contaminant solubility is linked to its mobility and bioavailability, chemical stabilization has the potential to reduce environmental risk [13], although the immobilizing effects may not last long enough and, consequently, repeated amendment additions may be needed to sustain the stabilization process.

Liming is a widely used practice for reducing the mobility of PHE in contaminated soils with different degrees of success [14,15]. Most research on the use of lime-based waste materials and their efficiencies for PHE immobilization in soil has been conducted under laboratory conditions in short-term studies [11,12], as the liming effects were observed only after the first few years of treatment. These results from lab-scale experiments need to be validated by further field work to verify long-term stability of immobilized PHE in amended soils [16–18], where natural processes controlling PHE mobility can be monitored over long time scales under realistic conditions. Long-term field monitoring provides direct evidence of the ageing process of amendments [19].

Specifically, the waste sludge (i.e., micronized calcium carbonate) generated by marble processing plants has been proven as an effective nanomaterial for acid soil neutralization and for enhanced PHE retention capacity of soils affected by mining activities [20–23]. In fact, a field trial in the historic mining district of Tharsis (southwestern Spain) showed the potential of marble waste sludge (MWS) as a promising soil additive for assisting re-vegetation of legacy mine lands [24]. The most remarkable features of the MWS are alkalinity (pH = 8.8–9.2), fineness (mean particle size = 8.24 μm), and purity (~95 wt% of calcite). Using this MWS, a single amendment of 22 $cmol_c$ of lime per kilogram of soil was applied by Fernández-Caliani and Barba-Brioso [24] to raise the pH from 3.2 to a pH level suitable for plant regrowth. The acid neutralizing effect of the soil amendment effectively reduced the concentrations of Al, Fe, sulfate and PHE, notably Cd, Cu, Pb and Zn, in the most labile and phytoavailable fraction enough to allow the settlement of spontaneous plant species (*Lolium perenne, Plantago coronopus* and *Spergularia rubra*). Even though the reported early findings showed promise, substantial uncertainty exists regarding the long-term effectiveness of PHE stabilization in soil.

To address this uncertainty, a mini plot field experiment was conducted to evaluate the sustainability of a single application of MWS on chemical immobilization of PHE in the mine soil of Tharsis, after a period of 12 years post-application. The specific objectives were to ascertain: (1) the effect of acid buffering capacity of the liming waste on the soil leachate chemistry; and (2) the influence of the MWS addition on fractionation of PHE and their environmental availability over a long time span.

2. Location and Description of the Experimental Site

The experimental plot was established at the historic mine site of Tharsis, in southwestern Spain (Figure 1), a world-class massive sulfide deposit hosted primarily by black shale sequences from the latest Devonian [25]. The biggest deposit is exposed in the Filón Norte open pit (Figure 1a), with total original reserves of about 90 million tons containing average grades of 46.5% S, 0.7% Cu, 2.7% Zn plus Pb, 35 g/t Ag, and 0.9 g/t Au [26]. Besides, a wide variety of PHE (As, Cd, Hg, Sb, and Tl, among others) are usually present in the ore as trace elements.

Tharsis has a long history of metal extraction dating back from prehistoric (third millennium B.C.) and Roman to modern times [27]. Past mining and smelting activities have left an extensive legacy of heavily contaminated soils. The surface soil has been subjected to chemical loading for decades in the absence of legal and regulatory frameworks for mine closure and environmental remediation. In the vicinity of the mining area, the soil is adversely affected by acid mine drainage (AMD) emanating from the waste dumps, thus being unable to support plant life [22,28,29]. However, small agricultural holdings have persisted by adopting traditional farming practices that enable cultivation of food crops [30], all at risk of contamination [31]. Elevated levels of PHE in soil and vegetation can be detected up to 2–3 km downwind of the Tharsis mines [32,33].

The experimental plot (1 × 1 m) is regarded as representative of an area impacted by AMD discharges arising from the mine wastes of Filón Norte pit (Figure 1b), with an extension of about 1.5 ha. The site (UTM coordinates: X = 666,533 and Y = 4,163,175) is located 250 m above sea level and subject to a Mediterranean climate (*Csa* in the Köppen climate classification system) characterized by hot, dry summers and mild winters. During the experimental period (2007 to 2019), the average minimum and maximum temperatures were 5 °C and 34 °C, respectively, and the average annual rainfall was 389 mm, according to data recorded in the nearest weather station.

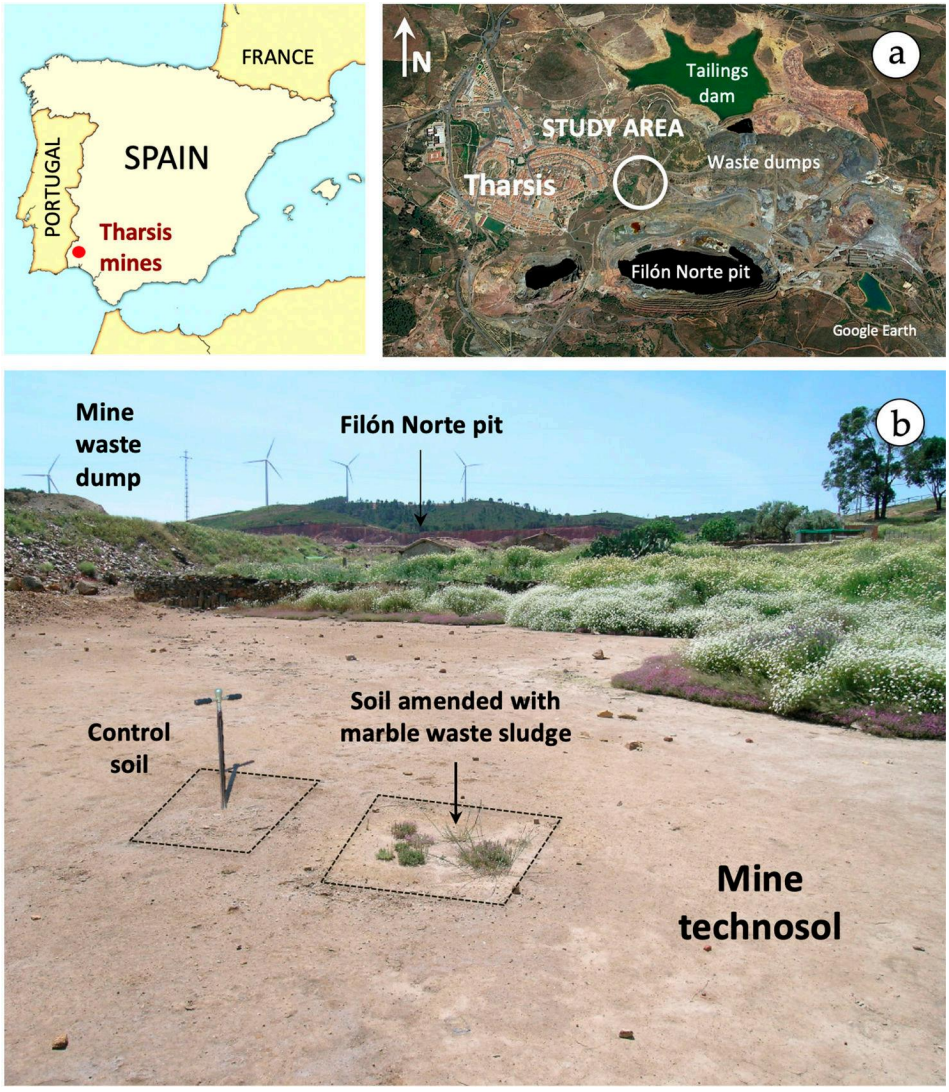

Figure 1. Location map of the study area showing a satellite view of the mining area of Tharsis (**a**), and a field picture of the field experimental site (**b**).

3. Materials and Methods

3.1. Soil Sampling

Two undisturbed soil cores were extracted by hand augering to a depth of 70 cm from the experimental mini plot amended with MWS in 2007 [24], and from an adjacent site of contaminated soil in which no amendment was applied (control soil) for comparative purposes. The cores were obtained using an Eijkelkamp auger (100 cm in length and 30 mm in diameter) after 12 years of MWS amendment application. The two soil cores were sectioned transversely into seven 10-cm thick slices that are assumed to be representative

samples of incremental depths within the soil profile (0–10, 10–20, 20–30, 30–40, 40–50, 50–60, and 60–70 cm) in both treated and control areas.

3.2. Analytical Procedures

The soil samples were air-dried, gently crushed to pass through a 2–mm sieve, and mixed thoroughly. Soil texture was determined by particle-size distribution analysis using a laser diffraction analyzer (Mastersizer 2000, Malvern Panalytical, Malvern, Worcestershire, UK). Soil reaction (pH), redox potential (Eh) and electrical conductivity (EC) were determined by stirring soil in deionized water at the ratio of 1:2.5 (g mL^{-1}). All measurements were performed in triplicate and averaged. Aliquots of the sieved material (<2 mm) were ground in an agate mortar until getting a fine powder (<63 μm) for analyses.

Major crystalline phases were identified by X-ray powder diffraction (XRPD) using a BRUKER AXS D8-Advance diffractometer (Bruker Corp., Karlsruhe, Germany), with monochromatic CuKα radiation operated at 40 kV and 30 mA. Scans of randomly oriented bulk powders were run from 3 to 70° 2θ with a step size of 0.02° and a counting time of 0.6 s per step. The XRPD raw data were processed with the software MacDiff 4.2.6 (from R. Petschick, Goethe-Universität Frankfurt, Frankfurt, Germany) to precisely determine the position, intensity, and area of the diffraction peaks. Semi-quantitative estimates of mineral abundance were made by empirical intensity factors weighting the integrated peak area values of diagnostic reflections [34], with absolute errors averaging less than 3% [35]. Samples were examined by environmental scanning electron microscopy (ESEM) on a JEOL JSM-IT500 instrument (JEOL, Tokyo, Japan) coupled with energy dispersive X-ray spectroscopy (EDS). Back-scattered electron (BSE) images and EDS spectra were acquired at 20 kV accelerating voltage to assist in the identification of accessory minerals of environmental concern.

The soil samples were subjected to multi-acid digestion (HF-$HClO_4$-HNO_3-HCl) followed by inductively coupled plasma-optical emission spectroscopy (ICP-OES) analysis to determine total concentrations of As, Cd, Cr, Cu, Ni, Pb, Sb, Tl, and Zn, all which are of environmental significance. The analyses were carried out at Activation Laboratories Ltd. (Ancaster, ON, Canada), which is compliant to the ISO/IEC 17,025 standard. Reliability of the analytical procedure was evaluated by the use of reagent blanks, certified reference materials (GRX-4, GRX-6, SDC-1, DNC-1a, OREAS-45d), and replicates to check accuracy and precision of the data. The average relative standard deviation (RSD) of the analyses was between 1.6 and 11.7%.

Chemical partitioning of PHE in the topsoil of both the amended and the control soil was determined using an improved Community Bureau of Reference (BCR) sequential extraction method [36]. This protocol fractionates PHE into three operationally defined pools: (F1) exchangeable and weak acid soluble fraction (extraction with 20 mL 0.11 mol L^{-1} acetic acid, CH_3COOH); (F2) reducible fraction (extraction with 20 mL 0.5 mol L^{-1} hydroxylammonium chloride, $NH_2OH{\cdot}HCl$); (F3) oxidizable fraction (digestion with 5 mL 8.8 mol L^{-1} hydrogen peroxide, H_2O_2, and extraction with 25 mL 1 mol L^{-1} ammonium acetate, CH_3COONH_4); and (F4) residual fraction (open vessel, hot plate acid digestion with 10 mL HF, 3.8 mL HNO_3, 5 mL $HClO_4$, and 1.2 mL HCl). Following each extraction step, the extract was centrifuged at 5000 rpm for 10 min, then the supernatant was filtered through a 0.45-μm membrane filter, and stored at 4° C until analysis. The PHE concentrations in the filtered soil extract were chemically analyzed by ICP-MS using an Agilent 7900 ICP-MS instrument (Agilent Technologies, Santa Clara, CA, USA), with detection and quantification limits of 0.01 μg L^{-1} and 0.03 μg L^{-1}, respectively, for all the determinations.

The sequential extraction procedure was repeated at least twice to ensure repeatability of results. The validity of the method was verified by carrying out analysis of a reference material (BCR-701) certified for extractable metal contents in the three steps of the modified BCR scheme [37]. The results showed a close agreement between observed and expected values for most PHE. The mean recovery was 102.6% with a standard deviation of 10.2% for PHE extracted in step 1, 102.2 ± 5.0% for those extracted in step 2, and 92.8 ± 16.0%

for those extracted in step 3. Moreover, the cumulative amount of PHE released from the three steps (F1 + F2 + F3) plus residual fraction (F4) compared well with the total PHE concentrations determined in soil samples, indicating acceptable levels of accuracy.

Easily leachable and potentially leachable fractions of PHE were assessed by single-reagent extraction tests with deionized water and with ethylene diamine tetraacetic acid (EDTA), respectively. Aliquots of each soil sample (<2 mm) were placed in 50-mL polypropylene centrifuge tubes and shaken for 2 h, with deionized water and with 0.05 mol L^{-1} EDTA (adjusted to pH 7.0) at a soil:solution ratio of 1:10 (w/v) [38,39]. Afterwards, the suspensions were centrifuged for 10 min at 5000 rpm, and then filtered through a 0.45-µm membrane filter. The PHE concentrations were measured in the filtrates by ICP-MS (Agilent 7900 ICP-MS instrument). Blank analyses were carried out to correct for contamination. The extraction procedure was repeated twice to assess reproducibility. Precision values were generally better than 10% RSD.

3.3. Analytical Analysis

The data obtained were statistically processed using the Statistica 10.0 (Stat Soft Inc., Tulsa, OK, USA) and MS Excel 2016 (Microsoft Co., USA) software packages. For statistical and graphical purposes, all values below detection limits (non-detects) were replaced with half of the detection limit [40]. Statistical differences between measured variables in treated and control samples were evaluated using Student's *t*-test and analysis of variance (one-way ANOVA). Prior to analysis, the homogeneity of variance was assessed by Levene's test. In this study, an α-value of 0.05 was used as critical level of significance for all statistical testing.

4. Results and Discussion

4.1. Mineral Composition and Soil Reaction

The soil affected by AMD discharges from the sulfide mine wastes is silt loam in texture (~68% silt, 25% sand and 7% clay), and mineralogically composed of quartz, clay minerals (illite and kaolinite) and jarosite, with minor feldspars, gypsum and hematite, as determined by XRPD analysis of control samples (Figure 2).

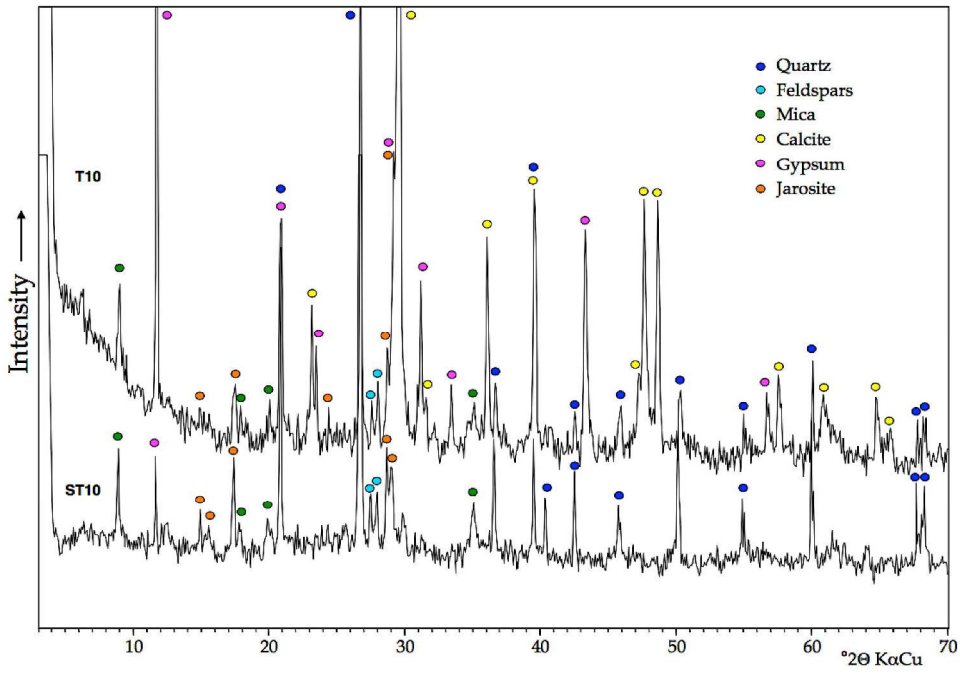

Figure 2. XRPD diffractograms of topsoil samples of amended soil (T10) and control soil (ST10).

In addition, a suite of accessory minerals was identified by ESEM-EDS, including barite, monazite, zircon, rutile, plumbogummite, cuprospinel and poorly crystallized iron oxides. Consistently, the contaminated mine soil has a poor buffering capacity to neutralize acid that is being produced, or has been produced, by AMD because it is completely free of carbonates and depleted in other acid-neutralizing minerals. Jarosite typically occurs as clusters of euhedral crystals of less than 1 μm in size, coexisting with iron oxides nanoparticles and soil clays, as observed by ESEM at high magnification (Figure 3a,b). The EDS spectra of some isolated crystals of a jarosite-group mineral that appear brighter in the ESEM-BSE images revealed a remarkable amount of Pb, by virtue of which they can be ascribed to plumbojarosite (Figure 3c).

Twelve years after amendment with MWS, the soil showed a silt loam texture with high contents of fine-grained calcite in the topsoil layer (0–20 cm) and lower proportions of the other constituents relative to control soil, with the exception of gypsum. It is interesting to note that most calcite crystals remain unaltered, maintaining their original rhombohedral morphology despite the long time since marble slurry application. Nevertheless, some of them showed signs of partial dissolution on their surface (Figure 3d), and some others appear to be coated by iron oxyhydroxides (Figure 3e). Direct precipitation of gypsum (Figure 3f) was induced by partial dissolution of the carbonates added to the soil, thus providing the Ca^{2+} ions necessary to combine with the sulfate ions. The neutralization reaction can explain not only the increase in gypsum concentration observed in the amended soil layer but also the occurrence of metal oxide coatings, as the Fe^{3+} solubility is controlled by the precipitation of ferric iron oxyhydroxides [2].

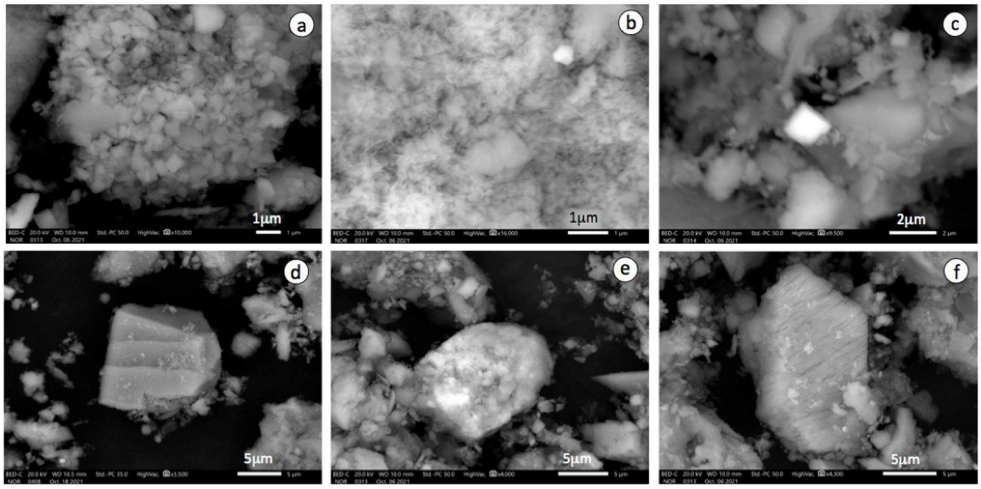

Figure 3. ESEM-BSE images showing salient mineralogical and textural features of the amended soil after 12 years of amendment application: (**a**) aggregate of jarosite with pseudocubic habit of euhedral crystals; (**b**) iron oxide nanoparticle aggregate; (**c**) isolated pseudocubic crystal of plumbojarosite; (**d**) calcite grain with dissolution grooves on its surface; (**e**) iron oxide coating calcite grain; and (**f**) newly-formed crystal of gypsum.

Soil reaction measured on control samples was ultra-acid, with pH values ranging from 3.1 to 3.5 (Table 1), whereas in the amended plot the soil samples had pH values in the range of 5.8–6.4, with an average of 6.2. Therefore, the soil solution appears to be neutralized to slightly acidic reaction throughout the entire sampled profile (0–70 cm) in the response to MWS amendment. Moreover, the long-term measurement of soil redox potential changed noticeably from strongly oxidizing conditions (Eh = 535–647 mV) to moderately oxidizing conditions (Eh = 343–525 mV) after treatment. The mean values of soil electrical conductivity were 2.62 mS cm^{-1} in the amended soil and 3.04 mS cm^{-1} in the unamended soil, indicating a low soluble salt content in both soil solutions.

Table 1. Electrochemical properties and semiquantitative mineral composition of the samples.

Sample		Depth (cm)	Electrochemical Parameters			Mineral Composition (wt %)						
			pH	Eh (mV)	EC (mS/cm)	Quartz	Clay Minerals *	Feldspars	Jarosite	Gypsum	Hematite	Calcite
Amended soil	T10	0–10	6.3	343	3.32	10–15	5–10	<5	10–15	10–15	<5	55–60
	T20	10–20	6.4	458	3.01	30–35	25–30	<5	10–15	5–10	<5	25–30
	T30	20–30	6.3	421	2.85	40–45	30–35	<5	15–20	<5	<5	n.d.
	T40	30–40	5.8	472	1.72	40–45	30–35	<5	15–20	<5	<5	n.d.
	T50	40–50	6.1	502	1.95	35–40	30–35	<5	15–20	<5	<5	n.d.
	T60	50–60	6.3	407	2.90	35–40	35–40	<5	15–20	<5	<5	n.d.
	T70	60–70	6.2	525	2.61	40–45	30–35	<5	15–20	<5	<5	n.d.
Control soil	ST10	0–10	3.2	619	4.02	40–45	35–40	5–10	10–15	<5	<5	n.d.
	ST20	10–20	3.3	647	3.10	35–40	25–30	<5	15–20	10–15	<5	n.d.
	ST30	20–30	3.1	644	3.07	40–45	25–30	5–10	15–20	<5	<5	n.d.
	ST40	30–40	3.3	632	2.90	40–45	30–35	5–10	15–20	<5	<5	n.d.
	ST50	40–50	3.3	627	1.92	40–45	30–35	<5	15–20	<5	<5	n.d.
	ST60	50–60	3.5	600	2.98	35–40	40–45	<5	10–15	5–10	<5	n.d.
	ST70	60–70	3.4	535	3.26	30–35	45–50	<5	10–15	<5	<5	n.d.

* illite and kaolinite; EC (electrical conductivity); n.d. (not detected).

As compared to soil electrochemical properties after one year of treatment, the soil pH declined but not to detrimental levels, from 6.8 to 6.3, and the electrical conductivity remained practically constant at 3.3–3.5 mS cm^{-1} twelve years after amendment application. Given the long lapse of time since the treatment, the soil system seems to be well buffered by carbonate equilibria, and thereby further potential acid production could be consumed with little or no decrease in pH through acid-neutralization reactions [41].

4.2. Total Trace Element Concentrations

Results of the total concentrations of PHE analyzed in the amended and control (no amendment) soil samples are listed together in Table 2, and displayed in Figure 4 to graphically show the variation of concentration with depth.

Table 2. Total trace element concentrations (in mg kg^{-1}) analyzed by ICP-OES.

Element (mg kg^{-1})		As	Cd	Cr	Cu	Ni	Pb	Sb	Tl	Zn
Detection limit		3	0.3	1	1	1	3	5	5	1
Amended soil	T10	268	1.4	34	1210	38	655	64	BDL	851
	T20	689	0.7	46	808	20	1800	35	BDL	296
	T30	1290	BDL	60	607	18	2310	22	7	176
	T40	1450	BDL	64	816	17	2420	26	11	153
	T50	1860	BDL	61	636	18	2660	20	9	134
	T60	1390	BDL	72	734	19	2380	20	11	217
	T70	1830	BDL	60	743	20	2620	37	9	162
Control soil	ST10	711	0.3	69	756	20	2010	129	BDL	157
	ST20	964	0.5	68	474	14	1990	20	BDL	129
	ST30	1130	BDL	61	504	20	2080	34	BDL	121
	ST40	980	BDL	70	1630	22	2080	34	6	156
	ST50	1090	BDL	59	1350	20	2080	42	12	141
	ST60	1110	BDL	81	825	13	3410	36	BDL	171
	ST70	1060	BDL	73	777	15	3320	42	6	132

BDL (below detection limit).

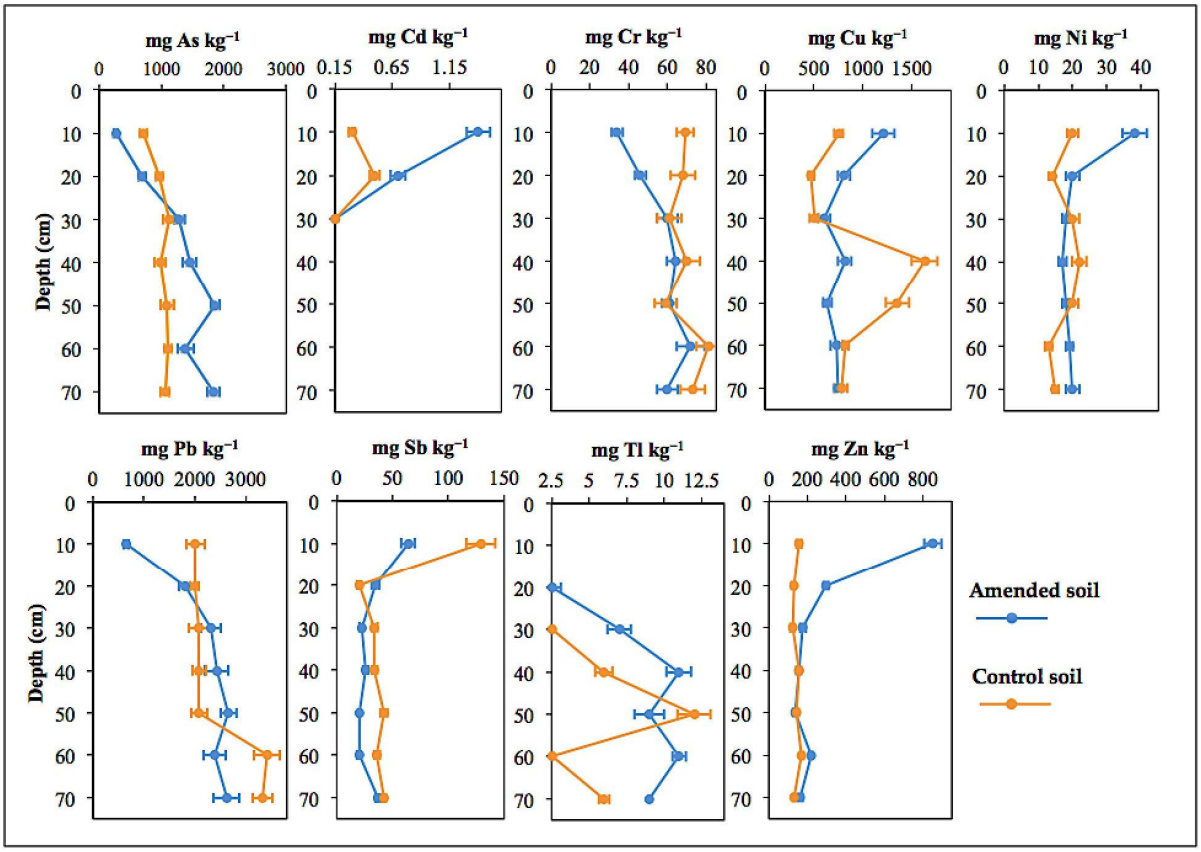

Figure 4. Vertical distribution of trace elements along the two sampling sections (amended and control) of the soil profile.

Total concentrations of As, Cr, and Pb increased significantly ($p < 0.01$) with depth in the amended soil up to a maximum of 1860 mg kg^{-1} As at 40–50 cm depth, 72 mg kg^{-1} Cr (50–60 cm), and 2660 mg kg^{-1} Pb (40–50 cm). Compared to the control, the concentrations of As, Pb, and Cr in the amended soil were noticeably low at the upper sampling layers (up to 20 cm depth), and then increased with depth to levels comparable to even higher than baseline concentration. Such vertical distribution pattern may be related to a dilution effect caused by the incorporation of MWS to the plough layer. It is nevertheless noteworthy that As showed a contrasted soil profile distribution, with increasing downward concentrations suggesting leaching from the upper horizons and subsequent re-deposition.

The levels of Cu, Cd, Ni, and Zn in the surface horizon were significantly ($p < 0.01$) higher than in the lower sampling depths. Notwithstanding the diluting effect due to MWS addition, the amounts of Cu (1210 mg kg^{-1}), Cd (1.4 mg kg^{-1}), Ni (38 mg kg^{-1}), and Zn (851 mg kg^{-1}) found in the topsoil (0–10 cm) of the amended mini plot were higher by a factor of 5.4 for Zn, 4.7 for Cd, 1.9 for Ni, and 1.6 for Cu relative to control soil (Figure 5). This increased upward trend is clearly indicative of metal enrichment in the amended surface layer. It was further found that the vertical distribution of such PHE in the two sampling sections (i.e., MWS-amended and control) was rather similar, with the concentration factor values ranging from 0.5 to 1.5, except for Cu that seemed to be more depleted in the 30–50 cm depth layer.

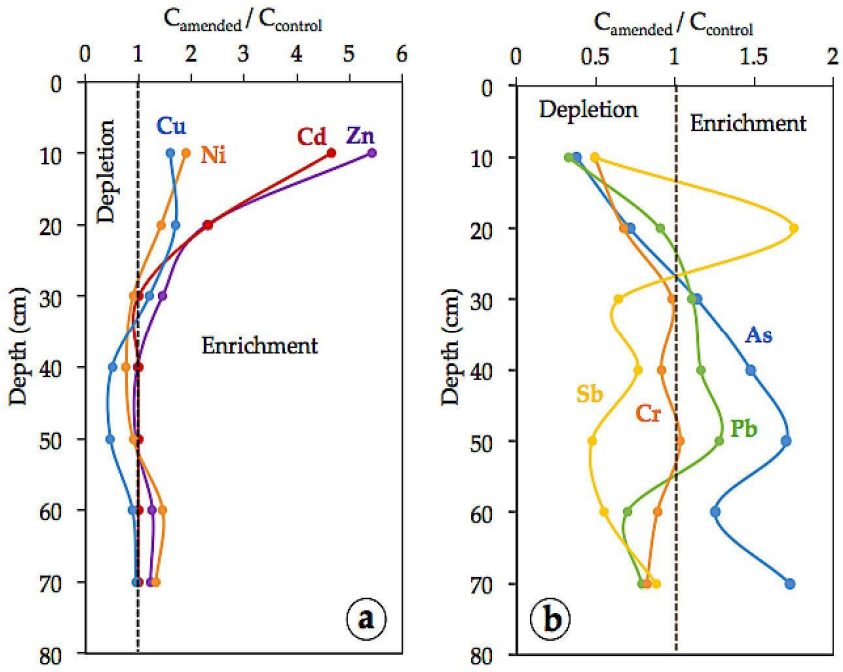

Figure 5. Soil profile distribution of the concentration factor (calculated by dividing the total content of each trace element in the amended soil by that in the unamended soil) for: (**a**) Cd, Cu, Ni, and Zn; and (**b**) As, Cr, Sb, and Pb.

A similar distribution pattern was observed when comparing the ratio between the concentrations of PHE in the amended topsoil 12 years after treatment and those previously reported for the surface soil before treatment [24]. Zinc, Cd, Ni, and to a lesser extent, Cu were found enriched in the amended surface layer (Figure 6), clearly indicating retention by the soil, while As, Cr, and Pb were relatively depleted by the dilution effect of the soil amendment.

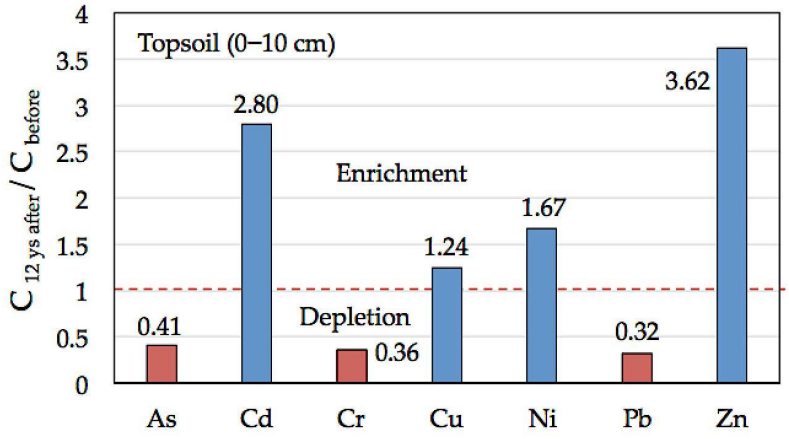

Figure 6. Quotient between total concentration (C) of trace elements in the amended surface soil 12 years after amendment application (this study) and before treatment [24].

4.3. Chemical Partitioning

Trace elements were unevenly distributed among the four operationally defined soil fractions, as determined by sequential chemical extraction (Table 3), which has been proven to be a useful procedure for assessing the long-term mobility of PHE [37].

Table 3. Total trace element concentrations (in mg kg^{-1}) analyzed by ICP-OES.

Trace Element (mg kg^{-1})	F1 (Exchangeable + Acid Soluble)	F2 (Reducible)	F3 (Oxidizable)	F4 (Residual)
Amended soil (sample T10)				
Cr	0.096 ± 0.012	0.201 ± 0.011	4.80 ± 0.16	20.4 ± 1.77
Ni	2.79 ± 0.29	17.7 ± 1.16	9.64 ± 0.99	14.2 ± 0.4
Cu	23.2 ± 2.2	554 ± 24	282 ± 22	398 ± 12
Zn	116 ± 17	436 ± 46	158 ± 9	203 ± 17
As	0.545 ±0.078	0.406 ± 0.028	9.94 ± 0.85	263 ± 6
Cd	0.538 ± 0.043	0.878 ± 0.026	0.180 ± 0.017	0.267 ± 0.008
Sb	1.30 ± 0.23	2.32 ± 0.16	1.03 ± 0.10	65.6 ± 3.37
Tl	0.068 ± 0.03	0.104 ± 0.006	0.029 ± 0.011	1.26 ± 0.04
Pb	0.089 ± 0.013	0.604 ± 0.014	0.173 ± 0.08	639 ± 18
Control soil (sample ST10)				
Cr	0.375 ± 0.010	9.7 ± 0.77	6.65 ± 0.53	38.6 ± 5.52
Ni	2.43 ± 0.19	1.20 ± 0.13	0.848 ± 0.082	12.4 ± 2.1
Cu	149 ± 4	182 ± 13	95 ± 9	335 ± 43
Zn	35.6 ± 1.1	14 ± 1.0	8.39 ± 0.8	96 ± 15
As	0.671 ± 0.056	139 ± 10	3.19 ± 0.32	553 ± 69
Cd	0.095 ± 0.007	0.089 ± 0.010	0.030 ± 0.003	0.283 ± 0.037
Sb	0.423 ± 0.067	14.2 ± 0.16	1.33 ± 0.12	185 ± 11
Tl	0.026 ± 0.003	0.105 ± 0.011	0.039 ± 0.003	2.20 ± 0.05
Pb	0.047 ± 0.004	52.2 ± 3.6	0.284 ± 0.055	1619 ± 60

Fraction F1 represents the labile fraction of PHE that would be released into the environment when soil conditions become acidic, including water-soluble, exchangeable (non-specifically sorbed), and weak acid soluble (bound to carbonates) pools. Trace element concentrations in the fraction F1 of the amended soil appeared insignificant (generally less than 1 mg kg^{-1}), except for Cu and Zn which reached 23.2 mg kg^{-1} and 116 mg kg^{-1}, respectively. Despite the low level of Cd (0.54 mg kg^{-1}) measured in this readily available fraction, it accounted for a relatively high extractability (28.9%).

Fraction F2 includes PHE bound to Fe and Mn oxyhydroxides, which would be easily released into the solution as a result of reductive dissolution. Copper (554 mg kg^{-1}) and Zn (436 mg kg^{-1}) were again the most extractable PHE in the reducible fraction of the amended soil, with an extraction yield of 44.1% and 47.7%, respectively. In addition, Cd and Ni were solubilized in the second step of the sequential extraction (F2) to a considerable extent in terms of percent extraction, accounting for 47.1% and 39.9% of their respective total concentration in the surface soil.

The results showed once again that Cu (282 mg kg^{-1}) and Zn (158 mg kg^{-1}) were the PHE removed at highest grade from the oxidizable fraction (F3) of the amended soil, which theoretically involves PHE bound to sulfides and/or organic matter. These released concentrations represent 22.4% and 17.3% of their respective total contents in soil and they scored the highest proportion of extractable PHE together with the extraction yield of Ni (21.7%).

The amounts of PHE solubilized in the amended soil samples after multi-acid digestion ranged widely depending on the element studied, with Pb (639 mg kg^{-1}), Cu (398 mg kg^{-1}), As (263 mg kg^{-1}), and Zn (203 mg kg^{-1}) being the most abundant contaminants in the extracts. This residual fraction (F4) was the dominant pool for Pb (99.8%), As (96.0%), Sb (93.4%), and Tl (86.2%). It must be emphasized that this residual fraction comprises not only the PHE tightly bound to the crystal structure of silicates but also those associated with secondary sulfates, such as jarosite-group minerals, which have not been effectively solubilized during the first three steps of the BCR sequential extraction procedure. It is generally agreed that jarosite-group minerals can scavenge Pb, As, Sb, and Tl in AMD-impacted areas through structural incorporation and/or adsorption mechanisms [2,42,43].

The lability of PHE in the amended soil, expressed as the ratio between the most labile fraction (F1) and the sum of all other fractions (F2 + F3 + F4), decreased in the following order (values shown in brackets): Cd (0.41) > Zn (0.15) > Ni (0.07) > Cu, Sb (0.02) > As, Cr, Pb, Tl (<0.01). Accordingly, Cd is the most labile PHE in soil under the current conditions of the amended mini plot whereas mobility of the other PHE remains very low unless specific environmental conditions are induced in the soil system. Interestingly, the most labile PHE (Cd, Zn, Ni, and Cu) are those that have been concentrated in a greater proportion in the soil surface as a result of the MWS amendment.

By comparing the fractionation pattern of PHE in topsoil, there are significant statistical differences between treated and untreated soil (Figure 7). The fraction of Cu, Zn, and Ni soluble in acetic acid (F1) was significantly lower in the amended soil than in the control soil ($p < 0.01$). In contrast, the extractability of Cd, Sb, and Tl was significantly higher in the amended soil ($p < 0.01$). The increased association of Cd with fraction F1 after soil amendment may suggest immobilization through carbonate precipitation by increased soil pH rather than sorption by cation exchange. It seems possible that adsorption could have been inhibited or limited due to the competition with Ca^{2+} ions for binding sites [41].

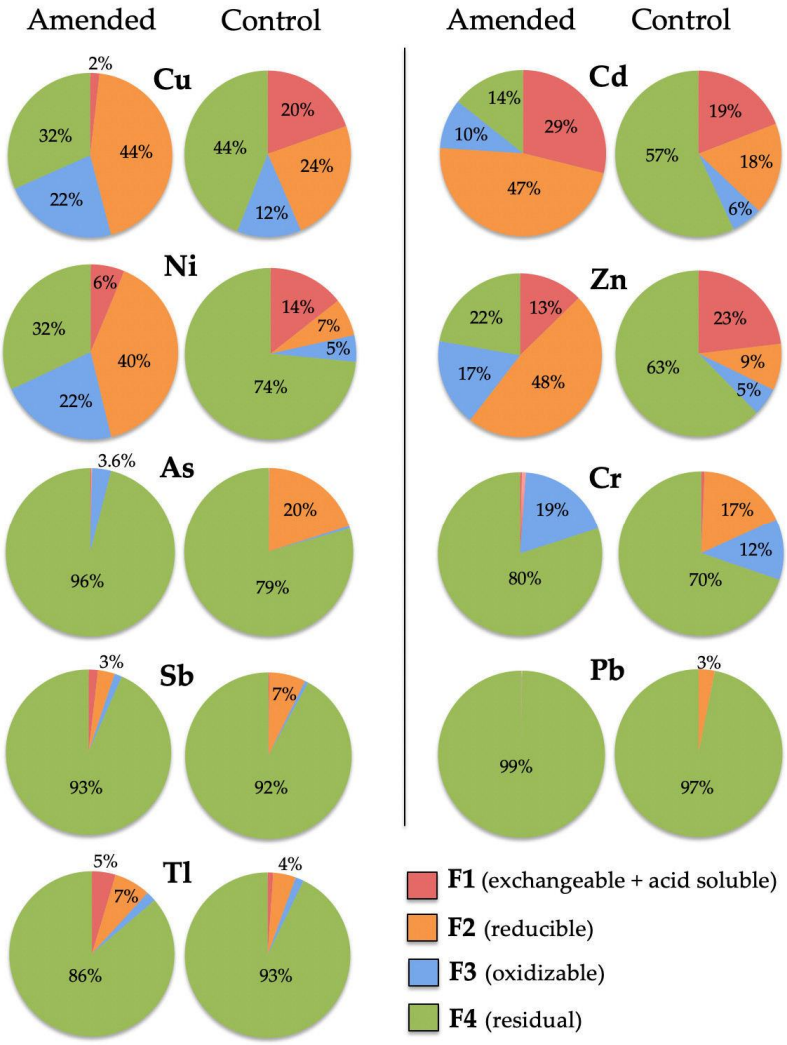

Figure 7. Geochemical partitioning of trace elements in amended soil (sample T10) and control soil (sample ST10). Extraction yields are expressed as percentage of extracted trace elements in operationally defined soil chemical fractions: (F1) water soluble, exchangeable and weak acid soluble; (F2) reducible; (F3) oxidizable; and (F4) residual.

The proportions of As, Cr, Pb, and Sb linked to reducible soil components (F2) of the amended plot were found to be significantly low relative to the control soil ($p < 0.01$), while those of Cu, Zn, Ni, and Cd showed a significant increase ($p < 0.01$). These findings indicate that iron oxyhydroxides were potentially responsible for retention of considerable levels of contaminants in soil after amendment, either by adsorption or coprecipitation processes [11].

In general, the percentages of PHE extracted from the treated soil sample under oxidizing conditions (F3) were significantly higher ($p < 0.01$) than those of the control sample, with the exception of Pb and Tl. The increase was particularly noteworthy for Cu and Ni, suggesting that a considerable proportion of them (up to 22%) seem to be bound to naturally occurring organic substances derived from plants growing on the amended soil.

In brief, most Pb, As, Sb, Tl, and Cr were found accumulated in the residual fraction (F4) of both treated and untreated soil; the fractionation patterns of Cu and Ni were fairly similar as they appear more or less evenly distributed among F2, F3, and F4 fractions; and Cd and Zn seemed preferentially partitioned among the most labile compartments (F1 and F2).

4.4. Environmental Availability

For most soil samples from the plot treated with MWS, the concentrations of PHE released after reaction with deionized water were generally less than 1 μg kg^{-1} with a few exceptions (Table 4), resulting in trivial fractions of less than 0.10%, calculated as the percentage of the total PHE concentration that was removed by the water extraction. In environmental terms, the fraction of PHE that may be available for plant uptake and easily leachable from the soil was assessed to be negligible. Zinc, Ni, and Cu were the PHE that showed the highest water-extractable concentrations, with their maximum values being measured in the leachates of the samples T50 (154 μg kg^{-1}), T40 (41.38 μg kg^{-1}), and T10 (31.4 μg kg^{-1}), respectively.

Table 4. Trace element concentrations (μg kg^{-1}) extracted with deionized water from amended soil and control soil samples.

Element (μg kg^{-1})	As	Cd	Cr	Cu	Ni	Pb	Sb	Tl	Zn
Amended soil									
T10	4.94 ± 0.39	0.45 ± 0.04	0.13 ± 0.01	31.4 ± 2.72	4.71 ± 0.44	0.29 ± 0.03	7.56 ± 0.67	0.03 ± 0.003	52.9 ± 3.3
T20	3.75 ± 0.33	0.25 ± 0.02	0.16 ± 0.01	26.4 ± 2.5	2.06 ± 0.17	0.34 ± 0.07	4.47 ± 0.38	0.02 ± 0.002	9.55 ± 0.67
T30	1.07 ± 0.10	0.06 ± 0.01	0.12 ± 0.01	3.70 ± 0.33	6.46 ± 0.64	0.42 ± 0.04	0.68 ± 0.06	0.04 ± 0.004	3.47 ± 0.25
T40	0.84 ± 0.08	0.16 ± 0.02	0.11 ± 0.01	13.8 ± 1.23	41.38 ± 3.20	0.11 ± 0.01	0.62 ± 0.06	0.1 ± 0.01	126.5 ± 9.51
T50	0.99 ± 0.10	0.16 ± 0.02	0.11 ± 0.01	14.1 ± 1.0	11.58 ± 1.15	0.18 ± 0.02	1.05 ± 0.08	0.1 ± 0.01	154 ± 13
T60	2.38 ± 0.22	0.04 ± 0.004	0.11 ± 0.008	5.18 ± 0.46	0.86 ± 0.08	0.09 ± 0.007	5.03 ± 0.5	0.07 ± 0.006	0.73 ± 0.07
T70	1.36 ± 0.10	0.04 ± 0.004	0.21 ± 0.02	2.97 ± 0.27	1.96 ± 0.16	0.25 ± 0.02	1.85 ± 0.14	0.12 ± 0.01	12.6 ± 1.26
Control soil									
ST10	5.99 ± 0.58	7.29 ± 0.52	4.21 ± 0.40	6646 ± 614	162 ± 14	1.61 ± 0.16	6.39 ± 0.06	0.06 ± 0.004	3267 ± 224
ST20	3.03 ± 0.26	2.87 ± 0.27	1.92 ± 0.18	2045 ± 127	35.2 ± 2.4	2.69 ± 0.26	1.25 ± 0.11	0.09 ± 0.007	641 ± 61
ST30	2.26 ± 0.17	3.43 ± 0.39	2.01 ± 0.18	2831 ± 209	66.9 ± 5.8	0.44 ± 0.04	1.35 ± 0.13	0.12 ± 0.008	1309 ± 130
ST40	2.31 ± 0.21	2.91 ± 0.20	1.57 ± 0.10	2727 ± 204	61.1 ± 5.0	0.97 ± 0.07	1.45 ± 0.11	0.16 ± 0.02	1051 ± 84
ST50	1.89 ± 0.19	2.20 ± 0.22	1.13 ± 0.10	2191 ± 178	43.9 ± 4.2	0.46 ± 0.04	1.06 ± 0.07	0.2 ± 0.02	831 ± 76
ST60	35.9 ± 2.31	5.00 ± 0.48	4.80 ± 0.48	3136 ± 241	47.0 ± 3.3	0.39 ± 0.04	33.99 ± 3.37	0.43 ± 0.04	781 ± 78
ST70	45.1 ± 2.8	6.02 ± 0.58	7.80 ± 0.68	4437 ± 313	64.8 ± 4.8	0.61 ± 0.04	33.64 ± 2.82	0.56 ± 0.04	993 ± 74

Remarkable differences were observed when comparing the PHE concentrations extracted with water from both groups of soil samples under study. The contents of Cu, Zn, Ni, Cd, Cr, and Pb in the extracts from the upper sampling layers (up to 20 cm depth) of the amended plot were significantly lower than those from the control soil sample ($p < 0.01$). No meaningful changes were detected in the concentrations of As and Sb released from the surface soil, although they were higher in the 10–20 cm depth interval of the amended soil compared to control. A significant decrease ($p < 0.01$) was also observed in the water-extractable amounts of all PHE at the amended soil depth of 20–50 cm, with the exception of Pb (at 20–30 cm depth) and Sb (at 40–50 cm depth). At deeper depths (50–70 cm), the

water-extracted concentrations of PHE in the amended soil remained consistently lower than those of the control.

The amounts of PHE extracted with EDTA varied noticeably depending on the element concerned and the sampling depth, in both the amended and the non-amended soil (Table 5). The use of EDTA as extracting reagent led to much higher ($p < 0.01$) extraction yields than those determined with deionized water (Figure 8), as expected given its strong complexing capacity [44]. The EDTA extraction method is capable of extracting PHE from all non-silicate bound phases, likely reflecting the metal availability in the long term [45].

Table 5. Trace element concentrations (μg kg^{-1}) extracted with 0.05 mol L^{-1} EDTA from amended soil and control soil samples.

Element (μg kg^{-1})	As	Cd	Cr	Cu	Ni	Pb	Sb	Tl	Zn
Amended soil									
T10	29.8 ± 2.6	39.2 ± 3.5	3.08 ± 0.29	10,877 ± 1739	101 ± 8	129 ± 11	16.7 ± 1.3	0.07 ± 0.006	13,419 ± 940
T20	10.9 ± 0.9	23.5 ± 1.9	5.59 ± 0.5	6517 ± 639	42 ± 3	162 ± 14	12.3 ± 0.8	0.07 ± 0.004	3951 ± 388
T30	5.9 ± 0.6	4.08 ± 0.39	4.58 ± 0.3	3261 ± 266	42 ± 3	334 ± 28	5.8 ± 0.5	0.40 ± 0.03	1577 ± 118
T40	11.2 ± 0.9	3.15 ± 0.27	4.21 ± 0.38	2383 ± 223	36.1 ± 2.5	289 ± 19	14.4 ± 1.3	0.75 ± 0.005	873 ± 77
T50	15.4 ± 1.4	4.34 ± 0.32	3.87 ± 0.32	3062 ± 246	31.5 ± 2.3	444 ± 42	18.4 ± 1.7	0.93 ± 0.07	813 ± 81
T60	37.7 ± 2.2	10.2 ± 0.7	11.5 ± 1.1	4775 ± 408	201 ± 18	589 ± 36	44.7 ± 3.9	0.71 ± 0.07	3315 ± 294
T65	25.0 ± 2.0	5.35 ± 0.93	4.76 ± 0.45	3557 ± 302	41.1 ± 3.9	402 ± 30	24.9 ± 2.4	1.23 ± 0.10	1101 ± 108
Control soil									
ST10	116 ± 11	7.37 ± 0.73	30.9 ± 2.2	13,126 ± 1260	154 ± 12	142 ± 12	69.8 ± 6.9	0.07 ± 0.01	2624 ± 213
ST20	13.3 ± 1.2	3.67 ± 0.32	8.87 ± 0.67	4479 ± 434	38.1 ± 3.2	473 ± 42	7.77 ± 0.66	0.16 ± 0.01	898 ± 56
ST30	77.6 ± 4.9	3.79 ± 0.37	23.1 ± 2.1	6143 ± 355	68.2 ± 4.4	190 ± 14	32.9 ± 2.4	0.53 ± 0.04	1206 ± 108
ST40	57.9 ± 5.5	3.09 ± 0.26	117 ± 7	6642 ± 660	63.4 ± 5.4	179 ± 16	35.1 ± 3.2	0.69 ± 0.05	788 ± 46
ST50	42.4 ± 4.1	3.17 ± 0.31	8.28 ± 0.82	4723 ± 359	45.7 ± 3.9	145 ± 12	22.3 ± 1.4	1.15 ± 0.11	624 ± 55
ST60	578 ± 49	8.87 ± 0.77	35.1 ± 3.1	14,663 ± 1371	57.2 ± 5.3	452 ± 40	125 ± 7	1.71 ± 0.15	1017 ± 97
ST70	477 ± 40	8.09 ± 0.81	44.4 ± 3.7	15,627 ± 1561	75.5 ± 7.3	579 ± 57	135 ± 10	1.75 ± 0.12	1137 ± 99

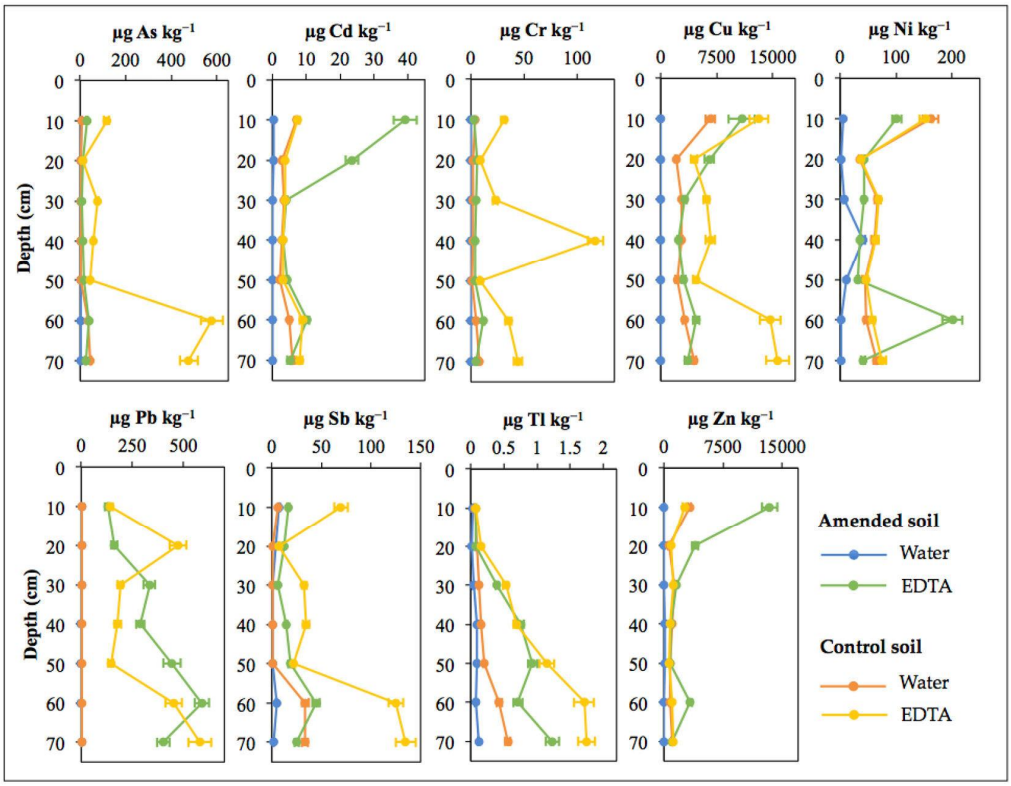

Figure 8. Vertical distribution of trace element concentrations extracted by deionized water and EDTA from the two sampling sections (amended and control) of the soil profile.

Certainly, Zn and Cu were the most abundant PHE in the topsoil extracts of the amended plot, where the EDTA-extracted concentrations reached up to 13,419 μg kg^{-1} and 10,877 μg kg^{-1}, respectively. Despite the high levels of Zn and Cu measured in the extracts, the mobilizable fraction of Zn was 1.58%, and that for Cu accounted for only 0.90%. The maximum contents of Pb (402–589 μg kg^{-1}) were extracted from the subsoil samples (50–70 cm depth), while the remaining PHE were at lower concentration in the extracts (mostly below 50 μg kg^{-1}) over the entire soil profile.

The amended upper surface layer (0–10 cm depth) had a significant increase ($p < 0.01$) in the levels of Zn and Cd in comparison with the control soil. It was also found that the soil cores were significantly enriched ($p < 0.01$) in the EDTA-extracted concentrations of Zn over the entire profile of the amended plot, as well as in those of Cd, Cu, and Sb at the depth of 10–20 cm, and Pb at 20–60 cm depth. Conversely, As, Cr, Cu, Ni, Sb, and Tl were generally most abundant in the EDTA extracts from the control soil samples. Furthermore, the comparison also revealed a generalized significant decrease ($p < 0.01$) in the PHE levels extracted with EDTA from the deeper sample (60–70 cm depth) of the amended soil.

To give a clearer picture of the effects of soil amendment on environmental availability of PHE with time, Figure 9 shows a bar chart comparing water-soluble and EDTA-extracted concentrations of PHE in the surface layer (0–10 cm depth) of the untreated soil, one year after and twelve years after amendment application. The extractable levels of PHE did differ statistically between the three groups of samples (one-way ANOVA, $p < 0.01$).

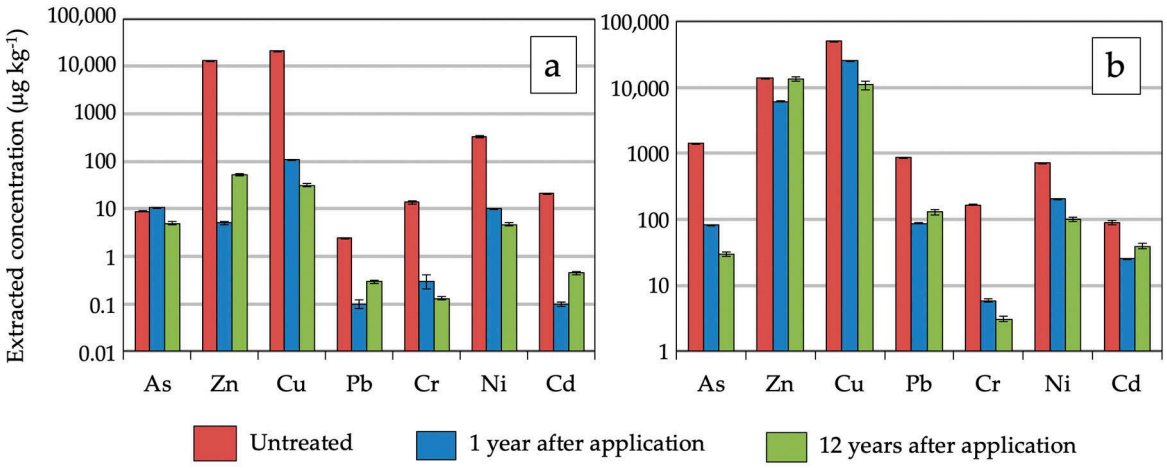

Figure 9. Bar chart comparing trace element availability before and after marble slurry waste application, at years one and twelve after soil amendment. (**a**) Water-extracted concentration; (**b**) EDTA-extracted concentration.

Before soil amendment, substantial amounts of PHE were released from the mine soil, as indicated in previous work [24]. The leachability risk was particularly high for Zn and Cu. Given that metal sorption and many metal precipitation processes increase with pH [11,46], amelioration of soil acidity by use of MWS amendment was the major factor driving the immobilization of contaminants, by reducing the activity of H^+ ions in soil solution and increasing negatively charged sites on soil particles. This in turn boosted the adsorption capacity of amended soil as the water-soluble levels of PHE and their uptake by plants dropped following MWS addition, except for As. Increased As mobility observed in the treated soil one year after amendment may also be linked to the increase in the negatively-charged surfaces of soil particles after acid neutralization [47], thus preventing the adsorption of water-soluble As oxyanion species.

When comparing soil treated with MWS at years one and twelve after amendment application, a salient decrease in the water-soluble concentrations (Figure 9a) of As, Cu, and Ni was observed with treatment time ($p < 0.01$), while the opposite trend was apparent for Zn, Pb, and Cd ($p < 0.01$). A plausible mechanism for reduced As leaching could be

formation of low-solubility calcium arsenates [48–50], due to reaction of dissolved calcium with arsenic, as reported in other acid mine soils reclaimed with sugar beet lime and composted biosolids [41]. Decreased Cu and Ni availability can be ascribed to adsorption onto organic matter or formation of stable complexes with organic ligands [51]. On the contrary, the release of Zn, Pb, and Cd from the amended soil increased after 12 years. The competition with Ca^{2+} ions for sorption sites could have displaced such PHE from the soil binding sites increasing their labile fractions, although they were limited in comparison with those determined in the unamended soil.

The extractable amounts of PHE by EDTA (Figure 9b) showed a similar pattern of results for the same time period excepting that of Cu, which increased from 12 to 22% with treatment. This could be explained by the fact that EDTA is a chelating agent that has the ability to release the fraction of Cu associated through complexation with various forms of organic material [52].

5. Conclusions

A mini plot field study was conducted to test the long-term effects of amending a heavily contaminated mine Technosol with a single application of MWS, with emphasis on soil reaction, chemical partitioning, and PHE retention. Soil acidity (pH = 3.1–3.5) and release of PHE were effectively reduced by amendment after its incorporation and these improvements were still observed after 12 years of its application. The addition of MWS provided a high pH-buffering capacity (pH = 5.8–6.4) to soil, making it less susceptible to eventual re-acidification over time, and therefore to PHE mobilization. Soil acidity neutralization affected the status and occurrence mode of PHE, rendering them less potentially phytotoxic and available for plant absorption, as indicated by the presence of plant species spontaneously growing in the amended site. Decreased mobility of Cu, Zn, Ni, and Cd most likely occurred by retention in reducible phases, mainly poorly crystallized Fe oxides, while Pb, As, Sb, Tl, and Cr were mostly found accumulated in the residual fraction, linked to insoluble secondary oxidation minerals and undissolved phases.

Consistently, application of MWS amendment is a promising option for assisting sustainable natural remediation of degraded mining landscapes with long-term efficacy on PHE immobilization, as well as an attractive way of industrial waste recycling. However, it is important to note that, in the event of re-acidification, a considerable proportion of Zn and Cd retained in topsoil as exchangeable and weak acid soluble forms could be released by ion exchange and dissolution reactions. It has also been shown that the competitive effect of Ca^{2+} ions for sorption sites could displace PHE from soil binding sites into soil solution enhancing the mobility of weakly adsorbed metallic cations. Therefore, further monitoring would be required to assess the chemical stability of PHE over a longer time span, the ageing process of the amendment, and the potential risk of transfer from soil to growing plants.

Author Contributions: Conceptualization, J.C.F.-C.; methodology, J.C.F.-C. and I.G.; validation, J.C.F.-C. and I.G.; formal analysis, I.G. and E.M.; investigation, I.G., S.F.-L., C.B.-B. and E.M.; data curation, S.F.-L. and C.B.-B.; writing—review and editing, J.C.F.-C.; visualization, I.G., S.F.-L., and C.B.-B.; supervision, J.C.F.-C.; project administration and funding acquisition, J.C.F.-C. All authors have read and agreed to the published version of the manuscript.

Funding: This research was partially supported by the Regional Government of Andalusia (Spain) and the European Regional Development Fund Andalusia 2014–2020, through the Project P-18-TP-3503.

Institutional Review Board Statement: Not applicable.

Informed Consent Statement: Not applicable.

Data Availability Statement: Not applicable.

Conflicts of Interest: The authors declare no conflict of interest.

References

1. Plumlee, G.S.; Morman, S.A. Mine wastes and human health. *Elements* **2011**, *7*, 399–404. [CrossRef]
2. Grantcharova, M.M.; Fernández-Caliani, J.C. Soil acidification, mineral neoformation and heavy metal contamination driven by weathering of sulphide wastes in a Ramsar wetland. *Appl. Sci.* **2022**, *12*, 249. [CrossRef]
3. Niu, A.; Lin, C. Managing soils of environmental significance: A critical review. *J. Hazard. Mater.* **2021**, *417*, 125990. [CrossRef] [PubMed]
4. Song, B.; Zeng, G.; Gong, J.; Liang, J.; Xu, P.; Liu, Z.; Zhang, Y.; Zhang, C.; Cheng, M.; Liu, Y.; et al. Evaluation methods for assessing effectiveness of in situ remediation of soil and sediment contaminated with organic pollutants and heavy metals. *Environ. Int.* **2017**, *105*, 43–55. [CrossRef]
5. Liu, L.; Li, W.; Song, W.; Guo, M. Remediation techniques for heavy metal-contaminated soils: Principles and applicability. *Sci. Total Environ.* **2018**, *633*, 206–219. [CrossRef]
6. Séré, G.; Schwartz, C.; Ouvrard, S.; Sauvage, C.; Renat, J.C.; Morel, J.L. Soil construction: A step for ecological reclamation of derelict lands. *J. Soils Sediments* **2008**, *8*, 130–136. [CrossRef]
7. Kumpiene, J. Trace element immobilization in soil using amendments. In *Trace Elements in Soils*; Hooda, P.S., Ed.; Wiley: Chichester, UK, 2010; pp. 353–379.
8. Firpo, B.A.; Weiler, J.; Schneider, I.A.H. Technosol made from coal waste as a strategy to plant growth and environmental control. *Energy Geosci.* **2021**, *2*, 160–166. [CrossRef]
9. IUSS Working Group WRB. *World Reference Base for Soil Resources 2014, Update 2015*; International Soil Classification System for Naming Soils and Creating Legends for Soil Maps; World Soil Resources Reports 106; FAO: Rome, Italy, 2015.
10. Asensio, V.; Vega, F.A.; Andrade, M.L.; Covelo, E.F. Technosols made of wastes to improve physico-chemical characteristics of a copper mine soil. *Pedosphere* **2013**, *23*, 1–9. [CrossRef]
11. Kumpiene, J.; Lagerkvist, A.; Maurice, C. Stabilization of As, Cr, Cu, Pb and Zn in soil using amendments—A review. *Waste Manag.* **2008**, *28*, 215–225. [CrossRef]
12. Bolan, N.S.; Kunhikrishnan, A.; Thangarajan, R.; Kumpiene, J.; Park, J.; Makino, T.; Kirkhamg, M.B.; Schecke, K. Remediation of heavy metal(loid)s contaminated soils—To mobilize or to immobilize? *J. Hazard. Mater.* **2014**, *266*, 141–166. [CrossRef]
13. Basta, N.T.; Gradwohl, R.; Snethen, K.L.; Schroder, J.L. Chemical immobilization of lead, zinc, and cadmium in smelter-contaminated soils using biosolids and rock phosphate. *J. Environ. Qual.* **2001**, *30*, 1222–1230. [CrossRef] [PubMed]
14. Bolan, N.S.; Adriano, D.C.; Curtin, D. Soil acidification and liming interactions with nutrient and heavy metal transformation and bioavailability. *Adv. Agron.* **2003**, *78*, 5–272.
15. Holland, J.; Bennett, A.; Newton, A.; White, P.; McKenzie, B.; George, T.; Pakeman, R.; Bailey, J.; Fornara, D.; Hayes, R. Liming impacts on soils, crops and biodiversity in the UK: A review. *Sci. Total Environ.* **2018**, *610*, 316–332. [CrossRef] [PubMed]
16. Madejón, P.; Pérez de Mora, A.; Burgos, P.; Cabrera, F.; Lepp, N.W.; Madejón, E. Do amended, polluted soils require re-treatment for sustainable risk reduction?—Evidence from field experiments. *Geoderma* **2010**, *159*, 174–181. [CrossRef]
17. Palansooriya, K.N.; Shaheen, S.M.; Chen, S.S.; Tsang, D.C.W.; Hashimoto, Y.; Hou, D.; Bolan, N.S.; Rinklebe, J. Soil amendments for immobilization of potentially toxic elements in contaminated soils: A critical review. *Environ. Int.* **2020**, *134*, 105046. [CrossRef]
18. Kumpiene, J.; Carabante, I.; Kasiuliene, A.; Austruy, A.; Mench, M. Long-term stability of arsenic in iron amended contaminated soil. *Environ. Pollut.* **2021**, *269*, 116017. [CrossRef]
19. Wang, L.; Huang, J.; Li, G.; Luo, J.; Bolan, N.S.; Hou, D. Long-term immobilization of soil metalloids under simulated aging: Experimental and modeling approach. *Sci. Total Environ.* **2022**, *806*, 150501. [CrossRef]
20. Pérez-Sirvent, C.; García-Lorenzo, M.L.; Martínez-Sanchez, M.J.; Navarro, M.C.; Marimón, J.; Bech, J. Metal-contaminated soil remediation by using sludges of the marble industry: Toxicological evaluation. *Environ. Int.* **2007**, *33*, 502–504. [CrossRef]
21. Zornoza, R.; Faz, A.; Carmona, D.M.; Kabas, S.; Martínez-Martínez, S.; Acosta, J.A. Plant cover and soil biochemical properties in a mine tailing pond five years after application of marble wastes and organic amendments. *Pedosphere* **2012**, *22*, 22–32. [CrossRef]
22. Tozsin, G.; Arol, A.I.; Oztas, T.; Kalkan, E. Using marble wastes as a soil amendment for acidic soil neutralization. *J. Environ. Manag.* **2014**, *133*, 374–377. [CrossRef]
23. Tozsin, G.; Oztas, T.; Arol, A.I.; Kalkan, E. Changes in the chemical composition of an acidic soil treated with marble quarry and marble cutting wastes. *Chemosphere* **2015**, *138*, 664–667. [CrossRef] [PubMed]
24. Fernández-Caliani, J.C.; Barba-Brioso, C. Metal immobilization in hazardous contaminated minesoils after marble slurry waste application. A field assessment at the Tharsis mining district (Spain). *J. Hazard. Mater.* **2010**, *181*, 817–826. [CrossRef] [PubMed]
25. González, F.; Moreno, C.; Sáez, R.; Clayton, J. Ore genesis age of the Tharsis Mining District (Iberian Pyrite Belt): A palynological approach. *J. Geol. Soc. Lond.* **2002**, *159*, 229–232. [CrossRef]
26. Tornos, F.; González-Clavijo, E.; Spiro, B.F. The Filón Norte orebody (Tharsis, Iberian Pyrite Belt): A proximal low-temperature shale-hosted massive sulphide in a thin-skinned tectonic belt. *Miner. Deposita* **1998**, *33*, 150–169. [CrossRef]
27. O'Brien, W. *Prehistoric Copper Mining in Europe: 5500-500 BC*; Oxford University Press: Oxford, UK, 2015.
28. Fernández-Caliani, J.C.; Barba-Brioso, C.; De la Rosa, J. Mobility and speciation of rare earth elements in acid minesoils and geochemical implications for river waters in the southwestern Iberian margin. *Geoderma* **2009**, *149*, 393–401. [CrossRef]
29. Fernández-Caliani, J.C.; Barba-Brioso, C.; González, I.; Galán, E. Heavy metal pollution in soils around the abandoned mine sites of the Iberian Pyrite Belt (Southwest Spain). *Water Air Soil Pollut.* **2009**, *200*, 211–226. [CrossRef]

30. Madejón, P.; Barba-Brioso, C.; Lepp, N.W.; Fernández-Caliani, J.C. Traditional agricultural practices enable sustainable remediation of highly polluted soils in Southern Spain for cultivation of food crops. *J. Environ. Manag.* **2011**, *92*, 1828–1836. [CrossRef]
31. Fernández-Caliani, J.C.; Giráldez, M.I.; Barba-Brioso, C. Oral bioaccessibility and human health risk assessment of trace elements in agricultural soils impacted by acid mine drainage. *Chemosphere* **2019**, *237*, 124441. [CrossRef]
32. Chopin, E.I.B.; Alloway, B.J. Trace element partitioning and soil particle characterization around mining and smelting areas at Tharsis, Riotinto and Huelva, SW Spain. *Sci. Total Environ.* **2007**, *373*, 488–500. [CrossRef]
33. Chopin, E.I.B.; Alloway, B.J. Distribution and mobility of trace elements in soils and vegetation around the mining and smelting areas of Tharsis, Riotinto and Huelva, Iberian Pyrite Belt, SW Spain. *Water Air Soil Pollut.* **2007**, *182*, 245–261. [CrossRef]
34. Kahle, M.; Kleber, M.; Jahn, R. Review of XRD-based quantitative analyses of clay minerals in soils. The suitability of mineral intensity factors. *Geoderma* **2002**, *109*, 191–205. [CrossRef]
35. Underwood, M.B.; Lawler, N.; McNamara, K. Data report: Standard mineral mixtures, normalization factors, and determination of error for quantitative X-ray diffraction analyses of bulk powders and clay-sized mineral assemblages. Hikurangi Subduction Margin Coring, Logging, and Observatories. In Proceedings of the International Ocean Discovery Program, 372B/375, Timaru, New Zealand, 8 March–5 May 2020.
36. Rauret, G.; López-Sánchez, J.F.; Sahuquillo, A.; Rubio, R.; Davidson, C.M.; Ure, A.M.; Quevauviller, P. Improvement of the BCR three step sequential extraction procedure prior to certification of new sediment and soil reference materials. *J. Environ. Monit.* **1999**, *1*, 57–61. [CrossRef] [PubMed]
37. Pueyo, M.; Sastre, J.; Hernández, M.; Vidal, E.; López-Sánchez, J.F.; Rauret, G. Prediction of trace element mobility in contaminated soils by sequential extraction. *J. Environ. Qual.* **2003**, *32*, 2054–2066. [CrossRef] [PubMed]
38. Sahuquillo, A.; Rigol, A.; Rauret, G. Overview of the use of leaching/extraction tests for risk assessment of trace metals in contaminated soils and sediments. *Trends Anal. Chem.* **2003**, *22*, 152–159. [CrossRef]
39. Rivera, M.B.; Giráldez, M.I.; Fernández-Caliani, J.C. Assessing the environmental availability of heavy metals in geogenically contaminated soils of the Sierra de Aracena Natural Park (SW Spain). Is there a health risk? *Sci. Total Environ.* **2016**, *560–561*, 254–265. [CrossRef]
40. Singh, A.; Nocerino, J. Robust estimation of mean and variance using environmental data sets with below detection limit observations. *Chemom. Intell. Lab. Syst.* **2002**, *60*, 69–86. [CrossRef]
41. Fernández-Caliani, J.C.; Giráldez, M.I.; Waken, W.H.; Del Río, Z.M.; Córdoba, F. Soil quality changes in an Iberian pyrite mine site 15 years after land reclamation. *Catena* **2021**, *206*, 105538. [CrossRef]
42. Aguilar-Carrillo, J.; Herrera-García, L.; Reyes-Domínguez, I.A.; Gutiérrez, E.J. Thallium(I) sequestration by jarosite and birnessite: Structural incorporation vs. surface adsorption. *Environ. Pollut.* **2019**, *257*, 113492. [CrossRef]
43. Asta, M.P.; Cama, J.; Martínez, M.; Giménez, J. Arsenic removal by goethite and jarosite in acidic conditions and its environmental implications. *J. Hazard. Mater.* **2009**, *171*, 965–972. [CrossRef]
44. Sun, B.; Zhao, F.J.; Lombi, E.; McGrath, S.P. Leaching of heavy metals from contaminated soils using EDTA. *Environ. Pollut.* **2001**, *113*, 111–120. [CrossRef]
45. Ure, A.M. Single extraction schemes for soil analysis and related applications. *Sci. Total Environ.* **1996**, *178*, 3–10. [CrossRef]
46. Basta, N.T.; Rayan, J.A.; Chaney, R.L. Trace element chemistry in residual-treated soil: Key concepts and metal bioavailability. *J. Environ. Qual.* **2005**, *34*, 49–63. [CrossRef] [PubMed]
47. Hartley, W.; Eduards, R.; Lepp, W.N. Arsenic and heavy metal mobility in iron oxide-amended contaminated soils as evaluated by short and long term leaching tests. *Environ. Pollut.* **2004**, *131*, 495–504. [CrossRef] [PubMed]
48. Bothe, J.V.; Brown, P.W. Arsenic immobilization by calcium arsenate formation. *Environ. Sci. Technol.* **1999**, *33*, 3806–3811. [CrossRef]
49. Juillot, F.; Ildefonse, P.; Morin, G.; Calas, G.; De Kersabiec, A.M.; Benedetti, M. Remobilization of arsenic from buried wastes at an industrial site: Mineralogical and geochemical control. *Appl. Geochem.* **1999**, *14*, 1031–1048. [CrossRef]
50. Porter, S.K.; Scheckel, K.G.; Impellitteri, C.A.; Ryan, J.A. Toxic metals in the environment: Thermodynamic considerations for possible immobilisation strategies for Pb, Cd, As, and Hg. *Crit. Rev. Environ. Sci. Tech.* **2004**, *34*, 495–604. [CrossRef]
51. Uchimiya, M.; Lima, I.M.; Klasson, K.T.; Wartelle, L.H. Contaminant immobilization and nutrient release by biochar soil amendment: Roles of natural organic matter. *Chemosphere* **2010**, *80*, 935–940. [CrossRef]
52. Rao, C.R.M.; Sahuquillo, A.; López-Sánchez, J.F. A review of the different methods applied in environmental geochemistry for single and sequential extraction of trace elements in soils and related materials. *Water Air Soil Pollut.* **2008**, *189*, 291–333. [CrossRef]

4.4. Aplicación de tecnosuelos para estimular el crecimiento vegetal en suelos mineros de Río Tinto, un análogo geoquímico y mineralógico de Marte

Basado en el artículo:

Unveiling a Technosol-based remediation approach for enhancing plant growth in an iron-rich acidic mine soil from the Rio Tinto Mars analog site. Science of the Total Environment 922 (2024) 171217

Los suelos mineros de Rio Tinto se caracterizan por una acidez extrema, altas concentraciones de hierro y EPT, así como por la falta o escasez de nutrientes. Estas condiciones inhiben el crecimiento de la vegetación, dificultando la restauración ecológica y la estabilidad del ecosistema. Además de su importancia local, los suelos del distrito minero de Rio Tinto se consideran un análogo terrestre de Marte debido a sus características geoquímicas y mineralógicas semejantes a las condiciones de algunos sitios marcianos. Esto convierte a Rio Tinto en un laboratorio natural único para investigar nuevas soluciones tecnológicas de remediación ambiental con implicaciones astrobiológicas.

Este estudio propone el uso de tecnosuelos elaborados a partir de RNP como una alternativa para mejorar las propiedades del suelo, reducir la toxicidad y promover el crecimiento vegetal. El objetivo principal fue evaluar la eficacia de diferentes formulaciones de tecnosuelos en la mitigación de los efectos de la acidez y de los metales pesados en el suelo, y en la promoción del crecimiento vegetal (*Brassica juncea*).

4.4.1. Resultados más relevantes y discusión

La investigación se llevó a cabo mediante experimentos en macetas, donde se probó la capacidad de diferentes tecnosuelos para mejorar un suelo del entorno de la mina Peña de Hierro (PH), contaminado con cenizas de tostación de pirita. Las enmiendas utilizadas fueron una mezcla de residuos orgánicos (lodos de clarificación

de agua, residuo R3) y residuos inorgánicos (escoria blanca de acero, residuo R5; y escoria de horno de hierro, residuo R6) en diferentes proporciones.

El suelo sin tratar (control) produjo lixiviados altamente ácidos (pH= 2,5), favoreciendo la movilización de Pb (26,16 mg kg^{-1}), Zn (4,94 mg kg^{-1}) y Cu (2,29 mg kg^{-1}). Por el contrario, los lixiviados de los tecnosuelos fueron moderadamente alcalinos y su contenido de cationes divalentes, como Cu^{2+}, Zn^{2+}, Pb^{2+} y Cd^{2+}, experimentó una disminución notable con el tratamiento, entre 2 y 9,5 veces dependiendo del elemento.

Por otro lado, elementos como As, Cr y Sb, que tienden a formar oxianiones complejos, mostraron ligeros incrementos en algunos lixiviados de tecnosuelos en relación al suelo sin tratar, lo que se atribuye a la reducción de la capacidad de sorción aniónica del suelo por el aumento del pH. No obstante, la fracción lixiviable de estos elementos fue insignificante.

En base a los resultados de los ensayos de lixiviación, se seleccionaron los tecnosuelos más eficaces (S2T8-25 y S2T13-25) para la experimentación en macetas con plantación de *Brassica juncea*. Los resultados más destacados obtenidos en esta fase experimental fueron:

- **Neutralización de la acidez.** Las formulaciones de tecnosuelos lograron una reducción significativa de la acidez neta del suelo, elevando los niveles de pH desde valores extremadamente ácidos (pH 2.1-3.0) a rangos más neutros o ligeramente alcalinos (pH 6.8-8.2).

- **Inmovilización de elementos potencialmente tóxicos.** Se observó una drástica reducción en las concentraciones de metales lixiviables. Específicamente, los niveles de Pb, Zn y Cu disminuyeron a concentraciones despreciables (< 1 mg/L) y se transformaron en especies menos tóxicas y más estables.

- **Mejora de las propiedades del suelo.** Las enmiendas contribuyeron a mejorar las propiedades físico-químicas del suelo, como la disponibilidad de nutrientes y la

capacidad de intercambio catiónico, creando un medio más favorable para el crecimiento de las plantas.

- **Promoción del crecimiento vegetal.** Los tecnosuelos mostraron una notable capacidad para fomentar la germinación de semillas y el crecimiento de plántulas. La respuesta de *Brassica juncea* (tasas de germinación y supervivencia, altura de la planta y número de hojas) fue significativamente mejor en los suelos tratados en comparación con el suelo minero original, donde la tasa de germinación fue nula. La mejora en el crecimiento de las plantas es una prueba directa de la eficacia de la remediación.

- **Formulación óptima.** Entre las formulaciones evaluadas, el tecnosuelo S2T8-25 demostró ser el más efectivo para superar las limitaciones del suelo minero, favoreciendo un crecimiento más vigoroso de las plantas y una mayor tasa de supervivencia, similar al control con mantillo.

4.4.2. Conclusiones

Este estudio demuestra que los tecnosuelos lograron neutralizar eficazmente la acidez, inmovilizar significativamente los EPT y mejorar sustancialmente las condiciones del suelo, dando lugar un crecimiento exitoso de las plantas. Por tanto, contribuye a los objetivos generales de la tesis al demostrar la viabilidad de la revegetación en suelo mineros complejos, y ampliando la aplicación del concepto de tecnosuelo a ambientes extremos.

La formulación del tecnosuelo S2T8-25, con una mezcla de lodos de clarificación de agua y escoria blanca de la industria del acero, mostró el mayor potencial para superar las limitaciones del suelo minero, facilitando la adaptación de las plantas y la estabilización de los contaminantes.

Para futuras investigaciones, se recomienda validar los resultados en ensayos de campo con diferentes especies vegetales, para evaluar la aplicabilidad a gran escala y la resiliencia a largo plazo de esta estrategia de remediación.

El reconocimiento de Rio Tinto como análogo de Marte también abre una vía para la investigación en astrobiología y la posibilidad de extender estos principios de revegetación a ambientes extraterrestres con características geoquímicas similares.

Science of the Total Environment 922 (2024) 171217

Contents lists available at ScienceDirect

Science of the Total Environment

journal homepage: www.elsevier.com/locate/scitotenv

Unveiling a Technosol-based remediation approach for enhancing plant growth in an iron-rich acidic mine soil from the Rio Tinto Mars analog site

Juan Carlos Fernández-Caliani [a,*], Sandra Fernández-Landero [a], María Inmaculada Giráldez [b], Pablo J. Hidalgo [c], Emilio Morales [b]

[a] Department of Earth Sciences, University of Huelva, Campus El Carmen, s/n, 21071 Huelva, Spain
[b] Department of Chemistry, University of Huelva, Campus El Carmen, s/n, 21071 Huelva, Spain
[c] Department of Integrated Sciences, RENSMA, University of Huelva, Campus El Carmen, s/n, 21071 Huelva, Spain

HIGHLIGHTS

- Circular economy for sustainable Technosol-based soil remediation
- Soil stabilization and plant growth in extreme environments is challenging but achievable.
- Reduction of soil acidity and metal mobility to environmentally sustainable levels
- Promising results for future applications in Martian soil simulants

GRAPHICAL ABSTRACT

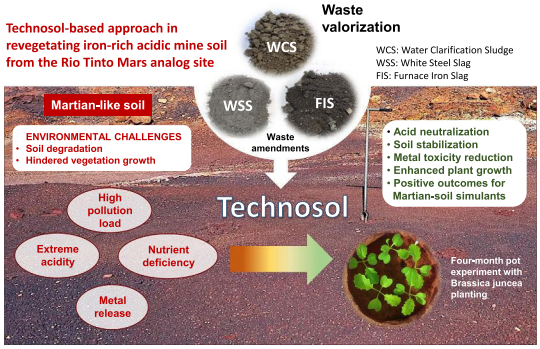

ARTICLE INFO

Editor: Paulo Pereira

Keywords:
Technosol
Martian-like soil
Waste amendments
Circular economy
Revegetation
Brassica juncea

ABSTRACT

This paper explores the potential of Technosols made from non-hazardous industrial wastes as a sustainable solution for highly acidic iron-rich soils at the Rio Tinto mining site (Spain), a terrestrial Mars analog. These mine soils exhibit extreme acidity (pH_{H2O} = 2.1–3.0), low nutrient availability (non-acid cation saturation < 20 %), and high levels of Pb (3420 mg kg^{-1}), Cu (504 mg kg^{-1}), Zn (415 mg kg^{-1}), and As (319 mg kg^{-1}), hindering plant growth and ecosystem restoration. To address these challenges, the study systematically analyzed selected waste materials, formulated them into Technosols, and conducted a four-month pot trial to evaluate the growth of *Brassica juncea* under greenhouse conditions. Technosols were tailored by adding varying weight percentages of waste amendments into the mine Technosol, specifically 10 %, 25 %, and 50 %. The waste amendments comprised a blend of organic waste (water clarification sludge, WCS) and inorganic wastes (white steel slag, WSS; and furnace iron slag, FIS). The formulations included: (T0) exclusively mine Technosol (control); (T1) 60 % WCS + 40 % WSS; (T2) 60 % WCS + 40 % FIS; and (T3) 50 % WCS + 16.66 % WSS + 33.33 % FIS. The analyses covered leachate quality, soil pore water chemistry, and plant response (germination and survival rates, plant height, and leaf number). Results revealed a significant reduction in leachable contaminant concentrations, with Pb (26.16 mg kg^{-1}), Zn (4.94 mg kg^{-1}), and Cu (2.29 mg kg^{-1}) dropping to negligible levels and shifting

* Corresponding author.
E-mail addresses: caliani@uhu.es (J.C. Fernández-Caliani), sandra.fernandez@dct.uhu.es (S. Fernández-Landero), giraldez@uhu.es (M.I. Giráldez), hidalgo@uhu.es (P.J. Hidalgo), albornoz@uhu.es (E. Morales).

https://doi.org/10.1016/j.scitotenv.2024.171217
Received 27 November 2023; Received in revised form 26 January 2024; Accepted 21 February 2024
Available online 26 February 2024

towards less toxic species. These changes improved soil conditions, promoting seed germination and seedling growth. Among the formulations tested, Technosol T1 showed promise in overcoming mine soil limitations, enhancing plant adaptation, buffering against acidification, and stabilizing contaminants through precipitation and adsorption mechanisms. The paper stresses the importance of tailoring waste amendments to specific soil conditions, and highlights the broader implications of the Technosol approach, such as waste valorization, soil stabilization, and insights for *Brassica juncea* growth in extreme environments, including Martian soil simulants.

1. Introduction

The exploration of Martian surface and its potential for supporting plant growth is an active area of research in Astrobiology (Eichler et al., 2021; Medina et al., 2021). The challenges posed by Martian soil for sustaining plant life under terrestrial conditions such as nutrient scarcity and potential toxicity requires substantial modifications. This involves creating an environment suitable for plant survival and growth, including the addition of organic matter, nutrients, water, and pH adjustments. Studies have shown that certain plant species can germinate and grow in Mars soil simulants under optimal conditions (Silverstone et al., 2005; Wamelink et al., 2014; Kasiviswanathan et al., 2022; Caporale et al., 2023). However, these simulants may not accurately replicate actual Martian soil, and there are uncertainties about the extent to which they can support plant growth.

An alternative approach to explore the potential of Martian soil is to investigate analogous extreme environments on Earth (Marlow et al., 2008; Preston and Dartnell, 2014). These terrestrial analog sites provide valuable insights into physical, geochemical, and microbiological processes that might have taken place on the red planet (Navarro-González et al., 2003; Peters et al., 2008; Valdivia-Silva et al., 2016). They can also serve as a testing ground for Mars exploration instruments, and aid in interpreting the formation mechanisms of iron oxide-rich soils (Marlow et al., 2008).

The Rio Tinto mine site (Fig. 1), in southwestern Spain, is recognized as a terrestrial analog site of significant interest for studying the Terra Meridiani hematite region of Mars due to mineralogical and geochemical similarities (Fernández-Remolar et al., 2004; Amils et al., 2007, 2014; Edwards et al., 2007; Sánchez-García et al., 2020). The NASA's Mars Exploration Rovers have detected the presence of hematite, jarosite, and evaporitic sulfate minerals (Klingelhöfer et al., 2004; Chevrier and Mathé, 2007; Edwards et al., 2007; Hazen et al., 2023) providing in situ evidence for an ancient aqueous environment at Meridiani Planum (Squyres et al., 2004). In terrestrial environments, the inferred mineral assemblage is often linked to near-surface processes involving the oxidative dissolution of pyrite and the subsequent acid-sulfate chemical reactions that drive under highly acidic and oxidizing conditions, similar to the environment found at the Rio Tinto analog site (Fernández-Remolar et al., 2005).

Historically, the Rio Tinto mining district engaged in extensive open-air sulfide roasting operations to extract copper from low-grade ores (Salkield, 1987). The roasted mineral was subjected to acid leaching with mine water leaving a solid residue of ferric iron oxide (red waste) on the calcination grounds (Fig. 1a). Meanwhile, the leach liquors were transferred into cementation tanks where dissolved copper was precipitated by using iron scrap chips. Interestingly, the iron-rich contaminated soil resulting from this ancient metallurgical process (Fig. 1b) shares similarities with hematite-rich Martian regions in terms of its chemical and mineralogical composition. Nutrient deficiencies coupled with extreme acidity, and elevated levels of sulfate and phytotoxic trace elements create an inhospitable environment for plant growing in this mine Technosol (Fernández-Landero et al., 2023).

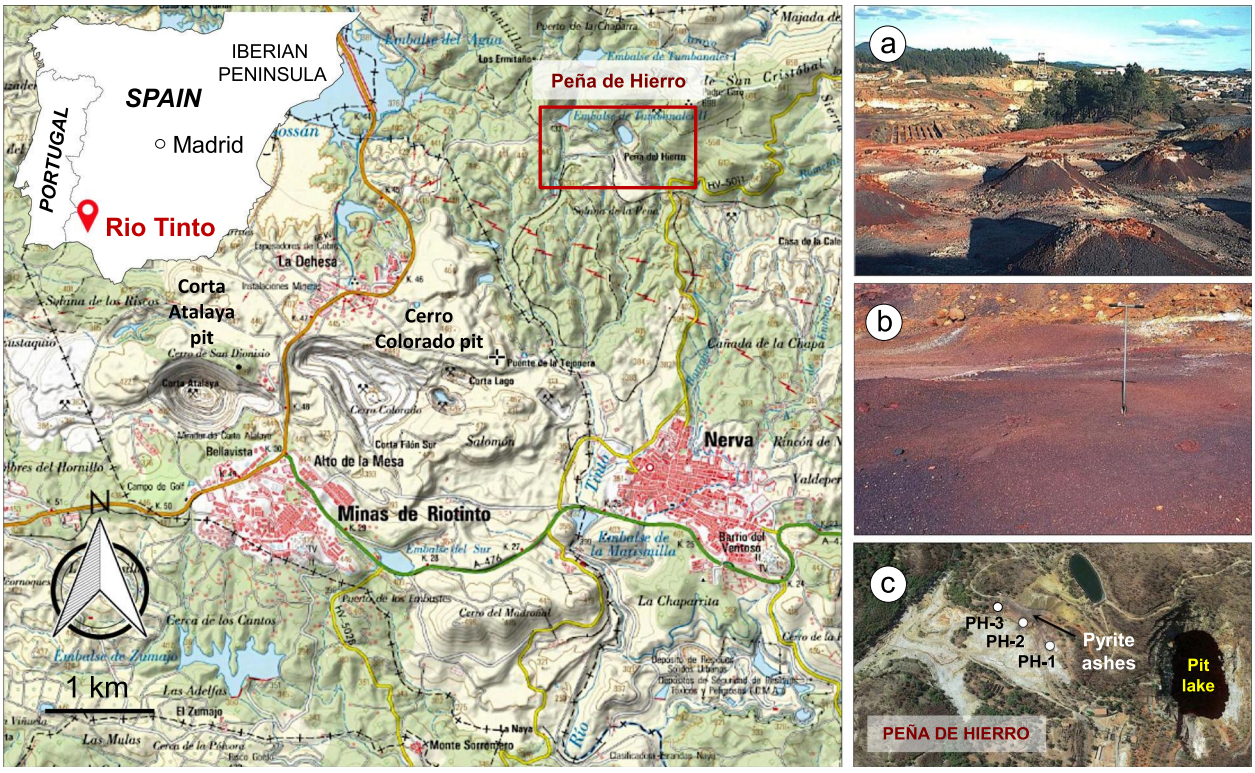

Fig. 1. Map of the Rio Tinto mining area (viewfinder SIGPAC) and illustrative images showing (a) roasted pyrite heaps; (b) mine Technosol contaminated with roasted pyrite wastes; and (c) sampling locations at the Peña de Hierro mine site.

Moreover, prolonged exposure to pollutants could lead to chronic health issues for human and wildlife populations. As such, effective management of this environmentally significant soil requires the adoption of sustainable remediation strategies to minimize the dispersion of contaminants and their potential associated risks. The application of Technosol-based methods for in situ immobilization of contaminant trace elements may offer a cost-effective and eco-friendly approach to land reclamation (Séré et al., 2008; Novo et al., 2013; Watkinson et al., 2017; Forján et al., 2018; Santos et al., 2019; Weiler et al., 2020; Ruiz et al., 2023). This remediation strategy involves the use of soil amendments derived from non-hazardous waste materials to create a conducive environment for the establishment of plants. The combined use of waste amendments and revegetation in mine soils offers several advantages (Tordoff et al., 2000; Fernández-Caliani et al., 2021), including: (i) immobilization of contaminants in the rhizosphere; (ii) reduction of risk exposure to wind-blown or re-entrained toxic particulates through ingestion or inhalation; (iii) aesthetically pleasing and publicly accepted landscape; (iv) beneficial habitat for wildlife.

By adopting a circular economy approach, this study addresses challenges linked to plant growth within a Martian-like mine soil, offering insights for optimizing soil properties and plant development. Specifically, it was aimed to assess the effectiveness of chemical stabilization in alleviating soil acidity and reducing the availability of toxic elements for plants. Additionally, it seeks to analyze the adaptability and resilience of *Brassica juncea* (L.) Czern, a known metal-tolerant plant, under tailored waste amendment combinations, focusing on germination and seedling growth patterns.

2. Materials and methods

2.1. The mine Technosol

The study area, located at the Peña de Hierro site in the Rio Tinto mining district (Fig. 1c), features a unique mine soil characterized by significant amounts of technogenic artifacts (red waste) resulting from past pyrite roasting processes. This residue poses a challenge to vegetation establishment, hindering the application of phytoremediation techniques. Classified as a Spolic Toxic Technosol according to World Reference Base for Soil Resources (Schad, 2018), the mine soil is composed mainly of well-crystallized hematite, lending it a distinct reddish hue (dry soil color Munsell chart 10R 4/2) reminiscent of the iron oxide prevalent on the Martian surface (Chevrier and Mathé, 2007). It also includes jarosite, quartz, amorphous or poorly ordered Fe phases, and minor constituents such as mica, kaolinite, feldspars, barite, anglesite, and efflorescent salts of iron sulfates (Fernández-Landero et al., 2023). Unlike relatively insoluble sulfate minerals (barite, anglesite, jarosite), the efflorescent salts undergo cycles of dissolution and reprecipitation due to dynamic wetting and drying conditions.

Soil analysis (Table 1) of the top layer (0–20 cm), extracted with an Edelman hand auger and previously analyzed by Fernández-Landero et al. (2023), revealed silt loam texture, extremely acidic soil reaction (pH_{H2O} = 2.1–3.0), strongly oxidizing conditions (Eh = 751 ± 46 mV), and relatively low electrical conductivity (< 1.8 mS cm^{-1}). Upon exposure to hydrogen peroxide, pH_{H2O2} values fall within the range of pH_{H2O} values, indicating a scarcity of sulfide minerals. Pyritic sulfur content was relatively low (0.15–0.18 %), confirming minimal unroasted sulfide ores in the red waste. Notably, sulfate was the predominant sulfur form (0.78–1.71 %), mainly due to jarosite-group minerals, resulting in an estimated modest release of latent acidity from sulfide oxidation (approx. 100 mmol H^+ per kg of soil or 3.06 kg of H_2SO_4 per ton). Importantly, results from an H_2O_2-based static test (Fernández-Landero et al., 2023) revealed that potential acid-consuming phases were ineffective in neutralizing sulfidic acidity, as evidenced by the mean value of net acid generation (NAG = 114 mmol H^+ kg^{-1}). Nutrient deficiencies are evident with low total carbon content (0.07 %) and reduced levels of exchangeable non-acid cations (mean non-acid cation saturation of 12 %), reflecting the limited nutrient-supplying capacity of the highly acidic mine soil.

Table 1
Soil properties and total concentrations of major and trace elements determined by ICP-OES on the <2 mm size fraction.

Parameter	Mine soil samples				
	PH-1	PH-2	PH-3	Mean	Std. Dev.
Sand (%)	15.9	15.0	18.0	16.3	1.5
Silt (%)	69.0	74.3	71.0	71.4	2.6
Clay (%)	15.1	10.7	11.1	12.3	2.4
Electrical conductivity (mS cm^{-1})	1.66	1.49	1.78	1.64	0.15
Eh (mV)	698	786	768	751	46
pH_{H2O}	3.0	2.5	2.1	2.5	0.4
pH_{H2O2}	2.8	2.5	2.4	2.6	0.2
Net acid generation ($mmolH^+/kg$)	144	104	93.3	114	26.9
$S_{sulfate}$ (g kg^{-1})	17.1	7.8	10.7	11.9	4.8
S_{pyrite} (g kg^{-1})	1.8	1.5	1.6	1.6	0.2
C_{total} (g kg^{-1})	0.8	0.5	0.7	0.7	0.2
Cation exchange capacity ($cmol^+kg^{-1}$)	14.2	2.5	4.0	6.9	6.3
Base saturation (%)	5.6	18.7	11.7	12.0	6.5
Major elements (g kg^{-1})					
Al	22.6	3.0	4.6	10.1	10.9
Ca	<0.1	<0.1	<0.1	<0.1	<0.1
Fe	352	461	470	428	65.7
K	7.1	1.3	1.9	3.4	3.2
Mg	0.4	0.1	0.1	0.2	0.2
Na	1.4	0.3	0.8	0.8	0.6
Trace elements (mg kg^{-1})					
As	319	150	152	207	97
Bi	86	108	100	98	11
Cd	3	3.3	3.1	3.1	0.2
Co	46	46	47	46	0.6
Cr	18	7	9	11	5.9
Cu	504	400	384	429	65
Ni	8	8	9	8	0.6
Pb	2340	3420	2980	2913	543
Tl	12	17	15	15	3
Zn	415	314	311	347	59

Given the dominance of iron-rich minerals, particularly hematite, iron was the most abundant major element in the mine soil samples, with an average content of 42.8 wt%. Other major elements such as Al, Mg, Ca, Na, and K were present at concentrations generally below 1 wt %. Total concentrations of potentially hazardous elements consistently remained at elevated levels, with Pb (up to 3420 mg kg^{-1}), Cu (up to 504 mg kg^{-1}), Zn (up to 415 mg kg^{-1}), and As (up to 319 mg kg^{-1}) being the major contributors to the trace element budget. Moreover, the mean contents of Bi, Co, Tl, and Cd peaked at 98 mg kg^{-1}, 46 mg kg^{-1}, 15 mg kg^{-1}, and 3.1 mg kg^{-1}, respectively. Trace element concentrations surpassed regional geochemical background by one to two orders of magnitude (Galán et al., 2008), collectively pointing to an extremely high degree of multi-elemental contamination (Romero et al., 2006; Fernández-Landero et al., 2023; Yesares et al., 2023). Concentrations of Pb, As, and Tl exceeded screening levels for evaluating contaminated soils in Southern Spain (Junta de Andalucía, 2015), posing unacceptable risks to potential receptors. Consequently, effective measures are imperative to mitigate potential exposure to soil contaminants.

2.2. Experimental setup

The experimental setup encompassed several key steps, including the selection and characterization of non-hazardous waste materials, formulation and blending process, physical and chemical testing, and trials with plants in pots. All these steps were designed to ensure the development of Technosols capable of enhancing soil quality for vegetation restoration.

2.2.1. Selection of waste materials for Technosol-based remediation

Three industrial wastes were selected as secondary raw materials for constructing Technosols: (i) sludge generated during the process of water clarification (WCS); (ii) white slag from steel making industry (WSS); and (iii) furnace slag from iron production (FIS). These waste materials, classified as non-hazardous under the codes 19 09 02, 10 02 02, and 10 09 03, respectively, within the European Waste Catalogue (Commission Decision 2000/532/EC), are abundantly generated and readily available on a global scale. Annually, drinking water treatment plants produce millions of tons (Mt) of sludge, with the volume steadily increasing due to the growing demand for water (Nguyen et al., 2022). In 2022, the global production of blast furnace slags ranged from 330 to 390 Mt., while steel-making slags amounted to between 190 and 290 Mt. (USGS, 2023). WCS sludge typically contains solid particles, organic matter, and other substances that have been removed by coagulation and flocculation processes during drinking water treatment. This residual material was incorporated as an organic component into the Technosol, enhancing soil structure and water retention capacity, while also providing essential macronutrients (N, P, K, S, and Mg) for improved soil fertility (Dassanayake et al., 2015; Watkinson et al., 2017). WSS and FIS slags have potential as liming agents, for assisting acid-neutralization and removal of trace elements and Fe(II) from acid mine drainage systems (Yang et al., 2022). Currently, these materials have no further utility and are being consistently disposed of in a landfill located at Nerva, within the Rio Tinto mining area. The company managing the landfill provided representative samples of the waste materials specifically for this study.

Before constructing Technosols, a comprehensive characterization of the chosen waste materials was performed, analyzing physical and chemical properties to ensure their suitability for chemical stabilization and potential adverse effects on soil quality and plant growth. The waste samples were air-dried, gently disaggregated, and sieved to 2 mm. Analysis covered particle size distribution, pH (in water), Eh, electrical conductivity, carbon contents (total, organic, and inorganic), nutrient contents (total nitrogen, assimilable phosphorus and potassium), mineral composition, and total concentrations of major elements (Fe, Al, Mg, Ca, Na, K, P, Ti, S) and trace elements of environmental significance (As, Bi, Cd, Co, Cr, Cu, Hg, Ni, Pb, Tl, Zn). In addition, a leaching test was conducted following European Standard EN-12457-4, using a liquid-to-solid ratio of 10 L kg^{-1} with end-over-end agitation for 24 h. This aimed to quantify potentially toxic trace elements that could leach from the waste material when exposed to rainfall. The leachate solutions were filtered through 0.45 μm syringe filters, acidified with dilute nitric acid, and stored in polyethylene bottles at 4 °C until analysis.

2.2.2. Constructed soil formulation

The Technosol-based remediation strategy involved the formulation of engineered soils tailored for remediating mining areas contaminated with red wastes. Waste amendments were prepared by manually blending WCS, WSS, and FIS in predetermined ratios to achieve a balanced combination of organic and inorganic components, allowing for enhanced fertility and contaminant immobilization capability. The chosen formulation ratio was 60:40 (*w*/w), meaning 60 % organic waste and 40 % inorganic waste on a dry weight basis. An exception was made for one Technosol, which tested an equal proportion of organic (50 % WCS) and inorganic (16.66 % WSS and 33.33 % FIS) waste materials. Similar ratios are usually reported in the literature for the formulation of tailor-made Technosols from wastes for the restoration of degraded mining areas (e.g. Yao et al., 2009a, 2009b; Santos et al., 2016; Asensio et al., 2019).

The Technosols were created through a blending process, where the waste material mixture, referred to as waste amendments, was thoroughly hand-mixed with the most representative sample of the mine soil (PH-2). To tailor the Technosols to the unique characteristics of the red mine soil, adjustments were made to the amendment mixtures. Thus, distinct Technosols were crafted by adding varying weight percentages of waste amendments into the mine soil, specifically 10 %, 25 %, and 50 %, in order to test the effect of the waste content on Technosol performance. The mine soil sample PH-2 was selected as the control for the laboratory experiment, providing a baseline measurement to assess the influence of the amendments on soil properties. Overall, there were eight mixtures (T0, T1a, T1b, T1c, T2a, T2b, T2c, and T3) including the control (Table 2).

Additionally, both untreated soil and soil treated with waste amendments were subjected to the EN-12457-4 leaching test to evaluate leachability and the quality of the resulting leachates. This evaluation played a crucial role in selecting optimal blends for growing purposes. The chosen blends were manually homogenized thoroughly and then moistened with distilled water to water-holding capacity (24–34 % dry weight). Subsequently, they were placed in polypropylene containers and left at room temperature (20 ± 4 °C) for two weeks to allow for equilibration before being transferred to pots.

2.2.3. Pot experiment with Brassica juncea growth

In the next phase of the experimental setup, a pot trial was carried out with Indian mustard (*Brassica juncea*, var. scala) to assess the effects of waste amendments on plant establishment and development. *B. juncea* is a versatile herbaceous plant native to the Indian subcontinent, cultivated globally due to its adaptability to diverse climatic conditions and various soil types. The selection of this species was based on its rapid growth rate and dense root system, which significantly contributes to enhanced soil fertility and stability. Given its remarkable tolerance to potentially toxic trace elements, *B. juncea* is suitable for phytostabilization and revegetating mine soils (Novo and González, 2014; Pérez-Esteban et al., 2014; Forján et al., 2018). It also serves as a valuable indicator of phytoavailability, assessing the effectiveness of potential remediation treatments in metal-contaminated soils (Clemente et al., 2005). High-quality seeds were supplied by AgroEcology (El Ejido, Almería, Spain) and carefully selected to ensure uniformity and viability.

Potting mixtures, each weighing approximately 3.5 kg, were prepared by mixing predetermined ratios of mine soil and waste amendments, and filled into individual pots of appropriate size (15 cm depth and 15 cm diameter) with tiny drainage holes at the base to prevent

Table 2
Formulation of the Technosols produced from water clarification sludge (WCS), white steel slag (WSS), and furnace iron slag (FIS), with the mixing percentage expressed in weight percent.

Sample	Technosol	Technosol composition		Amendment composition		
PH-2	Control	100 % mine soil	0 % amendment	–	–	–
T1a	S2T8–10	90 % mine soil	10 % amendment	60 % WCS	40 % WSS	-
T1b	S2T8–25	75 % mine soil	25 % amendment	60 % WCS	40 % WSS	–
T1c	S2T8–50	50 % mine soil	50 % amendment	60 % WCS	40 % WSS	–
T2a	S2T11–10	90 % mine soil	10 % amendment	60 % WCS	–	40 % FIS
T2b	S2T11–25	75 % mine soil	25 % amendment	60 % WCS	–	40 % FIS
T2c	S2T11–50	50 % mine soil	50 % amendment	60 % WCS	–	40 % FIS
T3	S2T13–25	75 % mine soil	25 % amendment	50 % WCS	16.66 % WSS	33.33 % FIS

WCS: Water Clarification Sludge. WSS: White Steel Slag. FIS: Furnace Iron Slag.

waterlogging. A layer of gravel was placed beneath of each pot to prevent soil leakage. Before planting, germination testing was conducted on *B. juncea* seeds to assess seed viability and evaluate the suitability of the constructed Technosols for promoting seedling establishment. For each Technosol, the seeds were spread on Petri dishes (30 seeds per plate), moistened with tap water, and subjected to day (10 h)-night (14 h) light cycles at temperatures ranging from 18 to 22 °C. Germination progress was observed and recorded over a period of 4–6 days. Following successful germination, five *B. juncea* seedlings, having reached the stage with two fully expanded cotyledons, were carefully transferred to the pots filled with Technosol, allowing enough space for plant growth. For quality control and accurate testing, three replicate pots of each Technosol were prepared. Additionally, a single pot was exclusively filled with mine soil (sample PH-2), without any sown seeds, while another pot was filled with mulch and used for planting, serving as the control treatment.

The pots were placed inside a glasshouse environment under natural sunlight conditions. Over the experimental period, extending from February to May 2023, temperatures ranged from 10 °C to 42 °C, air humidity levels varied between 25 % and 80 %, and daily light exposure lasted 10.5 to 14.5 h. The pots were regularly irrigated with tap water (pH = 6.85; EC = 0.65 mS cm^{-1}) to maintain optimal moisture levels for plant growth, avoiding overwatering or waterlogging. The moisture levels typically ranged from 65 % to 75 % of the soil water-holding capacity. Tap water was administered three times a week at a rate of either 50 mL or 100 mL, depending on the evaporation rate. Throughout the experiment, relevant parameters including pH, electrical conductivity and chemical composition of soil pore water, were regularly measured and recorded for both Technosols and the control sample. These measurements were conducted monthly for four months.

Soil solution sampling was performed under moisture conditions equivalent to field capacity using Rhizon soil moisture samplers (Eijkelkamp, The Netherlands) inserted into the soil at a 45° angle. This consists of a porous polymer tube with a pore size of 0.15 μm connected to a PVC tube and a Luer-Lock connector (Clemente et al., 2008). Soil pore water was sampled by pulling a vacuum with a 50 mL syringe and used immediately for pH, Eh, and electrical conductivity measurements. The extracted solution was then acidified with dilute nitric acid for the subsequent analysis of element concentrations in the soluble fraction. Furthermore, survival rate and parameters such as plant height and leaf number were measured to monitor the growth and development of *B. juncea*. These measurements were consistently recorded at regular intervals, weekly over a span of four months.

2.3. Analytical methods

The analysis of grain-size distribution and specific surface area was conducted using the Mastersizer 3000 laser diffraction particle size analyzer. The pH, redox potential (Eh), and electrical conductivity of the samples were determined through potentiometric measurements in the supernatant suspension obtained by mixing 10 g of soil with 25 mL of deionized water, followed by stirring for 5 min and allowing it to stand for 30 min.

Total carbon (C_{total}) and total nitrogen contents were determined using an ELTRA CHS-580 A analyzer through a dry combustion method. Inorganic carbon (C_{inorg}) measurement involved a two-step process: initially, the samples were calcined in a muffle furnace set at 400 °C for 16 h. Prior to this, a dehydration step was performed, wherein the samples were subjected to 110 °C heat for 1 h to remove moisture. Organic carbon (C_{org}) quantification was derived as the difference between C_{total} and C_{inorg} (Nelson and Sommers, 1996). To convert organic carbon to organic matter, a conversion factor of 1.724 was applied. Plant-available phosphorus concentration was assessed using Olsen's method, which relies on alkaline phosphate extraction with a 0.5 N NaH (CO_3) solution (Olsen and Sommers, 1982), while the content of assimilable forms of potassium was determined through a 0.01 M $CaCl_2$ extract (Houba et al., 1996).

Chemical analysis of total concentrations of major and trace element was performed by ICP-OES after a four-acid ($HClO_4$-HNO_3-HCl-HF) digestion process at Actlabs (Ancaster, Ontario, Canada), an accredited laboratory compliant with ISO 9001 and ISO/IEC 17025 standards. Quality control measures, including the use of reagent blanks, duplicate analysis, and certified reference materials (OREAS 101b, OREAS 98, and OREAS 13b), were employed to ensure accuracy and precision. The analysis of reference materials indicated deviations from certified concentrations with a relative standard deviation (RSD) of <10 %, and the precision of analytical data consistently was better than 5 % RSD for all reported elements.

Element concentrations in both the leachate solution and soil pore water extracted with Rhizon samplers were subjected to chemical analysis. Major elements were measured using an Agilent 5110 ICP-OES, while trace elements were analyzed by inductively coupled plasma mass spectrometry (ICP-MS) with an Agilent 7700 instrument. For quality control, external calibration, internal standard, replicates, blank analysis and standard reference material (SRM 1640a) were used. All elements in the standard reference material fell within the range of 95 % and 106 % of the certified concentrations. Analytical data for the majority of studied elements displayed accuracy and precision with an RSD better than 10 %. Furthermore, soil solution analysis for chloride, fluoride, and nitrate anions was conducted using ion chromatography with a Metrohm 883 Basic IC plus instrument. Mineral saturation indices and distribution of aqueous species in the soil solution were computed using the geochemical modeling software PHREEQC (Parkhurst and Appelo, 2013) and the Minteq.v4 thermodynamic database (Allison et al., 1999), enlarged with data from Bigham et al. (1996) to account for schwertmannite. The saturation index (SI) for each predicted mineral was calculated using the formula:

$$SI = log\ (IAP/Ks)$$

where IAP is the ion activity product and K_s is the solubility product constant. This index provides insights into potential dissolution-precipitation reactions, thereby influencing the availability of toxic elements to plants. A SI approaching zero indicates solubility equilibrium in the pore water composition. A positive SI implies potential oversaturation and precipitation, while a negative value indicates undersaturation, suggesting potential dissolution.

Additionally, a mineralogical analysis was carried out by powder X-ray diffraction (XRD) on a BRUKER D8-Advance diffractometer, using monochromatic CuKα radiation at 40 kV and 30 mA. XRD patterns were obtained from randomly oriented powders scanned from 3° to 70° 2θ, with a step size of 0.02° and a counting time of 0.6 s per step. Soil minerals were visualized by high-resolution field emission scanning electron microscopy (FESEM) using a JEOL JSM-IT500HR instrument operated at 20 kV, and chemically analyzed with an energy-dispersive X-ray (EDS) spectrometer coupled to the FESEM.

2.4. Statistical analysis

The collected data underwent statistical analysis to evaluate the effects of the treatment on the chemistry of the soil pore water. Left-censored data, representing values below the detection limit, were managed by assuming them as half of the detection limit. Standard errors were calculated to gauge the variability between replicates. Statistical differences between the sample means of the Technosols and the control soil (mine soil without treatment) were assessed using the Student's *t*-test and one-way analysis of variance (ANOVA). Before conducting the ANOVA analysis, the homogeneity of variance was examined through Levene's test. A significance level of $\alpha = 0.05$ (95 % confidence interval) was set for all statistical tests.

3. Results and discussion

3.1. Characteristics of waste materials used as amendments

To avert potential environmental issues stemming from the use of non-hazardous wastes in tailor-made Technosol formulation, a thorough understanding of the properties and constituents of these residual materials is crucial (Yao et al., 2009a). The waste materials used as components of the Technosols showed distinct compositions and characteristics in terms of particle size distribution, electrical conductivity, pH, carbon content, nitrogen content, and nutrient availability (Table 3).

Specifically, WCS showed a light olive brown hue (2.5Y 5/3), a slightly acid to neutral reaction ($pH_{H2O} = 6.7$), and the lowest electrical conductivity (0.69 mS cm^{-1}), indicating a limited presence of soluble salts. Remarkably, it displayed the highest total carbon content at 11.80 %, coupled with a substantial organic carbon content of 11.50 %. In addition, WCS boasted the largest organic matter content at 19.83 %, highlighting its rich organic composition. With the highest total nitrogen content at 2.12 %, WCS could serve as a nitrogenous organic fertilizer. The C/N ratio of 5.6 is indicative of a good balance between carbon and nitrogen. Further enhancing its profile, WCS contained 16.7 mg kg^{-1} of available phosphorus and 57.7 mg kg^{-1} of available potassium, thus providing a source of essential nutrients for plant growth.

Regarding to WSS, it is characterized by a gray color (2.5Y 6/1) and an exceptionally high alkaline pH_{H2O} of 12.44, coupled with a remarkable electrical conductivity of 7.27 mS cm^{-1}. WSS showed an inorganic carbon content of 1.50 %, while organic carbon remained undetected. Despite having the lowest total nitrogen content among the tested wastes, WSS contained the highest levels of available phosphorus (22.8 mg kg^{-1}) and available potassium (151 mg kg^{-1}).

As for FIS, it is a gray-colored (10YR 4/1) waste material with an alkaline pH of 10.0 and low electrical conductivity (0.78 mS cm^{-1}). In terms of composition, FIS showed a total carbon of 1.70 %, with 1.00 % accounting for organic carbon, along with a total nitrogen content of 0.09 %. Moreover, the concentrations of available phosphorus and available potassium measured in this waste material measured 18.7 mg kg^{-1} and 56 mg kg^{-1}, respectively.

Each waste material displayed a distinctive chemical composition, indicative of its origin and treatment process. WCS had remarkably high concentrations of Al (> 10 wt%) due to the use of Al-based coagulants and the prevalence of aluminosilicate clay minerals, as revealed by XRD analysis. Its composition also included quartz, feldspars, iron oxides, and gypsum. On the other hand, WSS showed relatively higher levels of Ca (> 10 wt%) and Mg (6.67 wt%), suggesting its potential for soil improvement if used as alkaline amendment to raise the pH and reduce soil acidity. FESEM-EDS analysis revealed distinct metallurgical phases, with a notable presence of Ca primarily combined with Si, forming calcium silicate phases, which are significant in neutralizing acidity and removing trace elements from mine discharges (Fernández-Caliani et al., 2008). Additionally, calcite was identified, while Mg predominately occurred in the form of oxides and aluminates. FIS exhibited an elevated Fe content (7.56 wt%) in comparison to the other waste materials, due to the presence of poorly crystallized iron-silicate phases. Mineralogically, it was characterized by abundant quartz with minor anorthite and calcite, as crystalline phases identified by XRD analysis.

In contrast to the mine soil, the waste materials contained low total concentrations of potentially hazardous trace elements (Table 3). However, the presence of certain toxic elements, even at these reduced levels, such as 42 mg kg^{-1} of As in WCS and 294 mg kg^{-1} of Cu in FIS, raises concerns about their potential impact on soil and environmental quality before being used for land applications. Particularly worrisome is the potential for leaching elevated levels of trace elements, especially in agricultural and landscaping contexts (Siddique et al., 2010). Yet, elemental measurements of leachate from these wastes (Table 3) revealed negligibly low values, with concentrations falling below the detection limits for all reported elements (in mg L^{-1}): < 0.01 for Hg, < 0.05 for Cd, < 0.1 for As, Cu, and Pb, < 0.2 for Zn, and < 0.5 for Cr and Ni. Therefore, the waste materials used as amendments displayed a low potential for leaching contaminants, with none of the analyzed trace elements surpassing the soil solution concentration considered as toxic for vegetation establishment (Ross, 1996). The concentration of sulfate measured in the leach solutions was 37 mg L^{-1}, while chloride was found to be <50 mg L^{-1}, indicating a minimal presence of soluble salts. The concentrations of all dissolved cations and anions in the leachates adhere to the standards outlined in Spanish legislation for the formulation of Technosols derived from waste materials.

Table 3
Properties and chemical composition of the waste materials and their leachates.

Parameter	WCS	WSS	FIS
Specific surface area (m^2 g^{-1})	0.598	0.640	0.474
Electrical conductivity (mS cm^{-1})	0.69 ± 0.07	7.27 ± 0.06	0.78 ± 0.04
$pH_{(H2O)}$	6.74 ± 0.21	12.44 ± 0.11	10.00 ± 0.13
C_{total} (g kg^{-1})	118.0	15.0	17.0
$C_{inorganic}$(g kg^{-1})	3.0	15.0	7.0
$C_{organic}$(g kg^{-1})	115.0	n.d.	10.0
Organic matter (g kg^{-1})	198.3	n.d.	17.2
N_{total} (g kg^{-1})	21.2	0.1	0.9
$P_{available}$ (mg kg^{-1})	16.7	22.8	18.7
$K_{available}$ (mg kg^{-1})	57.7	151	56.0
Major elements (g kg^{-1}) — Solid waste			
Al	> 100	37.9	9.7
Ca	1.8	> 100	16.8
Fe	13.4	9.3	75.6
K	6.0	0.2	0.9
Mg	1.6	66.7	8.3
Na	0.6	0.9	2.9
P	1.75	0.01	0.24
S	7.8	4.2	0.4
Ti	< 0.1	1.2	0.3
Trace elements (mg kg^{-1}) — Solid waste			
As	42	< 2	26
Bi	< 2	< 2	< 2
Cd	< 0.5	< 0.5	< 0.5
Co	3	1	5
Cr	14	121	73
Cu	84	42	294
Hg	2	< 1	< 1
Ni	15	12	54
Pb	23	16	88
Tl	< 2	< 2	< 2
Zn	71	252	226
Trace elements (mg L^{-1}) — Leachate			
As	< 0.1	< 0.1	< 0.1
Cd	< 0.05	< 0.05	< 0.05
Cr	< 0.5	< 0.5	< 0.5
Cu	< 0.1	< 0.1	< 0.1
Hg	< 0.01	< 0.01	< 0.01
Ni	< 0.5	< 0.5	< 0.5
Pb	< 0.1	< 0.1	< 0.1
Zn	< 0.2	< 0.2	< 0.2
Anions (mg L^{-1}) — Leachate			
Sulfate	37	6.9	< 4
Chloride	< 50	< 50	< 50
Fluoride	0.1	< 0.1	5.7

WCS: Water Clarification Sludge. WSS: White Steel Slag. FIS: Furnace Iron Slag.

3.2. Effects of waste amendments on chemical stabilization

3.2.1. Leachate quality

The leaching test results (Table S1) provide valuable insights into potential pollutant release from Technosols. Fig. 2 graphically compares trace element concentrations leached from treated samples with the total contents in the untreated mine soil sample. The line chart in Fig. 2

enhances this comparison by depicting the proportion of the total trace element pool removed from the mine soil by leaching.

The untreated soil (sample PH-2) yielded highly acidic leaching solutions (pH = 2.5) resulting from the mine soil-water interaction, leading to varying degrees of solubilization of potentially toxic trace elements. Among these elements, Pb (26.16 mg kg^{-1}), Zn (4.94 mg kg^{-1}), and Cu (2.29 mg kg^{-1}) were the most prevalent in the leachates. Other deleterious trace elements, including As, Cd, Sb, Cr, and Ni, generally occurred at levels below 1 mg kg^{-1}. In contrast, leach solutions from the Technosols were moderately alkaline. The leaching of soluble divalent cations with low ionic potential, notably Cu^{2+}, Zn^{2+}, Pb^{2+}, and Cd^{2+}, experienced a noticeable decrease with treatment. All waste amendments demonstrated the ability to reduce the mobility of these trace elements by at least 9.5, 8.3, 4.5, and 2.0, times respectively, with the Technosols S2T8–25 and S2T13–25 proving the most effective. Interestingly, Ni concentrations in most Technosol leachates exceeded

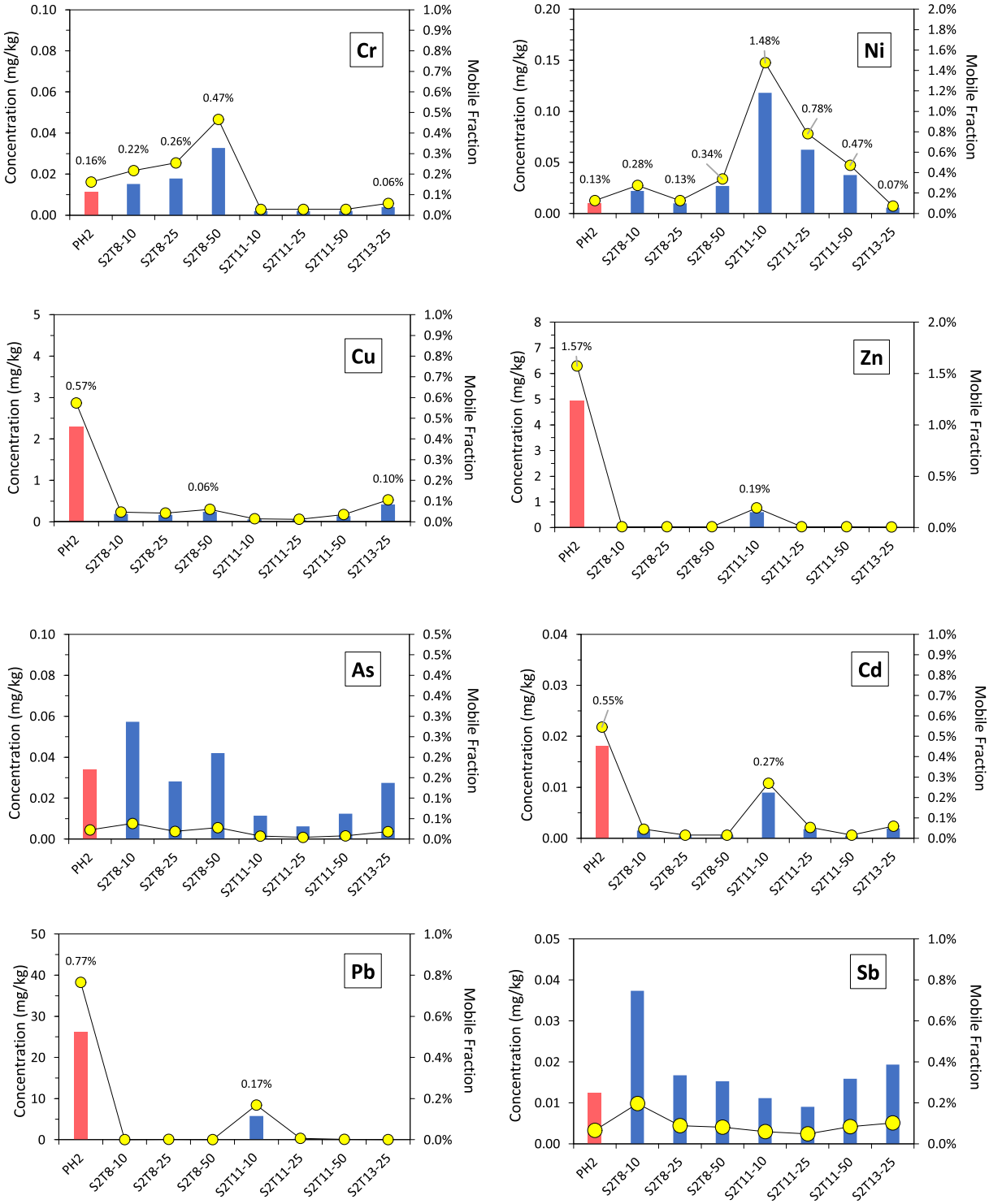

Fig. 2. Bar charts contrasting leaching concentrations of potentially toxic trace elements in untreated soil versus Technosols, and line charts showing the mobile fraction (%) released from the mine soil (sample PH2).

those in the control, attributed to the relatively high levels of this contaminant introduced by waste amendments, although the leaching fraction was limited to <1.5 %.

On the other hand, elements with high ionic potential, typically occurring as complex oxyhydroxy anions, such as As (up to 0.057 mg kg^{-1}), Cr (up to 0.033 mg kg^{-1}), and Sb (up to 0.037 mg kg^{-1}), showed increased concentrations in leachates from certain Technosols compared to those from untreated soil. This finding is consistent with the commonly noted observation that increased soil pH can weaken anion sorption onto soil minerals due to the increase in surface negative charge (Carabante et al., 2009). Nevertheless, these concentrations remained below regulatory limits (2 mg kg^{-1}, 10 mg kg^{-1}, and 0.7 mg kg^{-1}, respectively) established in Spain for Technosols derived from waste materials. Moreover, the leachable fraction of trace elements was negligibly low, with maximum release values of 0.47 % for Cr, 0.20 % for Sb and 0.04 % for As.

3.2.2. Soil pore water chemistry throughout the pot experiment

Despite significant reduction in trace element leachability from most treatments, formulations S2T8–25 and S2T13–25 were selected as first choices for a growth test in a pot experiment with *B. juncea*. As contaminants are primarily taken up by plant through the root system, analyzing the interstitial water in soil pores provides valuable insights into of trace element availability and a more accurate indication of environmental risk (Nolan et al., 2003). Therefore, the concentration of trace elements in the soil solution, extracted using Rhizon samplers, holds particular importance as it represents the fraction of soil water available for plant uptake (Clemente et al., 2008).

The Technosol-based treatment significantly influenced the pH, electrical conductivity, and redox status (Eh) of the soil-water system. The soil solution extracted from the untreated control soil showed extremely acidic pH values, ranging from 1.8 to 2.4 (Fig. S1a), nearly matching or slightly lower than the soil pH measured in water. This acidity persisted throughout the entire experimental period. Technosol S2T8–25 treatment initially shifted pore water pH from extremely acidic to slightly acidic (pH = 6.6), maintaining an alkaline level consistently. Technosol S2T13–25 induced initial acidity, with pH values around 4 in the first month of treatment, stabilizing at near-neutral values (pH = 6.7–6.8) after three months. The pH variations in both Technosols arise from complex interactions between the amendments and the mine soil, with the higher acid-neutralizing capacity of WSS playing a substantial role in determining pH trends. The pH increase in Technosols was significant compared to the control soil ($p < 0.00008$). The application of the highest dose of WSS not only induced a rapid pH increase in the Technosol S2T8–25 (40 % WSS) compared to Technosol S2T13–25 (16.66 % WSS) but also sustained an acid-neutralizing action throughout the four-month trial. Hence, the Technosol treatment efficiently neutralized the acid generated (104 mmol H^+ kg^{-1}) by the mine soil, fostering a more conducive environment for plant growth.

The pore water extract from the untreated mine soil initially had an electrical conductivity of 26.7 mS cm^{-1}, decreasing over time to recorded values (15.6–17.8 mS cm^{-1}) in the second month of treatment and thereafter (Fig. S1b). This decline in leachate conductivity, attributed to the dissolution and washing out of sulfate salts, is consistent with the presence of a finite pool of readily soluble sulfate for release. Similarly, the Technosols showed decreasing electrical conductivity over time, ranging from 21.0 mS cm^{-1} to 7.9 mS cm^{-1} (Technosol S2T13–25) and from 12.0 mS cm^{-1} to 6.7 mS cm^{-1} (Technosol S2T8–25). The treatment significantly reduced electrical conductivity compared to the control soil ($p < 0.004$), reflecting a decrease in sulfate concentration in the soil solution. Therefore, the observed decline in electrical conductivity values following treatment was another noticeable effect of the applied waste amendments.

The initial soil solution extracted from the mine soil showed a redox potential of 717 mV, indicating highly oxidizing conditions. Following waste amendment application, the Eh decreased to 398 mV in Technosol S2T8–25 and 528 mV in Technosol S2T13–25 two weeks later. At the end of the pot experiment, the pore water extracts exhibited Eh values of 370.4 ± 0.9 mV and 372.1 ± 1.9 mV, respectively, indicating a shift to moderately oxidizing conditions. In contrast, the mine soil control remained under oxidizing conditions with an Eh of 695 mV.

Rising soil pH and maintaining oxidizing conditions had a beneficial impact on soil pore water quality by boosting the retention of trace elements through chemical stabilization processes (Basta and McGowen, 2004; Kumpiene et al., 2008; Bolan et al., 2014). These immobilization mechanisms led to the redistribution of contaminants from the soil solution to the solid phase, thereby reducing their bioavailability and phytotoxicity for the restoration of vegetation. Concentrations of trace elements in pore water extracts from both treated and untreated (control) soil samples are listed in Table S2, and graphically depicted in Fig. 3 for comparison. The application of Technosol buffered the soil pH to moderately alkaline (Technosol S2T8–25) or near-neutral (Technosol S2T13–25) values, enhancing the attenuation of trace element contaminants.

Remarkably, there was a significant and substantial decrease in the dissolved metal(loid) load of the Technosols compared to the untreated soil ($p < 0.05$). Concentrations of all measured trace elements in the pore water extracts dropped by several orders of magnitude owing to the treatment-induced rise in pH. This reduction was particularly pronounced for trace elements influenced by pH, displaying their lowest mobility within the neutral to slightly alkaline range. For instance, the concentrations of initially dissolved Cu and Zn in the mine soil solution dropped from 481.1 mg L^{-1} and 789.9 mg L^{-1}, respectively, to <1 mg L^{-1} by the end of the four-month monitoring period. Therefore, the alleviation of soil acidity was a major factor driving the immobilization of metallic cations by reducing the activity hydrogen ions in the soil solution, thereby minimizing their competition for metal binding sites. Mineral saturation indices computed with PHREEQC revealed that the addition of waste amendments to mine soil triggered the precipitation of various Cu-bearing phases, especially copper ferrite ($CuFe_2O_4$) (SI = 12.8–16.9), and carbonates like azurite ($Cu_3(CO_3)_2(OH)_2$) (SI = 1.3) and malachite ($Cu_2(CO_3)(OH)_2$) (SI = 2.0) in Technosol S2T8–25, indicating reduced mobility but allowing potential plant uptake upon re-acidification. Conversely, minerals bearing Cd, Pb, or Zn, did not exhibit positive SI values, suggesting that their dissolved concentrations were controlled most likely by adsorption rather than precipitation.

Despite the potential risk of As mobilization associated with the pH increase to the alkaline region (Hartley et al., 2004; Kumpiene et al., 2008), the soluble concentrations of As interestingly dropped from 38.27 mg L^{-1} to either 23 μg L^{-1} (Technosol S2T8–25) or 8 μg L^{-1} (Technosol S2T13–25) by the end of the observation period. Clearly, this reduction in the concentration of As and other trace elements suggests a potential decrease in the mobility and phytoavailability of these potentially harmful elements. In Technosol S2T8–25, the decline in As mobility cannot be solely attributed to the adsorption of soluble oxyanion species, as the negatively-charged surfaces of soil particles increased after acid neutralization. Instead, it might be linked to the precipitation of low-solubility As-Ca complexes (Bothe and Brown, 1999; Porter et al., 2004; Fernández-Caliani et al., 2022).

On the other hand, concentrations of key major elements such as Al, Fe, and S in the pore water of the Technosols were significantly lower ($p < 0.004$) than in the control soil. Remarkably, the soluble concentration of Al dramatically dropped from 5200 mg L^{-1} to undetectable levels, mitigating one of the most severe toxicity issues in acid mine soils (Fernández-Caliani and Barba-Brioso, 2010). Potential control over the solubility of dissolved Al within the pH range of 6–9 may arise from the formation of aluminum hydroxide solid phases (Sánchez-España et al., 2011). Saturation indices predicted by PHREEQC for gibbsite ($Al(OH)_3$) (SI = 2.75), boehmite (γ-AlOOH) (SI = 2.46), and diaspore (α-AlOOH) (SI = 4.16) indicate that the reduction in dissolved Al concentrations was likely governed by the precipitation of aluminum hydroxide phases, which provides the soil with additional sorption capacity.

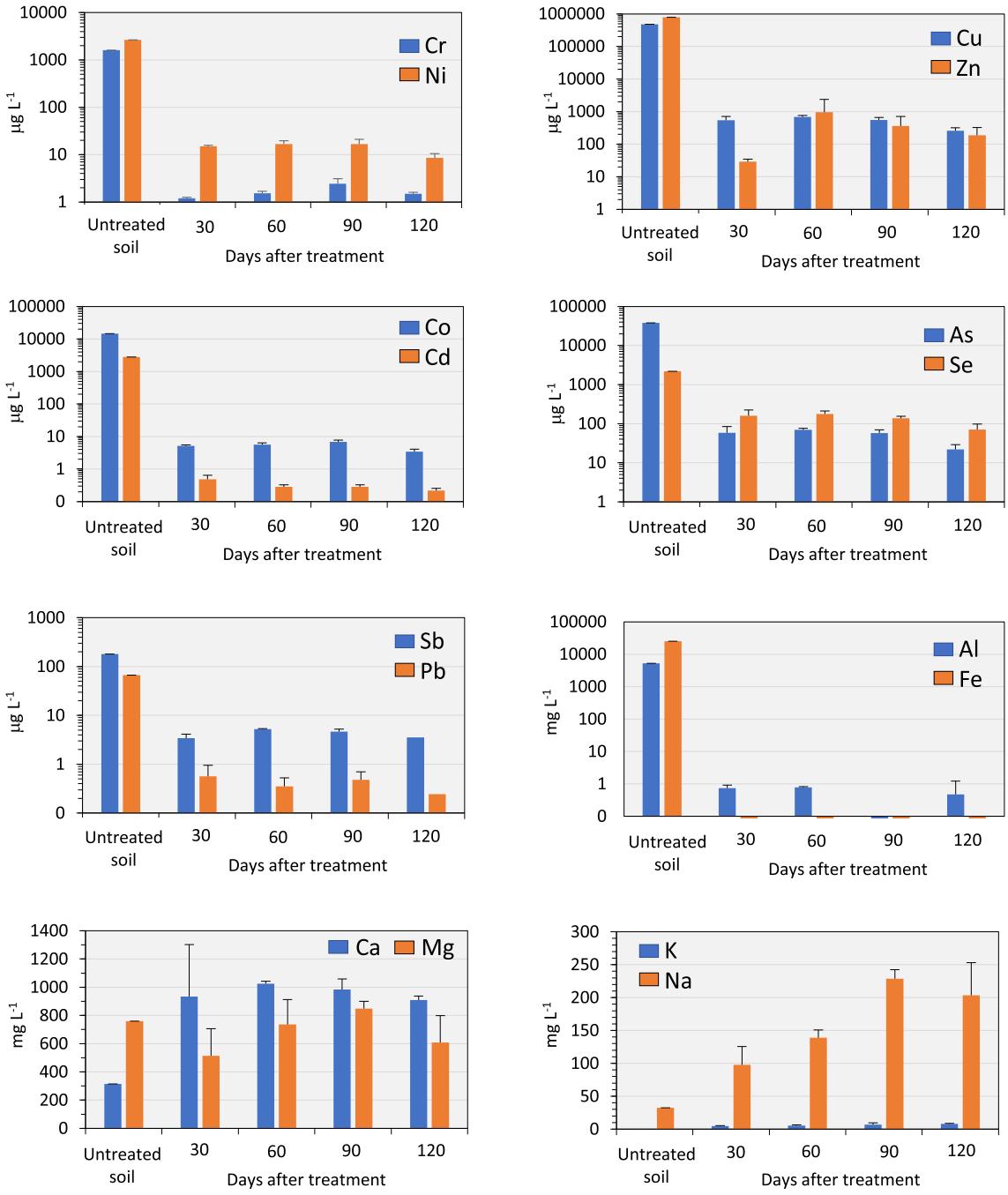

Fig. 3. Comparative bar charts displaying element concentrations in the untreated mine soil (control) and the Technosol S2T8–25. Error bars denote the standard deviation of the means ($n = 3$).

Fig. 3 (continued). Comparative bar charts displaying element concentrations in the untreated mine soil (control) and the Technosol S2T13–25. Error bars denote the standard deviation of the means (n = 3).

Moreover, a fraction of trace elements may have been removed from the soil solution and sequestered by newly-formed hydrous ferric oxides (HFO) through adsorption, complexation and (co)precipitation processes (Carlson et al., 2002; Sherman and Randall, 2003). HFO surfaces are known to be involved in As adsorption in soils (Waychunas et al., 1993; Hartley and Lepp, 2008; Kumpiene et al., 2021). Equilibrium speciation calculations revealed supersaturation concerning ferrihydrite ($Fe_{10}O_{14}(OH)_2$) (SI = 3.8), which is thermodynamically unstable and can be transformed to either lepidocrocite (γ-FeOOH) or goethite (α-FeOOH). Hence, it can be inferred that these HFO precipitates played a pivotal role in controlling iron activity in the soil solution of both Technosols. This is consistent with the significant reduction in water-soluble Fe concentrations, decreasing from 25 g L^{-1} to values below 1 mg L^{-1}. The most likely HFO precipitate under neutral or mildly alkaline pH conditions is ferrihydrite, a nanocrystalline phase commonly found in ochreous precipitates from Fe-rich surface waters with a pH >5 (Bigham et al., 1992; Murad and Rojík, 2003). Consequently, HFO surfaces might have efficiently removed contaminants from the soil solution through adsorption and co-precipitation mechanisms.

In contrast, concentrations of Ca, Mg, Na, and K in the soil solution

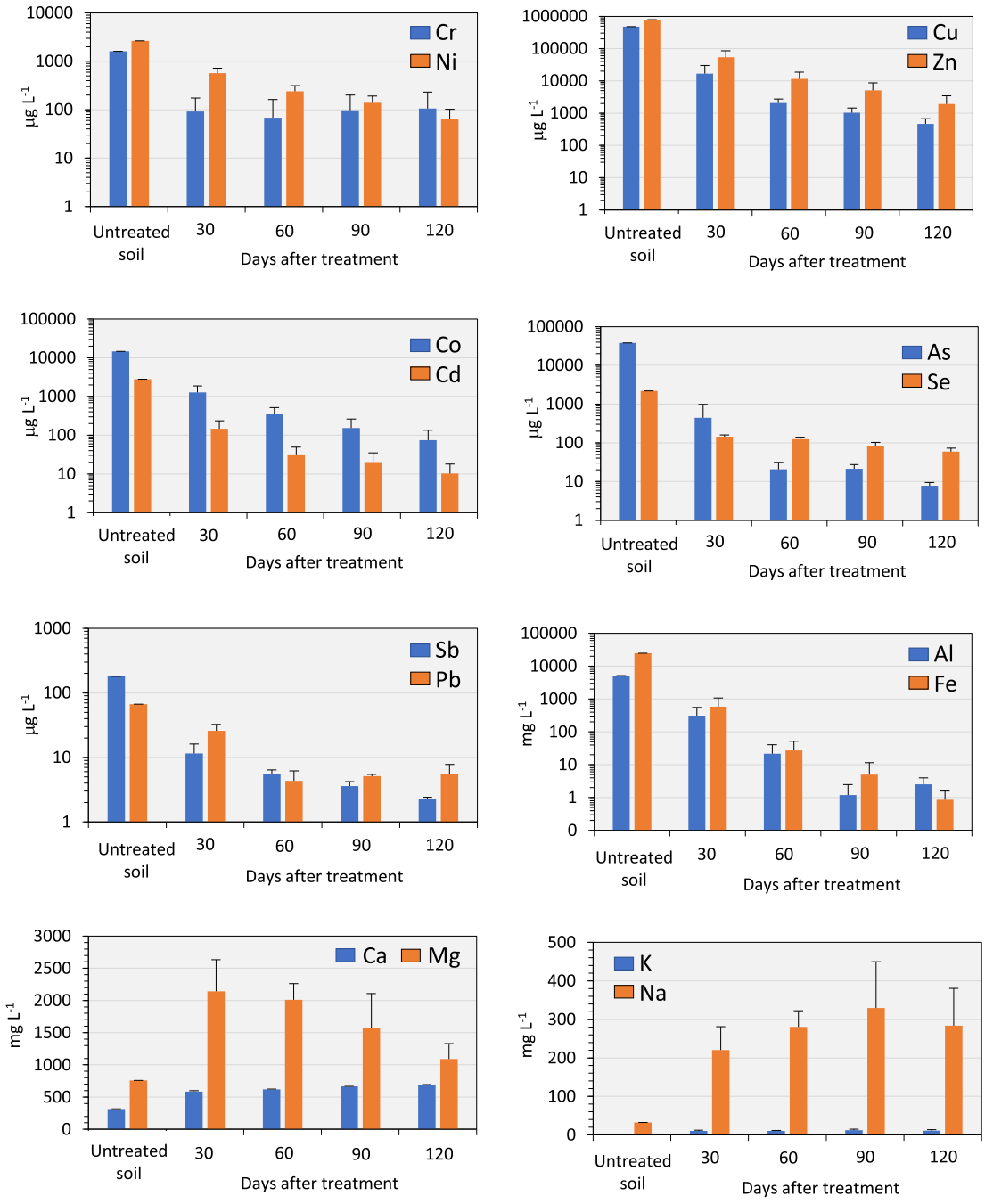

Fig. 3. (*continued*).

showed a significant increase compared to the control ($p < 0.01$). Technosol application led to an increase in soluble Ca content from to 315 mg L^{-1} (control soil) to 1024 mg L^{-1} (S2T8–25) and 683 mg L^{-1} (S2T13–25). Furthermore, there was an increase in soluble Mg content, particularly in S2T13–25 (from 760 mg L^{-1} up to 2141 mg L^{-1}), although the Mg concentration gradually decreased over time to 1089 mg L^{-1}. The minerals most prone to dissolution in the waste amendments were notably calcite, but also calcium silicate compounds, as well as magnesium oxides and aluminates. This boost in the solubility of essential nutrients was advantageous for promoting soil fertility and vegetation establishment.

Concerning anions (Fig. S2), sulfate stood out as the dominant species in all pore water solutions, initially reaching a concentration of 82.95 g L^{-1} in the untreated soil. Over time, this concentration significantly decreased to 22.45 g L^{-1} due to the washing out of efflorescent sulfate salts formed on the topsoil. During the experiment, the addition of water to restore moisture content resulted in the dissolution of sulfate salts, with partial reprecipitation observed on the pot walls of the control sample. Conversely, higher concentrations of chloride (up to 1509 mg L^{-1}), nitrate (up to 122 mg L^{-1}), and fluoride (up to 44 mg L^{-1}) were detected in the extract soil solutions of the Technosols compared to the untreated mine soil. Moreover, the concentration of bicarbonate anions in pore water emerged as a notable species following the Technosol-based treatment, peaking at 866 mg L^{-1}. This substantial increase was most pronounced and sustained at the higher dose of WSS (Technosol S2T8–25).

On the other hand, the rise in pH induced by the waste amendment to alkaline levels might theoretically destabilize metal-bearing minerals

like jarosite, impacting soil acidity and triggering the re-release of sulfate and trace elements back into the soil solution (Hudson-Edwards et al., 1999). However, this potential concern does not appear to be supported by the data, as indicated by consistently low concentrations of Fe, sulfate, and K in the pore water extracts of the Technosols throughout the entire pot experiment.

3.2.3. Soil solution speciation modeling

Understanding the mobility, availability, and toxicity of contaminants in the soil solution, requires a focus on trace element speciation rather than total dissolved concentration (Kalis et al., 2008). PHREEQC speciation calculations provided insights into the distribution of trace element of concern among various chemical species in both untreated soil and Technosols after the four-month pot trial (Fig. 4).

In untreated soil, aluminum was mainly associated with sulfate ions, existing in monomeric ($AlSO_4^+$) and dimeric ($Al(SO_4)_2^-$) forms, with free ions comprising about 6 % of the dissolved fraction. The highly toxic Al^{3+} form poses a significant limitation for plant growth (Chandra and Keshavkant, 2021). Waste amendments prompted a shift towards hydroxylated species, particularly with $Al(OH)_4^-$ being the dominant aqueous species in both Technosols. In this state, aluminum is less toxic to plant roots. Predicted $Al(OH)_3$ suggests some aluminum hydroxide precipitation, and $Al(OH)_2^+$ in Technosol S2T13–25 does not exhibit phytotoxicity under slightly acidic conditions (Bojórquez-Quintal et al., 2017). The rise in pH likely alleviated aluminum toxicity by rendering it less soluble and more prone to form less toxic species. Consequently, nutrient availability to plants improved as competition for root uptake sites with toxic Al^{3+} ions decreased.

Trace element speciation was clearly dominated by sulfate complexes and free (uncomplexed) ions. Specifically, Cu, Cd, Pb, and Zn were predicted to be associated mainly with sulfate anions, forming prevalent species such as $CuSO_4$, $Cd(SO_4)_2^{2-}$, $Pb(SO_4)_2^{2-}$, and $Zn(SO_4)_2^{2-}$, respectively. Furthermore, remarkable concentrations of free ions, accounting for 45 % Cu^{2+}, 16 % Cd^{2+}, 11 % Pb^{2+}, and 15 % Zn^{2+} of the

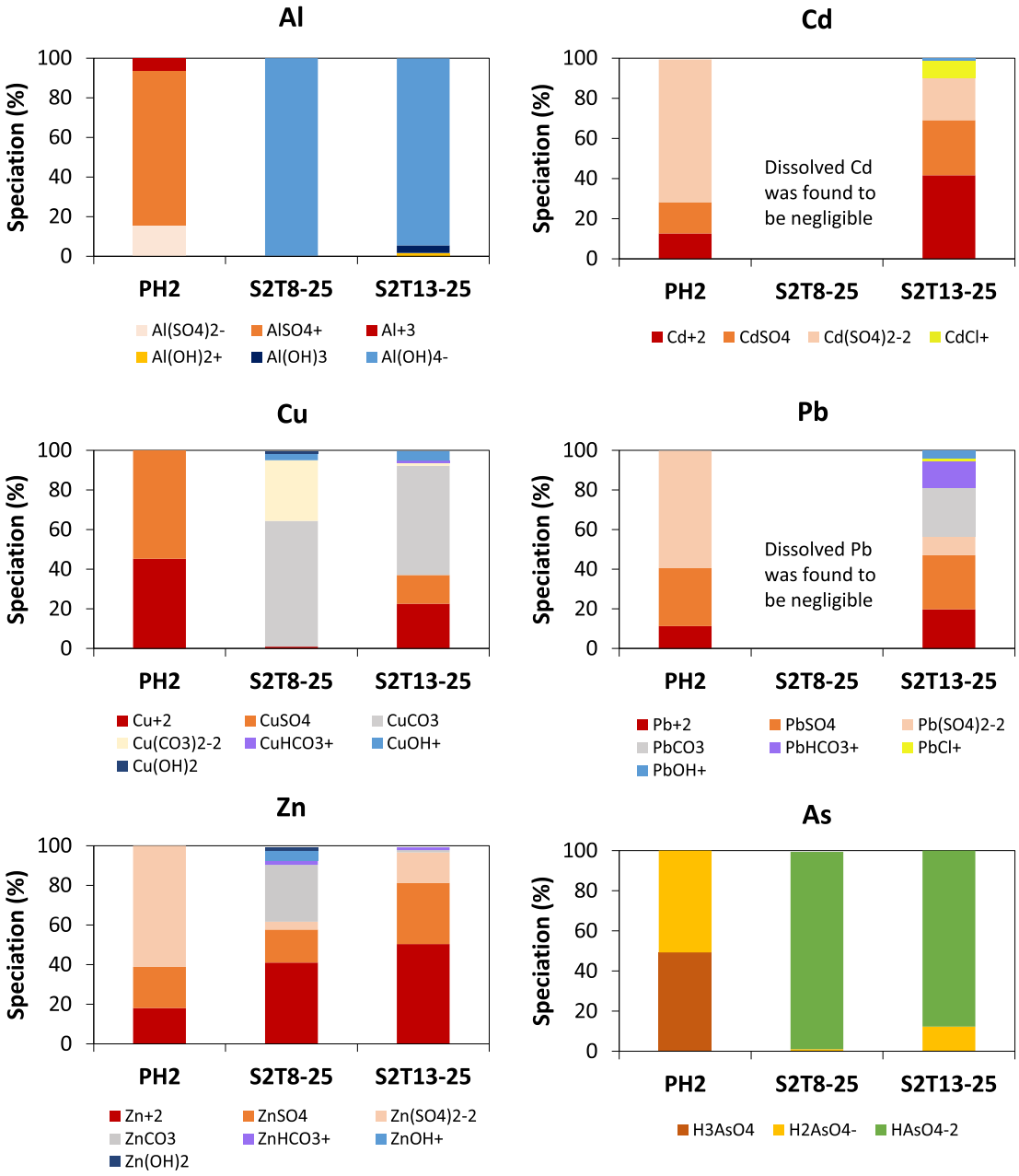

Fig. 4. Predicted speciation of trace elements of concern in the soil solution.

dissolved fraction, had the potential to induce phytotoxicity and hinder plant growth (Kumar et al., 2021).

The Technosol-based remediation approach induced substantial alterations in chemical speciation, resulting in a diverse distribution of species (hydroxide, carbonate, bicarbonate, chloride, sulfate, and free ions), which had a significant impact on trace element mobility and plant availability. Copper speciation was dominated by $CuCO_3$ in both Technosols, contributing to a favorable environment for plant growth by decreasing the activity of toxic Cu^{2+} ions. Lead speciation exhibited a mix of carbonate, sulfate, free ions and other soluble complexes with inorganic ligands. Zinc displayed a variety of species, including, sulfate, carbonate, and free ions. Meanwhile, Cd primarily existed as free Cd^{2+}, sulfate complexes, and chloride ions. Shifts in Pb and Zn speciation suggest decreased mobility, influencing plant availability, though a fraction of free Zn^{2+} ions remained available to plants. Similarly, the proportion of free Cd^{2+} ions in Technosol S2T13–25 raises concerns about plant uptake risk, and the occurrence of $Cd(SO_4)$ and $Cd(SO_4)_2^{2-}$ suggests limited changes in Cd speciation compared to untreated soil.

Arsenic speciation shifted towards less toxic forms ($HAsO_4^{2-}$) due to increased pH and oxygenation, thereby contributing to improved soil health. Oxidized forms of As(V) prevailed in the soil solution, aligning with positive and high measured values of Eh. Initially, As existed in the untreated mine soil in nearly equal distribution as arsenous acid (H_3AsO_4) and dihydrogen arsenate ($H_2AsO_4^-$). However, the treatment induced a significant shift towards the dominance of hydrogen arsenate ($HAsO_4^{2-}$), with a slightly higher proportion of dihydrogen arsenate ions in S2T13–25 compared to S2T8–25. The rise in soil pH and maintenance of an oxygenated environment enhanced the prevalence of $HAsO_4^{2-}$, which is typically less mobile than H_3AsO_4 and $H_2AsO_4^-$, and much less toxic than arsenite species (Yamauchi and Fowler, 1994).

Substantial changes in chemical speciation, particularly of Al, Cu, and As, and the saturation status of the soil solution indicate that Technosol treatment effectively transformed soil pore water chemistry. Reduced dissolution potential of metal-bearing minerals may contribute to improving soil health by minimizing the release of potentially toxic contaminants bound to such phases. Ultimately, these modifications may enhance nutrient cycling and availability, aligning with the goal of mitigating trace element toxicity and fostering overall soil conditions for plant growth.

3.3. Effects of waste amendments on plant establishment and growth

Mine soils pose significant obstacles to conventional direct sowing practices due to their inherently challenging environmental conditions (e.g. Arenas-Lago et al., 2022; Carvalho et al., 2022; Mourinha et al., 2022), including elevated trace element content, acidic pH, and poor nutrient availability. These factors impede the establishment of sustainable plant populations, leading to limited success with direct sowing methods. As a result, alternative approaches such as the transplantation of pre-treated seedlings in controlled environments have shown promising potential in revegetating abandoned mine lands (Fernández-Caliani et al., 2021). Additionally, hydroseeding techniques have been used to enhance vegetation cover on slopes of waste rock piles (Madejón et al., 2021). To address these challenges, our study intentionally adopted a germination test in seedbeds as a preliminary step before transplanting into pots. This approach aimed to evaluate seed viability and initial growth, given the adverse soil conditions and potential limitations of direct sowing. The validity of this strategy is supported by findings from previous studies that have employed similar germination tests (e.g. Rodríguez-Vila et al., 2014, 2016; Baragaño et al., 2021).

The germination assay conducted on *B. juncea,* assessing seed viability and the suitability of the Technosols for seedling establishment, yielded distinct outcomes. As expected, seeds in the untreated mine soil failed to germinate due to various constraints for plant life, including strong acidity, nutrient scarcity, high pollution load, and contaminant phytotoxicity. It is noteworthy that, this Fe-rich acidic soil at the mine site is currently barren due to severe degradation (Fernández-Landero et al., 2023). In contrast to the untreated soil, germination and seedling growth of *B. juncea* were observed in Technosols. The seeds sown on Technosols successfully hydrated, sprouted and developed fully expanded cotyledons within a week. Seeds were deemed to have germinated when the emerged radicle reached at least 3 mm in length (ISTA, 2005). Thus, the percentages of seed germination varied across treatments (Fig. 5a): untreated mine soil (0 %), Technosol S2T13–25 (56.7 %), Technosol S2T8–25 (86.7 %), and mulch control (90 %).

Fig. 6 illustrates the evolution of *B. juncea* plants during the four-month pot trial. All seedlings transferred to pots filled with Technosols S2T8–25 and S2T13–25 developed true leaves after a week, but remarkable differences were observed between the treatments in terms of plant establishment and vegetative growth. In Technosol S2T8–25, all plants survived until week 11, with four persisting by week 12 (Fig. 5b). By the end of the experiment, two plants were still thriving, yielding a 40 % survival rate, which was comparable to the seedlings in the mulched control pot. This suggests the success of waste amendments in promoting plant adaptation and resilience. The plants grew to an average maximum height of 5.7 cm during weeks 7 and 8, maintaining a stable height of 4.5–5 cm until the end of the observation period (Fig. 5c). The height of the plant after four month of growth in the mulched control pot was 8.5 cm. *B. juncea* displayed leaves with an alternate arrangement, elongated shapes, and serrated margins. The leaf count per pot (Fig. 5d) varied from 19 (week 5) to 6 (week 16), while in the mulched reference pot it ranged between 23 (weeks 10 and 11) and 4 (week 16).

In Technosol S2T13–25, one out of the initially planted five plants died at the early seedling stage (80 % survival rate). By week 7, only one plant remained, accounting for a 20 % survival rate, and by week 12 all plants died, indicating a reduced capacity for *B. juncea* to thrive in this Technosol. These plants attained an average peak height of 3.1 cm during weeks 4 and 5. Beyond week 7, a distinct inhibition in plant growth became apparent by reduced height and leaf expansion. The decline in growth can be traced to the demise of larger plants, shedding mature leaves, and the emergence of smaller leaves that failed to reach previous heights. The leaf count per pot peaked at 14 in week 4. Compared to plants in the mulch control pot, *B. juncea* in Technosol S2T13–25 showed stress-related morpho-physiological effects, including stunted growth, development of small leaves, delayed maturity, and foliar chlorosis, resembling symptoms of nutrient deficiency and metal stress (Chandra and Keshavkant, 2021; Kumar et al., 2021).

The results clearly establish Technosol S2T8–25, which combines 60 % WCS and 40 % WSS, as the superior choice for fostering the growth of *B. juncea*. This conclusion is supported by a higher survival rate, greater average height, and a more consistent leaf count observed in this Technosol compared to Technosol S2T13–25 (*t*-test, $p < 0.05$). Plants grown in Technosol S2T8–25 also exhibited healthy growth characteristics, while those in Technosol S2T13–25 displayed signs of stress. The higher concentration of potentially toxic elements in the pore water of Technosol S2T13–25 (t-test, $p < 0.05$) may account for the reduced survival rate, stunted growth, and chlorosis observed in plants grown in this Technosol. In contrast, Technosol S2T8–25 showed a significantly lower concentration of potentially toxic elements and a higher concentration of Ca and bicarbonate ions in the pore water of (t-test, $p < 0.035$). By neutralizing acidity, the addition of WSS not only mitigated the potential risk of metal toxicity but also increased the availability of Ca and other essential nutrients, suggesting that the chemical environment of Technosol S2T8–25 was more conducive to plant growth and resilience.

However, larger-scale field trials may be necessary to assess Technosols under more realistic conditions. The effectiveness of Technosols may vary depending on the plant species being grown. Studies with a wider range of plant species are needed to fully understand the range of potential applications for Technosols.

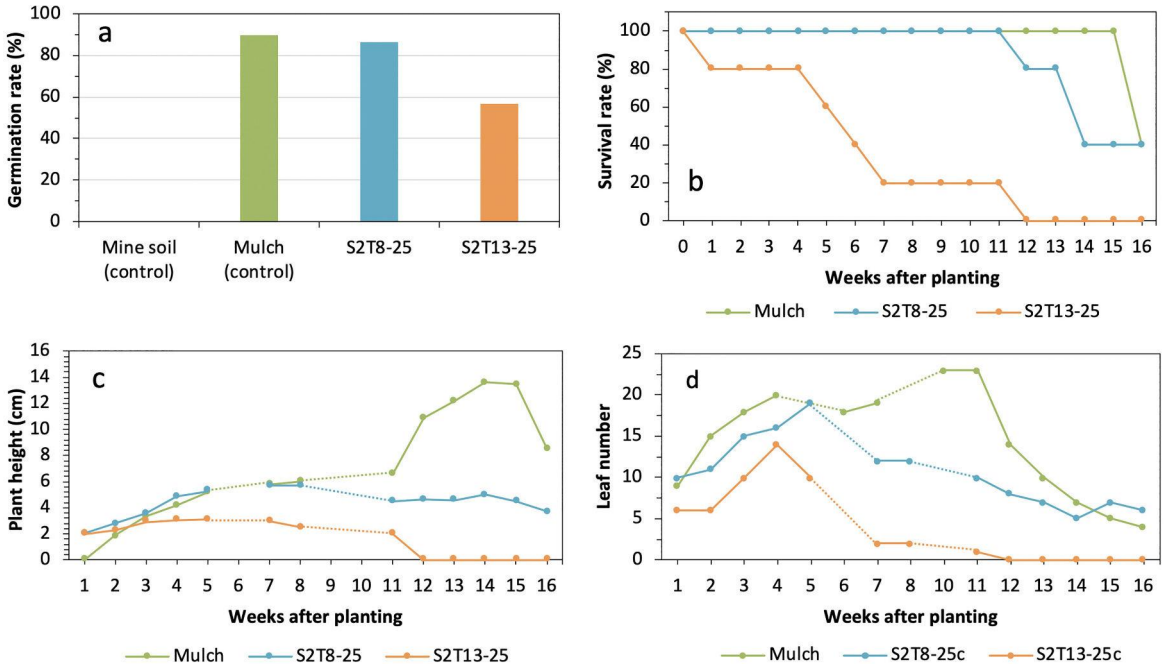

Fig. 5. Temporal dynamics of essential *Brassica juncea* plant parameters in formulated Technosols and control settings: (a) seed germination rate; (b) survival rate; (c) plant height; and (d) leaf number.

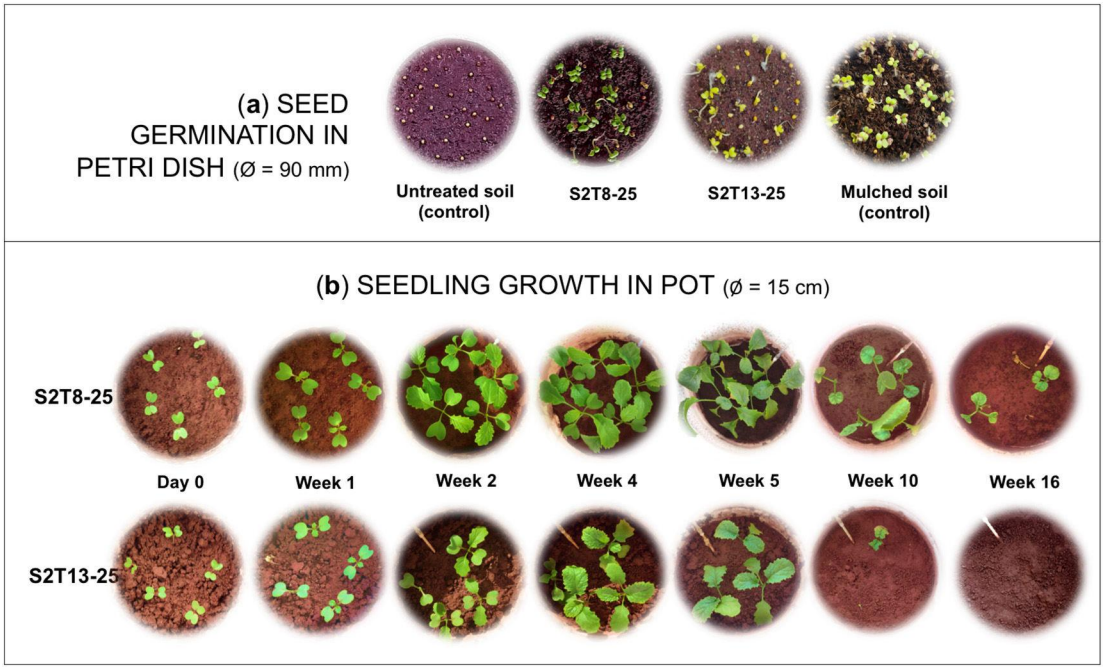

Fig. 6. Visual comparison of *Brassica juncea* outcomes in terms of: (a) seed germination assay; and (b) seedling growth in pots.

3.4. Potential for plant growth in Martian-like soil

The barren and harsh conditions of the Fe-rich acidic soil at the Rio Tinto site mirror challenges faced by plants in Martian soil simulants, marked by limited nutrient availability and potential toxicity. An examination of the red mine soil from the Rio Tinto Mars analog site reveals significant constraints to vegetation establishment, including: strong acidity, lack or deficiency of organic matter and essential nutrients, soil salinity due to high soluble sulfate content, and elevated concentrations of metallic cations dissolved in the soil solution. This complex interplay of acidic conditions, heightened trace element and sulfate levels, and nutrient deficiencies creates an inhospitable environment for plant growth, requiring a remediation strategy to overcome such limitations for successful germination and seedling growth.

The results of the germination assay indicate promising potential for *B. juncea* establishment and growth in Technosols compared to untreated mine soil. The failure of seeds to germinate in the mine soil underscores its hostile conditions. Plant growth and trace element availability were highly influenced by soil pH, as observed in soils contaminated with pyrite sludge (Clemente et al., 2005). Aluminum,

considered a potential growth-limiting factor in acidic environments, causes rhizotoxicity by inhibiting nutrient transportation (Chandra and Keshavkant, 2021). On Mars soil simulants, many germinated plants died or remained stunted due to low pH and the presence of free Al^{3+} ions (Wamelink et al., 2014).

In contrast, Technosols, notably S2T8–25, demonstrated substantial improvement, with 87 % germination rate, showcasing the effects of waste amendments on overcoming soil constraints. The subsequent pot experiment further confirmed the positive impact of waste amendments on supporting *B. juncea* growth by enhancing soil conditions. Successful germination, plant survival, and plant growth in Technosol S2T8–25 underlines the effectiveness of the Technosol construction approach in creating a conducive environment for plant establishment. The development of true leaves, coupled with a considerable survival rate and stable plant height, indicates improved soil fertility achieved through waste amendment addition. While the organic matter and assimilable P and K provided by WCS enhanced soil fertility, conditioner amendments, notably WSS, not only contributed effective acid neutralization capacity through base cation leaching, but also increased the availability of Ca, Mg, K, and Na to plants.

Positive outcomes in Technosol S2T8–25 highlight the potential of waste amendments for long-term buffering against acidification, improving soil fertility, and immobilizing contaminants, thus contributing to a more hospitable environment for plant growth. The waste amendment combining 60 % WCS and 40 % WSS proved the most effective, resulting in *B. juncea* grown with the highest biomass. However, Technosol S2T13–25 posed challenges in plant adaptation and growth, as indicated by the reduced survival rate, suggesting a need for further refinement in waste amendment composition to optimize plant growth. The observed growth inhibition, characterized by a decline in height and leaf expansion, emphasizes the importance of tailoring waste amendments to specific soil conditions.

In summary, the findings support the hypothesis that waste amendments in Technosols can address the factors limiting plant growth in Martian-like soil, such as the Fe-rich acidic mine soils of Rio Tinto. Overall, the success of Technosols in remediating challenging mine soils and supporting plant growth in Martian-like soils suggests their potential to transform extreme environments into habitable and productive spaces. Nevertheless, the variability in results between Technosols implies that the composition and characteristics of the amendments require careful consideration. The observed differences provide valuable insights into the complex interplay between waste amendments and soil-plant interactions, guiding future efforts in sustainable mine land reclamation.

4. Conclusions

This study delved into the complex and dynamic interactions among mine soil, waste amendments, soil water chemistry, and plant responses to assess the efficacy of the Technosol-based approach in revegetating iron-rich acidic mine soils, such as those at the Rio Tinto Mars analog site. The acidic and heavily polluted soil pore water posed challenges to plant growth, but the synergistic effects of waste amendments successfully stabilized contaminants and supported plant growth. The treatment not only alleviated acidity but also reduced trace element concentrations to environmentally sustainable levels, supplying essential nutrients for plant development. Copper removal from the soil solution occurred through precipitation reactions, while the immobilization of As and other trace elements likely took place through adsorption onto or co-precipitation with newly formed Fe oxyhydroxides and Al hydroxides. Predicted changes in aqueous chemical speciation indicated effective modification of soil pore water chemistry, reducing trace element toxicity and mitigating environmental risks.

Pot experiment with *B. juncea* showcased plant adaptability and resilience under stressful soil conditions, offering valuable insights into potential challenges and strategies for plant growth in Martian soil simulants. While positive impact on seed germination and seedling growth was evident, differential responses between Technosols emphasize the importance of optimizing waste amendment composition achieve optimal plant growth. Acknowledging hurdles like long-term performance and site-specific considerations, results suggest Technosols as a promising avenue for assisted natural remediation in managing similar mining-contaminated soils. Finally, to validate the approach and ensure lasting stability in immobilized contaminants and sustained plant life under actual field conditions, further research and field trials would be justified.

Supplementary data to this article can be found online at https://doi.org/10.1016/j.scitotenv.2024.171217.

CRediT authorship contribution statement

Juan Carlos Fernández-Caliani: Writing – review & editing, Writing – original draft, Visualization, Validation, Supervision, Project administration, Methodology, Investigation, Funding acquisition, Conceptualization. **Sandra Fernández-Landero:** Writing – review & editing, Visualization, Software, Resources, Investigation, Formal analysis, Data curation. **María Inmaculada Giráldez:** Writing – review & editing, Validation, Supervision, Software, Resources, Methodology, Investigation, Formal analysis, Data curation. **Pablo J. Hidalgo:** Writing – review & editing, Validation, Supervision, Methodology, Investigation, Funding acquisition, Formal analysis. **Emilio Morales:** Writing – review & editing, Validation, Software, Methodology, Investigation, Formal analysis.

Declaration of competing interest

Juan Carlos Fernandez-Caliani reports financial support, equipment, drugs, or supplies, and travel were provided by Regional Government of Andalusia (Spain). Juan Carlos Fernandez-Caliani reports equipment, drugs, or supplies and travel were provided by DSM Soluciones Medioambientales. Pablo J. Hidalgo reports financial support provided by EU project 101071300 Sustainable Horizons. If there are other authors, they declare that they have no known competing financial interests or personal relationships that could have appeared to influence the work reported in this paper.

Data availability

Data will be made available on request.

Acknowledgments

This research received financial support from the Regional Government of Andalusia (Spain) and the European Regional Development Fund Andalusia 2014–2020 under Project P-18-TP-3503, in partnership with DSM Soluciones Medioambientales. It was also funded by EU project 101071300 Sustainable Horizons (HORIZON). We express our gratitude to Nereida Pascual, Lourdes Vales, and Alicia Rodríguez (DSM, Centro Ambiental de Nerva) for their invaluable assistance in collecting waste samples and providing essential information about the waste materials. Funding for open access charge: Universidad de Huelva / CBUA.

References

Allison, J.D., Brown, D.S., Novo-Gradac, J., 1999. MINTEQA2/PRODEAFA2, a geochemical assessment model for environmental systems. In: User Manual Supplement for Version 4.0. US EPA, NERL, Athens, Georgia.

Amils, R., González-Toril, E., Fernández-Remolar, D., Gómez, F., Aguilera, A., Rodríguez, N., Malki, M., García-Moyano, A., Fairén, A.G., De la Fuente, V., Sanz, J. L., 2007. Extreme environments as Mars terrestrial analogs: the Rio Tinto case. Planet. Space Sci. 55, 370–381.

Amils, R., Fernández-Remolar, D., IPBSL Team, 2014. Río Tinto: a geochemical and mineralogical terrestrial analogue of Mars. Life 4, 511–534.

Arenas-Lago, D., Carvalho, L.C., Santos, E.S., Abreu, M.M., 2022. Influence of seed source and soil contamination on ecophysiological responses of *Lavandula pedunculata* in rehabilitation of mining areas. Plants 11, 1.
Asensio, V., Florido, F.G., Ruiz, F., Perlatti, F., Otero, X.L., Oliveira, D.P., Ferreira, T.O., 2019. The potential of a Technosol and tropical native trees for reclamation of copper-polluted soils. Chemosphere 220, 892–899.
Baragaño, D., Gallego, J.L.R., Forján, R., 2021. Comparison of the effectiveness of biochar vs. magnesite amendments to immobilize metals and restore a polluted soil. Environ. Geochem. Health 43, 5053–5064.
Basta, N.T., McGowen, S.L., 2004. Evaluation of chemical immobilization treatments for reducing heavy metal transport in a smelter-contaminated soil. Environ. Pollut. 127, 73–82.
Bigham, J.M., Schwertmann, U., Carlson, L., Skinner, H.C.W., Fitzpatrick, R.W., 1992. Mineralogy of precipitates formed by the biogeochemical oxidation of Fe(II) in mine drainage. In: Biomineralization Processes of Iron and Manganese, Catena, suppl. 21, pp. 219–232.
Bigham, J.M., Schwertmann, U., Traina, S.J., Winland, R.L., Wolf, M., 1996. Schwertmannite and the chemical modeling of iron in acid sulfate waters. Geochim. Cosmochim. Acta 60, 2111–2121.
Bojórquez-Quintal, E., Escalante-Magaña, C., Echevarría-Machado, I., Martínez-Estévez, M., 2017. Aluminum, a friend or foe of higher plants in acid soils. Front. Plant Sci. 8, 1767.
Bolan, N., Kunhikrishnan, A., Thangarajanan, R., Kumpiene, J., Park, J., Makino, T., Kirkhamg, M.B., Scheckel, K., 2014. Remediation of heavy metal(loid)s contaminated soils – to mobilize or to immobilize? J. Hazard. Mater. 266, 141–166.
Bothe, J.V., Brown, P.W., 1999. Arsenic immobilization by calcium arsenate formation. Environ. Sci. Technol. 33, 3806–3811.
Caporale, A.G., Palladino, M., De Pascale, S., Duri, L.G., Rouphael, Y., Adamo, P.J., 2023. How to make the lunar and Martian soils suitable for food production - assessing the changes after manure addition and implications for plant growth. J. Environ. Manag. 325 (Part A), 116455.
Carabante, I., Grahn, M., Holmgren, A., Kumpiene, J., Hedlund, J., 2009. Adsorption of As(V) on iron oxide nanoparticle films studied by in situ ATR-FTIR spectroscopy. Colloid Surface A 346, 106–113.
Carlson, L., Bigham, J.M., Schwertmann, U., Kyek, A., Wagner, F., 2002. Scavenging of As from acid mine drainage by schwertmannite and ferrihydrite: a comparison with synthetic analogues. Environ. Sci. Technol. 36, 1712–1719.
Carvalho, L.C., Santos, E.S., Saraiva, J.A., Magalhães, M.C.F., Macías, F., Abreu, M.M., 2022. The potential of *Cistus salviifolius* L. to phytostabilize gossan mine wastes amended with ash and organic residues. Plants 11, 588.
Chandra, J., Keshavkant, S., 2021. Mechanisms underlying the phytotoxicity and genotoxicity of aluminum and their alleviation strategies: a review. Chemosphere 278, 130384.
Chevrier, V., Mathé, P.E., 2007. Mineralogy and evolution of the surface of Mars: a review. Planet. Space Sci. 55, 289–314.
Clemente, R., Walker, D.J., Bernal, M.P., 2005. Uptake of heavy metals and as by *Brassica juncea* grown in a contaminated soil in Aznalcóllar (Spain): the effect of soil amendments. Environ. Pollut. 138, 46–58.
Clemente, R., Dickinson, N.M., Lepp, N.W., 2008. Mobility of metals and metalloids in a multi-element contaminated soil 20 years after cessation of the pollution source activity. Environ. Pollut. 155, 254–261.
Dassanayake, K.B., Jayasinghe, G.Y., Surapaneni, A., Hetherington, C., 2015. A review on alum sludge reuse with special reference to agricultural applications and future challenges. Waste Manag. 38, 321–335.
Edwards, H.G.M., Vandenabeele, P., Jorge-Villar, S.E., Carter, E.A., Rull, F., Hargreaves, M.D., 2007. The Rio Tinto Mars analogue site: an extremophilic Raman spectroscopic study. Spectrochim. Acta A Mol. Biomol. Spectrosc. 68, 1133–1137.
Eichler, A., Hadland, N., Pickett, D., Masaitis, D., Handy, D., Perez, A., Batcheldor, D., Wheeler, B., Palmer, A., 2021. Challenging the agricultural viability of martian regolith simulants. Icarus 354, 114022.
Fernández-Caliani, J.C., Barba-Brioso, C., 2010. Metal immobilization in hazardous contaminated minesoils after marble slurry waste application. A field assessment at the Tharsis mining district (Spain). J. Hazard. Mater. 181, 817–826.
Fernández-Caliani, J.C., Barba-Brioso, C., Pérez-López, R., 2008. Long-term interaction of wollastonite with acid mine water and effects on arsenic and metal removal. Appl. Geochim. 23, 1288–1298.
Fernández-Caliani, J.C., Giráldez, M.I., Waken, W.H., Del Río, Z.M., Córdoba, F., 2021. Soil quality changes in an Iberian pyrite mine site 15 years after land reclamation. Catena 206, 105538.
Fernández-Caliani, J.C., Giráldez, M.I., Fernández-Landero, S., Barba-Brioso, C., Morales, E., 2022. Long-term sustainability of marble waste sludge in reducing soil acidity and heavy metal release in a contaminated mine Technosol. Appl. Sci. 12, 6998.
Fernández-Landero, S., Fernández-Caliani, J.C., Giráldez, I., Morales, E., Barba-Brioso, C., González, I., 2023. Soil contaminated with hazardous waste materials at Rio Tinto mine (Spain) is a persistent secondary source of acid and heavy metals to the environment. Minerals 13, 456.
Fernández-Remolar, D., Gómez-Elvira, J., Gómez, F., Sebastian, E., Martín, J., Manfredi, J.A., Torres, J., González-Kesler, C., Amils, R., 2004. The Tinto River, an extreme acidic environment under control of iron, as an analog of the Terra Meridiani hematite site of Mars. Planet. Space Sci. 52, 239–248.
Fernández-Remolar, D., Morris, R.V., Gruener, J.E., Amils, R., Knoll, A.H., 2005. The Rio Tinto Basin, Spain: mineralogy, sedimentary geobiology and implications for interpretation of outcrop rocks of Meridiani Planum, Mars. Earth Planet. Sci. Lett. 240, 149–167.
Forján, R., Rodríguez-Vila, A., Covelo, E.F., 2018. Using compost and technosol combined with biochar and *Brassica juncea* L. to decrease the bioavailable metal concentration in soil from a copper mine settling pond. Environ. Sci. Pollut. Res. 25, 1294–1305.
Galán, E., Fernández-Caliani, J.C., González, I., Aparicio, P., Romero, A., 2008. Influence of geological setting on geochemical baselines of trace elements in soils. Application to soils of south-West Spain. J. Geochem. Explor. 98, 89–106.
Hartley, W., Lepp, N.W., 2008. Remediation of arsenic contaminated soils by iron-oxide application, evaluated in terms of plant productivity, arsenic and phytotoxic metal uptake. Sci. Total Environ. 390, 35–44.
Hartley, W., Edwards, R., Lepp, N.W., 2004. Arsenic and heavy metal mobility in iron oxide-amended contaminated soils as evaluated by short- and long-term leaching tests. Environ. Pollut. 131, 495–504.
Hazen, R.M., Downs, R.T., Morrison, S.M., Tutolo, B.M., Blake, D.F., Bristow, T.F., Chipera, S.J., McSween, H.Y., Ming, D., Morris, R.V., Rampe, E.B., Thorpe, M.T., Treiman, A.H., Tu, V.M., Vaniman, D.T., 2023. On the diversity and formation modes of Martian minerals. JGR Planets 128, e2023JE007865.
Houba, V.J.G., Lexmond, Th.M., Novozamsky, I., van der Lee, J.J., 1996. State of the art and future developments in soil analysis for bioavailability assessment. Sci. Total Environ. 178, 21–28.
Hudson-Edwards, K.A., Schell, C., Macklin, M.G., 1999. Mineralogy and geochemistry of alluvium contaminated by metal mining in the Rio Tinto area, Southwest Spain. Appl. Geochim. 14, 1015–1030.
ISTA, International Seed Testing Association, 2005. International Rules for Seed Testing. International Seed Testing Association, Zurich, Switzerland.
Junta de Andalucía, 2015. Decreto 18/2015, de 27 de enero, por el que se aprueba el reglamento que regula el régimen aplicable a los suelos contaminados. BOJA 38, 28–64.
Kalis, E.J.J., Temminghoff, E.J.M., Town, R.M., Unsworth, E.R., van Riemsdijk, W.H., 2008. Relationship between metal speciation in soil solution and metal adsorption at the root surface of ryegrass. J. Environ. Qual. 37, 2221–2231.
Kasiviswanathan, P., Swanner, E.D., Halverson, L.J., Vijayapalani, P., 2022. Farming on Mars: treatment of basaltic regolith soil and briny water simulants sustains plant growth. PLoS One 17, e0272209.
Klingelhöfer, G., Morris, R.V., Bernhardt, B., Schröder, C., Rodionov, D.S., De Souza Jr., P.A., Yen, A., Gellert, R., Evlanov, E.N., Zubkov, B., Foh, J., Bonnes, U., Kankeleit, E., Gütlich, P., Ming, D.W., Renz, F., Wdowiak, T., Squyres, S.W., Arvidson, R.E., 2004. Jarosite and hematite at Meridiani Planum from Opportunity's Mössbauer spectrometer. Science 306, 1740–1745.
Kumar, V., Pandita, S., Sidhu, G.P.S., Sharma, A., Khanna, K., Kaur, P., Bali, A.S., Setia, R., 2021. Copper bioavailability, uptake, toxicity and tolerance in plants: a comprehensive review. Chemosphere 262, 127810.
Kumpiene, J., Lagerkvist, A., Maurice, C., 2008. Stabilization of As, Cr, Cu, Pb and Zn in soil using amendments – a review. Waste Manag. 215–225.
Kumpiene, J., Carabante, I., Kasiuliene, A., Austruy, A., Mench, M., 2021. Long-term stability of arsenic in iron amended contaminated soil. Environ. Pollut. 269, 116017.
Madejón, P., Caro-Moreno, D., Navarro-Fernández, C.M., Rossini-Oliva, S., Marañón, T., 2021. Rehabilitation of waste rock piles: impact of acid drainage on potential toxicity by trace elements in plants and soil. J. Environ. Manag. 280, 111848.
Marlow, J.J., Martins, Z., Sephton, M.A., 2008. Mars on earth: soil analogues for future Mars missions. Astron. Geophys. 49, 2.20–2.23.
Medina, F.J., Manzano, A., Kamal, K.Y., Ciska, M., Herranz, R., 2021. Plants in space: Novel physiological challenges and adaptation mechanisms. In: Lüttge, U., Cánovas, F.M., Risueño, M.C., Leuschner, C., Pretzsch, H. (Eds.), Progress in Botany, Springer Nature, 83, pp. 1–36.
Mourinha, C., Palma, P., Alexandre, C., Cruz, N., Rodrigues, S.M., Alvarenga, P., 2022. Potentially toxic elements' contamination of soils affected by mining activities in the Portuguese sector of the Iberian Pyrite Belt and optional remediation actions: a review. Environments 9, 11.
Murad, E., Rojík, P., 2003. Iron-rich precipitates in a mine drainage environment: influence of pH on mineralogy. Amer. Min. 88, 1915–1918.
Navarro-González, R., Rainey, F.A., Molina, P., Bagaley, D.R., Hollen, B.J., De la Rosa, J., Small, A.M., Quinn, R.C., Grunthaner, F.J., Cáceres, L., Gomez-Silva, B., McKay, C.P., 2003. Mars-like soils in the Atacama Desert, Chile, and the dry limit of microbial life. Science 302, 1018–1021.
Nelson, D.W., Sommers, L.E., 1996. Total carbon, organic carbon, and organic matter. In: Sparks, D.L., Page, A.L., Helmke, P.A., Loeppert, R.H. (Eds.), Methods of Soil Analysis, SSSA Book Series, Madison, Part 3, pp. 961–1010.
Nguyen, M.D., Thomas, M., Moon, E.M., Nicholas, A., Milne, N.A., 2022. Beneficial reuse of water treatment sludge in the context of circular economy. Environ. Technol. Innov. 28, 102651.
Nolan, A.L., McLaughlin, M.J., Mason, S.D., 2003. Chemical speciation of Zn, Cd, Cu, and Pb in pore waters of agricultural and contaminated soils using Donnan dialysis. Environ. Sci. Technol. 37, 90–98.
Novo, L.A.B., González, L., 2014. Germination and early growth of *Brassica juncea* in copper mine tailings amended with Technosol and compost. Sci. World J. 506392, 1–9.
Novo, L.A.B., Covelo, E.F., González, L., 2013. The potential of *Salvia verbenaca* for phytoremediation of copper mine tailings amended with technosol and compost. Water Air Soil Pollut. 224, 1513.
Olsen, S.R., Sommers, L.E., 1982. Phosphorus. In: Page, A.L. (Ed.), Methods of Soil Analysis Part 2 Chemical and Microbiological Properties. American Society of Agronomy, Soil Science Society of America, Madison, pp. 403–430.
Parkhurst, D.L., Appelo, C.A.J., 2013. Description of input and examples for PHREEQC version 3—a computer program for speciation, batch-reaction, one-dimensional

transport, and inverse geochemical calculations. US Geol. Surv. Tech. Methods 6, 497.
Pérez-Esteban, J., Escolástico, C., Moliner, A., Masaguer, A., Ruiz-Fernández, J., 2014. Phytostabilization of metals in mine soils using *Brassica juncea* in combination with organic amendments. Plant Soil 377, 97–109.
Peters, G.H., Abbey, W., Bearman, G.H., Mungas, G.S., Smith, J.A., Anderson, R.C., Douglas, S., Beegle, L.W., 2008. Mojave Mars simulant – characterization of a new geologic Mars analog. Icarus 197, 470–479.
Porter, S.K., Scheckel, K.G., Impellitteri, C.A., Ryan, J.A., 2004. Toxic metals in the environment: thermodynamic considerations for possible immobilisation strategies for Pb, Cd, As, and Hg. Crit. Rev. Environ. Sci. Technol. 34, 495–604.
Preston, L.J., Dartnell, L.R., 2014. Planetary habitability: lessons learned from terrestrial analogues. Int. J. Astrobiol. 13, 81–98.
Rodríguez-Vila, A., Covelo, E.F., Forján, R., Asensio, V., 2014. Phytoremediating a copper mine soil with *Brassica juncea* L., compost and biochar. Environ. Sci. Pollut. Res. 21, 11293–11304.
Rodríguez-Vila, A., Asensio, V., Forján, R., Covelo, E.F., 2016. Assessing the influence of technosol and biochar amendments combined with *Brassica juncea* L. on the fractionation of Cu, Ni, Pb and Zn in a polluted mine soil. J. Soils Sediments 16, 339–348.
Romero, A., González, I., Galán, E., 2006. Estimation of potential pollution of waste mining dumps at Peña del Hierro (Pyrite Belt, SW Spain) as a base for future mitigation actions. Appl. Geochem. 21, 1093–1108.
Ross, S.M., 1996. Sources and forms of potentially toxic metals in soil-plant systems. In: Ross, S.M. (Ed.), Toxic Metals in Soil-Plant Systems. Wiley, Chichester, pp. 3–25.
Ruiz, F., Safanelli, J.L., Perlatti, F., Cherubin, M.R., Demattê, J.A.M., Cerri, C.E., Otero, X.L., Rumpel, C., Ferreira, T.O., 2023. Constructing soils for climate-smart mining. Commun. Earth Environ. 4, 219.
Salkield, L.U., 1987. A Technical History of the Rio Tinto Mines: Some Notes on Exploitation from Pre-Phoenician Times to the 1950s. London, UK, The Institution of Mining and Metallurgy, p. 116.
Sánchez-España, J., Yusta, I., Díez-Ercilla, M., 2011. Schwertmannite and hydrobasaluminite: a re-evaluation of their solubility and control on the iron and aluminium concentration in acidic pit lakes. Appl. Geochem. 26, 1752–1774.
Sánchez-García, L., Fernández-Martínez, M.A., Moreno-Paz, M., Carrizo, D., García-Villadangos, M., Manchado, J.M., Stoker, C.R., Glass, B., Parro, V., 2020. Simulating Mars drilling mission for searching for jife: ground-truthing lipids and other complex microbial biomarkers in the iron-sulfur rich Rio Tinto analog. Astrobiology 20, 1029–1047.
Santos, E.S., Abreu, M.M., Macías, F., de Varennes, A., 2016. Chemical quality of leachates and enzymatic activities in Technosols with gossan and sulfide wastes from the São Domingos mine. J. Soils Sediments 16, 1366–1382.
Santos, E.S., Abreu, M.M., Macías, F., 2019. Rehabilitation of mining areas through integrated biotechnological approach: Technosols derived from organic/inorganic wastes and autochthonous plant development. Chemosphere 224, 765–775.
Schad, P., 2018. Technosols in the world Reference Base for soil resources – history and definitions. Soil Sci. Plant Nutr. 64, 138–144.
Séré, G., Schwartz, C., Ouvrard, S., Sauvage, C., Renat, J.C., Morel, J.L., 2008. Soil construction: a step for ecological reclamation of derelict lands. J. Soils Sediments 8, 130–136.
Sherman, D.M., Randall, S.R., 2003. Surface complexation of arsenic(V) to iron(III) (hydr)oxides: structural mechanism from ab initio molecular geometries and EXAFS spectroscopy. Geochim. Cosmochim. Acta 67, 4223–4230.
Siddique, R., Kaur, G., Rajor, A., 2010. Waste foundry sand and its leachate characteristics. Resour. Conserv. Recycl. 54, 1027–1036.
Silverstone, S., Nelson, M., Alling, A., Allen, J.P., 2005. Soil and crop management experiments in the laboratory biosphere: an analogue system for the Mars on earth® facility. Adv. Space Res. 35, 1544–1551.
Squyres, S.W., Grotzinger, J.P., Arvidson, R.E., Bell, J.F., Calvin, W., Christensen, P.R., Clark, B.C., Crisp, J.A., Farrand, W.H., Herkenhoff, K.E., Johnson, J.R., Klingelhöfer, G., Knoll, A.H., McLennan, S.M., McSween Jr., H.Y., Morris, R.V., Rice Jr., J.W., Rieder, R., Soderblom, L.A., 2004. In situ evidence for an ancient aqueous environment at Meridiani Planum, Mars. Science 306, 1709–1714.
Tordoff, G.M., Baker, A.J.M., Willis, A.J., 2000. Current approaches to the revegetation and reclamation of metalliferous mine wastes. Chemosphere 41, 219–228.
USGS, 2023. Mineral Commodity Summaries 2023. U.S. Geological Survey, p. 210. https://doi.org/10.3133/mcs2023.
Valdivia-Silva, J.E., Karouia, F., Navarro-González, R., Mckay, C., 2016. Microorganisms, organic carbon, and their relationship with oxidant activity in hyper-arid Mars-like soils: implications for soil habitability. Palaios 31, 1–9.
Wamelink, G.W.W., Frissel, J.Y., Krijnen, W.H.J., Verwoert, M.R., Goedhart, P.W., 2014. Can plants grow on Mars and the Moon: a growth experiment on Mars and Moon soil simulants. PLoS One 9, e103138.
Watkinson, A.D., Lock, A.S., Beckett, P.J., Spiers, G., 2017. Developing manufactured soils from industrial by-products for use as growth substrates in mine reclamation. Restor. Ecol. 25, 587–594.
Waychunas, G.A., Rea, B.A., Fuller, C.C., Davies, J.A., 1993. Surface chemistry of ferrihydrite: part 1. EXAFS studies of the geometry of coprecipitated and adsorbed arsenate. Geochim. Cosmochim. Acta 57, 2251–2269.
Weiler, J., Firpo, B.A., Schneider, I.A.H., 2020. Technosol as an integrated management tool for turning urban and coal mining waste into a resource. Miner. Eng. 147, 106179.
Yamauchi, H., Fowler, B.A., 1994. Toxicity and metabolism of inorganic and methylated arsenicals. In: Nriagu, J.O. (Ed.), Arsenic in the Environment, Part II: Human Health and Ecosystem Effects. Wiley, New York, pp. 35–43.
Yang, M., Lu, C., Quan, X., Chang, H., Cao, D., Wu, Q., 2022. Steel slag as a potential adsorbent for efficient removal of Fe(II) from simulated acid mine drainage: adsorption performance and mechanism. Environ. Sci. Pollut. Res. 29, 25639–25650.
Yao, F.X., Macías, F., Santesteban, A., Virgel, S., Blanco, F., Jiang, X., Camps-Arbestain, M., 2009a. Influence of the acid buffering capacity of different types of Technosols on the chemistry of their leachates. Chemosphere 74, 250–258.
Yao, F.X., Macías, F., Virgel, S., Blanco, F., Jiang, X., Camps-Arbestain, M., 2009b. Chemical changes in heavy metals in the leachates from Technosols. Chemosphere 77, 29–35.
Yesares, L., González-Jiménez, J.M., Jiménez-Cantizano, F.A., González-Pérez, I., Caro-Moreno, D., Sánchez, I.M., 2023. Unveiling high-tech metals in roasted pyrite wastes from the Iberian Pyrite Belt, SW Spain. Sustainability 15, 12081.

Supplementary Figure S1

Bar charts comparing pH and electrical conductivity values measured in the pore water of Technosols, and line charts depicting the values of the untreated mine soil (control). Error bars denote the standard deviation of the means (n = 3).

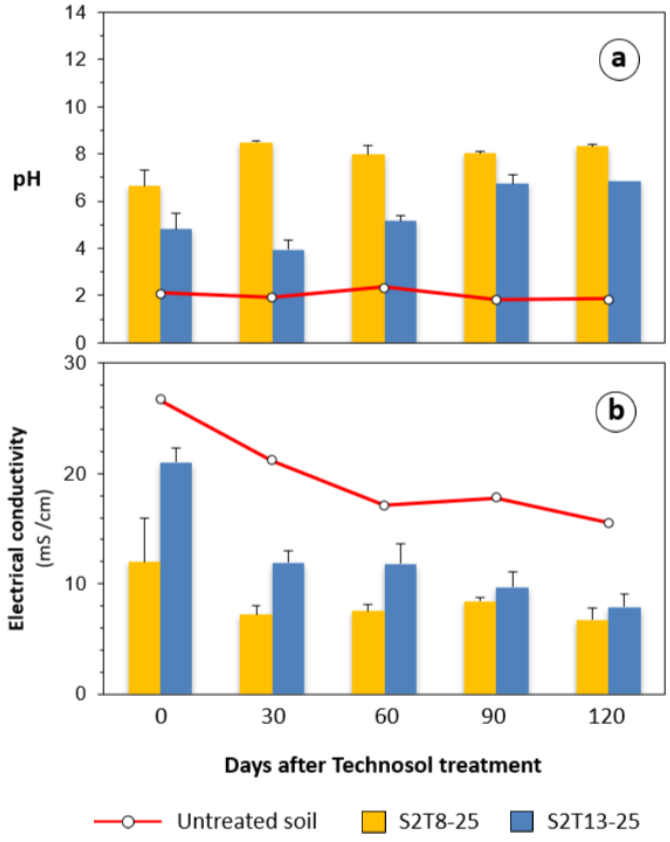

Supplementary Figure S2

Bar charts comparing anion concentrations between the untreated mine soil (control) and the Technosols S2T8-25 and S2T13-25. Error bars denote the standard deviation of the means (n = 3).

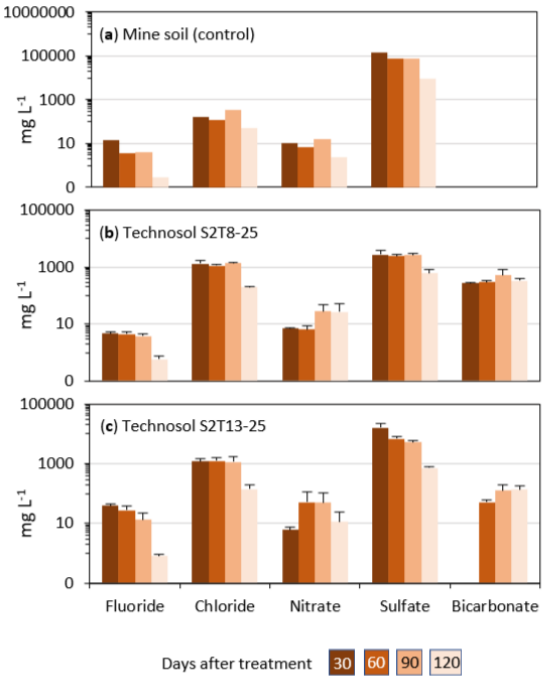

Supplementary Table S1

pH and Eh values of the leaching solutions and concentrations of potentially toxic trace elements leached from the Technosols

Technosol	pH	Eh	Cr	Ni	Cu	Zn	As	Cd	Sb	Pb
Unit	–	mV	mg kg^{-1}	mg kg^{-1}	mg kg^{-1}	mg kg^{-1}	mg kg^{-1}	mg kg^{-1}	mg kg^{-1}	mg kg^{-1}
PH-2 (Control)	2.50	747	0.011	<0.016	2.29	4.94	0.034	0.018	0.012	26.16
S2T8-10	9.49	297	0.015	<0.016	0.19	<0.05	0.057	0.001	0.037	0.034
S2T8-25	9.64	248	0.018	<0.016	0.17	<0.05	0.028	<0.001	0.017	0.051
S2T8-50	10.0	230	0.033	0.027	0.24	<0.05	0.042	<0.001	0.015	0.030
S2T11-10	6.47	344	<0.004	0.118	0.06	0.60	0.011	0.009	0.011	5.750
S2T11-25	7.29	282	<0.004	0.062	0.05	<0.05	0.006	0.002	0.009	0.227
S2T11-50	8.27	321	<0.004	0.038	0.14	<0.05	0.012	<0.001	0.016	0.053
S2T13-25	9.44	287	0.004	<0.016	0.42	<0.05	0.026	<0.001	<0.004	<0.017

SUPPLEMENTARY TABLE S2. SOIL PORE WATER CHEMISTRY

Unit	µg/L	µg/L	µg/L	µg/L	µg/L	µg/L	µg/L	µg/L	µg/L	µg/L	mg/L	mg/L	mg/L	mg/L
Day 30	Cr	Co	Ni	Cu	Zn	As	Se	Cd	Sb	Pb	Al	Ca	Fe	K
Control (PH2)	1609	14644	2662	481112	789893	38269	2204	2800	180,1	66,90	5203	314,8	25001	<0,10
S2T8-25a	1,187	4,759	15,61	360,7	35,69	32,71	91,58	0,595	2,662	1,000	0,54	535,5	<0,10	3,43
S2T8-25b	1,161	5,174	15,29	599,7	25,11	56,92	160,5	0,301	3,432	0,249	0,83	1008	<0,10	5,31
S2T8-25c	1,266	5,554	14,14	674,4	26,77	85,43	224,9	0,564	4,112	0,451	0,86	1259	<0,10	4,83
S2T13-25a	41,68	873,9	476,3	8672	34488	86,04	160,0	97,37	15,66	26,06	160,7	601,3	253,9	12,61
S2T13-25b	46,17	968,1	494,9	9515	37260	163,2	129,3	97,61	12,39	19,18	186,0	586,3	338,6	9,215
S2T13-25c	187,3	1977	746,4	32025	90270	1070	142,6	248,5	6,379	32,41	590,8	568,6	1156	9,607
Day 60	Cr	Co	Ni	Cu	Zn	As	Se	Cd	Sb	Pb	Al	Ca	Fe	K
Control (PH2)	1249	5239	2003	149234	241358	14402	1011	961,9	199,9	102,1	1623	115,1	7084	<0,10
S2T8-25a	1,352	4,866	14,29	618,4	233,24	64,80	147,4	0,292	5,161	0,279	0,74	1025	<0,10	5,70
S2T8-25b	1,554	5,675	15,84	697,5	73,75	69,24	170,6	0,234	5,143	0,230	0,81	1043	<0,10	6,16
S2T8-25c	1,668	6,406	20,03	754,2	2581	76,15	215,7	0,324	5,386	0,551	0,79	1005	<0,10	4,07
S2T13-25a	21,80	535,5	323,0	2806	19239	14,67	116,6	51,93	5,952	6,481	42,79	620,1	55,31	11,92
S2T13-25b	6,462	307,6	212,6	1919	9595	14,91	112,6	24,64	6,028	3,447	15,66	622,8	13,13	9,595
S2T13-25c	177,1	215,8	186,5	1404	5916	32,87	140,8	20,18	4,359	3,089	6,017	614,0	12,94	10,23
Day 90	Cr	Co	Ni	Cu	Zn	As	Se	Cd	Sb	Pb	Al	Ca	Fe	K
Control (PH2)	776,3	6451	985,3	207962	331271	3967	927,4	1298	99,28	177,5	2707	198,8	9642	<0,10
S2T8-25a	3,160	7,729	21,67	674,6	144,6	68,59	156,0	0,332	5,342	0,339	<0,10	984,3	<0,10	8,119
S2T8-25b	2,285	6,870	14,36	469,8	760,0	59,86	124,8	0,258	4,322	0,362	<0,10	1058	<0,10	8,788
S2T8-25c	1,871	6,150	14,01	504,4	174,6	44,32	132,8	0,262	4,239	0,733	<0,10	908,9	<0,10	4,002
S2T13-25a	82,48	265,2	200,7	1498	8472	16,62	65,21	36,22	3,285	5,351	<0,10	664,3	12,41	11,43
S2T13-25b	2,279	148,4	110,9	844,1	5474	19,29	69,05	16,77	3,212	5,312	2,584	664,9	<0,10	10,40
S2T13-25c	207,8	44,81	106,1	770,1	1206	28,27	106,3	7,620	4,299	4,715	0,974	666,8	2,525	15,16
Day 120	Cr	Co	Ni	Cu	Zn	As	Se	Cd	Sb	Pb	Al	Ca	Fe	K
Control (PH2)	7486	3805	6524	125648	206936	5384	1158	837,8	78,12	193,1	1483	122,4	5456	<0,10
S2T8-25a	1,466	3,848	9,613	276,9	142,6	28,83	62,75	0,192	3,813	0,240	<0,10	885,5	<0,10	7,443
S2T8-25b	1,420	2,669	6,304	190,1	342,1	14,72	49,12	0,198	2,991	0,260	1,326	901,6	<0,10	8,594
S2T8-25c	1,611	3,787	9,785	310,3	76,25	22,73	100,3	0,261	3,763	0,237	<0,10	940,2	<0,10	8,278
S2T13-25a	55,04	135,3	104,7	699,3	3528	9,111	51,43	18,86	2,279	8,079	4,146	693,2	1,124	10,08
S2T13-25b	12,32	71,52	59,08	360,3	1740	6,076	51,85	7,974	2,167	4,759	2,132	675,1	<0,10	8,963
S2T13-25c	250,3	18,18	27,31	319,9	516,8	8,278	74,69	4,086	2,411	3,588	1,322	680,2	1,420	13,90

SUPPLEMENTARY TABLE S2. SOIL PORE WATER CHEMISTRY

Unit	mg/L	mg/L	mg/L	mg/L	mg/L	mg/L	mg/L	mg/L	mg/L
Day 30	Mg	Mn	Na	S	Fluoride	Chloride	Nitrate	Sulfate	bicarbonate
Control (PH2)	759,6	41,44	32,34	27687	14,10	161,8	10,59	82948	0,0
S2T8-25a	303,0	0,18	66,14	491,0	5,540	1282	7,253	1471	256,3
S2T8-25b	565,8	0,24	111,4	939,7	3,888	1002	6,428	2815	280,7
S2T8-25c	675,2	0,17	116,2	949,5	4,656	1737	7,192	2845	292,9
S2T13-25a	2708	76,84	290,8	3846	43,96	1479	7,048	11521	0,00
S2T13-25b	1871	73,82	182,7	3057	33,24	977,8	7,280	9159	0,00
S2T13-25c	1845	114,7	186,7	4299	38,83	1065	4,240	12878	0,00
Day 60	Mg	Mn	Na	S	Fluoride	Chloride	Nitrate	Sulfate	bicarbonate
Control (PH2)	249,0	13,02	47,32	8660	3,510	124,0	6,500	25943	0,00
S2T8-25a	562,4	0,19	125,3	891,6	5,544	1101	6,008	2671	262,4
S2T8-25b	729,1	0,21	142,6	954,4	4,184	1254	8,676	2859	329,5
S2T8-25c	916,6	0,26	148,6	1070	3,368	1007	4,668	3206	280,7
S2T13-25a	1794	58,62	254,9	2442	40,06	1071	26,78	7316	36,61
S2T13-25b	1957	43,43	257,3	2592	22,12	1021	5,272	7765	61,02
S2T13-25c	2286	26,57	328,8	2782	20,26	1606	121,9	8334	54,92
Day 90	Mg	Mn	Na	S	Fluoride	Chloride	Nitrate	Sulfate	bicarbonate
Control (PH2)	444,3	22,14	55,85	12890	4,167	352,6	15,13	38617	0
S2T8-25a	814,7	<0,10	229,9	972,8	4,700	1339	17,77	2915	866,4
S2T8-25b	821,0	<0,10	241,6	901,3	3,496	1509	49,14	2700	323,4
S2T8-25c	908,6	<0,10	214,1	1058	3,300	1295	16,83	3170	390,5
S2T13-25a	1062	25,80	245,8	1651	24,12	759,5	16,58	4947	61,02
S2T13-25b	1496	21,15	275,8	2028	7,488	941,3	22,31	6076	109,8
S2T13-25c	2140	9,204	467,5	2440	9,007	1771	111,3	7311	207,5
Day 120	Mg	Mn	Na	S	Fluoride	Chloride	Nitrate	Sulfate	bicarbonate
Control (PH2)	285,9	14,03	63,00	<0.1	0,287	49,4	2,48	22487	0
S2T8-25a	544,8	0,195	173,6	856,2	0,785	182	5,69	2565	341,7
S2T8-25b	459,2	<0,10	176,3	776,8	0,511	184	52,6	2327	268,5
S2T8-25c	821,9	<0,10	260,6	989,7	0,421	214	21,7	2965	378,3
S2T13-25a	940,1	16,78	252,7	1405	0,935	126	3,44	4210	97,63
S2T13-25b	959,6	11,59	206,9	1446	0,650	99,1	3,61	4333	122,0
S2T13-25c	1368	4,666	392,2	1712	0,871	200	27,0	5129	183,1

4.5. Desarrollo eficiente de plantas en suelos afectados por drenaje ácido de mina mediante ensayos en macetas con enmiendas a base de residuos

Basado en el artículo:

Successful plant growth in acid mine drainage-impacted soil using pot-based experiments with waste amendments. Land Degradation & Development 922 (2024) 171217

La contaminación del suelo por DAM representa uno de los mayores problemas ambientales asociados con la actividad minera. La combinación de una acidez extrema y altas concentraciones de metales pesados crea un ambiente edáfico hostil, que imposibilita o limita severamente el crecimiento vegetal. Los suelos afectados por DAM pierden su capacidad natural para retener contaminantes, convirtiéndose en fuentes de lixiviados ácidos con altas concentraciones de hierro, sulfatos y EPT, lo que supone un peligro para los ecosistemas y la salud humana.

El objetivo principal de este estudio fue evaluar la efectividad de los tecnosuelos, elaborados con una combinación estratégica de residuos orgánicos (lodos de la clarificación del agua bruta) e inorgánicos (escorias siderúrgicas y yeso rojo), para mitigar los efectos perjudiciales del DAM en las propiedades del suelo, la química del agua intersticial y el crecimiento de las plantas. El estudio se basó en un experimento controlado en macetas, permitiendo una evaluación precisa de los cambios en el suelo (procedente de Tharsis) y la respuesta de la planta *Brassica juncea*.

4.5.1. Resultados más relevantes y discusión

El suelo afectado por DAM en Tharsis presenta condiciones extremadamente ácidas (pH 2,7–3,4), hiperoxidantes (706 mV) y deficiencias severas de nutrientes esenciales (N y P). Además, se encuentra fuertemente contaminado por Pb (hasta 1610 mg kg^{-1}), Cu (hasta 942 mg kg^{-1}) y As (hasta 783 mg kg^{-1}), superando ampliamente

los niveles genéricos de referencia. La principal fuente de acidez es la jarosita, que representa entre el 86 % y el 90 % de la capacidad de generación ácida total del suelo. Según la prueba estática NAG, la generación neta de acidez fue de 296 mmol H^+ kg^{-1}.

De las doce formulaciones diseñadas, las que mostraron mejores resultados en los ensayos de lixiviación (S3T2-25, S3T8-5 y S3T11-35) fueron seleccionadas para evaluar su eficacia en un ensayo en macetas con plantación de *B. juncea*. A continuación, se resumen los principales resultados del experimento:

- **Neutralización de la acidez.** Se observó una notable neutralización de la acidez neta del suelo, lo que elevó el pH de niveles extremadamente ácidos a valores ligeramente alcalinos o moderadamente ácidos (pH 8,0; 7,7; y 5,3, respectivamente).

- **Inmovilización de elementos potencialmente tóxicos**. Se redujeron las concentraciones de EPT en el agua de poro. Las disminuciones de Al y Fe se atribuyeron a la formación de hidróxidos y ferrihidrita, mientras que Cu, Zn, Cd y Pb fueron inmovilizados mediante procesos de adsorción, coprecipitación y/o precipitación de metales en nuevas fases minerales. Sin embargo, se detectó un incremento de movilidad de As y Sb en los tecnosuelos alcalinos, probablemente debido a la mayor disponibilidad de sitios con carga negativa, aunque las concentraciones se mantuvieron por debajo de niveles críticos. En contraste, S3T11-35, con condiciones más ácida, logró inmovilizar eficazmente estos metaloides.

- **Aumento de la disponibilidad de nutrientes.** Las enmiendas de RNP, especialmente el lodo de la clarificación del agua, mejoraron la disponibilidad de nutrientes, con concentraciones de nitrato que aumentaron hasta 417 mg L^{-1}, lo que fue determinante para el establecimiento de las plántulas.

- **Crecimiento exitoso de las plantas.** El ensayo de germinación con *B. juncea* reflejó una mejora sustancial en el establecimiento vegetal en los tecnosuelos frente al suelo minero sin tratar. El análisis de componentes principales mostró una fuerte correlación entre los indicadores de salud de las plantas

(tasa de supervivencia, altura de la planta, número de hojas, producción de biomasa) y la mejora de los parámetros del agua de poro del suelo (pH, EPT, aluminio, calcio, bicarbonato y nitrato).

- **Formulación óptima.** Las formulaciones S3T2-25 y S3T8-5 fueron las que presentaron mayores tasas de supervivencia, un crecimiento vigoroso, una elevada producción de biomasa aérea y, además, alcanzaron la floración. Por el contrario, S3T11-35 mostró baja supervivencia, síntomas de estrés vegetal y un escaso desarrollo, indicando su limitada idoneidad para la revegetación.

4.5.2. Conclusiones

El estudio experimental en macetas demostró que los tecnosuelos formulados con RNP tienen un alto potencial para revegetar suelos afectados por DAM. Los tecnosuelos modificaron profundamente la química del agua del suelo, reduciendo la toxicidad de metales y metaloides, mejorando la disponibilidad de nutrientes y creando condiciones más favorables para el crecimiento vegetal.

La inmovilización de los EPT se atribuye una combinación de varios mecanismos: a) formación de nuevas fases minerales estables por precipitación, y b) adsorción sobre oxihidróxidos de hierro y aluminio. La modelización de la especiación acuosa mostró cambios significativos hacia formas menos tóxicas de aluminio y EPT, favoreciendo la germinación y el crecimiento de *Brassica juncea* en los tecnosuelos más eficaces (S3T2-25 y S3T8-5), con una alta tasa de supervivencia y producción de biomasa. El análisis de componentes principales confirmó la relación positiva entre la mejora de la calidad del suelo y la respuesta vegetal.

Los resultados de esta investigación tienen amplias implicaciones para la recuperación de espacios degradados por la minería, ofreciendo un ejemplo de revegetación exitosa y de producción de biomasa en entornos que antes eran estériles.

Received: 8 April 2024 | Revised: 22 May 2024 | Accepted: 30 May 2024

DOI: 10.1002/ldr.5211

RESEARCH ARTICLE

WILEY

Successful plant growth in acid mine drainage-impacted soil using pot-based experiments with waste amendments

Sandra Fernández-Landero[1] | Juan Carlos Fernández-Caliani[1] | María Inmaculada Giráldez[2] | Pablo J. Hidalgo[3] | Emilio Morales[2]

[1]Department of Earth Sciences, University of Huelva, Huelva, Spain

[2]Department of Chemistry, University of Huelva, Huelva, Spain

[3]Department of Integrated Sciences, RENSMA, University of Huelva, Huelva, Spain

Correspondence
Sandra Fernández-Landero, Department of Earth Sciences, University of Huelva, Campus El Carmen, s/n., Huelva 21071, Spain.
Email: sandra.fernandez@dct.uhu.es

Funding information
Regional Government of Andalusia; European Regional Development Fund; EU project 101071300 Sustainable Horizons (HORIZON); Horizon Europe Framework Programme

Abstract

This paper addresses the challenge of remediating soil impacted by acid mine drainage (AMD) using an innovative and sustainable Technosol-based approach to stabilize soil and facilitate vegetation recovery. The study assessed the effectiveness of Technosols made from recycled organic (water clarification sludge) and inorganic (siderurgical slags and red gypsum) wastes in mitigating the detrimental effects of AMD on soil properties, pore water chemistry, and plant growth through a 4-month pot experiment. Technosols significantly improved soil health by neutralizing net acidity (296 mmol H^+ kg^{-1}), raising pH levels from extremely acidic (3.3) to mildly alkaline (7.7–8.0), and limiting the mobility of potentially toxic elements (PTEs). Dissolved Cu and Zn concentrations dropped from 80.21 and 72.08 mg L^{-1}, respectively, to below 1 mg L^{-1} by the end of the monitoring period. The experiment identified several concomitant mechanisms of PTE retention, such as decreased dissolution of metal-bearing minerals, precipitation reactions and adsorption onto Fe and Al (oxy)hydroxides. Aqueous speciation modelling indicated a decline in toxic metal forms (e.g. Al^{3+}, $AlSO_4^+$, Cu^{2+}, Zn^{2+} and $H_2AsO_4^-$) in soil pore water after treatment, thus reducing phytotoxicity. Additionally, waste amendments enhanced nutrient availability, with nitrate concentrations reaching up to 417 mg L^{-1}, supporting seed germination and seedling establishment. The most effective Technosol, combining water treatment sludge and white steel slag (60:40 w/w), enabled robust growth of *Brassica juncea*. Principal component analysis showed a strong correlation between healthy plant responses (survival rate, plant height, leaf number, biomass production) and improved soil pore water parameters (pH, PTEs, aluminium, calcium, bicarbonate and nitrate ions), highlighting the benefits of waste amendments. These findings underscore the potential of waste-derived Technosols in stabilizing AMD-impacted soils and promoting thriving plant growth. However, further validation in field trials with diverse plant species is recommended for real-world applications.

KEYWORDS
Brassica juncea, ecological restoration, non-hazardous wastes, soil reclamation, Technosol, Tharsis mines

1 | INTRODUCTION

Acid mine drainage (AMD) poses a significant environmental challenge arising from the exposure of sulphide minerals, notably pyrite, to air and water (Blowes et al., 2003; Nordstrom, 2011). Sulphide oxidative weathering leads to acid generation and the release of potentially toxic elements (PTEs) into the surrounding environment. This process raises substantial concerns in abandoned mine sites (Fernández-Caliani et al., 2009, 2019; Madejón et al., 2011, 2021), causing severe soil degradation, hindering plant growth, and posing health risks. AMD-affected soils often lose their natural resilience and capacity to immobilize harmful contaminants, becoming sources of acidic leachates with high levels of iron, sulphate and PTEs (Fernández-Landero et al., 2023). Sustainable remediation strategies are essential to mitigate contaminant dispersion and protect ecosystems and human health (Niu & Lin, 2021) in these environmental significant soils.

Remediating AMD-impacted soils is a complex, site-specific process that requires effective techniques for chemical stabilization and ecological restoration. In situ treatment involves using soil amendments to reduce contaminant leachability and bioavailability (Adriano et al., 2004; Bolan et al., 2014; Fernández-Caliani et al., 2021; Kumpiene et al., 2008; Palansooriya et al., 2020; Uchimiya et al., 2010). Common amendments for acidic, metal-contaminated soils include liming materials combined with organic additives (compost, biochar or manure) to improve soil fertility, enhance water holding capacity and stimulate microbial activity.

In recent years, Technosols (technogenic soils) have emerged as a promising alternative to traditional post-mining reclamation methods (Aguilar-Garrido et al., 2023; Ahirwal & Maiti, 2018; Arán et al., 2022; Asensio et al., 2013; Fernández-Caliani et al., 2024; Santos et al., 2019; Watkinson et al., 2017). This innovative approach involves blending non-hazardous waste materials or by-products with contaminated soil to create environments conducive to vegetation recovery and no-food biomass production. The benefits include cost-effectiveness, reduced resource reliance and waste reuse, aligning with circular economy principles (Ruiz et al., 2020; Séré et al., 2008; Watkinson et al., 2017; Weiler et al., 2020).

After achieving soil stabilization, ecological restoration becomes feasible, playing a crucial role in maintaining ecological balance and preventing further erosion. Selecting plant species depends on various factors like soil conditions, hydrology and climate, especially in AMD-impacted regions where species resilient to high PTE levels are needed (Barba-Brioso et al., 2023; Tordoff et al., 2000). Certain metal-tolerant plants, such as Indian mustard (*Brassica juncea* L.), are valuable for phytostabilization and soil revegetation (Forján et al., 2018; Lai et al., 2008; Novo & González, 2014; Pérez-Esteban et al., 2014) due to their ability to absorb and accumulate PTEs without succumbing to toxicity. Moreover, *B. juncea* serves as a reliable indicator of metal phytoavailability (Clemente et al., 2005), aiding in the assessment of remediation effectiveness.

This study explores the potential of using strategic combinations of non-hazardous waste materials to create sustainable Technosols for supporting plant growth in AMD-degraded landscapes. Through controlled pot-scale experiments, the research aimed to (1) elucidate the specific challenges associated with AMD-impacted soils; (2) evaluate the effectiveness of waste amendments in mitigating the adverse effects of AMD and (3) unveil how Technosols influence the establishment of *B. juncea* in remediated soil and the capacity to support healthy vegetation growth. By addressing these objectives, the study seeks to contribute to the development of sustainable practices for reclaiming AMD-affected soils and promoting broader ecological restoration efforts in post-mining landscapes.

2 | MATERIALS AND METHODS

2.1 | Mine soil and wastes used for Technosol construction

Soil samples were randomly collected from three locations within a barren area severely affected by AMD discharges (Fernández-Caliani et al., 2022; Fernández-Caliani & Barba-Brioso, 2010; Madejón et al., 2011) in the Tharsis mining district, Spain (Figure 1). Composite samples from the topsoil layer (0–20 cm) were air-dried, gently disaggregated and sieved to 2 mm. A portion of the sieved sample was then finely ground and passed through a 63 μm sieve for subsequent chemical analysis.

The AMD-affected soil was analysed for particle size, pH, redox potential (Eh), electrical conductivity, mineral composition, carbon and sulphur content, nitrogen and phosphorous levels, cation exchange capacity, exchangeable cations and total concentrations of major and PTEs. Acid soil drainage prediction was accomplished using an acid–base accounting approach, which assesses the total acid generating and neutralizing capacities through the acid–base accounting equation (Ahern et al., 2004): Net acid generation (NAG) = potential sulphidic acidity (PSA) + titratable actual acidity (TAA) + retained acidity − acid neutralizing capacity.

Four locally sourced waste materials were selected for Technosol construction: (1) water clarification sludge (WCS), (2) white slag from steel production (WSS), (3) furnace slag from iron production (FIS) and (4) red gypsum (RGY), a by-product of titanium dioxide pigment production. These materials, classified as non-hazardous wastes according to the European Waste Catalogue (Commission Decision 2000/532/EC), served specific roles in Technosol formulation, with WCS contributing organic nutrients (Dassanayake et al., 2015), WSS and FIS acting as liming agents (Yang et al., 2022) and RGY potentially improving soil structure while reducing contaminant mobilization (Peacock & Rimmer, 2000; Rodríguez-Jordá et al., 2010). These materials are currently landfilled 60 km from the reclamation site.

2.2 | Experimental setup

The experimental setup aimed to tailor waste amendments to reclaim AMD-impacted soils and promote vegetation restoration. Waste materials were characterized for specific surface area, pH, Eh,

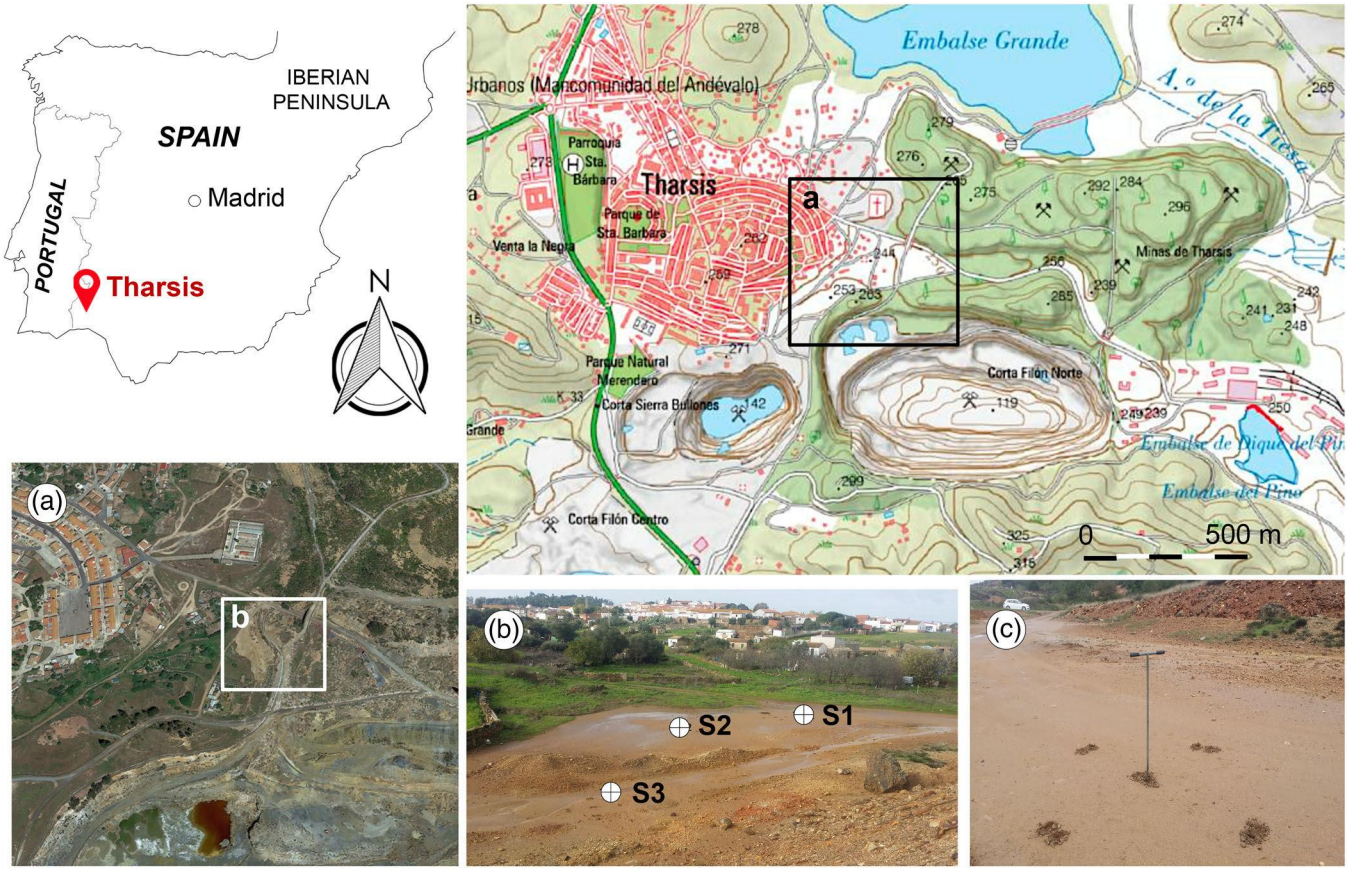

FIGURE 1 Location map of the Tharsis mining area showing: (a) an aerial view of the study area, (b) the sampling sites and (c) the soil sampling technique using a hand auger. [Colour figure can be viewed at wileyonlinelibrary.com]

TABLE 1 Composition of Technosols derived from water clarification sludge (WCS), white steel slag (WSS), furnace iron slag (FIS), and red gypsum (RGY).

Technosol	Technosol composition		Waste amendment	Amendment composition		
Control	100% mine soil (S3)		–	–		
S3T2-10	90% S3	10% WA1	WA1	60% WCS	20% WSS	20% RGY
S3T2-25	75% S3	25% WA1	WA1	60% WCS	20% WSS	20% RGY
S3T2-50	50% S3	50% WA1	WA1	60% WCS	20% WSS	20% RGY
S3T5-25	75% S3	25% WA2	WA2	60% WCS	20% FIS	20% RGY
S3T5-40	60% S3	40% WA2	WA2	60% WCS	20% FIS	20% RGY
S3T5-50	50% S3	50% WA2	WA2	60% WCS	20% FIS	20% RGY
S3T8-5	95% S3	5% WA3	WA3	60% WCS	40% WSS	–
S3T8-25	75% S3	25% WA3	WA3	60% WCS	40% WSS	–
S3T8-50	50% S3	50% WA3	WA3	60% WCS	40% WSS	–
S3T11-25	75% S3	25% WA4	WA4	60% WCS	40% FIS	–
S3T11-35	65% S3	35% WA4	WA4	60% WCS	40% FIS	–
S3T11-50	50% S3	50% WA4	WA4	60% WCS	40% FIS	–

Note: Mixing percentages are expressed in weight.

electrical conductivity, carbon content, nutrient levels and total concentrations of major and PTEs.

Soil amendments involved blending WCS, WSS, FIS and RGY waste materials in a 60:40 (w/w) ratio to achieve a balanced mixture of organic and inorganic components (Asensio et al., 2019; Santos et al., 2016; Yao et al., 2009). The waste amendments were mixed with mine soil at various rates (Table 1), with untreated mine soil (sample S3) serving as the control. The resulting Technosols

underwent leaching tests to assess leachability and guide optimal blend selection for planting.

Selected planting blends were homogenized, moistened with distilled water and equilibrated for 14 days at room temperature before being transferred to pots (15 cm depth and diameter) and planted with *B. juncea* for 4 months. Germination assays in 90 mm Petri dishes confirmed the viability of *B. juncea* seeds. The dishes were kept at room temperature under a 10–14 h day/night photoperiod and monitored daily for germination progress. Five seedlings with expanded cotyledons were transplanted into Technosol pots. Each treatment had three replicates, including negative (mine soil) and positive (mulch) controls. The pots were placed in a glasshouse environment with controlled temperature, humidity and light exposure, while regular irrigation was applied to maintain optimal soil moisture levels.

A 4-month pot trial monitored the soil solution chemistry in both Technosol and control pots. Soil solution was sampled monthly at maximum water holding capacity using Rhizon samplers (Clemente et al., 2008). The extracted solution was analysed for pH, electrical conductivity and total concentrations of major elements and PTEs. Plant health, growth and development were evaluated by monitoring survival rate, height, leaf number, flowering time and biomass production.

2.3 | Analytical procedures

Phase identification was conducted by X-ray diffraction (XRD) on a BRUKER D8-Advance diffractometer, using monochromatic CuKα radiation (40 kV, 30 mA). Selected particles were examined using field emission scanning electron microscopy (FESEM) with a JEOL JSM-IT500HR instrument operating at 20 kV, and were chemically analysed with an energy-dispersive X-ray spectrometer coupled to the FESEM. Grain-size distribution and specific surface area were determined using a Mastersizer 3000 laser diffraction analyser. For pH, Eh and electrical conductivity measurements, a 10 g soil sample was mixed with 25 mL of deionized water. Additional pH measurements were performed in 1 M KCl (1:2.5 m/v) and 30% H_2O_2 (1:20 m/v) suspensions, with H_2O_2 added until bubbling ceased (Urrutia et al., 1992).

PSA was determined by extracting pyrite sulphur (S_{pyr}) with hot 6 M HNO_3, following the ASTM D2492-02 standard test method for sulphate removal prior to pyrite extraction. The extracted S_{pyr} was quantified by inductively coupled plasma optical emission spectroscopy (ICP-OES) with an Agilent 5110 instrument and converted to PSA assuming complete pyrite oxidation, which releases two moles of protons per mole (Dold, 2017; Nordstrom, 1982).

TAA measured readily available acidity in the soil, considering soluble sulphates and exchangeable acid cations. This was achieved by titrating a 1 M KCl soil suspension with 0.1 M NaOH until reaching a pH endpoint of 7.0 (McElnea et al., 2002). The acidity retained in sparingly soluble hydroxy-sulphate minerals, like jarosite, was estimated by quantifying extractable sulphate sulphur (S_{jar}) using 0.2 M NH_4-oxalate. The extracted S_{jar} was analysed by ICP-OES and converted to equivalent acidity units (mmol H^+ kg^{-1}) based on the assumption that one mole of sulphur in jarosite releases 1.5 moles of protons (Dold, 2003).

A static NAG test assessed the overall acid-forming potential of the mine soil. This test mimics pyrite oxidation by reacting the soil with a 30% H_2O_2 solution while monitoring pH variations. The solution is then titrated with 0.1 M NaOH until reaching a neutral pH, accounting for any acid neutralizing minerals present in the soil (Monterroso & Macías, 1998).

Total carbon and nitrogen were determined via dry combustion using an ELTRA CHS-580A analyser. Plant-available phosphorus and assimilable potassium were extracted with 0.5 N $NaHCO_3$ (Olsen & Sommers, 1982) and 0.01 M $CaCl_2$ (Houba et al., 1996) respectively. Effective cation exchange capacity was assessed by leaching the soil with a 1 M NH_4Cl solution. The extracted base cations were analysed using flame atomic absorption spectroscopy, while exchangeable acid cations were measured through titration with 0.01 N NaOH.

Major and trace element contents in mine soil and waste samples were analysed by ICP-OES following a four-acid digestion method. Quality control measures ensured data accuracy, including reagent blanks, duplicates and certified reference materials (OREAS series). Element concentrations deviated from reference values by less than 10% relative standard deviation (RSD), with most elements showing excellent reproducibility (RSD below 5%).

A standardized leaching test (EN-12457-4) evaluated PTE mobilization from Technosols. Leachates were filtered (0.45 µm pore size), acidified, and analysed for major elements by ICP-OES, while PTE concentrations were measured by ICP mass spectrometry (Agilent 7700 ICP-MS). Quality control measures, including external calibration, replicates, blanks and analysis of SRM 1640a, ensured outstanding accuracy (SRM recovery within 5%) and precision (RSD below 10%). Nitrate, fluoride and chloride concentrations were determined using ion chromatography (Metrohm 883 Basic IC plus instrument), while bicarbonate content was measured via titration with 0.02 M HCl.

2.4 | Statistical analysis and geochemical modelling

Statistical analysis was performed using SPSS 27.0 to assess Technosol influence on soil pore water chemistry. Left-censored data were imputed as half of the detection limit, and replicate variability was quantified by standard errors. Differences between Technosol-based treatments and controls were assessed using Student's *t*-test and one-way ANOVA, preceded by Levene's test to confirm homogeneity of variance. All tests adopted a significance level of $p < 0.05$. Principal component analysis (PCA) explored relationships between soil pore water chemistry and plant responses.

The PHREEQC chemical equilibrium modelling software (Parkhurst & Appelo, 2013) was employed to predict the aqueous speciation of PTEs and determine mineral saturation states using Equation (1):

$$SI = \log (IAP/K_s) \quad (1)$$

where SI is the saturation index, IAP denotes the ion activity product and K_s represents the solubility product constant. A SI value of 0 indicates equilibrium solubility, positive values suggest oversaturation and potential precipitation, while negative values imply undersaturation and potential dissolution.

3 | RESULTS AND DISCUSSION

3.1 | Properties and constituents of the mine soil

The AMD-impacted soil exhibited loam texture, extremely acidic reaction (pH_{H_2O} 2.7–3.4), strongly oxidizing conditions (Eh = 706 mV) and moderate salinity. Similar pH values were obtained using a 1 M KCl solution, suggesting potential constraints for plant growth and microbial activity. XRD analysis identified quartz, mica, kaolinite and jarosite as the dominant soil minerals, with minor feldspars, gypsum and hematite. Importantly, the absence of carbonates indicates limited buffering capacity against further acidification.

The observed $pH_{H_2O_2}$ values aligned with the low S_{pyr} content (0.10%), resulting in relatively low PSA (65 mmol H^+ kg^{-1}) linked to the oxidation of mineral dust particles derived from nearby mine waste dumps (Chopin et al., 2003; Fernández-Caliani et al., 2013; Fernández-Caliani & Barba-Brioso, 2010). Low TAA values (57–87 mmol H^+ kg^{-1}) imply a limited capacity of the soil to generate acidity through the dissolution of readily soluble sulphate minerals and the release of acid cations from exchange sites.

Considerable differences between S_{total} and S_{pyr} levels denote the occurrence of sulphate minerals, primarily jarosite, as confirmed by XRD analysis. S_{jar} was the dominant form of sulphur, ranging from 1.70% to 2.53%, representing retained acidity released through slow jarosite hydrolysis, estimated at 797–1186 mmol H^+ kg^{-1}. This finding underscores the significance of jarosite as the main reservoir of acidity, accounting for 86%–90% of the total acid-generating capacity, and its role in predicting long-term acidification trends.

The H_2O_2-based static test revealed a mean NAG value of 296 mmol H^+ kg^{-1}, which reflects the net acid production, assuming simultaneous acid generation and acid neutralization reactions (Karlsson et al., 2018; Miller et al., 1997). This result is consistent with those from nearby Rio Tinto mine soils (Fernández-Landero et al., 2023), highlighting persistent acidity and limited acid neutralizing potential.

Mine soil analysis showed severe limitations in essential plant nutrients, including nitrogen (0.32%) and plant-available phosphorus (P_{Olsen} = 0.014%), aligning with observations from other regional mine soils (Alvarenga et al., 2022). The high prevalence of exchangeable acid cations (over 52% of effective cation exchange capacity) can further exacerbate nutrient deficiencies for plant uptake. Organic carbon content varied widely (0.2%–3.7%), with the higher values being likely due to the presence of carbonaceous shale fragments derived from nearby mine waste dumps.

As shown in Table 2, the AMD-impacted soil showed a distinctive geochemical signature characterized by relatively high levels of Fe (9.6%–11.0%) and Al (6.9%–7.3%), with smaller contributions from K and S. This elemental profile aligns with the mineralogical composition of the mine soil, reflecting the occurrence of jarosite, iron oxides and aluminosilicate minerals. A concerning aspect of the AMD impact was the consistently elevated levels of PTEs. Total concentrations of Pb (up to 1610 mg kg^{-1}), Cu (up to 942 mg kg^{-1}) and As (up to 783 mg kg^{-1}) exceeded regional baseline levels (Galán et al., 2008; Martín-Méndez et al., 2023) by one to two orders of magnitude, indicating severe multi-elemental contamination. Of particular concern is the surpassing of As concentrations beyond the screening level (40 mg kg^{-1}) set for industrial land use in southern Spain (Junta de Andalucía, 2015), indicating an unacceptable risk to potential receptors.

3.2 | Characterization of waste materials used as amendments

The tested waste materials (WCS, WSS, FIS and RGY) displayed diverse characteristics across particle size distribution, pH, electrical conductivity, agronomic properties and element concentrations (Table 3), reflecting their varied origins and compositions.

WCS exhibited a slightly acidic to near-neutral pH, low electrical conductivity, and a high organic carbon content (11.50%), making it suitable as an organic fertilizer. It boasts significant amounts of available phosphorus (16.7 mg kg^{-1}) and potassium (57.7 mg kg^{-1}), providing a source of essential nutrients. The observed high Al content (>10%) is attributed to aluminosilicate clay minerals and the use of Al-based coagulants during drinking water treatment. XRD analysis further revealed a diverse mineral assemblage encompassing quartz, feldspars, iron oxides and gypsum.

WSS showed exceptional alkalinity (pH_{H_2O} = 12.4), indicating its potential to counteract soil acidity, along with high electrical conductivity (7.27 mS cm^{-1}). FESEM-energy-dispersive X-ray spectrometer analysis revealed distinct calcium silicate phases, calcite and Mg oxides and aluminates. Despite lacking organic carbon, WSS compensates with remarkable levels of plant-available phosphorus (22.8 mg kg^{-1}) and potassium (151 mg kg^{-1}), serving as a valuable nutrient source. High contents of Ca (>10%) and Mg (6.67%) further enhance its potential as an alkaline soil amendment.

FIS displayed an alkaline pH_{H_2O} (10.0) and low electrical conductivity. It showed 1.70% total carbon, with 1.00% being organic carbon, and low total nitrogen content (0.09%). Moderate levels of available phosphorus (18.7 mg kg^{-1}) and potassium (56 mg kg^{-1}) further enhanced its potential as a soil amendment. Additionally, it exhibited a relatively high Fe content (7.56%) ascribed to iron-silicate phases. XRD analysis identified abundant quartz with minor anorthite and calcite.

RGY had a slightly alkaline pH_{H_2O} (7.76) and moderate electrical conductivity. It is composed mainly of gypsum with minor iron oxides, rutile, ilmenite and zircon. Despite its predominantly inorganic nature,

TABLE 2 Soil properties, acidity pools and chemical composition of mine soil samples.

	Mine soil samples (<2 mm fraction)				
Parameter	**S1**	**S2**	**S3**	**Mean**	**Std. dev.**
Color (dry)	10YR 6/4	10YR 6/3	10YR 6/4	–	–
Sand (%)	51.6	30.9	41.4	41.3	10.4
Silt (%)	41.4	56.9	47.1	48.5	7.8
Clay (%)	7.0	12.2	11.5	10.2	2.8
Electrical conductivity (mS cm^{-1})	3.59	1.94	2.02	2.52	0.93
Eh (mV)	656	694	767	706	56
pH_{H_2O}	3.4	3.2	2.7	3.09	0.39
pH_{KCl}	3.3	3.0	2.4	2.92	0.46
pH_{Ox}	2.7	2.6	2.3	2.5	0.2
Acidity (mmol H^+ kg^{-1})					
Potential sulphidic acidity	81	69	44	65	19
Titratable actual acidity	57	64	87	69	16
Retained acidity	1073	1186	797	1019	200
Total acid generation	1211	1319	928	1153	202
Net acid generation	417	281	189	296	115
S_{jar} (%)	2.29	2.53	1.70	2.17	0.43
S_{py} (%)	0.13	0.11	0.11	0.10	0.03
C_{inorg} (%)	0.0	0.1	0.2	0.1	0.1
C_{org} (%)	3.7	1.8	0.2	1.9	1.7
N_{total} (%)	0.50	0.34	0.10	0.32	0.20
P_{Olsen} (%)	0.027	0.013	0.001	0.014	0.013
Exchangeable cations (cmol$^+$ kg^{-1})					
Ca^{2+}	6.9	11.1	10.8	9.6	2.3
Mg^{2+}	4.7	3.2	3.0	3.6	0.9
Na^+	0.2	0.1	n.d.	0.1	0.1
K^+	n.d.	n.d.	n.d.	n.d.	n.d.
$H^+ + Al^{3+}$	19.4	14.3	10.6	14.8	4.4
Cation exchange capacity (cmol$^+$ kg^{-1})	31.2	28.8	24.5	28.2	3.4
Non-acid cation saturation (%)	37.7	50.3	56.7	48.2	9.7
Major element concentrations (wt %)					
Al	6.91	7.26	6.90	7.02	0.21
Ca	0.22	0.26	0.15	0.21	0.06
Fe	10.5	11.0	9.60	10.37	0.71
K	1.76	2.48	2.73	2.32	0.50
Mg	0.44	0.45	0.34	0.41	0.06
Mn	0.019	0.017	0.018	0.018	0.001
Na	0.40	0.54	0.49	0.48	0.07
Ti	0.31	0.38	0.43	0.37	0.06
S	2.25	2.44	1.93	2.21	0.26
P	0.835	0.333	0.048	0.045	0.398
Trace element concentrations (mg kg^{-1})					
As	714	556	783	684	116
Bi	14	12	10	12	2
Cd	0.7	0.4	0.5	0.53	0.15
Co	13	11	10	11.3	1.5

TABLE 2 (Continued)

Parameter	Mine soil samples (<2 mm fraction)				
	S1	S2	S3	Mean	Std. dev.
Cr	103	102	87	97	9
Cu	942	540	339	607	307
Ni	22	24	19	21.7	2.5
Pb	1610	1010	1200	1273	307
Sb	86	27	<5	56	44
Tl	<5	<5	<5	<5	<5
Zn	190	136	111	146	40

Abbreviation: n.d., not detected.

it provided some nutrient value with 130 mg kg^{-1} of assimilable potassium and 3 mg kg^{-1} of plant-available phosphorus. High levels of Ca and S (>10% each) are attributed to the abundance of gypsum, while the significant Fe content (5.39%) stems from iron oxides.

Although the overall PTE concentrations in these waste materials are generally lower than those observed in the AMD-impacted soil and adhere to Spanish legislation for Technosol formulation (ITR, 2008), elevated levels of Cu (294 mg in FIS) and Zn (315 mg kg^{-1} in RGY and 252 mg in WSS) may require careful consideration.

3.3 | Leachate quality

The leaching test provided valuable insights into the acidity/alkalinity and pollutant release of both mine soil and the tested waste amendments (WA1, WA2, WA3 and WA4). All waste amendments yielded alkaline leachates (Figure 2a), with WA1 and WA3 showing the highest alkalinity due to the incorporation of WSS as a liming material. Electrical conductivity ranged from 0.66 to 2.60 mS cm^{-1}, with RGY-bearing wastes (WA1 and WA2) registering the highest values. Leachate solutions revealed varying concentrations of diverse anions (Figure 2b), with sulphate particularly elevated (around 12,000 mg kg^{-1}) in WA1 and WA2 due to their gypsum content. Chloride levels ranged from 324 to 838 mg kg^{-1}, while nitrate concentrations varied between 124 and 230 mg kg^{-1}.

A significant concern when utilizing waste-derived amendments in agriculture and landscaping is the potential release of high levels of PTEs into the environment (Siddique et al., 2010). However, leachate analysis showed negligible concentrations of dissolved PTEs in the amendments, typically below 0.1 mg kg^{-1}. Conversely, the AMD-impacted soil produced highly acidic leachate (pH 2.8) with concerning levels of Cu (39.54 mg kg^{-1}) and Zn (22.66 mg kg^{-1}), while other PTEs remained below 1 mg kg^{-1}. These results indicate minimal leaching risk of contaminants, complying with Spanish regulations for safe Technosol construction (ITR, 2008).

The Technosol treatments effectively reduced the leaching of PTEs from the mine soil, particularly for Cu and Zn. Leaching of other divalent metals (Ni, Cd and Pb) was minimized to negligible or undetectable levels (Figure 2c). However, there was a slight increase in the leaching of As and Sb attributed to reduced anion adsorption onto soil particles under alkaline conditions (Bradl, 2004; Carabante et al., 2009; Fan et al., 2020). Importantly, despite this increase, the concentrations of leached As and Sb remained well below regulatory limits for Technosol construction (2 mg kg^{-1} for As and 0.7 mg kg^{-1} for Sb).

3.4 | Technosol pore water chemistry

Dissolved pore water PTE concentrations are a crucial indicator of environmental risk, revealing the fraction readily available for plant uptake (Clemente et al., 2008; Nolan et al., 2003). To gain insights into this, interstitial water from Technosols S3T2-25, S3T8-5 and S3T11-35 was analysed over a 4-month pot trial.

All Technosols displayed significantly higher pH values compared to the untreated control soil ($p < 0.002$) throughout the experiment (Figure S1). Technosols amended with WSS (S3T2-25 and S3T8-5) experienced a rapid and sustained increase in pore water pH, shifting from extremely acidic to mildly alkaline or near-neutral conditions. Conversely, Technosol S3T11-35, amended with FIS, demonstrated a less pronounced effect, remaining moderately acidic. These findings suggest that WSS holds significant promise for neutralizing net acidity. The strongly oxidizing state (Eh 712 mV) of the mine soil solution displayed a noteworthy shift towards less oxidizing conditions upon amendment application. The shift was most pronounced in Technosols S3T2-25 and S3T8-5, which reached moderately oxidizing states. In contrast, the untreated control soil maintained its highly oxidizing character throughout the experiment. The electrical conductivity of the pore water in the soil control exhibited a steady decline, stabilizing between 6.0 and 8.1 mS cm^{-1}. This decrease reflects the depletion of readily soluble sulphate salts through irrigation water leaching. However, Technosol treatments maintained consistent electrical conductivity ranges throughout the study period.

Technosols showed differential effects on the major element concentrations in the pore water (Figure 3). Waste amendments significantly reduced the levels of Al and Fe compared to the control soil

TABLE 3 Properties and chemical composition of the waste materials used as ingredients in Technosols.

		Waste materials (<2 mm fraction)			
Parameter	**Unit**	**WCS**	**WSS**	**FIS**	**RGY**
Munsell colour (dry)	–	2.5Y 5/3	2.5Y 6/1	10YR 4/1	7.5YR 6/6
Specific surface area	$m^2\ g^{-1}$	0.598	0.640	0.474	0.756
Electrical conductivity	$mS\ cm^{-1}$	0.69 ± 0.07	7.27 ± 0.06	0.78 ± 0.04	4.33 ± 0.25
pH_{H_2O}	–	6.74 ± 0.21	12.44 ± 0.11	10.00 ± 0.13	7.76 ± 0.61
C_{total}	%	11.82 ± 0.31	1.48 ± 0.13	1.67 ± 0.63	0.84 ± 0.02
C_{inorg}	%	0.34 ± 0.04	1.48 ± 0.60	0.70 ± 0.06	0.53 ± 0.22
C_{org}	%	11.49 ± 0.31	n.d.	0.98 ± 0.51	0.31 ± 0.02
Organic matter	%	19.83 ± 0.53	n.d.	1.72 ± 0.71	0.52 ± 0.04
N_{total}	%	2.12	0.01	0.09	0.08
C/N	–	5.6	150	18.9	3.9
$P_{available}$	$mg\ kg^{-1}$	16.7	22.8	18.7	3.0
$K_{available}$	$mg\ kg^{-1}$	57.7 ± 4.2	151 ± 8.2	56.0 ± 0.2	130 ± 5.8
Major elements	Detection limit (wt %)				
Al	0.01	>10	3.79	0.97	0.45
Ca	0.01	0.18	>10	1.68	>10
Fe	0.01	1.34	0.93	7.56	5.39
K	0.01	0.06	0.02	0.09	0.02
Mg	0.01	0.16	6.67	0.83	0.50
Na	0.01	0.06	0.09	0.29	0.07
P	0.001	0.175	0.001	0.024	0.006
S	0.01	0.78	0.42	0.04	11.0
Ti	0.01	< 0.01	0.12	0.03	0.47
Trace elements	Detection limit ($mg\ kg^{-1}$)				
As	2	42	<2	26	4
Bi	2	<2	<2	<2	<2
Cd	0.5	<0.5	<0.5	<0.5	2
Co	1	3	1	5	8
Cr	1	14	121	73	69
Cu	1	84	42	294	41
Hg	1	2	<1	<1	<1
Ni	1	15	12	54	26
Pb	3	23	16	88	58
Tl	2	<2	<2	<2	<2
Zn	1	71	252	226	315

Abbreviations: FIS: furnace iron slag; n.d., not detected; RGY, red gypsum; WCS, water clarification sludge; WSS, white steel slag.

($p < 0.00001$). Notably, Al concentration dropped dramatically from 1178 $mg\ L^{-1}$ to practically undetectable levels, addressing a major toxicity concern in acid mine soils (Fernández-Caliani & Barba-Brioso, 2010). This improvement is likely due to the formation of Al hydroxide solid phases (Sánchez-España et al., 2011). This hypothesis is supported by saturation indices predicted by PHREEQC modelling, which indicates a likelihood of precipitation for gibbsite (SI = 1.8–2.9), boehmite (SI = 1.5–2.6) and diaspore (SI = 3.1–4.3). These precipitates not only remove harmful Al from the solution but also provide additional binding sites for other contaminants, boosting the sorption capacity of the Technosols. Similarly, dissolved Fe concentrations decreased significantly from 10 $mg\ L^{-1}$ to below 0.5 $mg\ L^{-1}$. Equilibrium modelling suggests this decrease is due to the formation of ferrihydrite (SI = 3.6–3.8), a mineral prevalent in ochreous sediments precipitated from Fe-rich waters with neutral to mildly alkaline pH (Bigham et al., 1992; Murad & Rojík, 2003).

All three amended soils displayed a significant increase ($p < 0.00001$) in dissolved Ca concentrations. This notable increase, particularly evident in Technosol S3T2-25 (peaking at 948 $mg\ L^{-1}$), can be attributed to the dissolution of calcite and calcium silicate

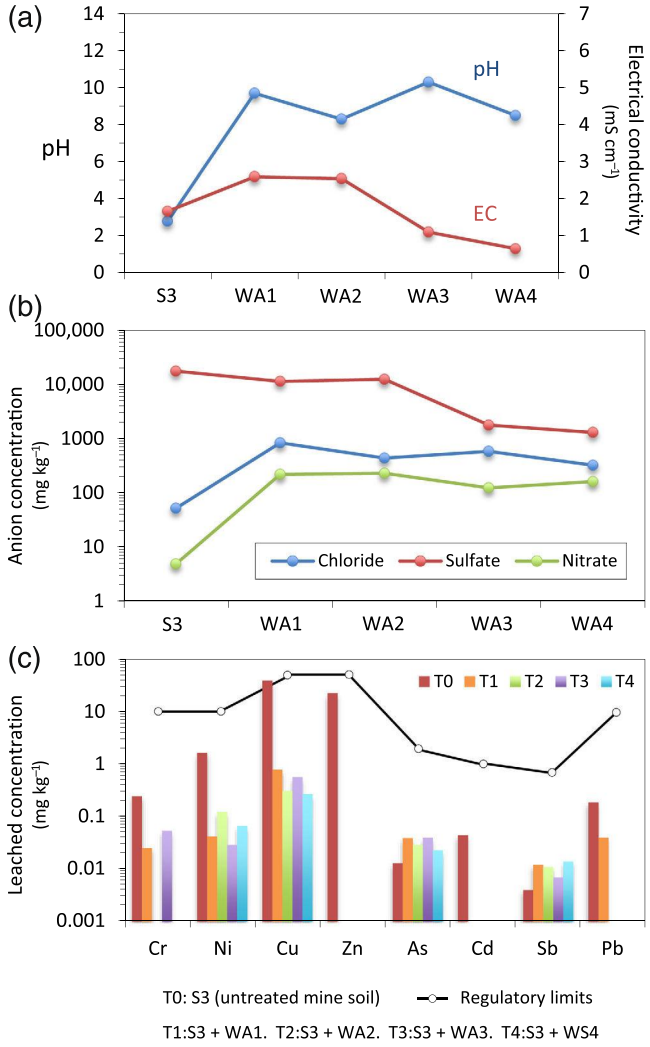

FIGURE 2 Effects of waste amendments on mine soil leachate composition: (a) pH and electrical conductivity of leachates from mine soil and waste amendments; (b) anion concentrations in leachates and (c) concentrations of potentially toxic trace elements leached from Technosols compared to regulatory limits for safe Technosol construction. S3, untreated mine soil; T, Technosol; WA, waste amendment. Composition details of waste amendments are provided in Table 1. [Colour figure can be viewed at wileyonlinelibrary.com]

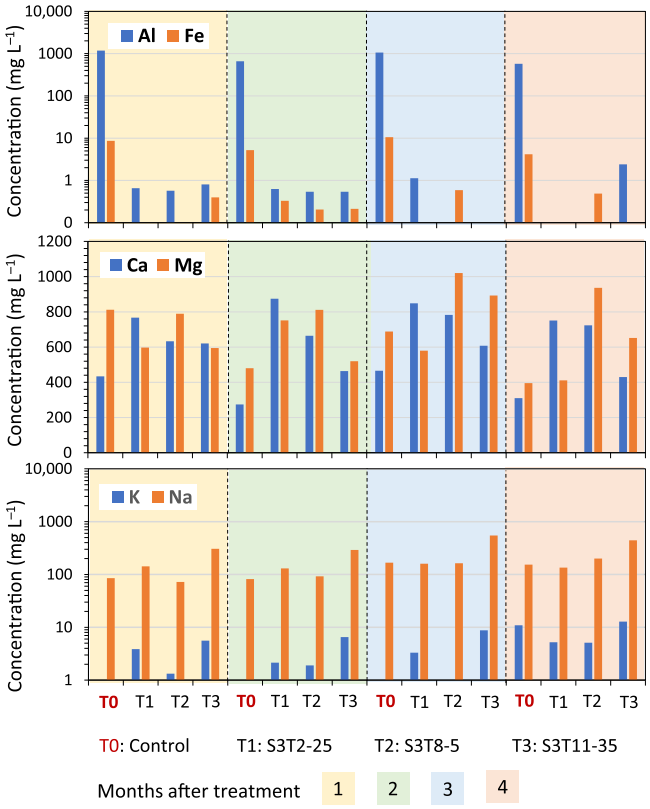

FIGURE 3 Comparative bar charts showing the temporal evolution of major element concentrations dissolved in the pore water extracts of the Technosols (T1, T2 and T3) and the control mine soil (T0) during the 4-month pot trial. [Colour figure can be viewed at wileyonlinelibrary.com]

compounds present in the waste amendments. Dissolved Mg concentration decreased significantly ($p < 0.01$) in Technosols S3T2-25 and S3T11-35, but increased ($p < 0.01$) in Technosol S3T8-5 due to its higher WSS content. Technosol S3T11-35 showed a noteworthy elevation in Na concentration compared to the control ($p < 0.00005$), whereas no significant changes were observed in Technosols S3T2-25 and S3T8-5 ($p > 0.05$). Overall, Technosol S3T11-35 proved most effective in promoting the solubilization of alkaline elements, while S3T8-5 displayed enhanced Mg mobilization.

As noted previously, waste amendments caused a pH increase, shifting towards moderately alkaline or near-neutral levels, while maintaining oxidizing conditions. This combined effect improved soil pore water quality by enhancing PTE retention through chemical stabilization (Basta & McGowen, 2004; Bolan et al., 2014; Kumpiene et al., 2008). Figure 4 illustrates the significant reduction in dissolved metal load within Technosols relative to the untreated (control) soil ($p < 0.00001$). In fact, treatments lowered mean concentrations of Cr, Co, Ni, Cu, Zn, Cd and Pb in pore water, with some declining by several orders of magnitude, clearly indicating reduced mobility and phytoavailability. Particularly, Cu and Zn concentrations dropped from initial levels of 80.21 and 72.08 mg L^{-1} to below 1 mg L^{-1} by the end of the monitoring period. The observed improvement in PTE immobilization can be ascribed to the alleviation of soil acidity, which reduces the activity of hydrogen ions in the soil solution, thereby decreasing competition for metal binding sites. This finding supports recent studies (e.g. Díaz et al., 2024; Paniagua-López et al., 2024) that demonstrate metal immobilization through soil amendment practices.

Waste amendment application in the mine soil triggered the precipitation of Cu-bearing phases, primarily copper ferrites. This is supported by positive saturation indices computed using PHREEQC (SI = 12.7–16.7). However, minerals containing Cd, Pb or Zn lacked positive SI values, suggesting that their mobility is likely controlled by adsorption processes onto newly formed phases rather than precipitation. Ferrihydrite may play a role in sequestering some of these PTEs through adsorption and co-precipitation mechanisms (Carlson et al., 2002; Michel et al., 2007; Sherman & Randall, 2003).

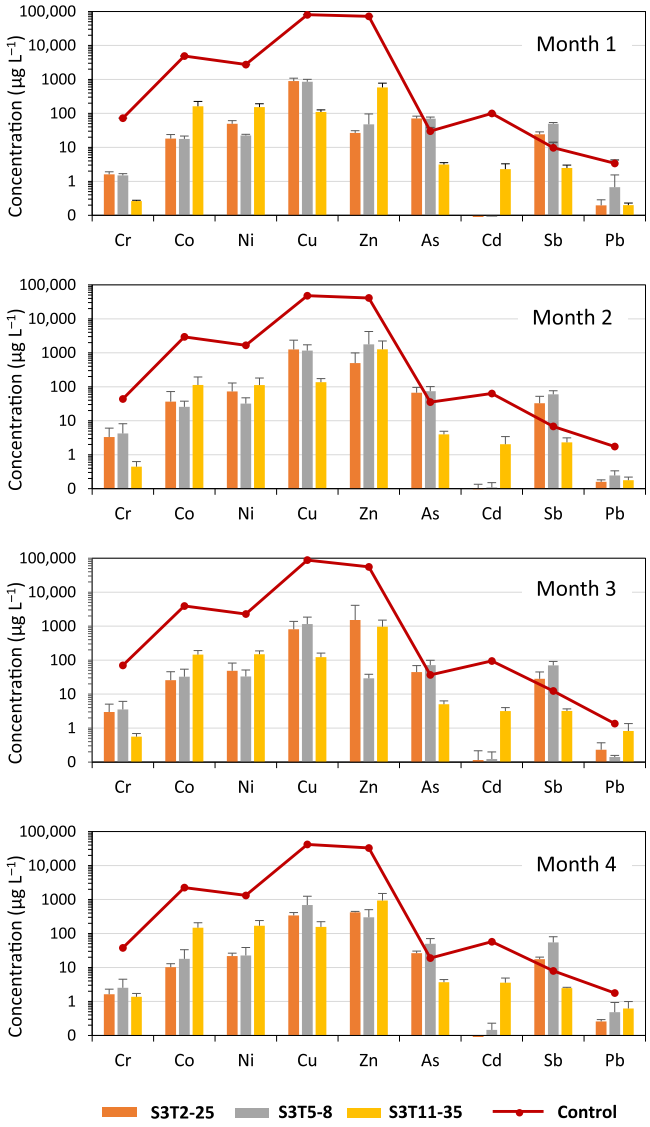

FIGURE 4 Comparative bar charts displaying trace element concentrations dissolved in the pore water extracts of the Technosols during the 4-month pot trial. Line charts show the trace element contents in the pore water of untreated mine soil (control). Error bars denote the standard deviation of the means ($n = 3$). [Colour figure can be viewed at wileyonlinelibrary.com]

Rising the pH to near-neutral and mildly alkaline levels in Technosols S3T2-25 y S3T8-5 increased the mobility of metalloids, specifically As and Sb, evidenced by their higher concentrations in pore water compared to the control ($p < 0.00003$). Despite concerns about potential As mobilization associated with the pH increase to the alkaline region (Hartley et al., 2004; Kumpiene et al., 2008), dissolved As concentrations remained below 50 µg L^{-1} in both Technosols after treatment. The enhanced mobility of As and Sb may result from an increase in negatively charged soil surface sites following acid neutralization (Bradl, 2004; Carabante et al., 2009), hindering the adsorption of harmful oxyanions. Conversely, Technosol S3T11-35, with an acidic soil solution, showed significant reductions in metalloid concentrations compared to the control ($p < 0.0001$), indicating its effectiveness as the most suitable treatment for all PTEs, including metalloids.

Sulphate was initially the predominant anion in the untreated mine soil solution, peaking at 23.04 g L^{-1}. This concentration decreased to 4.19 g L^{-1} over time due to the washing out of efflorescent sulphate salts formed on the soil surface. Upon treatment, mean chloride concentrations increased up to 1824 mg L^{-1} and nitrate concentrations up to 417 mg L^{-1}, exceeding untreated counterparts, which peaked at 376 mg L^{-1} and 61.2 respectively. Elevated nitrate levels benefit for plant growth as an essential nutrient. Bicarbonate also emerged as a prominent anion, peaking at 382 mg L^{-1} in Technosol S3T2-25.

Following the pot trial, sulphate remained the dominant anion in the mine soil solution (control), comprising 98% of the total anionic composition. However, Technosol treatments induced a shift in the species distribution pattern. Although sulphate remained significant (50%–66%), a new speciation model emerged (Figure S2), with chloride, bicarbonate and nitrate accounting for up to 31%, 28% and 25% respectively. This shift in the anionic balance can influence soil properties, affecting the mobility and speciation of contaminants.

Understanding the mobility, availability and toxicity of contaminants in the soil solution requires paying attention to their specific chemical forms rather than solely focusing on total dissolved concentration (Kalis et al., 2008). Through PHREEQC speciation calculations, insights into the distribution of PTEs among different aqueous species were gained by comparing untreated soil with Technosols after the 4-month pot trial (Figure 5).

In the untreated control soil solution, Al mainly formed harmful sulphate complexes, with the monomeric form ($AlSO_4^+$) comprising 83% of dissolved Al species. Notably, around 10% existed as highly toxic Al^{3+} ions, detrimental to plant growth (Chandra & Keshavkant, 2021). Waste amendment applications effectively mitigated this concern by promoting a shift towards less toxic hydroxylated species, such as $Al(OH)_4^-$ and $Al(OH)_2^+$. This shift, driven by the increased pH, reduces Al phytotoxicity by rendering it less soluble and more prone to form less harmful species (Bojórquez-Quintal et al., 2017).

Heavy metal speciation revealed a dominance of sulphate complexes in the mine soil solution, including neutral and negatively charged species ($CuSO_4$, $CdSO_4$, $Cd(SO_4)_2^{2-}$, $PbSO_4$, $ZnSO_4$ and $Zn(SO_4)_2^{2-}$). Moreover, a significant fraction of the dissolved metal load existed as free metal ions, posing a threat to plant growth through phytotoxicity (Kumar et al., 2021). Technosol application demonstrably altered this speciation pattern, leading to a greater diversity of metal species compared to the control. In Technosols S3T2-25 and S3T8-5, Cu speciation was dominated by $CuCO_3$ (77.5%–81.0%), creating a thriving environment for plants by reducing the activity of toxic Cu^{2+} ions. Zinc speciation was more complex, with a mixture of free metal, sulphate, carbonate and nitrate ions, while Cd primarily existed as free Cd^{2+}, along with sulphate complexes, and chloride ions. Changes in Cu and Zn speciation suggest a decrease in their mobility, although some free ions remained available to plants. While dissolved Pb and Cd concentrations decreased to

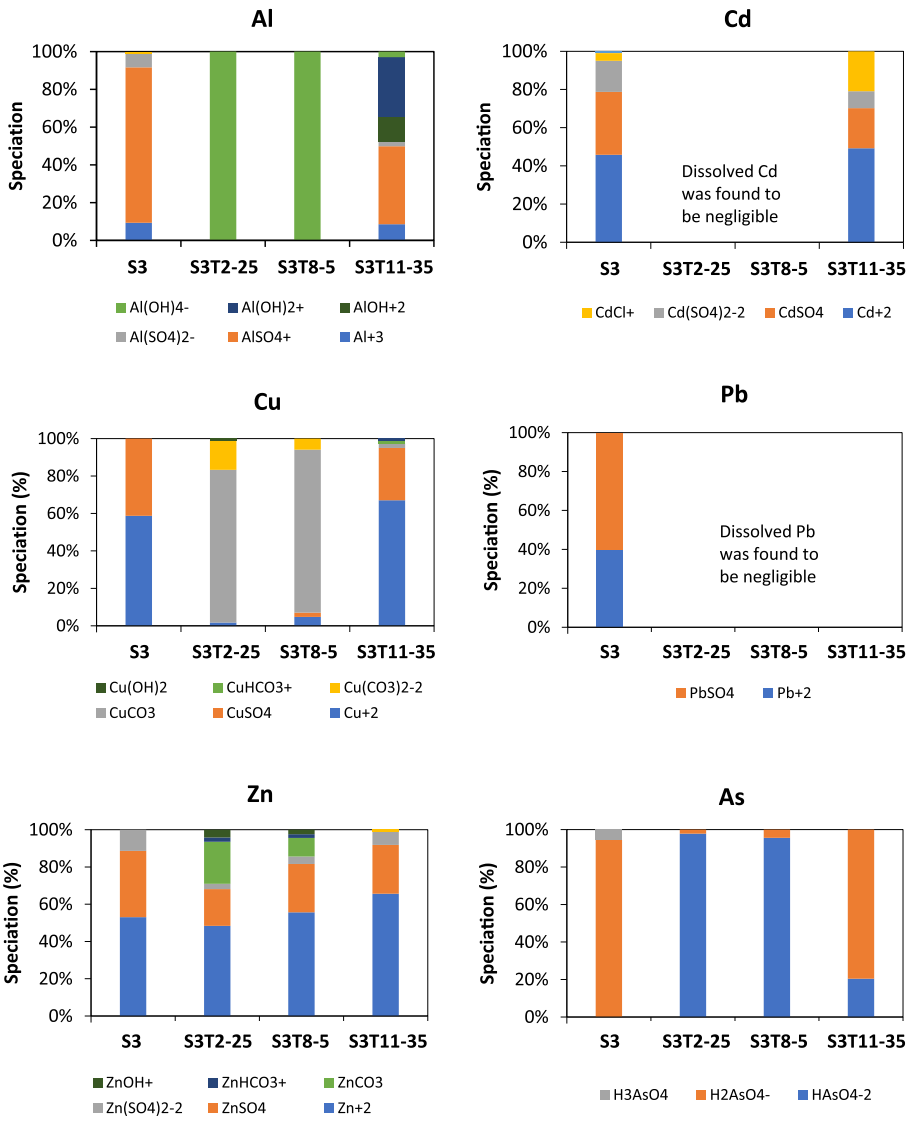

FIGURE 5 Aqueous speciation of trace elements of concern in the soil solution of Technosols (S3T2-25, S3T8-5 and S3T11-35) and control mine soil (sample S3) after the end of the pot trial, as predicted by PHREEQC geochemical modelling. [Colour figure can be viewed at wileyonlinelibrary.com]

negligible levels in Technosols S3T2-25 and S3T8-5, the presence of Cd^{2+} ions in Technosol S3T11-35 raises concerns regarding potential plant uptake.

Similar to other PTEs, the aqueous speciation of As in the amended soils shifted towards less harmful forms due to increased pH and oxygenation. Initially dominated by dihydrogen arsenate ($H_2AsO_4^-$), treatment induced a transition towards hydrogen arsenate ($HAsO_4^{2-}$), which is less mobile than H_3AsO_4 and $H_2AsO_4^-$ and much less toxic than arsenite species (Yamauchi & Fowler, 1994). Notably, Technosols S3T2-25 and S3T8-5 showed a remarkable dominance of this less harmful species, with 95%–99% of As existing as $HAsO_4^{2-}$.

3.5 | Effectiveness of waste amendments on plant growth

A seed germination assay using *B. juncea* revealed a significant positive effect of waste amendments on plant establishment in Technosols. The inherent limitations of the mine soils (strong acidity, nutrient deficiencies and high levels of dissolved PTEs) severely hampered germination. Conversely, Technosols enhanced both germination and early seedling growth, with seeds readily absorbing water, sprouting and developing cotyledons within a week. Germination was confirmed when the radicle reached 3 mm in length (ISTA, 2005). Germination rates varied across treatments (Figure 6a): untreated mine soil (0%), Technosol S3T11-35 (73.3%), Technosol S3T8-5 (80.0%), Technosol S3T2-25 (86.7%) and mulch control (90%).

Figure 7 depicts the 4-month progression of *B. juncea* plants in the pot trial. Although all seedlings successfully developed true leaves within a week, remarkable differences in plant establishment and growth were observed among treatments.

Technosol S3T2-25 demonstrated outstanding plant survival (100%), comparable to the mulched control (Figure 6b), indicating its effectiveness in fostering plant adaptation and resilience. Plants grew vigorously, reaching a maximum height of 59.4 cm with up to 51 leaves per pot by week 13 (Figure 6c,d). Technosol S3T8-5 maintained an 80% survival rate throughout the trial, with surviving plants

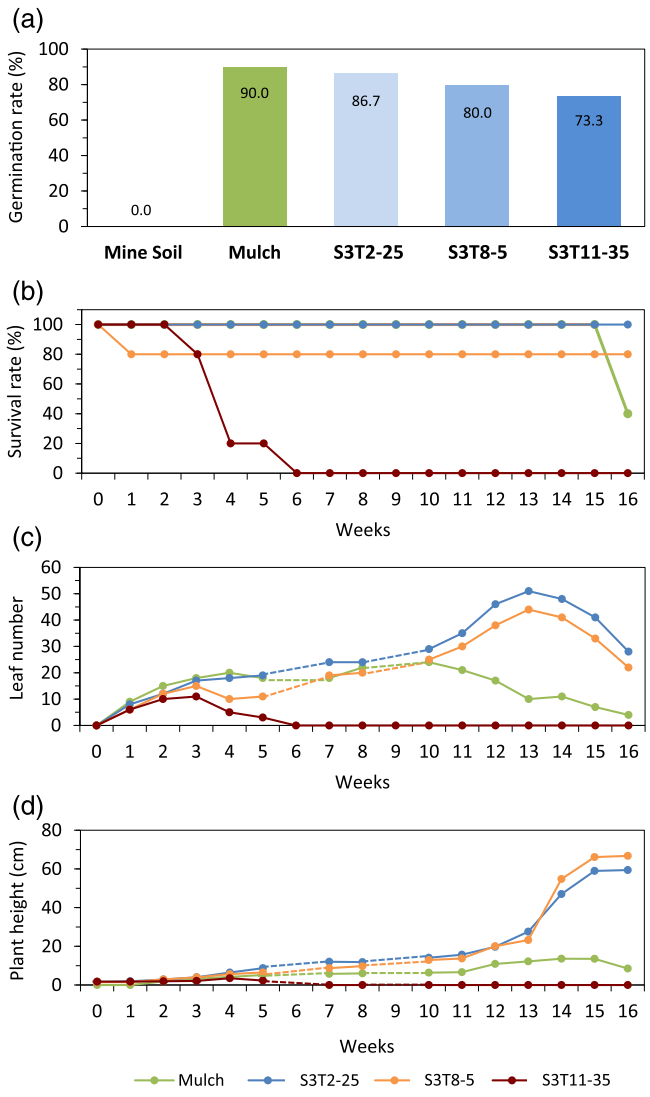

FIGURE 6 Bar chart comparing (a) seed germination rate of *Brassica juncea* in Technosols and mulch control, alongside line charts showing plant growth dynamics throughout the pot-based trial: (b) survival rate; (c) maximum plant height and (d) leaf number. [Colour figure can be viewed at wileyonlinelibrary.com]

achieving an even taller average height (66.8 cm) and a maximum leaf count of 44 by week 13. Notably, there were no statistically significant differences ($p > 0.053$) in plant growth parameters between the two Technosols, suggesting comparable effectiveness. Flowering commenced in both Technosols by week 12, mirroring the mulched control, with plants displaying vibrant yellow flowers and successfully completing seed production by week 13. At the conclusion of the trial, Technosol S3T2-25 yielded 6.734 g per pot of aboveground dry biomass, while Technosol S3T8-5 produced 5.574 g per pot.

In contrast, plant survival in Technosol S3T11-35 sharply declined, with only 20% survival by week 4 and complete mortality by week 6, indicating a limited capacity for *B. juncea* growth. The surviving plants displayed stunted growth, reaching an average peak height of just 3.5 cm by week 4, with limited leaf production (peaking at 11 leaves in week 3). Unlike the healthy growth observed in other Technosols, plants in Technosol S3T11-35 showed stress symptoms like limited growth, reduced leaf number, and foliar chlorosis, resembling effects typically associated with nutrient deficiency and metal stress (Chandra & Keshavkant, 2021; Kumar et al., 2021). By week 6, when all plants succumbed, cumulative aboveground dry biomass production was only 0.155 g.

PCA analysis elucidated the relationships between plant responses (survival rate, plant height, leaf number, biomass) and soil pore water variables (pH, trace elements, aluminium, calcium, bicarbonate, nitrate), providing further insights into how changes in soil solution chemistry influenced plant health and growth. The scores projected onto the two principal components (PC1 and PC2) delineated distinct clusters (Figure 8). PC1 explained 87% of the total variance and was driven by strong positive loadings for healthy plant responses and favourable soil conditions. High positive PC1 scores correlated with heightened survival rates and biomass production, taller plants, increased leaf count and higher levels of pH, bicarbonate, calcium and nitrate. Conversely, PC1 displayed strong negative loadings for aluminium and PTEs, indicating their detrimental effects on plants. PC2 played a minor role (10% variance), with all loadings remaining below 0.54. Overall, the PCA unveiled a clear link between thriving *B. juncea* plants and improved soil pore water quality, characterized by lower acidity, reduced stress from aluminium and PTEs and optimal nutrient availability. These findings are consistent with previous research on the beneficial effects of soil amendments on *B. juncea* growth in contaminated soils (Clemente et al., 2005; Fernández-Caliani et al., 2024; Pérez-Esteban et al., 2014).

In the PCA plot, Technosols S3T2-25 and S3T8-5 clustered closely together, indicating similar effects on both plant response and soil solution chemistry. Conversely, Technosol S3T11-35 displayed a notable separation, reflecting distinctive effects on plant growth (e.g. reduced survival rate and biomass) and pore water parameters (e.g. lower pH and higher toxic elements). The distant positioning of the untreated mine soil (control) from these clusters underscores the effectiveness of Technosol-based treatments in promoting plant growth and modifying soil chemistry.

The successful germination, growth and flowering observed in Technosols S3T2-25 and S3T8-5 provide promising evidence of their potential to overcome growth limitations in mine soils. These technogenic soil blends not only enhance plant survival rates but also support flourishing development under controlled pot experiment conditions. Nevertheless, field trials with a variety of plant species may be necessary to fully validate the impact of Technosol amendments on PTE mobility and bioavailability in the soil–plant system, under realistic environmental conditions.

4 | CONCLUSIONS

This pot-based study used *B. juncea* as a model plant to explore the potential of waste-derived Technosols as a sustainable and multifunctional approach for revegetating AMD-impacted soils. The results

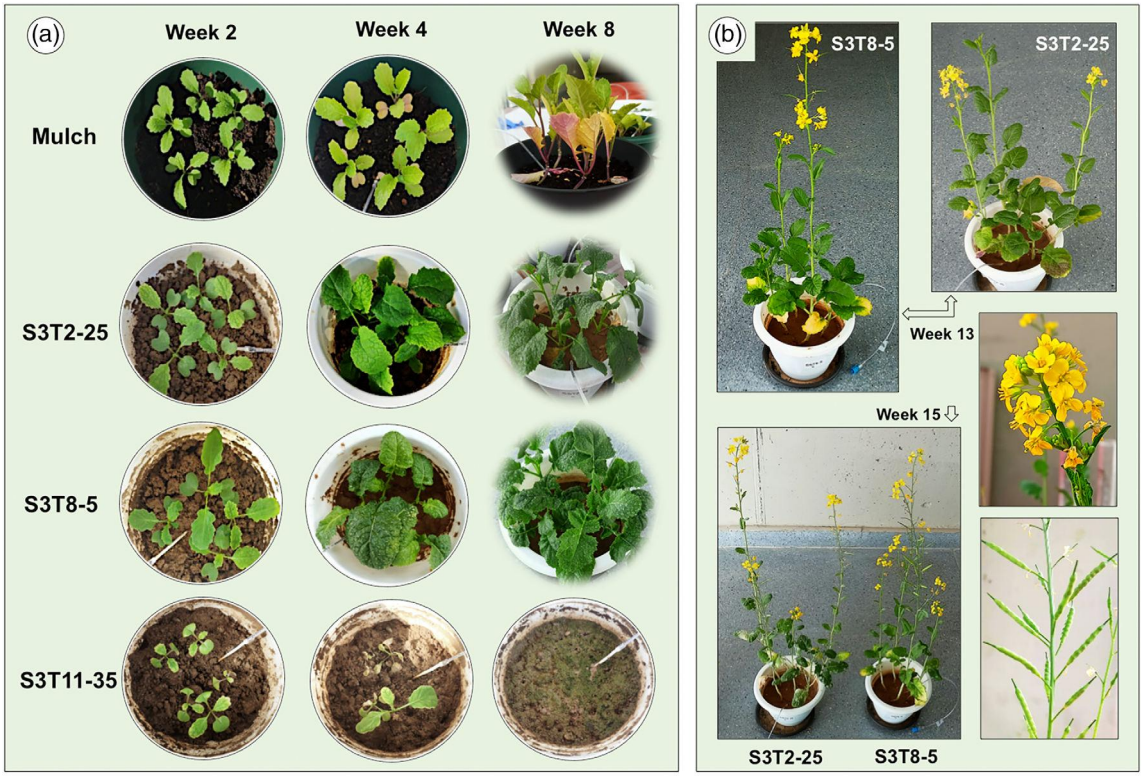

FIGURE 7 Visual comparison of *Brassica juncea* growth in Technosols and mulch control pots (⌀ = 15 cm) during the: (a) seedling and early vegetative growth stages; and (b) flowering and fruiting periods. [Colour figure can be viewed at wileyonlinelibrary.com]

FIGURE 8 PCA plot depicting the relationships between plant response parameters and soil pore water chemistry variables in mine soil and Technosols. The percentage of variance explained by each principal component is indicated on the corresponding axis label. [Colour figure can be viewed at wileyonlinelibrary.com]

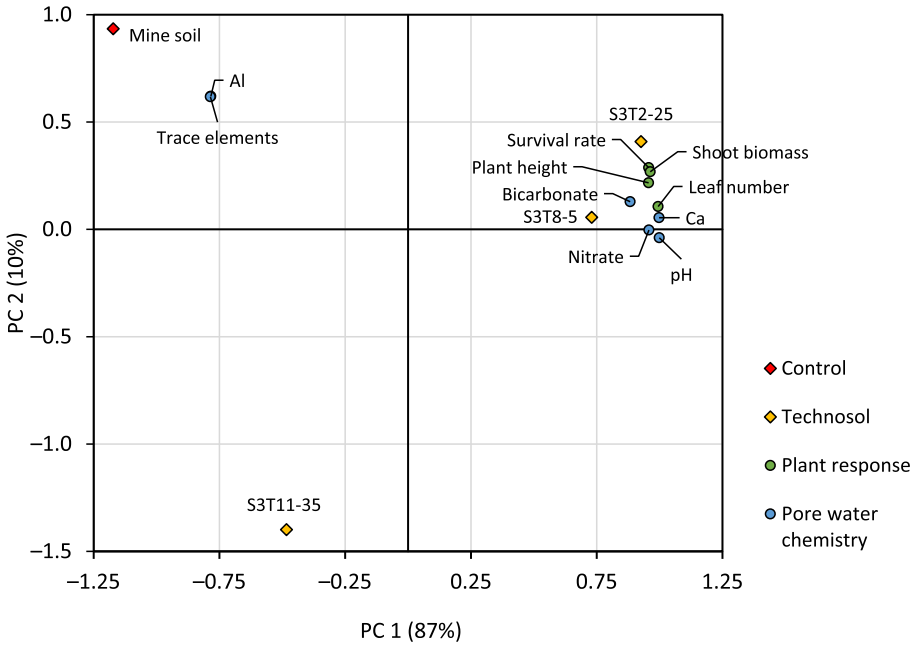

consistently demonstrated the effectiveness of Technosols in mitigating the extreme acidity of the mine soil, improving nutrient availability and reducing the leaching of PTEs to environmentally sustainable levels. The study identified several concomitant mechanisms for PTE immobilization: reduced dissolution of metal-bearing minerals, precipitation reactions forming stable mineral phases and adsorption onto Fe and Al (oxy)hydroxides. These processes collectively contribute to decrease PTE mobility and bioavailability in the leachate. Aqueous speciation modelling indicated a shift towards less phytotoxic forms of aluminium and heavy metals following treatment. This aligns with the observed germination and robust growth of *B. juncea* in specific Technosol formulations. Technosols S3T2-25 and S3T8-5 supported

high survival rates and optimal biomass production, underscoring their capacity to transform barren AMD-impacted landscapes into fertile and revitalized soils. PCA analysis corroborated this positive correlation between improved soil conditions and healthy plant responses. However, Technosol S3T11-35 showed limited effectiveness, emphasizing the importance of carefully selecting and formulating waste amendments to achieve optimal reclamation outcomes. Further research, particularly through field trials, is warranted to confirm these findings and assess the long-term effects of waste amendments on soil quality. This will provide valuable insights for informed decision-making regarding the large-scale implementation of Technosols in real-world settings.

ACKNOWLEDGEMENTS

This research received financial support from the Regional Government of Andalusia (Spain) and the European Regional Development Fund Andalusia 2014–2020 under Project P-18-TP-3503, in partnership with DSM Soluciones Medioambientales. It was also funded by EU project 101071300 Sustainable Horizons (HORIZON) Horizon Europe Framework Programme- HORIZON-WIDERA-2021-ACCESS-05. We express our gratitude to Nereida Pascual, Lourdes Vales, and Alicia Rodríguez (DSM, Centro de Nerva) for their invaluable assistance in collecting waste samples and providing essential information about the waste materials. Funding for open access charge: Universidad de Huelva / CBUA.

CONFLICT OF INTEREST STATEMENT

The authors declare no conflict of interest.

DATA AVAILABILITY STATEMENT

The data that support the findings of this study are available from the corresponding author upon reasonable request.

ORCID

Sandra Fernández-Landero https://orcid.org/0000-0003-2710-8348

Juan Carlos Fernández-Caliani https://orcid.org/0000-0002-1580-7929

Pablo J. Hidalgo https://orcid.org/0000-0001-9704-8139

REFERENCES

Adriano, D. C., Wenzel, W. W., Vangronsveld, J., & Bolan, N. S. (2004). Role of assisted natural remediation in environmental cleanup. *Geoderma*, *122*, 121–142.

Aguilar-Garrido, A., Reyes-Martín, M. P., Vidigal, P., & Abreu, M. M. (2023). A green solution for the rehabilitation of marginal lands: The case of *Lablab purpureus* (L.) sweet grown in Technosols. *Plants*, *12*, 2682.

Ahern, C. R., McElnea, A. E., & Sullivan, L. A. (2004). *Acid sulfate soils laboratory methods guidelines*. Queensland Department of Natural Resources, Mines and Energy, Indooroopilly.

Ahirwal, J., & Maiti, S. K. (2018). Development of Technosol properties and recovery of carbon stock after 16 years of revegetation on coal mine degraded lands, India. *Catena*, *166*, 114–123.

Alvarenga, P., Mourinha, C., Palma, P., Cruz, N., & Rodrigues, S. M. (2022). Assessment of soil physicochemical characteristics and As, Cu, Pb and Zn contamination in non-active mines at the Portuguese sector of the Iberian Pyrite Belt. *Environments*, *9*, 105.

Arán, D., Santos, E. S., Abreu, M. M., Antelo, J., & Macías, F. (2022). Use of combined tools for effectiveness evaluation of tailings rehabilitated with designed Technosol. *Environmental Geochemistry and Health*, *44*, 1857–1873.

Asensio, V., Florido, F. G., Ruiz, F., Perlatti, F., Otero, X. L., Oliveira, D. P., & Ferreira, T. O. (2019). The potential of a Technosol and tropical native trees for reclamation of copper-polluted soils. *Chemosphere*, *220*, 892–899.

Asensio, V., Vega, F. A., Andrade, M. L., & Covelo, F. (2013). Technosols made of wastes to improve physico-chemical characteristics of a copper mine soil. *Pedosphere*, *23*, 1–9.

Barba-Brioso, C., Hidalgo, P. J., Fernández-Landero, S., Giráldez, M. I., & Fernández-Caliani, J. C. (2023). Phytoaccumulation of trace elements (As, Cd, Co, Cu, Pb, Zn) by *Nicotiana glauca* and *Euphorbia segetalis* growing in a Technosol developed on legacy mine wastes (Domingo Rubio wetland, SW Spain). *Environmental Geochemistry and Health*, *45*, 9541–9557.

Basta, N. T., & McGowen, S. L. (2004). Evaluation of chemical immobilization treatments for reducing heavy metal transport in a smelter-contaminated soil. *Environmental Pollution*, *127*, 73–82.

Bigham, J. M., Schwertmann, U., & Carlson, L. (1992). Mineralogy of precipitates formed by the biogeochemical oxidation of Fe(II) in mine drainage. In H. C. W. Skinner & R. W. Fitzpatrick (Eds.), *Biomineralization processes of iron and manganese: Catena supplement 21* (pp. 219–232). Catena Verlag.

Blowes, D. W., Ptacek, C. J., Jambor, J. L., & Weisener, C. G. (2003). The geochemistry of acid mine drainage. In H. D. Holland & K. K. Turekian (Eds.), *Treatise on geochemistry* (Vol. 9, pp. 149–204). Elsevier.

Bojórquez-Quintal, E., Escalante-Magaña, C., Echevarría-Machado, I., & Martínez-Estévez, M. (2017). Aluminum, a friend or foe of higher plants in acid soils. *Frontiers in Plant Science*, *8*, 1767.

Bolan, N., Kunhikrishnan, A., Thangarajanan, R., Kumpiene, J., Park, J., Makino, T., Kirkhamg, M. B., & Scheckel, K. (2014). Remediation of heavy metal(loid)s contaminated soils – To mobilize or to immobilize? *Journal of Hazardous Materials*, *266*, 141–166.

Bradl, H. B. (2004). Adsorption of heavy metal ions on soils and soils constituents. *Journal of Colloid and Interface Science*, *277*, 1–18.

Carabante, I., Grahn, M., Holmgren, A., Kumpiene, J., & Hedlund, J. (2009). Adsorption of As(V) on iron oxide nanoparticle films studied by in situ ATR-FTIR spectroscopy. *Colloid Surface A*, *346*, 106–113.

Carlson, L., Bigham, J. M., Schwertmann, U., Kyek, A., & Wagner, F. (2002). Scavenging of As from acid mine drainage by schwertmannite and ferrihydrite: A comparison with synthetic analogues. *Environmental Science & Technology*, *36*, 1712–1719.

Chandra, J., & Keshavkant, S. (2021). Mechanisms underlying the phytotoxicity and genotoxicity of aluminum and their alleviation strategies: A review. *Chemosphere*, *278*, 130384.

Chopin, E. I. B., Black, S., Hodson, M. E., Coleman, M. L., & Alloway, B. J. (2003). A preliminary investigation into mining and smelting impacts on trace element concentrations in the soils and vegetation around Tharsis, SW Spain. *Mineralogical Magazine*, *67*, 279–288.

Clemente, R., Dickinson, N. M., & Lepp, N. W. (2008). Mobility of metals and metalloids in a multi-element contaminated soil 20 years after cessation of the pollution source activity. *Environmental Pollution*, *155*, 254–261.

Clemente, R., Walker, D. J., & Bernal, M. P. (2005). Uptake of heavy metals and As by *Brassica juncea* grown in a contaminated soil in Aznalcóllar (Spain): The effect of soil amendments. *Environmental Pollution*, *138*, 46–58.

Dassanayake, K. B., Jayasinghe, G. Y., Surapaneni, A., & Hetherington, C. (2015). A review on alum sludge reuse with special reference to agricultural applications and future challenges. *Waste Management*, *38*, 321–335.

Junta de Andalucía. (2015). Decreto 18/2015, de 27 de enero, por el que se aprueba el reglamento que regula el régimen aplicable a los suelos contaminados. *Boletín Oficial de la Junta de Andalucía*, *38*, 28–64.

Díaz, A. M., Forján, R., Gallego, J. R., Benavente, L., Menéndez-Aguado, J. M., & Baragaño, D. (2024). Nanoscale zero-valent iron mitigates arsenic mobilization and accumulation in *Sinapis alba* grown on a metal(loid)-polluted soil treated with a dunite mining waste-compost amendment. *Plant and Soil*, *497*, 241–255.

Dold, B. (2003). Speciation of the most soluble phases in a sequential extraction procedure adapted for geochemical studies of copper sulfide mine waste. *Journal of Geochemical Exploration*, *80*, 55–68.

Dold, B. (2017). Acid rock drainage prediction: A critical review. *Journal of Geochemical Exploration*, *172*, 120–132.

Fan, Y., Zheng, C., Liu, H., He, C., Shen, Z., & Zhang, T. C. (2020). Effect of pH on the adsorption of arsenic(V) and antimony(V) by the black soil in three systems: Performance and mechanism. *Ecotoxicology and Environmental Safety*, *191*, 110145.

Fernández-Caliani, J. C., & Barba-Brioso, C. (2010). Metal immobilization in hazardous contaminated minesoils after marble slurry waste application. A field assessment at the Tharsis mining district (Spain). *Journal of Hazardous Materials*, *181*, 817–826.

Fernández-Caliani, J. C., Barba-Brioso, C., González, I., & Galán, E. (2009). Heavy metal pollution in soils around the abandoned mine sites of the Iberian Pyrite Belt (Southwest Spain). *Water, Air, and Soil Pollution*, *200*, 211–226.

Fernández-Caliani, J. C., De la Rosa, J. D., De la Campa, A. M. S., González-Castanedo, Y., & Castillo, S. (2013). Mineralogy of atmospheric dust impacting the Rio Tinto mining area (Spain) during episodes of high metal deposition. *Mineralogical Magazine*, *77*, 2793–2810.

Fernández-Caliani, J. C., Fernández-Landero, S., Giráldez, M. I., Hidalgo, P. J., & Morales, E. (2024). Unveiling a Technosol-based remediation approach for enhancing plant growth in an iron-rich acidic mine soil from the Rio Tinto Mars analog site. *Science of the Total Environment*, *922*, 171217.

Fernández-Caliani, J. C., Giráldez, M. I., & Barba-Brioso, C. (2019). Oral bioaccessibility and human health risk assessment of trace elements in agricultural soils impacted by acid mine drainage. *Chemosphere*, *237*, 124441.

Fernández-Caliani, J. C., Giráldez, M. I., Fernández-Landero, S., Barba-Brioso, C., & Morales, E. (2022). Long-term sustainability of marble waste sludge in reducing soil acidity and heavy metal release in a contaminated mine Technosol. *Applied Sciences*, *12*, 6998.

Fernández-Caliani, J. C., Giráldez, M. I., Waken, W. H., Del Río, Z. M., & Córdoba, F. (2021). Soil quality changes in an Iberian pyrite mine site 15 years after land reclamation. *Catena*, *206*, 105538.

Fernández-Landero, S., Fernández-Caliani, J. C., Giráldez, M. I., Morales, E., Barba-Brioso, C., & González, I. (2023). Soil contaminated with hazardous waste materials at Rio Tinto mine (Spain) is a persistent secondary source of acid and heavy metals to the environment. *Minerals*, *13*, 456.

Forján, R., Rodríguez-Vila, A., & Covelo, E. F. (2018). Using compost and technosol combined with biochar and *Brassica juncea* L. to decrease the bioavailable metal concentration in soil from a copper mine settling pond. *Environmental Science and Pollution Research*, *25*, 1294–1305.

Galán, E., Fernández-Caliani, J. C., González, I., Aparicio, P., & Romero, A. (2008). Influence of geological setting on geochemical baselines of trace elements in soils. Application to soils of Southwest Spain. *Journal of Geochemical Exploration*, *98*, 89–106.

Hartley, W., Edwards, R., & Lepp, N. W. (2004). Arsenic and heavy metal mobility in iron oxide-amended contaminated soils as evaluated by short- and long-term leaching tests. *Environmental Pollution*, *131*, 495–504.

Houba, V. J. G., Lexmond, T. M., Novozamsky, I., & van der Lee, J. J. (1996). State of the art and future developments in soil analysis for bioavailability assessment. *Science of the Total Environment*, *178*, 21–28.

ISTA, International Seed Testing Association. (2005). *International rules for seed testing*. International Seed Testing Association.

ITR, Instrucción Técnica de Residuos. (2008). ITR/01/08, de 8 de enero de 2008, de la Dirección General de Calidad y Evaluación Ambiental, referente a la elaboración de suelos (tecnosoles) derivados de residuos. *Diario Oficial de Galicia*, *18*, 1499–1511.

Kalis, E. J. J., Temminghoff, E. J. M., Town, R. M., Unsworth, E. R., & van Riemsdijk, W. H. (2008). Relationship between metal speciation in soil solution and metal adsorption at the root surface of ryegrass. *Journal of Environmental Quality*, *37*, 2221–2231.

Karlsson, T., Räisänen, M. L., Lehtonen, M., & Alakangas, L. (2018). Comparison of static and mineralogical ARD prediction methods in the Nordic environment. *Environmental Monitoring and Assessment*, *190*, 719.

Kumar, V., Pandita, S., Sidhu, G. P. S., Sharma, A., Khanna, K., Kaur, P., Bali, A. S., & Setia, R. (2021). Copper bioavailability, uptake, toxicity and tolerance in plants: A comprehensive review. *Chemosphere*, *262*, 127810.

Kumpiene, J., Lagerkvist, A., & Maurice, C. (2008). Stabilization of As, Cr, Cu, Pb and Zn in soil using amendments – A review. *Waste Management*, *28*, 215–225.

Lai, H. Y., Chen, S. W., & Chen, Z. S. (2008). Pot experiment to study the uptake of Cd and Pb by three Indian mustards (*Brassica juncea*) grown in artificially contaminated soils. *International Journal of Phytoremediation*, *10*, 91–105.

Madejón, P., Barba-Brioso, C., Lepp, N. W., & Fernández-Caliani, J. C. (2011). Traditional agricultural practices enable sustainable remediation of highly polluted soils in southern Spain for cultivation of food crops. *Journal of Environmental Management*, *92*, 1828–1836.

Madejón, P., Caro-Moreno, D., Navarro-Fernández, C. M., Rossini-Oliva, S., & Marañón, T. (2021). Rehabilitation of waste rock piles: Impact of acid drainage on potential toxicity by trace elements in plants and soil. *Journal of Environmental Management*, *280*, 111848.

Martín-Méndez, I., Llamas, J., Bel-lan, A., & Locutura, J. (2023). Geochemical distribution in residual soils of Iberian Pyrite Belt (Spain). *Journal of Iberian Geology*, *49*, 97–114.

McElnea, A. E., Ahern, C. R., & Menzies, N. W. (2002). The measurement of actual acidity in acid sulfate soils and the determination of sulfidic acidity in suspension after peroxide oxidation. *Australian Journal of Soil Research*, *40*, 1133–1157.

Michel, F. M., Ehm, L., Antao, S. M., Lee, P. L., Chupas, P. J., Liu, G., Strongin, D. R., Schoonen, M. A. A., Phillips, B. L., & Parise, J. B. (2007). The structure of ferrihydrite, a nanocrystalline material. *Science*, *316*, 1726–1729.

Miller, S., Robertson, A., & Donahue, T. (1997). Advances in acid drainage prediction using the net acid generating (NAG) test. In *Proceedings of the fourth international conference on acid rock drainage, Vancouver, Canada* (Vol. 2, pp. 533–547).

Monterroso, C., & Macías, F. (1998). Prediction of the acid generating potential of coal mining spoils. *International Journal of Surface Mining, Reclamation, and Environment*, *12*, 5–9.

Murad, E., & Rojík, P. (2003). Iron-rich precipitates in a mine drainage environment: Influence of pH on mineralogy. *American Mineralogist*, *88*, 1915–1918.

Niu, A., & Lin, C. (2021). Managing soils of environmental significance: A critical review. *Journal of Hazardous Materials*, *417*, 125990.

Nolan, A. L., McLaughlin, M. J., & Mason, S. D. (2003). Chemical speciation of Zn, Cd, Cu, and Pb in pore waters of agricultural and contaminated soils using Donnan dialysis. *Environmental Science & Technology*, *37*, 90–98.

Nordstrom, D. K. (1982). Aqueous pyrite oxidation and the consequent formation of secondary iron minerals. In J. A. Kittrick, D. S. Fanning, & L. R. Hossner (Eds.), *Acid sulfate weathering* (Vol. 10, pp. 37–56). Soil Science Society of America.

Nordstrom, D. K. (2011). Mine waters: Acidic to circumneutral. *Elements*, *7*, 393–398.

Novo, L. A. B., & González, L. (2014). Germination and early growth of *Brassica juncea* in copper mine tailings amended with Technosol and compost. *Scientific World Journal*, *506392*, 1–9.

Olsen, S. R., & Sommers, L. E. (1982). Phosphorus. In A. L. Page (Ed.), *Methods of soil analysis part 2 chemical and microbiological properties* (pp. 403–430). American Society of Agronomy, Soil Science Society of America.

Palansooriya, K. N., Shaheen, S. M., Chen, S. S., Tsang, D. C. W., Hashimoto, Y., Hou, D., Bolan, N. S., & Rinklebe, J. (2020). Soil amendments for immobilization of potentially toxic elements in contaminated soils: A critical review. *Environment International*, *134*, 105046.

Paniagua-López, M., García-Robles, H., Aguilar-Garrido, A., Romero-Freire, A., Lorite, J., & Sierra-Aragón, M. (2024). Vegetation establishment in soils polluted by heavy metal(loid)s after assisted natural remediation. *Plant and Soil*, *497*, 257–275.

Parkhurst, D. L., & Appelo, C. A. J. (2013). *Description of input and examples for PHREEQC version 3—A computer program for speciation, batch-reaction, one-dimensional transport, and inverse geochemical calculations. U.S. Geological Survey Techniques and Methods* (Vol. 6, p. 497). U.S. Geological Survey.

Peacock, S., & Rimmer, D. L. (2000). The suitability of an iron oxide-rich gypsum by-product as a soil amendment. *Journal of Environmental Quality*, *29*, 1969–1975.

Pérez-Esteban, J., Escolástico, C., Moliner, A., Masaguer, A., & Ruiz-Fernández, J. (2014). Phytostabilization of metals in mine soils using *Brassica juncea* in combination with organic amendments. *Plant and Soil*, *377*, 97–109.

Rodríguez-Jordá, M. P., Garrido, F., & García-González, M. T. (2010). Potential use of gypsum and lime rich industrial by-products for induced reduction of Pb, Zn and Ni leachability in an acid soil. *Journal of Hazardous Materials*, *175*, 762–769.

Ruiz, F., Cherubin, M. R., & Ferreira, T. O. (2020). Soil quality assessment of constructed Technosols: Towards the validation of a promising strategy for land reclamation, waste management and the recovery of soil functions. *Journal of Environmental Management*, *276*, 111344.

Sánchez-España, J., Yusta, I., & Díez-Ercilla, M. (2011). Schwertmannite and hydrobasaluminite: A re-evaluation of their solubility and control on the iron and aluminium concentration in acidic pit lakes. *Applied Geochemistry*, *26*, 1752–1774.

Santos, E. S., Abreu, M. M., & Macías, F. (2019). Rehabilitation of mining areas through integrated biotechnological approach: Technosols derived from organic/inorganic wastes and autochthonous plant development. *Chemosphere*, *224*, 765–775.

Santos, E. S., Abreu, M. M., Macías, F., & de Varennes, A. (2016). Chemical quality of leachates and enzymatic activities in Technosols with gossan and sulfide wastes from the São Domingos mine. *Journal of Soils and Sediments*, *16*, 1366–1382.

Séré, G., Schwartz, C., Ouvrard, S., Sauvage, C., Renat, J. C., & Morel, J. L. (2008). Soil construction: A step for ecological reclamation of derelict lands. *Journal of Soils and Sediments*, *8*, 130–136.

Sherman, D. M., & Randall, S. R. (2003). Surface complexation of arsenic(V) to iron(III) (hydr)oxides: Structural mechanism from ab initio molecular geometries and EXAFS spectroscopy. *Geochimica et Cosmochimica Acta*, *67*, 4223–4230.

Siddique, R., Kaur, G., & Rajor, A. (2010). Waste foundry sand and its leachate characteristics. *Resources, Conservation and Recycling*, *54*, 1027–1036.

Tordoff, G. M., Baker, A. J. M., & Willis, A. J. (2000). Current approaches to the revegetation and reclamation of metalliferous mine wastes. *Chemosphere*, *41*, 219–228.

Uchimiya, M., Lima, I. M., Klasson, K. T., & Wartelle, L. H. (2010). Contaminant immobilization and nutrient release by biochar soil amendment: Roles of natural organic matter. *Chemosphere*, *80*, 935–940.

Urrutia, M. M., García-Rodeja, E., & Macías, F. (1992). Sulfide oxidation in coal-mine dumps: Laboratory measurement of acidifying potential with H_2O_2 and its application to characterize spoil materials. *Environmental Management*, *16*, 81–89.

Watkinson, A. D., Lock, A. S., Beckett, P. J., & Spiers, G. (2017). Developing manufactured soils from industrial by-products for use as growth substrates in mine reclamation. *Restoration Ecology*, *25*, 587–594.

Weiler, J., Firpo, B. A., & Schneider, I. A. H. (2020). Technosol as an integrated management tool for turning urban and coal mining waste into a resource. *Minerals Engineering*, *147*, 106179.

Yamauchi, H., & Fowler, B. A. (1994). Toxicity and metabolism of inorganic and methylated arsenicals. In J. O. Nriagu (Ed.), *Arsenic in the environment, part II: Human health and ecosystem effects* (pp. 35–43). Wiley.

Yang, M., Lu, C., Quan, X., Chang, H., Cao, D., & Wu, Q. (2022). Steel slag as a potential adsorbent for efficient removal of Fe(II) from simulated acid mine drainage: Adsorption performance and mechanism. *Environmental Science and Pollution Research*, *29*, 25639–25650.

Yao, F. X., Macías, F., Santesteban, A., Virgel, S., Blanco, F., Jiang, X., & Camps- Arbestain, M. (2009). Influence of the acid buffering capacity of different types of Technosols on the chemistry of their leachates. *Chemosphere*, *74*, 250–258.

SUPPORTING INFORMATION

Additional supporting information can be found online in the Supporting Information section at the end of this article.

How to cite this article: Fernández-Landero, S., Fernández-Caliani, J. C., Giráldez, M. I., Hidalgo, P. J., & Morales, E. (2024). Successful plant growth in acid mine drainage-impacted soil using pot-based experiments with waste amendments. *Land Degradation & Development*, 1–16. https://doi.org/10.1002/ldr.5211

Supplementary Figure S1

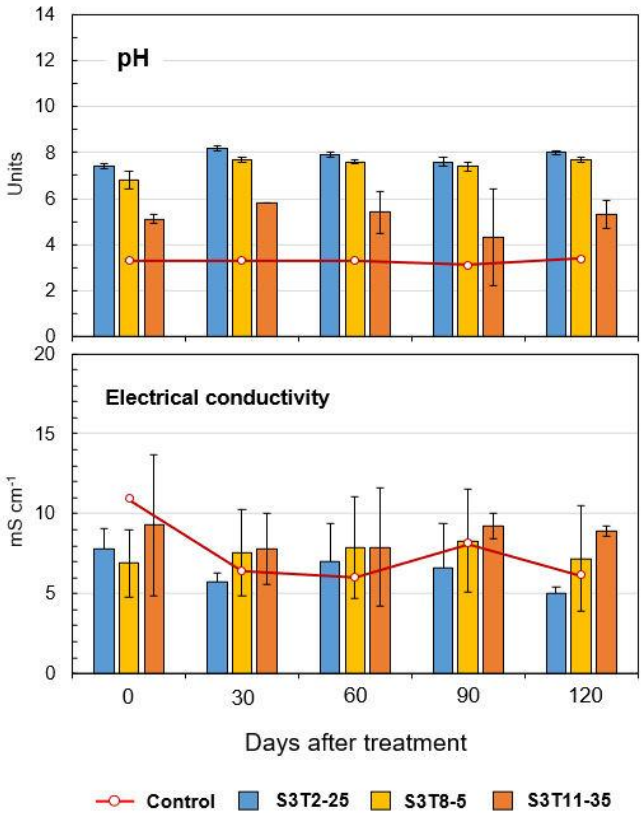

Figure S1. Bar charts illustrating the temporal evolution of pH and electrical conductivity values in the pore water of Technosols compared to the control mine soil (shown in line charts). Error bars denote the standard deviation of the means (n = 3).

Supplementary Figure S2

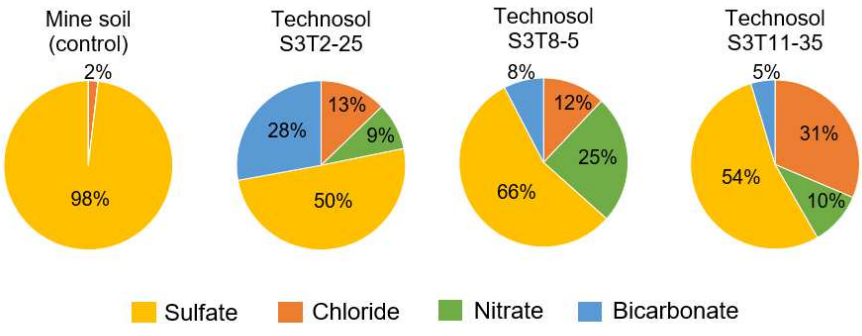

Figure S2. Pie charts illustrating the distribution of major anions in the pore water extract after the four-month pot trial period.

5. CONCLUSIONES GENERALES Y NUEVAS VÍAS DE INVESTIGACIÓN

5.1. Conclusiones generales

Los resultados de esta tesis han permitido profundizar en el conocimiento del comportamiento de los sistemas edáficos hiperácidos y extremadamente contaminados con arsénico y metales pesados en los entornos de Rio Tinto y Tharsis, y el estero de Domingo Rubio. Este avance en la caracterización ha sido imprescindible para calibrar la magnitud del problema y diseñar unos tecnosuelos efectivos. Asimismo, se ha progresado en la identificación de RNP que cumplen las especificaciones técnicas y ambientales requeridas para su empleo en la elaboración de tecnosuelos, siempre bajo las restricciones pertinentes en cada caso.

Los ensayos realizados han demostrado la viabilidad, a escala de laboratorio, de los tecnosuelos formulados con RNP como una solución para mejorar las propiedades físicas, químicas y biológicas de suelos mineros degradados. Los tecnosuelos son capaces de estabilizar químicamente estos entornos, reduciendo la acidez y la movilidad de los contaminantes, al mismo tiempo que promueven la fertilidad y el desarrollo de la vegetación. A continuación, se resumen las principales conclusiones de esta investigación:

1. **Avances en la caracterización de suelos mineros.** Se ha logrado un avance significativo en la caracterización de suelos mineros altamente ácidos y contaminados, proporcionando un diagnóstico ambiental exhaustivo de su estado previo al tratamiento. Los resultados obtenidos han demostrado que los suelos mineros han superado su carga crítica de acidez y capacidad amortiguadora de la contaminación, comportándose como fuentes secundarias de contaminantes. Por tanto, es imprescindible aplicar medidas correctivas para aminorar el riesgo que representan para los ecosistemas y la salud humana.

2. **Desarrollo de tecnosuelos sostenibles.** Se ha demostrado la viabilidad de valorizar RNP para la producción de tecnosuelos como una solución sostenible para la recuperación de suelos degradados por la actividad minera. Las mezclas propuestas representan un avance importante hacia estrategias de

restauración ambiental tendentes a minimizar el impacto de la minería metálica, aportando estabilidad química y mejorando las propiedades edáficas.

3. **Mejora de la calidad ambiental.** El tratamiento con tecnosuelos ha contribuido notablemente a mejorar la calidad ambiental, restaurando la salud del suelo y su capacidad de regeneración. Se ha logrado una reducción efectiva de la acidez, movilidad y la disponibilidad ambiental de los EPT en los suelos tratados, además de estabilizar carbono y aportar nutrientes esenciales.

4. **Revegetación exitosa.** Uno de los logros más notables es la evidencia de que los tecnosuelos formulados favorecen el crecimiento de plantas en macetas, lo que demuestra su potencial para la revegetación de áreas degradadas.

En definitiva, los avances alcanzados en la aplicación de tecnosuelos como técnica de recuperación natural asistida tienen un impacto positivo tanto en el medio ambiente como en la sociedad, abriendo el camino a soluciones más sostenibles para la gestión de suelos contaminados.

5.2. Trabajos en curso y nuevas líneas de investigación

En continuidad con la tesis, se han desarrollado análisis microbiológicos que permiten evaluar la salud de los suelos remediados, incluyendo cultivos bacterianos, extracción de ADN genómico y análisis de la actividad enzimática.

- **Cultivo bacteriano.** Se han cultivado bacterias a partir del agua de poro obtenida cuatro meses después de la plantación de *B. juncea*. Las muestras se cultivaron en medio Luria-Bertani para comparar la microbiota presente en suelos tratados y no tratados, con el fin de evaluar el impacto de los tecnosuelos sobre comunidad bacteriana.

- **Extracción y caracterización de ADN genómico.** Para identificar y comparar las especies microbianas en ambos tipos de suelos, se extrajo ADN genómico utilizando el kit QIAGEN DNeasy PowerMax Soil, específico para suelos con baja biomasa microbiana. El procedimiento de extracción consta de 6 pasos: 1) descomposición celular, 2) precipitación de impurezas, 3) purificación del ADN, 4) lavado, 5) elución, y 6) preconcentración.

- **Evaluación de la actividad enzimática.** Se analizaron las actividades de diversas enzimas indicadoras de salud del suelo (deshidrogenasas, β-glucosidasas, celulasas, fosfatasas, ureasas, proteasas y sulfatasas), mediante incubación con sustratos específicos, y posterior cuantificación colorimétrica de los productos liberados por las reacciones enzimáticas.

Los resultados de estas investigaciones microbiológicas son inéditos y las publicaciones derivadas de estos trabajos se encuentran en proceso de elaboración.

Asimismo, se están analizando las plantas (*Brassica juncea*) cultivadas en los suelos mineros recuperados para determinar el contenido de EPT en los órganos vegetales y evaluar la posible transferencia de metales desde el suelo a la planta, como indicador de su biodisponibilidad.

Otra línea de trabajo actualmente en curso pretende ampliar y diversificar la gama de RNP susceptibles de valorizar en la producción de tecnosuelos, mediante la caracterización de nuevos materiales residuales que se generan regularmente en grandes volúmenes, en colaboración con la empresa Green Soil Solutions.

Finalmente, se considera fundamental incorporar ensayos de campo a largo plazo en zonas piloto. Estos ensayos permitirán validar los resultados obtenidos en laboratorio a escala mayor y en condiciones ambientales reales, reforzando así la aplicabilidad práctica y la transferencia del conocimiento generado.

REFERENCIAS

Adriano, D.C., Wenzel, W.W., Vangronsveld, J., Bolan, N.S. (2004) Role of assisted natural remediation in environmental cleanup. *Geoderma,* 122, 121-142. https://doi.org/10.1016/j.geoderma.2004.01.003

Ahern, C.R., McElnea, A.E., Sullivan, L.A. (2004). *Acid Sulfate Soils Laboratory Methods Guidelines*; Queensland Department of Natural Resources, Mines and Energy: Indooroopilly, Australia.

Alberruche del Campo, E., Arranz González, J.C., Rodríguez Pacheco, R., Vadillo Fernández, L., Rodríguez Gómez, V., Fernández-Naranjo, F.J. (2014). *Manual para la evaluación de riesgos de instalaciones de residuos de industrias extractivas cerradas o abandonadas*. Instituto Geológico y Minero de España-Ministerio de Agricultura, Alimentación y Medio Ambiente. Madrid.

Allison, J.D., Brown, D.S., Novo-Gradac, J. (1999). *MINTEQA2/PRODEAFA2, a Geochemical Assessment Model for Environmental Systems: User Manual Supplement for Version 4.0*. US EPA, NERL, Athens, Georgia.

Alloway, B.J. (1996). Soil pollution and land contamination. En: R.M. Harrison (Ed.), *Pollution: Causes, Effects and Control* (pp. 352-377). Royal Society of Chemistry.

Aparicio, J.D., Raimondo, E.E., Saez, J.M., Costa-Gutiérrez, S.B., Álvarez, A., Benimeli, C.S., Polti, M.A. (2022). The current approach to soil remediation: A review of physicochemical and biological technologies, and the potential of their strategic combination. *Journal of Environmental Chemical Engineering*, 10(2), 107141. https://doi.org/10.1016/j.jece.2022.107141

Arán, D., Santos, E.S., Abreu, M.M., Antelo, J., Macías, F. (2022). Use of combined tools for effectiveness evaluation of tailings rehabilitated with designed

Technosol. *Environmental Geochemistry and Health*, 44, 1857-1873. https://doi.org/10.1007/s10653-021-01118-3

Arenas-Lago, D., Andrade, M.L., Lago-Vila, M., Rodríguez-Seijo, A., Vega, F.A. (2014). Sequential extraction of heavy metals in soils from a copper mine: Distribution in geochemical fractions. *Geoderma*, 230-231, 108-118. https://doi.org/10.1016/j.geoderma.2014.04.011

Barba-Brioso, C. (2011). Mineralogía, Geoquímica e Implicaciones Ambientales de los Suelos y Sedimentos del Paraje Natural Estero Domingo Rubio y su entorno (Huelva). (Tesis Doctoral). Universidad de Sevilla, Sevilla.

Barba-Brioso, C., Delgado, J., Fernández-Caliani, J.C. (2021). Sulfide oxidation, chemical partitioning and environmental availability of iron and trace elements in abandoned mine wastes affecting a coastal wetland ecosystem. *EGU General Assembly 2021*, EGU 21-5195. https://doi.org/10.5194/egusphere-egu21-5195

Barba-Brioso, C., Fernández-Caliani, J.C., Miras, A., Cornejo, J., Galán, E. (2010). Multi-source water pollution in a highly anthropized wetland system associated with the estuary of Huelva (SW Spain). *Marine Pollution Bulletin*, 60, 1259-1269. https://doi.org/10.1016/j.marpolbul.2010.03.018

Bigham, J.M., Schwertmann, U., Traina, S.J., Winland, R.L., Wolf, M. (1996). Schwertmannite and the chemical modeling of iron in acid sulfate waters. *Geochimica et Cosmochimica Acta*, 60 (16), 2111-2121. https://doi.org/10.1016/0016-7037(96)00091-9

Blowes, D.W., Ptacek, C.J., Jambor, J.L., Weisener, C.G. (2003). The geochemistry of acid mine drainage. En: H.D., Holland, K.K., Turekian (Eds.), *Treatise on Geochemistry* (Vol. 9, pp. 149–204). Elsevier.

Bolan, N., Kunhikrishnan, A., Thangarajan, R., Kumpiene, J., Park, J., Makino, T., Kirkham, M.B., Scheckel, K. (2014). Remediation of heavy metal(loid)s contaminated soils - to mobilize or to immobilize? *Journal of hazardous materials*, 266, 141-166. https://doi.org/10.1016/j.jhazmat.2013.12.018

Bolaños-Guerrón, D. (2014). Aplicación de Tecnosoles para la recuperación de suelos y aguas afectados por actividades de obras civiles, urbanas y mineras. (Tesis

Doctoral, Universidad de Santiago de Compostela). Minerva. http://hdl.handle.net/10347/12503

Blum, W.E.H. (2005). Functions of soil for society and the environment. *Reviews in Environmental Science and Biotechnology*, 4, 75–79. https://doi.org/10.1007/s11157-005-2236-x

Cánovas, C.R., Macías, F., Basallote, M.D., Olías, M., Nieto, J.M., Pérez-López, R. (2021). Metal(loid) release from sulfide-rich wastes to the environment: The case of the Iberian Pyrite Belt (SW Spain). *Current Opinion in Environmental Science & Health*, 20, 100240. https://doi.org/10.1016/j.coesh.2021.100240

Castillo, S., De la Rosa, J.D., Sánchez de la Campa, A.M., González-Castanedo, Y., Fernández-Caliani, J.C., González, I., Romero, A. (2013). Contribution of mine wastes to atmospheric metal deposition in the surrounding area of an abandoned heavily polluted mining district (Rio Tinto mines, Spain). *Science of the Total Environment*, 449, 363–372.

https://doi.org/10.1016/j.scitotenv.2013.01.076

Chopin, E.I.B., Alloway, B.J. (2007). Distribution and Mobility of Trace Elements in Soils and Vegetation Around the Mining and Smelting Areas of Tharsis, Ríotinto and Huelva, Iberian Pyrite Belt, SW Spain. *Water Air Soil Pollution,* 182, 245–261. https://doi.org/10.1007/s11270-007-9336-x

Clemente, R., Dickinson, N.M., Lepp, N.W. (2008). Mobility of metals and metalloids in a multi-element contaminated soil 20 years after cessation of the pollution source activity. *Environmental Pollution*, 155, 254–261. https://doi.org/10.1016/j.envpol.2007.11.024

Clemente, R., Walker, D.J., Bernal, M.P. (2005). Uptake of heavy metals and As by *Brassica juncea* grown in a contaminated soil in Aznalcóllar (Spain): The effect of soil amendments. *Environmental Pollution*, 138 (1), 46-58. https://doi.org/10.1016/j.envpol.2005.02.019

Decisión 96/350/CE de la Comisión Europea, de 24 de mayo de 1996, por la que se adaptan los Anexos II A y II B de la Directiva 75/442/CEE del Consejo relativa a

los residuos (Decisión 96/350/CE). https://eur-lex.europa.eu/legal-content/ES/TXT/?uri=CELEX%3A31996D0350

Delgado, A. (2023). *Hidrometalurgia del cobre en Rio Tinto (1725-1954)*. (Ed.) Universidad de Huelva, 240 pp.

Directiva 2008/98/CE del Parlamento Europeo y del Consejo, de 19 de noviembre de 2008, sobre los residuos y por la que se derogan determinadas Directivas (Directiva 2008/98/CE). https://eur-lex.europa.eu/legal-content/ES/TXT/?uri=CELEX%3A32008L0098

European Commission (2021). *The EU Soil Strategy for 2030*. https://environment.ec.europa.eu/publications/eu-soil-strategy-2030_en

Dold, B. (2003). Speciation of the most soluble phases in a sequential extraction procedure adapted for geochemical studies of copper sulfide mine waste. *Journal of Geochemical Exploration*, 80, 55–68. https://doi.org/10.1016/S0375-6742(03)00182-1

FAO (2015). *Status of the World's Soil Resources – Main Report*. Food and Agriculture Organization of the United Nations and Intergovernmental Technical Panel on Soils, Rome, Italy.

Fernández-Caliani, J.C. (2008). Una aproximación al conocimiento del impacto ambiental de la minería en la Faja Pirítica Ibérica. *Macla*, 10, 24-28.

Fernández-Caliani, J.C. (2022). La contaminación del suelo por la minería metálica de la Faja Pirítica Ibérica. *Macla*, 26, 1-3.

Fernández-Caliani, J.C., Álvarez-Lozano, J., García-Navarro, E., Fernández-Landero, S., Cantero, C., Giráldez, M.I. (2024). A novel Technosol formulation for sustainable landfill top covers using non-hazardous wastes. *Applied Sciences*, 14, 6166. https://doi.org/10.3390/app14146166

Fernández-Caliani, J.C., Barba-Brioso, C. (2010). Metal immobilization in hazardous contaminated minesoils after marble slurry waste application. A field assessment at the Tharsis mining district (Spain). *Journal of Hazardous Materials*, 181, 817-826. https://doi.org/10.1016/j.jhazmat.2010.05.087

Fernández-Caliani, J.C., Barba-Brioso, C., González, I., Galán, E. (2009). Heavy metal pollution in soils around the abandoned mine sites of the Iberian Pyrite Belt (Southwest Spain). *Water Air and Soil Pollution*, 200, 211–226. https://doi.org/10.1007/s11270-008-9905-7

Fernández-Caliani, J.C., De la Rosa, J.D, Sánchez de la Campa, A.M., González-Castanedo, Y., Castillo, S. (2013). Mineralogy of atmospheric dust impacting the Rio Tinto mining area (Spain) during episodes of high metal deposition. *Mineralogical Magazine*, 77 (6), 2793-2810. 10.1180/minmag.2013.077.6.07

Fernández-Caliani, J.C., Giráldez, M.I., Barba-Brioso, C. (2019). Oral bioaccessibility and human health risk assessment of trace elements in agricultural soils impacted by acid mine drainage. *Chemosphere*, 237, 124441. https://doi.org/10.1016/j.chemosphere.2019.124441

Fernández-Caliani, J. C., Giráldez, M. I., Waken, W. H., Del Río, Z. M., Córdoba, F. (2021). Soil quality changes in an Iberian pyrite mine site 15 years after land reclamation. *Catena*, 206, 105538. https://doi.org/10.1016/j.catena.2021.105538

Ficklin, W.H., Plumlee, G.S., Smith, K.S., McHu-gh, J.B. (1992). Geochemical classification of mine drainages and natural drainages in mineralized areas. En: *Proceedings of the 7th International Symposium on Water Rock Interaction Conference*, pp. 381–384. Park City, Utah.

Forján, R., Asensio, V., Rodríguez-Vila, A., Covelo, E.F. (2015). Contribution of waste and biochar amendment to the sorption of metals in a copper mine tailing. *Catena*, 137, 120-125. https://doi.org/10.1016/j.catena.2015.09.010

Forján, R., Rodríguez-Vila, A., Cerqueira, B., Covelo, E.F. (2018). Comparison of compost with biochar versus technosol with biochar in the reduction of metal pore water concentrations in a mine soil. *Journal of Geochemical Exploration*, 192, 103-111. https://doi.org/10.1016/j.gexplo.2018.06.007

Forján, R., Rodríguez-Vila, A., Covelo, E.F. (2017). Using compost and technosol combined with biochar and Brassica juncea L. to decrease the bioavailable metal concentration in soil from a copper mine settling pond. *Environmental*

Science and Pollution Research, 25, 1294–1305. https://doi.org/10.1007/s11356-017-0559-0

Gabari, V., Fernández-Caliani, J.C. (2017). Assessment of trace element pollution and human health risks associated with cultivation of mine soil. A case study in the Iberian Pyrite Belt. *Human and Ecologycal Risk Assessment*, 23, 2069-2086. https://doi.org/10.1080/10807039.2017.1364130

Galán, E., Fernández-Caliani, J.C., González, I., Aparicio, P., Romero, A. (2008). Influence of geological setting on geochemical baselines of trace elements in soils. Application to soils of Southwest Spain. *Journal of geochemical exploration*, 98, 89-106. https://doi.org/10.1016/j.gexplo.2008.01.001

Galán, E., Gómez-Ariza, J.L., González, I., Fernández-Caliani, J.C., Morales, E., Giráldez. I. (2003). Heavy metal partitioning in river sediments severely polluted by acid mine drainage in the Iberian Pyrite Belt. *Applied Geochemistry*,18 (3), 409–21. https://doi.org/10.1016/S0883-2927(02)00092-6

Grande, J.A., Valente, T., de la Torre, M.L., Santisteban, M., Cerón, J.C., Pérez-Ostalé, E. (2014). Characterization of acid mine drainage sources in the Iberian Pyrite Belt: base methodology for quantifying affected areas and for environmental management. *Environmental Earth Sciences*, 71, 2729-2738. https://doi.org/10.1007/s12665-013-2652-0

Grantcharova, M.M., Fernández-Caliani, J.C. (2022). Soil acidification, mineral neoformation and heavy metal contamination driven by weathering of sulphide wastes in a Ramsar wetland. *Applied Sciences*, 12, 249. https://doi.org/10.3390/app12010249

Houba, V.J.G., Lexmond, Th.M., Novozamsky, I., van der Lee, J.J. (1996). State of the art and future developments in soil analysis for bioavailability assessment. *Science of the Total Environment*, 178, 21–28. https://doi.org/10.1016/0048-9697(95)04793-X

Houba, V.J.G., Novozamsky, I., Lexmond, T.M., van ver Lee, J.J. (1990). Applicability of 0,01 M $CaCl_2$ as a single extraction solution for the assessment of the nutrient status of soils and other diagnostic purposes. *Communications in Soil*

Science and Plant Analysis, 21 (19-20), 2281-2290. https://doi.org/10.1080/00103629009368380

ISTA, International Seed Testing Association (2005). *International Rules for Seed Testing*. International Seed Testing Association, Zurich, Switzerland.

Jiménez-Ballesta, R. (2017). *Introducción a la contaminación de suelo*s. Editorial Mundi-Prensa.

Jones, A., Panagos, P., Barcelo, S., Bouraoui, F., Bosco, B., Dewitte, O., Gardi, C., Hervás, J., Hiederer, R., Jeffery, L., Montanarella, L., Penizek, V., Tóth, G., Van Den Eeckhaut, M., Van Liedekerke, M., Verheijen, F., Yigini, Y. (2012). *The State of Soil in Europe. A contribution of the JRC to the European Environment Agency's Environment State and Outlook Report*. https://publications.jrc.ec.europa.eu/repository/bitstream/JRC68418/lbna25186enn.pdf

Junta de Andalucía (2005). Caracterización ambiental de humedales de Andalucía. pp. 550. Junta de Andalucía, Sevilla.

Junta de Andalucía (2015). Decreto 18/2015, de 27 de enero, por el que se aprueba el reglamento que regula el régimen aplicable a los suelos contaminados. BOJA, 38, 28-64.

Junta de Andalucía (2023). Memoria del Plan Hidrológico (2022-2027) de la Demarcación Hidrográfica del Tinto, Odiel y Piedras. pp. 236.

Kabata-Pendias, A., Mukherjee, A.B. (2007). *Trace Elements from Soil to Human*. Springer.

Kahle, M., Kleber, M., Jahn, R. (2002). Review of XRD-based quantitative analyses of clay minerals in soils: The suitability of mineral intensity factors. *Geoderma*, 109, 191–205.

Kumpiene, J., Lagerkvist, A., Maurice, C. (2008). Stabilization of As, Cr, Cu, Pb and Zn in soil using amendments - A review. *Waste Management*, 28, 215-225. https://doi.org/10.1016/j.wasman.2006.12.012

Lal, R. (2004). Soil carbon sequestration impacts on global climate change and food security. *Science,* 304, 1623–1627. https://doi.org/10.1126/science.1097396

López, M., González, I., Romero, A. (2008). Trace elements contamination of agricultural soils affected by sulphide exploitation (Iberian Pyrite Belt, SW Spain). *Environmental Geology*, 54, 805-818. https://doi.org/10.1007/s00254-007-0864-x

Macías, F., 2001. Perspectivas de la aplicación de residuos orgánicos al suelo. En: J. Boixadera, M.E. Teira (Eds). *Aplicación de residuos orgánicos*. Lleida: Univ. Lleida, pp. 329-354.

Macías, F., 2004. Recuperación de suelos degradados, reutilización de residuos y secuestro de carbono. Una alternativa integral de mejora de la calidad ambiental. *Recursos Rurais*, 1, 49-56.

Macías, F. (2015). Retos y oportunidades de la ciencia del suelo: aprendiendo de los suelos, aprendiendo de la naturaleza. *Spanish Journal of Soil Science,* 5(1), 1-11.

Macías, F., Bao, M., Macías-García, F., Camps, M. (2007). Valorización biogeoquímica de residuos mediante la elaboración de Tecnosoles con diferentes aplicaciones ambientales. *Aguas & Residuos*, 5, 12-25.

Macías, F., Nieto, C. (2012). Didáctica de la mina de Touro: procesos de recuperación de suelos y aguas hiperácidas de minas de sulfuros metálicos mediante la valorización geoquímica de residuos. *Comunicaciones del XVII Simposio sobre Enseñanza de la Geología*, pp. 139-145.

Macías-García, F., Camps, M., Macías, F. (2009a). Utilización de Tecnosoles derivados de residuos en procesos de restauración de la mina de Touro. En: *Minería Sostenible. Cámara Oficial Mineira de Galicia*. A Coruña, pp. 651-661.

Macías-García, F., Fontán, L., Otero, X. L., Pérez Llaguno, C., Camps Arbestain, M., Macías, F. (2009b). Recuperación de aguas ácidas de la mina Touro mediante sistemas integrados de barreras reactivas con diferentes Tecnosoles y humedales. En: *Minería Sostenible. Cámara Oficial Mineira de Galicia*. A Coruña. 963-973.

Madejón, P., Barba-Brioso, C., Lepp, N.W., Fernández-Caliani J.C. (2011). Traditional agricultural practices enable sustainable remediation of highly polluted soils in Southern Spain for cultivation of food crops. *Journal of Environmental Management*, 92, 1828-1836. https://doi.org/10.1016/j.jenvman.2011.03.007

Madejón, P., Burgos, P., Murillo, J.M., Cabrera, F., Madejón, E. (2009). Bioavailability and accumulation of trace elements in soils and plants of a highly contaminated estuary (Domingo Rubio tidal channel, SW Spain). *Environmental Geochemistry and Health,* 31, 629–642. https://doi.org/10.1007/s10653-008-9221-6

Madejón, P., Caro-Moreno, D., Navarro-Fernández, C.M., Rossini-Oliva, S., Marañón, T. (2021). Rehabilitation of waste rock piles: Impact of acid drainage on potential toxicity by trace elements in plants and soil. *Journal of Environmental Management*, 280, 111848. https://doi.org/10.1016/j.jenvman.2020.111848

Martín-Méndez, I., Llamas Borrajo, J., Bel-lan, A., Locutura, J (2023). Geochemical distribution in residual soils of Iberian Pyrite Belt (Spain). *Journal of Iberian Geology*, 49, 97–114. https://doi.org/10.1007/s41513-023-00210-0

Meuser, H. (2013). *Soil Remediation and Rehabilitation. Treatment of Contaminated and Disturbed Land*. Springer.

Mirsal, I.A. (2008). *Soil pollution. Origin, monitoring and remediation*. Springer. https://doi.org/10.1007/978-3-540-70777-6

Moreno-Barriga, F., Díaz, V., Acosta, J.A., Muñoz, M.A., Faz, A., Zornoza, F. (2017). Creation of Technosols to decrease metal availability in pyritic tailings with addition of biochar and marble waste. *Land Degradation & Development*, 28, 1943-1951. https://doi.org/10.1002/ldr.2714

Nelson, D.W., Sommers, L.E. (1996) Total Carbon, Organic Carbon, and Organic Matter. En: D.L. Sparks, A.L. Page, P.A. Helmke, R.H. Loeppert, P.N. Soltanpour, M.A. Tabatabai, C.T. Johnston, M.E. Summer (Eds.). *Methods of Soil Analysis. Part 3. Chemical Methods* (pp. 961-1010), Madison, WI: Soil Science Society of America.

Nordstrom, D.K., Alpers, C.N. (1997). Geochemistry of acid mine waters. En: G.S Plumlee, M.J. Logsdon (Eds.), *The Environmental Geochemistry of Mineral Deposits* (Vol. 6A, pp. 133-160). Reviews in Economic Geology, Society of Economic Geologists, Littleton, USA.

Novo, L.A.B., González, L. (2014). Germination and early growth of Brassica juncea in copper mine tailings amended with Technosol and compost. *The Scientific World Journal*, 2014 (3), 506392. https://doi.org/10.1155/2014/506392

Olías, M., Nieto, J.M., Sarmiento, A.M., Cánovas, C.R. (2010). *La contaminación minera de los ríos Tinto y Odiel*. Junta de Andalucía. 166 p.

Olsen, S. R., Sommers, L. E. (1982). Phosphorus. En: A. L. Page (Ed.), *Methods of soil analysis part 2 chemical and microbiological properties* (pp. 403–430). American Society of Agronomy, Soil Science Society of America.

Pahalvi, H.N., Rafiya, L., Rashid, S., Nisar, B., Kamili, A.N. (2021). Chemical Fertilizers and Their Impact on Soil Health. En: G.H., Dar, R.A., Bhat, M.A., Mehmood, K.R. Hakeem, (Eds). *Microbiota and Biofertilizers* (Vol 2, pp 1-20). Springer.

Palansooriya, K.N., Shaheen, S.M., Chen, S.S., Tsang, D.C.W., Hashimoto, Y., Hou, D., Nanthi, N.S., Rinklebe, J., Ok, Y.S. (2020) Soil Amendments for Immobilization of Potentially Toxic Elements in Contaminated Soils: A Critical Review. *Environment International*, 134, 105046. https://doi.org/10.1016/j.envint.2019.105046

Parkhurst, D.L., Appelo, C.A.J. (2013). Description of input and examples for PHREEQC version 3—A computer program for speciation, batch-reaction, one-dimensional transport, and inverse geochemical calculations. US Geological Survey, Techniques and Methods, 6, 497.

Parviainen, A., Vázquez-Arias, A., Arrebola, J.P., Martín-Peinado, F.J. (2022). Human health risks associated with urban soils in mining areas. *Environmental Research*, 206, 112514. https://doi.org/10.1016/j.envres.2021.112514

Pérez-Esteban, J., Escolástico, C., Moliner, A., Masaguer, A., Ruiz-Fernández, J. (2014). Phytostabilization of metals in mine soils using Brassica juncea in combination

with organic amendments. *Plant and Soil*, 377, 97–109. https://doi.org/10.1007/s11104-013-1629-9

Pérez-Macías, J.A. (1998), *Las minas de Huelva en la Antigüedad*. (Ed.) Diputación Provincial de Huelva, Huelva.

Pinedo, I. (1963). *Piritas de Huelva: Historia, minería y aprovechamiento*. (Ed.) Suma, Madrid, 10003 pp.

Rabot, E., Wiesmeier, M., Schlüter, S., Vogel, H.J. (2018). Soil structure as an indicator of soil functions: A review. *Geoderma*, 314, 122-137. https://doi.org/10.1016/j.geoderma.2017.11.009

REDIAM. Red de Información Ambiental de Andalucía. https://www.juntadeandalucia.es/medioambiente/portal/acceso-rediam

Ribeiro de Mello, C., Tornos, F., Conde, C., Tassinari, C.C.G., Farci, A., Vega, R. (2022). Geology, Geochemistry, and Geochronology of the Giant Rio Tinto VMS Deposit, Iberian Pyrite Belt, Spain. *Economic Geology*, 117 (5), 1149-1177. https://doi.org/10.5382/econgeo.4907

Rivera, M.B., Giráldez, M.I., Fernández-Caliani, J.C. (2016). Assessing the environmental availability of heavy metals in geogenically contaminated soils of the Sierra de Aracena Natural Park (SW Spain). Is there a health risk? *Science of the Total Environment*, 560-561, 254-265. https://doi.org/10.1016/j.scitotenv.2016.04.029

Rodrigues, S.M., Henriques, B., Ferreira da Silva, E., Pereira, M.E., Duarte, A.C., Römkens, P.F.A.M. (2010). Evaluation of an approach for the characterization of reactive and available pools of twenty potentially toxic elements in soils: part I – the role of key soil properties in the variation of contaminants reactivity. *Chemosphere*, 81, pp. 1549-1559. https://doi.org/10.1016/j.chemosphere.2010.07.026

Rodríguez-Eugenio, N., McLaughlin, M., Pennock, D. (2019). *La contaminación del suelo: una realidad oculta*. Roma, FAO. https://openknowledge.fao.org/server/api/core/bitstreams/7d70ca8d-7503-4839-8d6b-8250e9add8ac/content

Rodríguez-Vila, A., Forján, R., Guedes, R.S., Covelo, E.F. (2016). Changes on the phytoavailability of nutrients in a mine soil reclaimed with compost and biochar. *Water, Air, & Soil Pollution*, 227, 453. https://doi.org/10.1007/s11270-016-3155-x

Rodríguez-Vila, A., Forján, R., Guedes, R.S., Covelo, E.F. (2017). Nutrient phytoavailability in a mine soil amended with technosol and biochar and vegetated with *Brassica juncea*. *Journal of Soils and Sediments,* 17, 1653-1661. https://doi.org/10.1007/s11368-016-1643-7

Romero, A., González, I., Galán, E., Fernández-Caliani, J.C. (2011). Caracterización y distribución espacial de las escombreras mineras de Riotinto: una base para valorar el potencial contaminante. *Macla*, 15, 179-180.

Romero-Baena, A., Barba-Brioso, C., Ross, A., González, I., Aparicio, P. (2021). Mobility of potentially toxic elements in family garden soils of the Riotinto mining area. *Applied Clay Science*, 203, 105999. https://doi.org/10.1016/j.clay.2021.105999

Ruiz de Almodóvar, G., Sáez, R. (1992). Los yacimientos de sulfuros masivos de la Faja Pirítica Sur-Ibérica". En: *Recursos minerales de España* (pp. 1309-1324). Consejo Superior de Investigaciones Científicas, CSIC.

Sáez, R., González, F., Donaire, T., Toscano, M., Yesares, L., Ruiz de Almodóvar, G., Moreno, C. (2024). Updating geological information about the metallogenesis of the Iberian Pyrite Belt. *Minerals*, 14 (9), 860. https://doi.org/10.3390/min14090860

Saiz, J.L. (2004). Estudio edafológico de suelos afectados por procesos de acidificación en las explotaciones piríticas del suroeste español (Huelva y Sevilla). Tesis Doctoral, Escuela Técnica Superior de Ingenieros de Montes, Universidad Politécnica de Madrid.

Saiz, J.L., Ceacero, C.J. (2008). Revegetación de suelos acidificados por minería metálica. Consejería de Medio Ambiente y Ordenación del Territorio, Junta de Andalucía, Sevilla, 150 p.

Salkield, L.U., (1987): *A technical history of the Rio Tinto mines: some notes on exploitation from pre-Phoenician times to the 1950s*. The Institute of Mining and Metallurgy, Londres, 114 pp.

Sánchez-España, J., Pamo, E.L., Pastor, E.S., Andrés, J.R., Martín Rubí, J.A. (2006). The Removal of Dissolved Metals by Hydroxysulphate Precipitates during Oxidation and Neutralization of Acid Mine Waters, Iberian Pyrite Belt. *Aquatic Geochemistry,* 12, 269–298. https://doi.org/10.1007/s10498-005-6246-7

Sandor, J.A., Burras, C.L., Thompson, T., Wills, S.A. (2023). Factors of soil formation-Human impacts. En: M.J., Goss, M. Oliver (Eds.). *Encyclopedia of Soils in the Environment* (2º ed., Vol. 4, pp. 54-68). Academic Press.

Santos, E.S., Magalhães, M.C.F., Abreu, M.M., Macías, F. (2014). Effects of organic/inorganic amendments on trace elements dispersion by leachates from sulfide containing tailings of the São Domingos mine, Portugal. Time evaluation. *Geoderma*, 226-227: 188-203. https://doi.org/10.1016/j.geoderma.2014.02.004

Santos, E., Abreu, M., Macías, F., Varennes, A. (2016). Chemical quality of leachates and enzymatic activities in Technosols with gossan and sulfide wastes from the São Domingos mine. *Journal of Soils & Sediments*, 16, 1366-1382. https://doi.org/10.1007/s11368-015-1068-8

Santos, E., Abreu, M.M., Macías, F., Magalhães, M.C.F. (2017). Potential environmental impact of technosols composed of gossan and sulfide-rich wastes from São Domingos mine: assay of simulated leaching. *Journal of soils and sediments*, 17, 1369-1383. https://doi.org/10.1007/s11368-016-1518-y

Sarmiento, A.M., Nieto, J.M., Olías, M., Cánovas, C.R. (2009). Hydrochemical characteristics and seasonal influence on the pollution by acid mine drenaje in the Odiel river Basin (SW Spain). *Applied Geochemistry*, 24, 697-714. https://doi.org/10.1016/j.apgeochem.2008.12.025

Schermerhörn, L.J.G. (1971). An outline stratigraphy of the Iberian Pyrite Belt. *Boletín Geológico y Minero*, 82, 239-268.

Tornos, F. (2006). Environment of formation and styles of volcanogenic massive sulfides: The Iberian Pyrite Belt. *Ore Geology Reviews*, 28 (3), 259-307. https://doi.org/10.1016/j.oregeorev.2004.12.005

Ure, A.M., Quevauviller, P.H., Muntau, H., Griepink, B. (1993). Speciation of heavy metalsin soils and sediments. An account of the improvement and harmonisation ofextraction techniques undertaken under the auspices of the BCR of the Commissionof the European Communities. *Interntional Journal of Environmental Analytical Chemistry*, 51, 135-151. https://doi.org/10.1080/03067319308027619

Urrutia, M.M., García-Rodeja, E., Macias, F. (1992). Sulfide oxidation in coal-mine dumps: Laboratory measurement of acidifying potential with H2O2 and its application to characterize spoil materials. *Environmental Management*, 16, 81–89. https://doi.org/10.1007/BF02393911

USEPA, U.S. Environmental Protection Agency (2024). Superfund National Priorities List Sites. https://www.epa.gov/superfund/superfund-national-priorities-list-npl

Weil, R.R., Brady, N.C. (2016). *The Nature and Properties of Soils* (15th Edition). Pearson, Columbus.

WRB (2006). *Base referencial mundial del recurso suelo 2006: Un marco conceptual para clasificación, correlación y comunicación internacional.* World Soil Resources Reports (2° ed.), 103. FAO, Roma.

Xunta de Galicia (2008). Resolución de 8 de enero de 2008, de la Dirección General de Calidad y Evaluación Ambiental, por lo que se da publicidad a la instrucción técnica de residuos ITR/01/08, de 8 de enero de 2008, de la Dirección General de Calidad y Evaluación Ambiental, referente a la elaboración de suelos (tecnosoles) derivados de residuos. *Diario Oficial de Galicia*, 18, 1499-1511.